Prepared in cooperation with Fairfax County, Virginia

Spatial and Temporal Patterns in Streamflow, Water Chemistry, and Aquatic Macroinvertebrates of Selected Streams in Fairfax County, Virginia, 2007–18

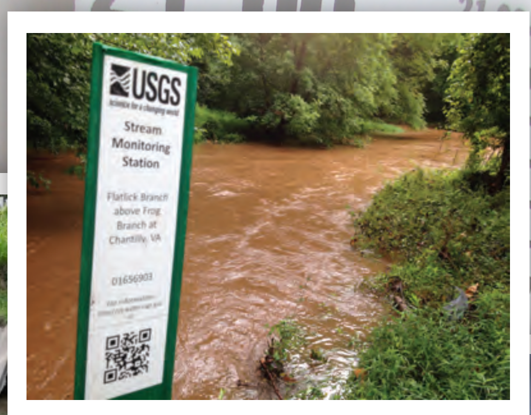

Scientific Investigations Report 2020–5061

U.S. Department of the Interior
U.S. Geological Survey

Top: Elevated stormflows at Flatlick Branch above Frog Branch at Chantilly, Virginia, on August 12, 2014; photograph by U.S. Geological Survey.

Right: *Optioservus* larva (a riffle beetle, family Elmidae) under the microscope collected during one of the annual benthic macroinvertebrate sampling trips; photograph by Chad Grupe of Fairfax County.

Bottom: Gage house at Long Branch near Annandale, Virginia, on February 3, 2015; photograph by U.S. Geological Survey.

Left: USGS hydrologic technician collecting water quality samples at a Fairfax County stream; photograph by U.S. Geological Survey.

Background: Image of USGS staff gage used for reading water level; photograph by U.S. Geological Survey.

Spatial and Temporal Patterns in Streamflow, Water Chemistry, and Aquatic Macroinvertebrates of Selected Streams in Fairfax County, Virginia, 2007–18

By Aaron J. Porter, James S. Webber, Jonathan W. Witt, and John D. Jastram

Prepared in cooperation with Fairfax County, Virginia

Scientific Investigations Report 2020–5061

U.S. Department of the Interior
U.S. Geological Survey

U.S. Department of the Interior
DAVID BERNHARDT, Secretary

U.S. Geological Survey
James F. Reilly II, Director

U.S. Geological Survey, Reston, Virginia: 2020

Suggested citation:
Porter, A.J., Webber, J.S., Witt, J.W., and Jastram, J.D., 2020, Spatial and temporal patterns in streamflow, water chemistry, and aquatic macroinvertebrates of selected streams in Fairfax County, Virginia, 2007–18: U.S. Geological Survey Scientific Investigations Report 2020–5061, 106 p., https://doi.org/10.3133/sir20205061.

Associated data for this publication:
Porter, A.J., Webber J.S., Witt, J.W., and Jastram, J.D., 2020, Inputs and selected outputs used to assess spatial and temporal patterns in streamflow, water-chemistry, and aquatic macroinvertebrates of selected streams in Fairfax County, Virginia, 2007-2018: U.S. Geological Survey data release, https://doi.org/10.5066/P95S9RFV.

ISSN 2328-031X (print)
ISSN 2328-0328 (online)

Acknowledgments

Ecologists with the Fairfax County Department of Public Works and Environmental Services, primarily Shannon Curtis and Joe Sanchirico, have contributed greatly to this effort through field work and program responsibilities. Their dedication to the success of this effort has been vital in the progress toward the achievement of program objectives. Staff at the Fairfax County Environmental Services Laboratory performed the nutrient analyses for the large number of samples collected. Their efforts to accommodate unpredictable sample collection schedules are greatly appreciated.

This study was designed by Doug Moyer and Ken Hyer of the U.S. Geological Survey (USGS), who continue to contribute to the success of the effort by sharing expertise in water-resources monitoring and data analysis. Alyssa Thornton and numerous USGS hydrologic technicians have spent substantial amounts of time in the field maintaining instrumentation and collecting data, and their efforts are greatly appreciated. We would also like to thank Guoxiang Yang for his analysis of long-term trends in continuously collected specific conductance data.

Contents

Figures

Tables

Conversion Factors

International System of Units to U.S. customary units

Multiply	By	To obtain
	Length	
centimeter (cm)	0.3937	inch (in.)
millimeter (mm)	0.03937	inch (in.)
meter (m)	3.281	foot (ft)
	Area	
square meter (m^2)	0.0002471	acre
hectare (ha)	2.471	acre
square kilometer (km^2)	0.3861	square mile (mi^2)
	Volume	
cubic meter (m^3)	35.31	cubic foot (ft^3)
	Flow rate	
meter per second (m/s)	3.281	foot per second (ft/s)
meter per year (m/yr)	3.281	foot per year ft/yr)
cubic meter per second (m^3/s)	35.31	cubic foot per second (ft^3/s)
cubic meter per second per square kilometer ($[m^3/s]/km^2$)	91.49	cubic foot per second per square mile ($[ft^3/s]/mi^2$)
cubic meter per day (m^3/d)	35.31	cubic foot per day (ft^3/d)
millimeter per year (mm/yr)	0.03937	inch per year (in/yr)
	Mass	
gram (g)	0.03527	ounce, avoirdupois (oz)
kilogram (kg)	2.205	pound avoirdupois (lb)

Temperature in degrees Celsius (°C) may be converted to degrees Fahrenheit (°F) as °F = (1.8 × °C) + 32.

Temperature in degrees Fahrenheit (°F) may be converted to degrees Celsius (°C) as °C = (°F – 32) / 1.8.

Datum

Horizontal coordinate information is referenced to the North American Datum of 1983 (NAD 83).

Altitude, as used in this report, refers to distance above the vertical datum.

Supplemental Information

Specific conductance is given in microsiemens per centimeter at 25 degrees Celsius (µS/cm at 25 °C).

Concentrations of chemical constituents in water are given in either milligrams per liter (mg/L) or micrograms per liter (µg/L)

Abbreviations

AEP	annual exceedance probability
AMLE	adjusted maximum likelihood estimator
ANCOVA	analysis of covariance
BFI	baseflow index
BMP	best management practices
CB-NTN	Chesapeake Bay Non-tidal Network
CCH	*Chimarra, Cheumatopsyche*, and *Hydropsyche*
COTE	Coleoptera, Odonata, Tricoptera, and Ephemeroptera
DO	dissolved oxygen
DTKN	dissolved total Kjeldahl nitrogen
EPA	U.S. Environmental Protection Agency
EPT	Ephemeroptera, Plecoptera, and Trichoptera
FCSWPD	Fairfax County Stormwater Planning Division
FFG	functional feeding group
FN	flow normalization
FNU	Formazin nephelometric units
GAM	generalized additive model
IBI	Index of Biological Integrity
MDL	method detection limit
NPS	nonpoint source
NWIS	National Water Information System
OP	orthophosphate
PAR	photosynthetically active radiation
RBI	Richards-Baker Flashiness Index
SC	specific conductance
SCI	stream condition index
SEP	standard error of prediction
SFI	stormflow index
SS	suspended sediment
TDN	total dissolved nitrogen
TDP	total dissolved phosphorus
TMDL	total maximum daily load
TN	total nitrogen
TP	total phosphorus

TPN	total particulate nitrogen
TPP	total particulate phosphorus
USGS	U.S. Geological Survey
WRTDS	Weighted Regressions on Time, Discharge, and Season
WY	water year (October 1-September 30)

Spatial and Temporal Patterns in Streamflow, Water Chemistry, and Aquatic Macroinvertebrates of Selected Streams in Fairfax County, Virginia, 2007–18

By Aaron J. Porter,[1] James S. Webber,[1] Jonathan W. Witt,[2] and John D. Jastram[1]

Abstract

Urbanization substantially alters the landscape in ways that can impact stream hydrology, water chemistry, and the health of aquatic communities. Stormwater best management practices (BMPs) are the primary tools used to mitigate the effects of urban stressors such as increased runoff, decreased baseflow, and increased nutrient and sediment transport. To date, Fairfax County Virginia's stormwater management program has made substantial investments into the implementation of both structural and nonstructural BMPs aimed at restoring and protecting watersheds. The U.S. Geological Survey (USGS), in cooperation with Fairfax County, Virginia, established a long-term water-resources monitoring program to evaluate the watershed-scale effects of these investments. Monitoring began at 14 stations in 2007 and was expanded to 20 stations in 2013. This report utilized the first 10 years of data collection to (1) assess water quantity and quality, as well as ecological condition; (2) compute annual nutrient and sediment loads; and (3) evaluate trends in streamflow, water quality, and ecological condition. Efforts are underway to link the biotic and abiotic patterns described herein to watershed management practices as well as factors such as land use change, public works infrastructure, and climate.

Hydrologic, chemical, and benthic macroinvertebrate community conditions in the streams monitored were similar to those observed in other studies of urban streams. Multidecadal trends in baseflow indices and runoff ratios at long-term Chesapeake Bay Non-tidal Network streamgages (CB-NTN) indicate a decrease in groundwater recharge and increase in storm runoff as a result of urbanization. Streamflow yields varied spatially with land cover, geology, and soil characteristics, whereas flashiness was positively related to impervious area. Dissolved oxygen typically was lowest in the Coastal Plain and across all Triassic Lowlands streams, and highest in the Piedmont. Dissolved oxygen concentrations generally were above Virginia's minimum criterion of 4.0 milligrams per liter (mg/L), most violations occurred at Paul Spring Branch in the Coastal Plain during the warmest months of the year owing to increased chemical and biological oxygen demand. Typical pH values of the monitored streams centered on neutrality (pH = 7); however, diurnal fluctuations were most prevalent in the continuous pH data at Flatlick Branch (FLAT; a Triassic Lowlands station), as a result of increased photosynthesis catalyzed by phosphorus-rich geology. Specific conductance (SC) varied spatially owing to geology (highest at Triassic Lowlands stations) and anthropogenic disturbance (watersheds with high impervious land cover). Specific conductance typically was inversely related to streamflow except in winter months following deicing road salt applications, when values increased by several orders of magnitude. A significant increase in SC of about 2 percent per year was observed from the combined trend result of all monitoring stations over the 10-year period. Significant SC increases occurred at nearly all monitoring stations. Increasing trends were observed during winter and nonwinter months, which suggests that salts applied to deice roadways and other impervious surfaces are stored in the environment and released year-round.

Suspended-sediment (SS) concentrations in monthly samples did not vary significantly between most stations, but typically were highest in the spring and lowest in the fall as a result of seasonal differences in streamflow and climate. Suspended-sediment yields ranged from 62 to 1,428 tons per square mile (ton/mi^2), with a median of 302 ton/mi^2. Annual loads were greatest during the wettest water years (October 1-September 30; 2008, 2011, and 2014), with the greatest interannual variability occurring at Difficult Run above Fox Lake (DIFF) and South Fork Little Difficult Run (SFLIL). Suspended sediment was primarily composed of silts and clays; however, the proportion of sand in suspended sediment was related positively to streamflow. Cross-correlation analyses suggested the dominant sources of SS were streambank erosion and resuspension of in-channel material at DIFF and FLAT; whereas, upland sources and erosion of upper streambanks were more common at Dead Run (DEAD), Long Branch (LONG), and SFLIL.

Median total phosphorus (TP) concentrations ranged from 0.016 to 0.077 mg/L, with a networkwide median of 0.022 mg/L, were highest in the warm season (April-September), and were composed primarily of dissolved phosphorous. Although TP concentrations were relatively low across the network, the highest concentrations were

[1]U.S. Geological Survey.

[2]Fairfax County Department of Public Works and Environmental Services.

consistently at stations located in the Triassic Lowlands, owing to phosphorous-rich geology, and in the Coastal Plain, owing to the low-phosphorous sorptive capacity of those soils. A significant increase in TP concentration occurred in a few stations, but the combined trend results from all stations demonstrated a significant increase of about 4 percent per year. Networkwide increases were also observed in total dissolved phosphorus, orthophosphate, and total particulate phosphorus. The composition of TP shifted from dissolved to particulate as streamflow increased and for this reason loads primarily were composed of particulate phosphorous. Median annual TP loads were highest at FLAT and DEAD and ranged from 247 to 642 pounds per square mile (lbs/mi^2) networkwide. Interannual variability in phosphorous yields was apparent at most stations; the highest loading years were also the wettest years during the study period and coincident with the highest peak annual flows.

Total nitrogen (TN) concentrations typically were low throughout the network with exceptions occurring at stations located in watersheds with a high density of septic infrastructure. Elevated TN concentrations also were observed in some watersheds without a high density of septic systems and may be attributable to geologic and soil properties that limit denitrification as well as other unknown anthropogenic inputs. Total nitrogen typically was dominated by nitrate during baseflows; however, the proportion of particulate nitrogen increased during stormflows. Total nitrogen yields were similar across stations, with medians ranging from about 3,600 to 6,300 lbs/mi^2 and were related to annual streamflow volume. Total nitrogen concentrations and flow-normalized concentrations decreased over the 10-year period at 7 stations, with median reductions of about 2.5 percent. Increasing trends were observed at the two stations with the highest median TN concentration (Captain Hickory Run and SFLIL, 3–5 mg/L), both watersheds contain a high density of septic infrastructure. The combined trend results from all stations revealed no trend in TN and a declining trend in nitrate of about 2 percent per year.

Overall, benthic community metrics indicated that streams throughout Fairfax County were initially of poor health; however, many metrics show an improving trend (from poor to fair based on the Fairfax County Index of Biological Integrity [IBI]). Significant increasing trends in IBI occurred at the network-scale and at 4 individual stations; additionally, scores improved by at least 1 qualitative category (for example, poor to fair, fair to good) at 11 of the 14 stations between 2009 (the first year all 14 stations were sampled) and 2017. Changes in all metrics suggest that the biodiversity, function, and condition of streams in Fairfax County are improving, but some of these improvements are driven by increased diversity and percent composition of organisms that are tolerant of the urban environment.

Introduction

In 2018, 55 percent of the world's population lived in urban areas, and that figure is projected to increase to 68 percent by 2050 (United Nations, 2018). In the United States, the percent of the population living in urban areas increased from 64.2 percent in 1950 to 82.3 percent in 2018 and is projected to reach 89.2 percent by 2050 (United Nations, 2018). In particular, urban land is projected to nearly triple from 2009 to 2060 in the U.S. Environmental Protection Agency (EPA) level III Piedmont ecoregion (45) of the southeastern United States (Omernik, 1987; Terando and others, 2014), and is expected to negatively impact small urban streams (Van Metre and others, 2019). To accommodate these populations, infrastructure is developed that consequentially decreases the permeability of soils through soil compaction or construction of impervious surfaces such as pavement and rooftops. Many recent studies have focused on how the hydrologic cycle is altered in urban ecosystems in response to these land-use changes, and how these modifications affect water quality (O'Driscoll and others, 2010; Aulenbach and others, 2017; Bonneau and others, 2017; Hobbie and others, 2017). Studies have commonly concentrated on the relations between watershed development and direct surface runoff, groundwater recharge, and evapotranspiration dynamics, and have attempted to link watershed alterations to changes in water-chemistry, hydrology, biotic communities, and fluvial geomorphological processes.

Impervious surfaces reduce the volume of water that can infiltrate into soils, limiting groundwater recharge and increasing the volume of runoff to streams (Leopold, 1968). Engineered stormwater conveyances are designed to efficiently export water from impervious land surfaces to prevent local flooding, protect human safety, and prevent property damage, but until recent decades, had not been designed with the health of downstream ecosystems in mind. These older engineered systems shorten natural flow paths and amplify in-stream water velocity, resulting in increased runoff volume (Leopold and Dunne, 1978), reduced lag time between the onset of precipitation and peak flows (Hall, 1977), increased flood frequency (Hollis, 1975), and increased magnitude of peak storm discharges (Weiss, 1990). Soil moisture decreases as runoff volume increases, ultimately reducing low flows between storm events and affecting ecosystem health by altering stream temperature and biogeochemical processes (Bhaskar and others, 2016). Increased storm runoff can accelerate streambank erosion, channel incision, and habitat destruction; a phenomenon labeled as "urban stream syndrome" (Paul and Meyer, 2001; Meyer and others, 2005; Walsh and others, 2005). Channel incision, for example, reduces the horizontal and vertical hydrologic connectivity of streams, floodplains, and groundwater tables, consequently increasing the transport of nutrients, sediment, and other contaminants (Feminella and Walsh, 2005; Meyer and others, 2005; Lammers and Bledsoe, 2017). Increases in hydrograph flashiness and stream salinization related to anthropogenic activities have been linked to reduced biotic richness and a shift in community composition toward tolerant species (Paul and Meyer, 2001).

Nonpoint source (NPS) pollution is the leading cause of aquatic impairment in waterbodies throughout the United States, including critical waterbodies such as the Gulf of Mexico and Chesapeake Bay (Carpenter and others, 1998; U.S. Environmental Protection Agency, 2011). Nitrogen and phosphorus, common NPS pollutants, are essential to the health of aquatic communities, but excessive nitrogen and phosphorous loading can trigger algal blooms that reduce light availability and water clarity, as well as produce anoxic conditions (Carey and others, 2013). In 1987, Congress enacted Section 319 of the Clean Water Act, requiring states to develop and implement NPS pollution management programs (U.S. Environmental Protection Agency, 2011). This mandate led to the concept of best management practices (BMPs), which are measures designed to reduce or slow the transport of NPS pollution to receiving waterbodies (Muthukrishnan and others, 2004). Best management practices commonly are classified as structural or nonstructural. Structural BMPs are physical controls intended to reduce or slow the volume of storm runoff, remove pollutants, and promote groundwater infiltration and recharge. These BMPs include stream restoration, dry extended-detention ponds, wet ponds, stormwater wetlands, swales, porous pavement, bioretention beds, rain gardens, green roofs, and vegetated filter strips. Nonstructural BMPs are operational measures and educational programs which include community outreach programs and watershed planning aimed at reducing or disconnecting areas of impervious cover, concentrating or clustering new development, minimizing land disturbances, and restoring native vegetation.

Fairfax County, Virginia, has experienced rapid population growth since the 1940s (U.S. Census Bureau, 2012), which resulted in rapid urbanization, and, consequently, most streams within the county show signs of urban stream syndrome (Jastram, 2014; Fairfax County, 2017a). In the 1970s master drainage plans were initially developed that focused on flooding and erosion abatement; however, in the early 2000s this focus shifted away from structural repairs to water-quality improvements. In 2003, Fairfax County began developing and implementing updated watershed management plans that included plans for improvements over the following 25 years for all County watersheds (Fairfax County, 2017b). The principal goals of these watershed management plans were to (1) improve and maintain watershed functions, including water quality, habitat, and hydrology; (2) protect human health, safety, and property by reducing stormwater impacts; and (3) involve stakeholders in the protection, maintenance, and restoration of County watersheds (Fairfax County, 2017b). To date, Fairfax County's stormwater management program has made substantial investments (more than $100 million) into the implementation of both structural and nonstructural BMPs aimed at restoring and protecting watersheds (Fairfax County, 2017b).

In 2007, the U.S Geological Survey (USGS) partnered with Fairfax County to initiate a long-term water resources monitoring program to evaluate the watershed-scale effects of BMP implementation and land use change. Multiple years of monitoring are often required to begin assessing watershed-scale BMP effects because of delays between practice installation and water-quality response. Delays, or lag times, between BMP implementation and quantifiable improvements in water quality depend on the degree of impairment, the type of BMP implemented, and the appropriateness of that BMP to mitigate the type(s) of NPS present in the watershed (Meals and others, 2010). The degree of lag time depends on the NPS delivery pathway (overland flow, subsurface flow), the distance between the contaminant source to the stream, and the rate of travel from the source to the stream (for example, quick overland runoff versus a slow groundwater movement within a regional aquifer) (Chesapeake Bay Scientific and Technical Advisory Committee, 2005; Meals and others, 2010). As a result of these delays, a long-term approach to monitoring was required; this report synthesizes data collected over the first 10 years of monitoring. Although outside of the scope of this report, efforts are underway to link the water-quality patterns discussed herein to watershed-scale changes in land use and BMP implementations, as well as regional changes in climate.

Purpose and Scope

The purpose of this report is to summarize the spatial and temporal patterns in streamflow, water chemistry, and benthic macroinvertebrate communities across a 20-station monitoring network in Fairfax County, Virginia, during 2007–18. Although the monitoring network was designed to ultimately evaluate the watershed-scale effects of the substantial investments made by Fairfax County Virginia's stormwater management program, relating land use change and BMP implementations to monitored responses is not the focus of this report; however, efforts are currently underway to utilize the knowledge gained in this report to establish those links.

This monitoring network is cooperatively operated by USGS and Fairfax County Stormwater Planning Division (FCSWPD). Analyses varied by station based on data collection activities, but generally included assessments of

- streamflow variability using annual flashiness metrics, baseflow separations, and annual exceedance computations. Differences in these metrics were related to precipitation and land use;
- spatial, seasonal, and hydrologic water-chemistry variability in a suite of water-quality constituents including water temperature (WT), pH, specific conductance (SC), dissolved oxygen (DO), turbidity, nitrogen, phosphorous, and suspended sediment (SS);
- annual nutrient and sediment loads based on surrogate water-quality regression models;

- temporal trends in basic water-quality constituents (WT, pH, SC, DO, and turbidity) and in concentrations and loads of nitrogen, phosphorous, and SS; and
- temporal patterns in benthic macroinvertebrate community metrics.

Description of Study Area and Monitoring Network

Fairfax County is a 395-square mile (mi^2) predominantly suburban county in northern Virginia (fig. 1). The county is bordered by the Potomac River to the north and east, Bull Run and the Occoquan River to the south, and Loudon County to the northwest. Portions of the east boundary are shared with Arlington County, the City of Falls Church, and the City of Alexandria. The county surrounds the incorporated City of Fairfax City.

Fairfax County is the most populous jurisdiction in Virginia, with a population of just over 1.18 million in 2018 (fig. 2, Han and others, 2018). Approximately 75 percent of Fairfax County land use was composed of urban-land classifications in 2017 (Fairfax County, 2018). Most of this urban land is low- to medium-density residential housing, with commercial, industrial, transportation, and public utility lands representing smaller amounts. Land cover in low-density residential areas is composed mostly of turf grass and forest. Increased residential density and commercial intensity are associated with increased impervious cover. As of 2013, Fairfax County land cover was composed of approximately 24 percent impervious surfaces, 33 percent forest, and 32 percent turf grass. Total urban area increased countywide by about 15 percent between 1974 and 2012, primarily as a result of increased residential land use coincident with population increases (Falcone, 2015). County population and total housing units are expected to grow by about 20 and 25 percent, respectively, by 2040 (Han and others, 2018).

Geologic terranes are defined by the types of rock that underlie the area, whereas physiographic provinces are defined by landforms at the surface; however, landforms in Virginia are strongly influenced by subsurface geology, and therefore geologic terranes and physiographic provinces are commonly coincident. Fairfax County is underlain by three major geologic terranes: the Triassic Lowland, Piedmont, and Atlantic Coastal Plain (Froelich and Zenone, 1985a). These geologic terranes occur in association with the Mesozoic Basins physiographic subprovince, Outer Piedmont physiographic subprovince, and Coastal Plain physiographic province, respectively (Froelich and Zenone, 1985a). The geologic and physiographic differences between these regions strongly influence surface-water and groundwater flow patterns and water quality. The Mesozoic Lowlands subprovince collocated with the Triassic Lowland geologic terrane (hereafter referred to as “Triassic Lowlands,” EPA level III ecoregion 64), is in the western extent of the county and contains sedimentary bedrock and soils that are generally shallow and poorly drained. Most of the county is within the Outer Piedmont subprovince (hereafter referred to as “Piedmont,” EPA level III ecoregion 45), which contains highly weathered metamorphic crystalline bedrock that has been chemically weathered at the surface to form saprolite (Froelich and Zenone, 1985a). The thickness and permeability of this saprolite varies substantially from thin and nearly impervious to nearly 200 feet (ft) thick and well-drained, depending upon the parent material from which it was formed (Froelich and Zenone, 1985a). Low, rolling hills associated with the Outer Piedmont contrast the relatively flat topography present in other areas of the county. The eastern extent of the county is within the Coastal Plain (EPA level III ecoregion 65), which contains sedimentary deposits of sand and clay, capped by sheets of gravel with flat, low-velocity streams (Froelich and Langer, 1983; Froelich and Zenone, 1985a). There are more than 1,600 miles of streams in Fairfax County that drain portions of 18 hydrologic unit code (HUC)-12 watersheds that flow into the Potomac River. Most county stream miles are headwater, perennial streams with riffle-pool sequences. Although most streams drain suburban and urban land, some riparian areas are protected by Fairfax County Park Authority, which owns about 40 mi^2 of land throughout the county. Twenty watersheds that range in size from about 0.43 to 5.49 mi^2 and drain a representative gradient of Fairfax County land use and geologic settings have been included in this study (fig. 1; table 1).

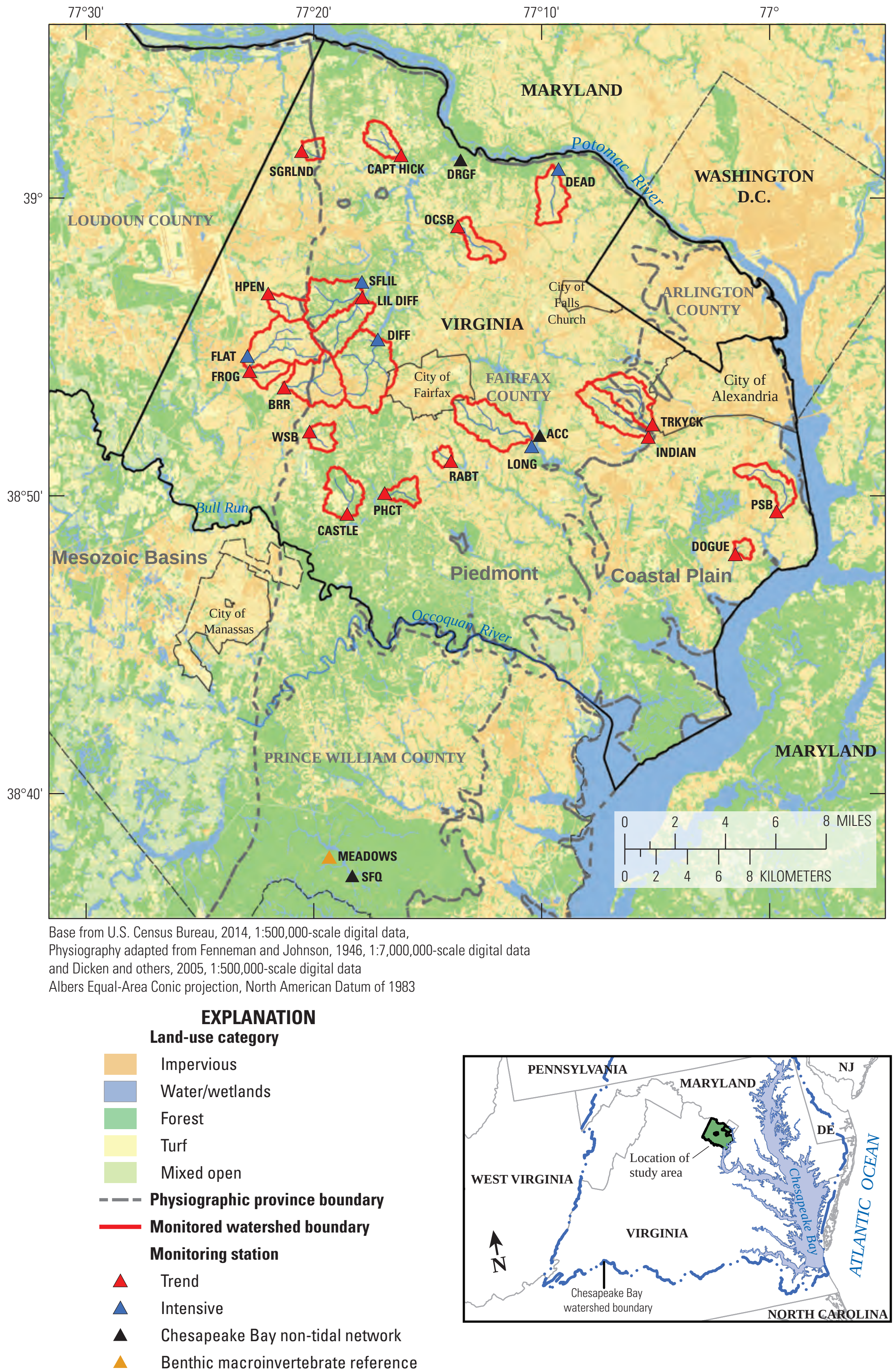

Figure 1. Monitoring stations and watersheds of Fairfax County, Virginia, used in this study. Station names are defined in table 1. Land-use categories from the Chesapeake Bay Program Office (2018).

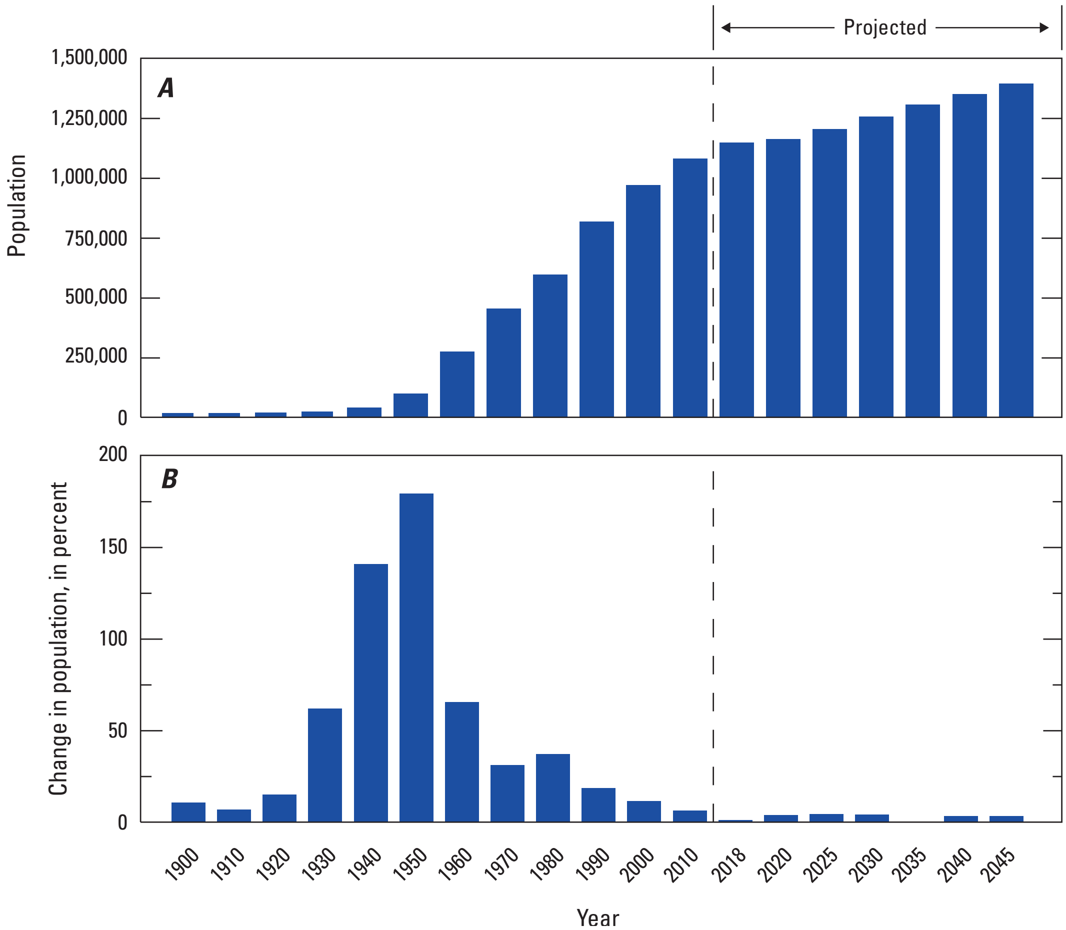

Figure 2. *A*, The population of Fairfax County, Virginia, from 1900 to 2010 derived from U.S Census Bureau (U.S. Census Bureau, 2012) and population estimates from 2018 to 2045 (Han and others, 2018). *B*, Percent change is presented as the difference between the population in a given year and that of the previous most recent year.

Methods of Investigation

This study was designed to better understand streamflow, water-chemistry, and biologic conditions in a network of Fairfax County streams and to document changes in those conditions over time as BMPs were implemented. The study design and data analyses were selected to characterize spatial conditions across a gradient of land uses and to characterize temporal patterns while accounting for seasonal and hydrologic effects. Annual metrics are based on water years (WY), which begin on October 1 and end on September 30; for example, WY 2017 began on October 1, 2016, and ended September 30, 2017.

Study Design

A long-term monitoring network was established using tiered monitoring intensity across a network of 20 monitoring stations. This network includes 5 intensive monitoring stations and 15 low-intensity monitoring stations; these 2 tiers were designed to specifically address different objectives of the overall effort. Data collection began at 14 monitoring stations in 2007 and at 6 additional stations in 2012–13. All watersheds are less than 6 mi^2 and were selected to represent land use, impervious coverage, physiographic province, and BMP conditions common to Fairfax County watersheds (fig. 3). Monthly water-chemistry samples, real-time water-level data, and annual benthic macroinvertebrate samples were collected at all monitoring stations. In addition, real-time water-quality and streamflow data, and high-flow water-chemistry samples were collected at five intensive monitoring stations (table 1). Collecting these additional data at all stations is cost prohibitive. The intensive monitoring stations are a representative subset of the studied watersheds and knowledge gained from their enhanced data collection activities will be applied in the nonintensive watersheds (hereafter referred to as "trend" stations).

Table 1. Monitoring stations and watershed information.

[mi², square mile; VA, Virginia; Rd, road; Br, bridge; Cr, creek; Tr, trail; Rn, run; –, no value]

Station identifier[1]	Station name	Short name	Station type	Watershed area (mi²)	Water year[2] established	Percent of watershed in Coastal Plain	Percent of watershed in Piedmont	Percent of watershed in Triassic Lowland
01646305	Dead Run at Whann Avenue near Mclean, VA	DEAD	Intensive	2.05	2008	–	100	–
01645704	Difficult Run above Fox Lake near Fairfax, VA	DIFF	Intensive	5.49	2008	–	100	0
01656903	Flatlick Branch above Frog Branch at Chantilly, VA	FLAT	Intensive	4.2	2008	–	1	99
01654500	Long Branch near Annandale, VA	LONG	Intensive	3.72	2013	–	100	–
01645762	South Fork Little Difficult Run above mouth near Vienna, VA	SFLIL	Intensive	2.71	2008	–	96	4
0165694286	Big Rocky Run at Stringfellow Rd near Chantilly, VA	BRR	Trend	3.4	2008	–	62	38
01645940	Captain Hickory Run at Route 681 near Great Falls, VA	CAPT HICK	Trend	1.38	2008	–	100	–
01657394	Castle Creek at Newman Road at Clifton, VA	CASTLE	Trend	2.21	2008	–	100	–
01653844	Douge Creek Tributary at Woodley Drive at Mount Vernon, VA	DOGUE	Trend	0.43	2013	100	–	–
0165690673	Frog Branch above Flatlick Branch at Chantilly, VA	FROG	Trend	0.99	2008	–	–	100
0164425950	Horsepen Rn above Horsepen Run Tributary near Herndon, VA	HPEN	Trend	1.19	2013	–	8	92
01652789	Indian Run at Bren Mar Drive at Alexandria, VA	INDIAN	Trend	2.45	2008	13	87	–
01645745	Little Difficult Run near Vienna, VA	LIL DIFF	Trend	2.99	2008	–	97	3
01645844	Old Courthouse Spring Branch near Vienna, VA	OCSB	Trend	1.45	2008	–	100	–
01657322	Popes Head Creek tributary near Fairfax Station, VA	PHCT	Trend	0.95	2008	–	100	–
01653717	Paul Spring Br above North Branch near Gum Springs, VA	PSB	Trend	1.89	2008	100	–	–
01655305	Rabbit Branch Tributary above Lake Royal near Burke, VA	RABT	Trend	0.57	2013	–	100	–
01644343	Sugarland Run Tributary below Crayton Road near Herndon, VA	SGRLND	Trend	0.64	2013	–	32	68
01652860	Turkeycock Run at Edsall Road at Alexandria, VA	TRKYCK	Trend	2.59	2008	57	43	–
01657100	Willow Springs Branch at Highway 29 near Centreville, VA	WSB	Trend	0.96	2013	–	100	–
01654000	Accotink Creek near Annandale, VA	ACC	Reference	23.8	1948	–	100	–
01646000	Difficult Run near Great Falls, VA	DRGF	Reference	57.8	1946	–	100	–
01658500	South Fork Quantico Creek near Independence Hill, Virginia	SFQ	Reference	7.62	2006	–	100	–
QCQB01	Unnamed Tributary of SF Quantico Cr near High Meadows Tr and Scenic Dr	MEADOWS	Reference	1.31	2008	–	100	–

[1]Station identifiers are U.S. Geological Survey station numbers with the exception of QCQB01 (MEADOWS), which is a Fairfax County Stormwater Planning Division identifier.

[2]A water year begins October 1 and ends September 30.

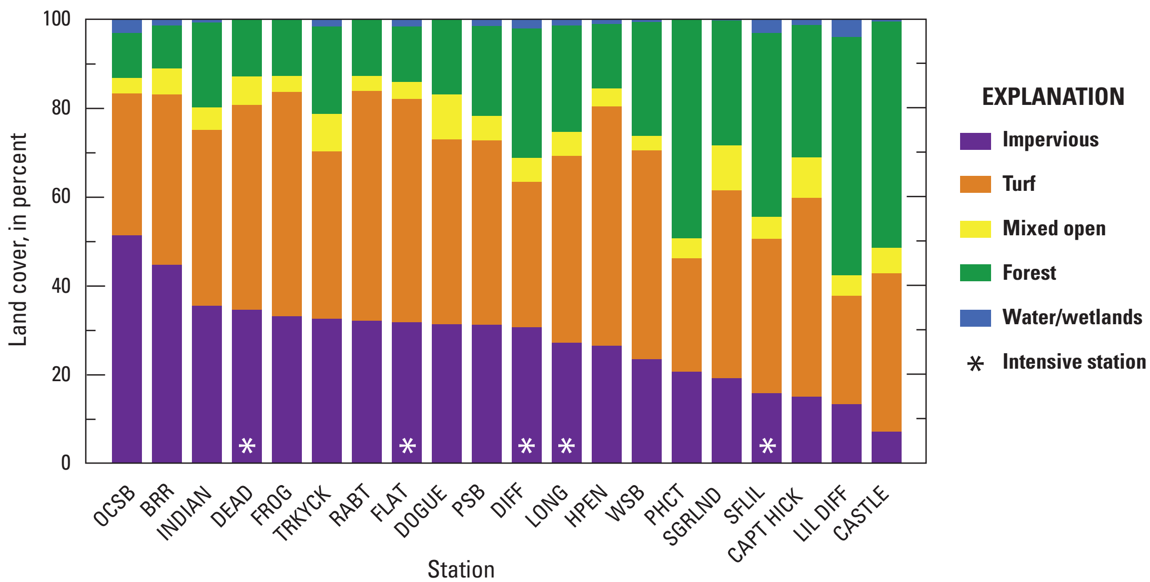

Figure 3. Percent of 5 land cover classifications in the 20 monitored watersheds, ordered by decreasing impervious land cover. Station names are defined in table 1. Land cover is based on the Chesapeake Conservancy, Chesapeake Bay Phase 6 High-Resolution Land Cover Dataset (Chesapeake Bay Program Office, 2018).

Data Collection, Sampling, and Laboratory Analysis

The five intensive monitoring stations were instrumented to collect 5-minute (min) measurements of streamflow and 15-min measurements of DO, pH, SC, turbidity, and WT (collectively referred to as continuous data), which were transmitted to the USGS National Water Information System database (NWIS; https://waterdata.usgs.gov/nwis) in near real-time (within 1 hour). Continuous nitrate data were collected at a single intensive location, SFLIL, since October 2016.

Standard USGS methods for continuously measuring and verifying stage, measuring streamflow, and computing continuous timeseries of streamflow using stage-discharge ratings (Rantz and others, 1982) were followed at the intensive monitoring stations. At the trend monitoring stations, non-vented internally logging pressure sensors, HOBO U-20 Water Level Data Loggers (Onset Computer Corp.), were used to continuously (15-min interval) measure water level. Periodic measurements of streamflow were paired with measurements of stage from the staff plate or by tape-down (measurement from a known reference point) to develop stage-discharge rating curves. These stations were not operated as traditional streamgages, so many of the elements required to support the computation of continuous streamflow were not present. Further, the stated 0.015-ft accuracy of HOBO loggers does not meet the established USGS technical specifications for stage sensors at streamgaging stations, set at 0.01 ft (Sauer, 2002). Nevertheless, the accuracy of these data do support the objectives of this component of the data-collection effort, to assign a measurement of streamflow to each water-quality sample and are consistent with other USGS studies with similar objectives (Gregory and Calhoun, 2007; Moring, 2006; Richards and others, 2006; Sprague and others, 2006; Cuffney and others, 2010).

The operation and maintenance of continuous water-quality monitors was conducted by USGS staff in accordance with published procedures (Wagner and others, 2006). Routine service visits were performed during which the instrument was cleaned and recalibrated when required based on published thresholds. Data collected during these visits were used to apply corrections to DO, pH, SC, turbidity, and WT timeseries records for periods of sensor fouling or calibration drift. A Satlantic SUNA in situ nitrate sensor was deployed at SFLIL prior to the start of WY 2017.

Monthly water-quality samples were collected at all stations and additional targeted stormflow samples were collected at the intensive monitoring stations in accordance with USGS methods (U.S. Geological Survey, variously dated). All samples were analyzed for a suite of nutrient and sediment constituents (table 2). Monthly nutrient and sediment samples were collected by USGS and FCSWPD staff using a grab (dip) sampling approach at the centroid of streamflow. These samples were collected on a fixed monthly interval during the first 5 years of the study with the intention of capturing random hydrologic variability. Analyses revealed that, as a result of the flashy nature of these streams, the monthly samples were capturing few high-flow conditions, so the monitoring design was modified to target wet conditions during 4 of the 12 monthly sampling events each year. All monitoring stations were sampled within the same day to limit variability in conditions across the stations for a given sample; additionally, the collecting agency and the order in which stations were visited was rotated each month. Each month, four stations were randomly selected for the collection of an additional quality assurance sample (replicate or blank). Along with the monthly samples, high-flow storm samples were collected at the intensive monitoring stations using an automated refrigerated sampler; these samples are referred to as storm samples throughout the report. The automated sampler was triggered to begin collection when station-specific water-level and turbidity thresholds were met. A subset of these collected storm samples that represent a broad range of hydrologic conditions were selected by USGS personnel and retrieved by FCSWPD staff for delivery to the laboratories for analyses.

Nutrient analyses were conducted by the Fairfax County Environmental Services Laboratory, as approved through the USGS Branch of Quality Systems Laboratory Evaluation Program. Samples were analyzed for total nitrogen (TN), total phosphorous (TP), and the dissolved and particulate fractions of nitrogen and phosphorous. Sediment analyses were conducted by the USGS Kentucky Sediment Laboratory in Louisville, Kentucky. All samples were analyzed for SS concentration (Guy, 1969; Shreve and Downs, 2005) and storm samples also were analyzed for sand-fine split—the percentage of material finer than 0.0625 millimeter (Guy, 1969; Shreve and Downs, 2005).

Annual benthic macroinvertebrate sampling was conducted each spring (late March or April) at all stations by FCSWPD staff with occasional assistance from USGS staff, in conjunction with the annual sampling performed for the Fairfax County Biological Stream Monitoring Program (Fairfax County, 2017a). Benthic macroinvertebrate samples were collected, stream habitat metrics recorded, and basic water-quality parameters were measured according to standard operating procedures (Fairfax County, 2019). Aquatic benthic macroinvertebrate samples were collected along a 100-meter (m) reach using the EPA’s Rapid Bioassessment Protocol multihabitat, 20-jab methodology (Barbour and others, 1999). Samples were subsorted to 200±40 individuals as in Barbour and others (1999), or until the entire sample was sorted. Taxa were identified to genus when possible, except for annelid worms (class Oligochaeta) and nonbiting midges (family Chironomidae), to evaluate community richness and composition. Benthic macroinvertebrate data are available online (Porter and others, 2020).

Statistical Analysis of Streamflow, Water-Chemistry, and Benthic Macroinvertebrate Data

Nonparametric analyses were used to describe statistical relations in water-chemistry and streamflow data following methods in Helsel and Hirsch (2002). Spatial variability in streamflow characteristics were evaluated with baseflow-separation models, stormflow to precipitation ratios, stream-flashiness metrics, and peak-streamflow exceedance

Table 2. Nutrient and sediment constituents as well as analysis methods used by the Fairfax County Environmental Services Laboratory and the U.S. Geological Survey (USGS) Kentucky Sediment Laboratory.

[USEPA, U.S. Environmental Protection Agency (U.S. Environmental Protection Agency, 2018); SM, Standard Methods (American Public Health Association, 1976); ASTM, American Society for Testing and Materials (American Society for Testing and Materials, 2007)]

Constituent	Abbreviation	Method	USGS parameter code
Nitrogen			
Total nitrogen	TN	USEPA 351.2 + USEPA 353.2	00600
Total dissolved nitrogen	TDN	USEPA 351.2 + USEPA 353.2	00602
Total particulate nitrogen	TPN	USEPA 351.2 + USEPA 353.2	00601
Total Kjeldahl nitrogen	TKN	USEPA 351.2	00625
Total dissolved Kjeldahl nitrogen	DTKN	USEPA 351.2	00623
Nitrate + nitrite	NO_3^-	USEPA 351.2	00631
Ammonia	NH3	USEPA 350.1	00608
Phosphorus			
Total phosphorus	TP	SM425C & 425E	00665
Total dissolved phosphorus	TDP	SM425C & 425E	00666
Total particulate phosphorus	TPP	SM425C & 425E	00667
Orthophosphate	OP	USEPA 365.2	00671
Sediment			
Suspended sediment concentration	SSC	ASTM D3977-97	80154
Suspended sediment, percent smaller than 0.0625 millimeter[1]	Percent fine	ASTM D3977-97	70331

[1]Only analyzed in stormflow samples.

probabilities. Spatial and seasonal patterns in water-chemistry data were evaluated using a nonparametric Kruskal-Wallace test and subsequent Steel-Dwass post-hoc test for multiple comparisons (Critchlow and Flinger, 1991). The Steel-Dwass test is preferable over the more common Wilcoxon method because it controls for the overall experiment-wide error rate, thus reducing the probability of Type-1 errors (rejection of a true null hypothesis; Critchlow and Flinger, 1991). Where applicable, data were subset by warm (March-September) and cool (October-February) seasons. Unless otherwise specified, the term "significant" is used throughout the text to denote a statistically significant difference based on a p-value less than or equal to 0.05.

Water quality is affected by numerous watershed processes that can be measured by streamflow and water chemistry. Computation of constituent loads requires input of both streamflow and concentration terms; therefore, annual loads were used to integrate the effects of streamflow and water chemistry on nitrogen, phosphorous, and SS transport in the five intensively monitored streams. Trends in streamflow, water chemistry, and benthic macroinvertebrate metrics were evaluated to assess change over time using a variety of methods (described below) that remove variability associated with seasonality and streamflow.

Baseflow Separation Models

Separation of the stormflow and baseflow components from total streamflow—termed baseflow separation—is useful for assessing the effects of urbanization and stormwater management actions on the hydrologic regime and can provide additional insight to the interpretation of water-quality and ecological-condition assessments. The terms "stormflow" and "baseflow" have been defined many ways (Dingman, 2002; Wittenberg, 2003; Peters and van Lanen, 2005; Blume and others, 2007); herein, the term baseflow represents groundwater discharged to surface waters (Hall, 1968), whereas stormflow represents the combination of direct surface runoff and interflow, the water that infiltrates the soil surface and travels through the unsaturated zone by means of gravity toward a stream channel. As such, stormflow represents new water that can be associated with a specific event, and baseflow represents old water that cannot be associated with a specific event.

A chemical mixing model was used for baseflow separation. The model assumes the two flow components (stormflow and baseflow) have a different chemical composition owing to differences in flow paths. Ion concentration, represented by proxy with SC, was used to approximate the ratio of stormflow to baseflow at any given time step (Hem, 1985). In minimally disturbed streams, SC correlates positively with time of contact with rocks and soils; therefore, streamflows become ionically enriched during periods of baseflow, and diluted by precipitation during higher flows. Specific conductance was an ideal surrogate owing to the availability of high frequency measurements (15-min interval) at each of the intensive monitoring stations; however, anthropogenic activities such as road deicing salt applications in winter months can complicate calculations. To account for typical seasonal variability in SC, the storm flow end member (SF_c) was computed as the monthly minimum SC and the baseflow end member (BF_c) was computed as the monthly 75th percentile of SC. During winter months, when the acute effects of road deicing salts were detected in continuous records of SC, the program HYSEP (Sloto and Crouse, 1996), using the USGS Groundwater Toolbox version 1.3.1 (Barlow and others, 2017), was used to supplement the mixing model in order to avoid overestimation of the baseflow component. The empirical HYSEP model, which operates on low-pass filter principles, used mean daily streamflow values to determine low points on the streamflow hydrograph and interpolate between those points using a fixed-interval method. The area under the curve of the resulting hydrograph was summed to compute the baseflow component of total streamflow. The chemical mixing model method is preferable over other available methods because it is the only approach to hydrograph separation that contains a physical basis, as end-member concentrations are related to physical and chemical processes in the watershed (Matsubayashi and others, 1993; Miller and others, 2014; Raffensperger and others, 2017). Baseflow was computed using the mass balance approach originally proposed by Steele (1969) and Pinder and Jones (1969), and later applied to SC by Yu and Schwartz (1999) and Stewart and others (2007), which relies on the principle of dilution. The form of the model is

$$Q_{BF} = Q_i[(SC_i - SF_c) \;/\; (BF_c - SF_c)] \tag{1}$$

where

Q_{BF} is the predicted baseflow component of total streamflow at time i,

Q_i is the streamflow at time i,

SC_i is the measured SC at time i,

SF_c is the SC end member of runoff, and

BF_c is the SC end member of baseflow.

If $[(SC_i - SF_c) / (BF_c - SF_c)] > 1$, then the result is adjusted to 1.

For the five intensive monitoring stations, baseflow separations were calculated on unit-values (15-min interval) when using the chemical mixing model and mean daily streamflow values were used in the HYSEP model and retroactively applied to unit values to match the chemical mixing model. Baseflow statistics generated by the HYSEP model were used to supplement those from the chemical mixing model for approximately 4–8 percent of unit values at each station over the 10 years of monitoring. Additionally, baseflow separations were calculated at two additional USGS monitoring stations within Fairfax County: Accotink Creek near Annandale, Virginia (ACC, 23.8 mi^2, USGS station identifier 01654000), which is the receiving body for LONG, and Difficult Run near Great Falls, Virginia (DRGF, 57.8 mi^2, USGS station identifier 01646000), which is located along the main stem of Difficult Run, and incorporates streamflow from both SFLIL and DIFF. For these two long-term monitoring locations, the

HYSEP model was used for the entire record because SC data were not available for much of the historical record. Unit-value estimations of baseflow and stormflow components were aggregated by water year for each station and used to calculate total annual stormflow and baseflow volumes. Subsequent analyses of these components such as annual baseflow (BFI) and stormflow (SFI) indices represent the proportion of total annual streamflow that was generated by either baseflows or stormflows.

Runoff Ratio

A ratio of stormflow to precipitation, hereafter termed "runoff ratio," was calculated to evaluate watershed responses to rainfall. A runoff ratio provides a holistic examination of watershed processes as it is a function of the interactions of precipitation, evapotranspiration, land use/land cover, watershed slope, and soil properties (Ratzlaff, 1994). Runoff ratio is a commonly reported statistic; however, the use of this terminology and the methods used to derive it are inconsistent throughout hydrologic literature. A runoff ratio may be calculated by including either total streamflow or separated stormflow (Ratzlaff, 1994; Bell and others, 2016), and either total precipitation or throughfall—precipitation that penetrates through tree canopy and reaches the soil surface (Brown and others, 1999; Blume and others, 2007). Runoff ratios computed using only stormflow are highly affected by the hydrograph separation method used (Blume and others, 2007); thus, care must be taken before comparing the results of different studies.

In this study, the runoff ratio was computed by first separating out the stormflow proportion of total streamflow in each unit value using the methods described above. Both county- and watershed-specific daily precipitation data were obtained from the Parameter-elevation Regressions on Independent Slopes Model (PRISM) for WYs 2008 through 2017 (Daly and others, 2002) to compute precipitation volumes. Watershed-specific daily precipitation data and unit-value stormflow volumes were converted to yields by dividing by watershed area and then aggregated by WY. Annual stormflow and precipitation yields were used in the following equation

$$C_r = SF_y / P_y , \qquad (2)$$

where

C_r is the runoff ratio,

SF_y is the area-normalized annual (WY) stormflow volume, and

P_y is the area-normalized annual (WY) precipitation volume.

Annual (WY) runoff ratios were calculated at the five intensive monitoring stations for 2008–17 (DEAD, DIFF, FLAT, and SFLIL) and 2013–17 (LONG). Additionally, runoff ratios were calculated for each water year from 1949 to 2017 and 1946 to 2017 at the two long-term monitoring stations ACC and DRGF, respectively.

Streamflow-Precipitation Relations

Precipitation is a primary driver of streamflow yield. Examination of the relation between streamflow and precipitation can elucidate patterns in the way a complex set of interdependent factors (in other words, land use, soil properties, BMPs, geology) influence hydrology across the monitored watersheds. For each monitoring station, streamflow and precipitation data were aggregated by month and separated into two periods (2008–12 and 2013–17) that represent the first and most recent 5 years of monitoring. Monthly streamflow yields were compared to monthly precipitation totals to explore these relations. Further, an analysis of covariance (ANCOVA) was used to explore differences in the slopes of those relations both between stations and across periods.

Streamflow duration curves show the distribution of streamflows over a given time period, contain the entire range of observed hydrologic conditions, and indicate how often a given streamflow occurs. The shape of the duration curve can be affected by factors such as climate, geology, topographic relief, land cover, and soil properties, and given that the curve is computed on streamflow yield, comparisons can be made across stations. The hydrologic characteristics of a watershed can be inferred based on the slope of the curve; a steep slope indicates rapid runoff of stormwater, high-peak flows, and a flashy storm hydrograph, whereas a flat slope indicates longer transit time of overland flows, storage of surface and groundwater, and shorter peak, longer duration events (Searcy, 1959). Duration curves were computed for each of the five intensive monitoring stations using mean hourly streamflow data divided by watershed area to produce a mean hourly yield. Mean hourly values were ranked based on the magnitude of streamflow, and probability scores were computed based on the distribution of ranks for each station using JMP 14 software (SAS Institute). For n nonmissing scores, the probability score of each value was computed as the averaged rank of that valued divided by n + 1, similar to a cumulative distribution function.

Streamflow Flashiness

Flashiness, or the rate of change in streamflow, is a commonly used metric to quantify a watershed's response to precipitation (Baker and others, 2004). This metric is generally computed using timeseries records of mean daily streamflow, although McMahon and others (2003) demonstrated that the use of stage (or water level) data provides a comparable measure of flashiness. At the five intensive monitoring stations where continuous records of streamflow were available, the Richards-Baker Flashiness Index (RBI) was applied to mean hourly streamflow data following the methods published in Baker and others (2004)) to estimate RBI for each WY.

The RBI measures oscillations in streamflow relative to total streamflow. This index is dimensionless and is positively correlated with the flashiness of a basin. The index is calculated as

$$\frac{\sum_{i=1}^{n}\left|q_i - q_{i-1}\right|}{\sum_{i=1}^{n}\left|q_i\right|}, \tag{3}$$

where

q is the streamflow at time i.

Stage-based stream flashiness was defined for all 20 stations in the monitoring network for WYs 2008–17 as the number of occurrences in which the hourly stage increase was 0.5 ft or greater (PERIOD5; McMahon and others, 2003). The PERIOD5 value was then divided by the total number of measurements in the analysis period to express flashiness as the percent of time that PERIOD5 occurred, and in doing so normalized data records of varying length. The percent change in flashiness between WY 2008–12 and WY 2013–17 was calculated for all 20 monitoring locations.

Peak Streamflow Exceedance Probabilities

Peak-flow annual exceedance probabilities (AEP) provide insight into how frequent a storm of a given magnitude is likely to occur. Annual exceedance probability estimates can be made for stream gages with a minimum of 10 years of streamflow data (Maidment, 1993). AEPs were developed for each of the four intensive monitoring stations with the requisite record length (DIFF, FLAT, SFLIL, and DEAD) using the USGS program PeakFQ version 7.2 (Flynn and others, 2006; Veilleux and others, 2013). AEP's ranging from 0.002 to 0.995 were computed using annual peak flow data from each monitoring station, following the procedures outlined in England and others (2018). Annual peak flows were fitted using a log-Pearson Type III distribution and the Expected Moments Algorithm (Cohn and others, 1997) and a multiple Grubbs-Beck Test (Cohn and others, 2013). There is large uncertainty in the at-site sample skewness coefficient in short length records owing to sensitivity to extreme events (Griffis and others, 2004); therefore, England and others (2018) recommend the application of a skew coefficient that is a weighted average of the mean square errors of the station skew and regional skew. Weighted regional skew values were not yet available in Virginia; therefore, station skews were used in the computation of AEPs for each of these watersheds and may be affected by the biases mentioned above.

Handling of Censored Water-Chemistry Data

Nutrient concentrations were below laboratory instrumentation detection limits in some dissolved total Kjeldahl nitrogen (DTKN), total particulate nitrogen (TPN), total dissolved phosphorous (TDP), orthophosphate (OP), and total particulate phosphorous (TPP) results. Results below the method detection limit (MDL), known as left-censored data, indicate that a concentration is somewhere between zero and the MDL, but the actual concentration is unknown. Statistical analyses that delete censored values or substitute a constant value such as one-half of the reporting limit may produce biased results and introduce patterns not present in the original dataset (Helsel, 2005) To properly handle censored data, nonparametric methods were used that do not rely on calculating a mean or standard deviation from an assumed distribution, but instead perform statistical analysis on the ranks of data.

Results below the MDL are stored in the USGS National Water Information System (NWIS) database at a reporting limit that is higher than the MDL. This handling of censored results can produce an upward bias in the data (Helsel, 2005) and was resolved by recoding censored results to the MDL. Analysis of monthly and storm sample data was performed by using the Nondetects and Data Analysis for Environmental Data (NADA) package for R Studio version 1.1.456 (R Core Team, 2018). A trend analysis that can handle multiple censoring limits (described later in this section) also was performed on these recoded data. Load computations were performed on the censored data as originally reported in NWIS because software (rloadest) was used that contains an algorithm to properly fit these data and eliminate bias in the estimation of model coefficients.

Turbidity Hysteresis and Cross-Correlation Analysis

The relation of peak turbidity and peak streamflow can help inform the source of SS during stormflows. These relations typically are evaluated graphically through examination of the timing and shape of turbidity—streamflow hysteresis loops. When turbidity, and by inference SS concentration, is greater on the rising limb than on the falling limb of a storm hydrograph at a given unit of streamflow, the hysteresis pattern is referred to as a clockwise loop (Landers and Sturm, 2013; Bussi and others, 2017). A clockwise loop typically indicates SS derived from the resuspension of previously deposited sediments, eroding streambanks or streambeds, or highly connected upland sources in close proximity to the stream (Williams, 1989; Gellis, 2013). Conversely, a counterclockwise hysteresis loop occurs when turbidity at a given unit of streamflow is greater on the falling limb of a hydrograph, which suggests either an upland source relatively far from the in-stream measurement point or erosion of upper streambank slopes following peak streamflow (Williams, 1989; Landers and Sturm, 2013).

Although hysteresis loops can be informative, they are event-specific and can be difficult to interpret in highly flashy streams where few data points are often collected during the rising limb of the hydrograph. Cross-correlation analyses were used to quantify the turbidity-streamflow relation for selected storm events at each of the intensive monitoring stations and were interpreted in the context of hysteresis loops. Storm events that met the station-specific turbidity and streamflow criteria used to trigger the autosampler were considered for cross- correlation analysis. The cross-correlation function (Schwientek and others, 2013) calculates multiple correlations between timeseries of streamflow and turbidity data where one variable is adjusted forward and backward by hourly increments while the other is held constant. The maximum correlation coefficient of these iterations is identified and represents the time offset at which streamflow and turbidity peaks are aligned. The function was calculated using the R stats package (v. 3.5.1) in version 0.4.5 of R Studio (R Core Team, 2018).

Nutrient and Suspended-Sediment Concentration and Load Models

Suspended-sediment and nutrient concentration and load timeseries were computed at the five intensive stations with surrogate regression models that include continuous (15-min interval) water-chemistry and streamflow data as explanatory variables. Annual loads were converted to yields, or the load per unit area, to remove the effect of watershed size and allow for comparisons between stations. Methods and rationale for estimating nutrient and suspended-sediment concentrations and loads using this surrogate regression approach have been well documented (Nash and Sutcliffe, 1970; Jastram and others, 2009; Rasmussen and others, 2009; Jastram, 2014; Schilling and others, 2017; Robertson and others, 2018), so only a summary of pertinent details is presented here.

Continuous records of streamflow data were available at 15-min intervals; however, concentration data were only available from discretely collected samples that provide a snapshot in time of constituent concentration. To compute a load at each instantaneous time step (15-min interval), constituent concentration had to be estimated for all time steps when samples were unavailable. To this aim, water-chemistry parameters that can be continuously measured were used as surrogates for the estimation of concentration.

Station-specific regression models were developed for TN, total dissolved nitrogen (TDN), nitrate + nitrite (hereafter termed nitrate or NO_3^-), TPN, TP, TDP, TPP, and SS concentrations using JMP 14 software (SAS Institute). Models were calibrated using discrete concentration data collected from both monthly and storm samples as the response variable: explanatory variables included water-quantity and -quality parameters such as streamflow, turbidity, SC, WT, and pH; temporal variables such as trend and season (dTime); and a binary indicator variable (BASE) for hydrologic condition (baseflow or stormflow). The trend variable does not indicate a trend over time in annual load, but rather a trend in the relation of other explanatory variables in the model to the constituent being predicted. The binary variable was included when the slope of the surrogate-concentration relation was consistent across hydrologic condition, but the y-intercept differed. In select cases, the slope of this relation also differed across hydrologic condition; therefore, an interaction term (natural logarithm of turbidity times the binary hydrologic condition variable) was included. For SFLIL, continuous NO_3^- data obtained from the Satlantic SUNA in situ nitrate sensor deployed prior to the start of WY 2017 was used to recalibrate TN and TDN models and recompute WY 2017 loads; additionally, the NO_3^- load was directly computed.

Models were selected to maximize explanatory power while minimizing systemic errors (bias) and random errors (variance) using a suite of criteria detailed in Helsel and Hirsch (2002) including (1) prediction error sum of squares (Allen, 1974), (2) Nash-Sutcliffe index (Nash and Sutcliffe, 1970), (3) partial-load ratio (Stenback and others, 2011), (4) Mallows' C_p (Mallows, 1973), (5) variance inflation factor, (5) autocorrelation, and (6) analysis of model residuals. Instantaneous constituent loads were computed from the selected models using rloadest—an R implementation of the LOAD ESTimator (LOADEST) FORTRAN program (Runkel and others, 2004)—in version 0.4.5 of R Studio (R Core Team, 2018; Lorenz and others, 2015). Instantaneous load timeseries were then aggregated to an annual (WY) time step.

The adjusted maximum likelihood estimator (AMLE) algorithm was used to properly fit models for constituents with censored observations. The AMLE method also corrects for retransformation bias introduced as a result of the nonlinear relation of predicted concentrations in natural logarithm transformed and original units (Cohn and others, 1992). The standard error of prediction (SEP) also was calculated for each load and used to compute 95-percent confidence intervals around each load estimate.

Annual (WY) nutrient and suspended-sediment yields were compared with similar information available for headwater urban streams in the Piedmont in Gwinnett County, Georgia (Aulenbach and others, 2017), and for nontidal streams throughout the Chesapeake Bay watershed (CB-NTN; Moyer and Blomquist, 2018), which vary in drainage area and land use. Computation methods and watershed characteristics differ between these studies, but published yields from long-term intensively monitored urban watersheds are uncommon, so this comparison provides relevant context for the conditions in Fairfax County streams.

Water-Chemistry and Streamflow Trends

A combination of methods was used to calculate monotonic trends in a suite of water-chemistry constituents and streamflow between April 1, 2008, and March 31, 2018, at the 14 monitoring stations that have been sampled for 10 years. Trends were computed for dissolved, particulate, and total fractionations of nitrogen and phosphorous, SS concentration, basic water-quality parameters (WT, SC, pH, DO, and turbidity), and streamflow. Trends were not reported from datasets with more than 50 percent of values below the MDL (in other words, ammonia and TPN). When possible, water-chemistry trends were adjusted for streamflow to remove streamflow-induced variability. Referred to as flow normalization (FN), these results are used to document water-quality trends more closely associated with watershed changes than with hydrologic variability.

Trend quantification methods varied based on data collection activities and included the following approaches:

1. Trend computation was performed for all chemical constituents across the 14 stations using a Seasonal Kendall test. These computations were performed using monthly discrete samples (n=120) with a streamflow value assigned to each sample. Computations were run in R version 3.4.3 (R Core Team, 2018) using the restrend version 0.4.2 package (Lorenz, 2017). Trends in concentration are reported for nitrogen, phosphorous, and SS and in common units of measurement for the basic water-quality parameters. The nonparametric Seasonal Kendall test accounts for seasonality by running the Mann-Kendall test on each month separately and then combining the results (Hirsch and others, 1982). This method is appropriate for monthly water-quality time-series data, can account for varying censoring limits, allows for streamflow normalization, and has been used to compute water-quality trends in other previous water-quality investigations (Langland and others, 2000; Johnson and others, 2009; Sullivan and others, 2009). The Seasonal Kendall test was performed on the residuals of a streamflow-constituent nonparametric regression to calculate a FN result. A censored local regression method was used to obtain the residuals from a streamflow-constituent relation (Loader, 2013) when a dataset contained greater than 10 percent censored values. The fit and residuals of each nonparametric regression were examined to ensure an accurate streamflow relation estimation. Significance trend results were assessed at a serial correlation adjusted p-value of ≤0.10.

2. The consistency of trend patterns reported in approach (1) were evaluated across the 14-station network using the Regional Seasonal Kendall test (Helsel and Frans, 2006). This test expands on the Seasonal Kendall test described in approach (1) by totaling the Mann-Kendall test scores for each station-season combination across a region, which in this report is defined as the 14-station monitoring network. The Regional Seasonal Kendall test was performed using the restrend version 0.4.2 package (Lorenz, 2017). Significance trend results were assessed at a serial and spatial correlation adjusted p-value of ≤0.1. Results from the Regional Seasonal Kendall test are referred to as combined trend results herein.

3. Computation of nitrogen, phosphorous, and SS concentration and load trends at the four intensive monitoring locations using the Weighted Regressions on Time, Discharge, and Season (WRTDS; Hirsch and others, 2010). This method uses mean daily streamflow and discrete samples collected from a range of hydrologic conditions to estimate trends and FN trends. Continuous streamflow, monthly samples, and high-flow discrete storm samples collected at the four intensive monitoring stations met these data requirements. The WRTDS approach was not applied to the 10 trend-monitoring stations because they lack discrete storm samples and continuous streamflow data necessary for the analysis. Mean daily streamflow may provide a suboptimal estimation of the hydrologic conditions in small, urban watersheds with flashy stormflow responses (Hirsch and others, 2010); however, there are no alternative methods to quantify trends in FN load.

4. Trends in mean daily streamflow, WT, pH, SC, DO, and turbidity were computed using continuous data collected at the four intensive monitoring stations between March 2008 and April 2018 (Hirsch, 2019). A trend result is computed for the 1st through 365th order statistic of mean daily values for each parameter. The first order statistic translates to a trend in the minimum mean daily value that occurred each year and the 365th order statistic refers to a trend in the maximum mean daily values. Trends are reported in percent/year based on the Thiel-Sen slope estimator computed from a Mann-Kendall test (Helsel and Hirsch, 2002). Significant trend results were interpreted from a serial correlation adjusted p-value (adjusted for serial correlation) of ≤0.1.

5. Trends in SC also were computed using a generalized additive model (GAM) run on the continuously collected data at the four intensive stations. There are an increasing number of continuously collected water-quality datasets that reach the minimum temporal scale (10 years) for trend analysis; consequently, it has been a long-standing goal to develop a method for the analysis of trends using these high-frequency data given that these datasets violate many of the assumptions of traditional methods (Yang and Moyer, 2020). The GAM is a semi-parametric regression modelling approach, composed of a sum of smooth functions of covariates, subject to smoothing penalties. This model structure allows a flexible specification for potentially important covariates. With its automatic smoothing parameter selection, GAM can determine the shape of the fitted trend objectively. The SC GAM employed here includes streamflow, seasonal, and time components. The GAM approach provides several benefits over traditional methods because it utilizes a richer dataset that may be more representative of actual conditions than the snapshots in time provided by discretely collected measurements, computes a nonlinear trend, and extracts the effects of seasonal patterns and changing streamflows.

Trend results for 10 years (April 2008–March 2018) were compared with long-term results computed from two additional USGS monitoring stations within Fairfax County, ACC and DRGF. Trends in WT, DO, pH, and SC were computed at these locations between 1985 and 2016 using the previously described Seasonal Kendall method described in item (1). Trends in streamflow were computed for 1948–2017 and 1946–2017 at ACC and DRGF, respectively, using method

(3). Trends in TN and NO_3^- were computed between 1985 and 2016 at both locations as part of the USGS nontidal monitoring network using the WRTDS approach described in item (2); the data are available online (Moyer and others, 2017).

Temporal Benthic Macroinvertebrate Analyses

Benthic macroinvertebrates, hereafter referred to as benthics, are widely used as indictors of water quality because these organisms are residents of the aquatic ecosystem, relatively ubiquitous, and have varied responses to stream degradation (Rosenberg and Resh, 1993; Resh and others, 1996; Barbour and others, 1999). Temporal trends in benthics at both the networkwide (132 samples) and station (n = maximum 10 samples per station) scale were computed for 20 metrics that are responsive to monitoring biological conditions in Fairfax County urban streams (O'Driscoll and others, 2010). The selected metrics include 19 richness (number of unique taxa) and percent composition (relative abundance calculated as the number of target taxa in a standardized sample with 100 total individuals) measures, as well as the Fairfax County Index of Biological Integrity (IBI), a multimetric index score (table 3; Fairfax County, 2019). The Fairfax IBI is a combination of several individual metrics based on tolerance, community composition, habitat type, and functional feeding group (FFG) (Fairfax County, 2019). The Fairfax IBI is calibrated to the Piedmont and should not be applied to Coastal Plain streams owing to the intrinsic variability in benthic assemblages across these regions. An index developed specifically for Coastal Plain streams (Maxted and others, 2000) was used to calculate IBI scores for the two stations (PSB and TKYCK) in this region. Both IBIs use the same scale (0–100), which reflects the relative stream condition compared to the best attainable condition. Six of the richness and percent composition metrics are based on taxonomy within FFGs, such as scraper richness and percent predator, whereas the remaining metrics are based on taxonomic classification alone, such as total taxa richness, dominance, and percent Odonata. The Ephemeroptera (mayflies), Plecoptera (stoneflies), and Trichoptera (caddisflies) (EPT) metric is commonly used because it includes many sensitive organisms and is thus a strong indication of good stream health (Rosenberg and Resh, 1993). The Coleoptera (beetles), Odonata (dragonflies and damselflies), Trichoptera (caddisflies), and Ephemeroptera (mayflies) (COTE) metric, which contains more tolerant species than EPT, was used because not all urban streams can support Plecopterans and may thus provide a more appropriate evaluation of stream health in an urban environment (Smith and others, 2017).

Mixed-effects models were used to evaluate networkwide trends and traditional regression models were used to evaluate station-specific trends. Each mixed-effects model produces a linear equation of change over time and fits the general form

$$y_{ij} = \beta_0 + \beta_1 \times x_{ij} + \varepsilon_{ij} \tag{4}$$

where

β_0 is the y-intercept,
β_1 is the slope for the year term,
y_{ij} is a metric value at station i, in year j,
x_{ij} is the year the sample was collected at a station i, in year j, and
ε_{ij} is the error term and is partitioned into three components, based on the equation

Table 3. Description of metrics and type of analyses used to explore trends in benthic macroinvertebrates.

Metric	Abbreviation	Type[1,2]
Fairfax County Index of Biological Integrity	IBI	Score (0–100)
Total taxa richness	Total	Richness
Dominance	Dominance	Composition
Ephemeroptera, Plecoptera, and Trichoptera	EPT	Richness, composition
Coleoptera, Odonata, Trichoptera, and Ephemeroptera	COTE	Richness, composition
Chimarra spp., *Cheumatopsyche* spp., and *Hydropsyche* spp.	CCH	Richness, composition
Chironomidae and oligochaetes	ChiroOligo	Composition
Gastropoda	Gastropoda	Richness, composition
Odonata	Odonata	Richness, composition
Filter feeder	Filterer	Richness, composition
Predator	Predator	Richness, composition
Scraper	Scraper	Richness, composition

[1]Richness metrics are presented as the number of unique taxa.

[2]Composition metrics are the percent of target taxa in the sample.

$$\varepsilon_{ij} = b_{0,i} + b_{1,i} + n_{ij} \tag{5}$$

where

$b_{0,I}$ represents the estimates of the variability among stations,

$b_{1,I}$ represents the variability in trends over time among stations, and

η_{ij} represents the unaccounted variability.

These models are similar to ANCOVA, in that there are repeated measures within groups, but the models account for sources of variability among groups, analogous to block designs in analysis of variance, rather than estimating differences in trends between groups. The type of model used was metric-specific and the significance of trend results was assessed at a p-value of ≤0.05. Richness and composition metrics were evaluated with either mixed-effects or traditional Poisson regression models with a log-link function. The response variables for richness and composition metrics were the number of unique target taxa and total number of target taxa in each sample. For composition metrics, an offset equal to the log of the total number of individuals in the sample was added to the model to produce estimates of percent composition. Mixed-effects and traditional linear regression models were used to evaluate the Fairfax IBI metric, for which the IBI score served as the response variable. Mixed-effect models were evaluated with restricted maximum likelihood using the lme4 and lmerTest packages in R (Bates and others, 2015; Kutznetsova and others, 2017; R Core Team, 2018). Models were run on a reference station (MEADOWS, 1.31 mi^2, FCSWPD station identifier QCQB01) located along an unnamed tributary of South Fork Quantico Creek between High Meadows Trail and Scenic Drive. The MEADOWS station is located within a relatively undeveloped watershed (0.5 percent impervious cover), which provides a useful comparison to the Fairfax County stations located in considerably more developed watersheds (7–51 percent impervious cover) and may provide some insight into the relative effects of station-specific urban stressors versus regional drivers of change in benthic macroinvertebrate metrics.

Data Availability

All continuous-stage and streamflow data (5-min interval) and basic water-quality parameters (15-min interval) collected at the 5 intensively monitored stations, continuous-stage data (15-min interval) collected at the 15 trend stations, and discrete laboratory-analyzed water samples from the full 20 station network are publicly available in the NWIS database (U.S. Geological Survey, 2018). Those data, or results of subsequent analyses, that could not be stored in NWIS are available as a data release (Porter and others, 2020). Specifically, the data release includes all benthic macroinvertebrate data and model results, computed unit values for stage-based and RBI flashiness indices, annual streamflow metrics (streamflow volume, baseflow separations, runoff ratios, peak streamflow, and so forth), annual nutrient and suspended-sediment loads, load model calibration and estimation files, and water-quality trends. The appendixes contain a summary of some of the analyses presented in the data release such as results from hypotheses tests, annual exceedance probabilities, general additive models, and load an concentration models as well as figures presenting results from monthly sampling at the 20 monitoring stations for water temperature and several subspecies of nitrogen and phosphorus.

Hydrologic Conditions

Stormwater management practices seek to improve water quality by reducing peak flows, lowering stream flashiness, and increasing riparian connectivity; therefore, analyses of hydrologic conditions are necessary to measure the effectiveness of these actions. Streamflow metrics were analyzed in association with precipitation to investigate the spatial and temporal patterns that occurred throughout the monitoring network. Analyses explore the relation of stream hydrology to the duration, intensity, and recurrence of precipitation events, degree of impervious cover, and the soil and geological properties of each monitored watershed.

Precipitation

Countywide annual rainfall totals fluctuated around the monitoring period mean (fig. 4), with the lowest annual precipitation in WY 2012 and above mean precipitation in WYs 2008, 2010, 2011, and 2014. In three of the wettest years, WYs 2008, 2011, and 2014, much of the total annual precipitation accumulated as a result of high-intensity events. In WY 2008, 7.06 inches (in.) of rain fell on the county during Hurricane Hanna; Tropical Storm Lee produced a single day total of 5.49 in. in WY 2011; and three separate storms each generated over 3.5 in. of daily rainfall in WY 2014. Conversely, the annual precipitation total in WY 2010 was elevated owing to the aggregation of many moderately intense storms (0.5–1.0 in.) but lacked extreme events. Monthly precipitation totals revealed a seasonal pattern of wetter conditions in late spring (May and June) and early fall (September and October), and drier conditions that began in late fall and extended through the winter months.

High precipitation periods have pronounced effects on hydrologic and water-quality conditions with the potential for altering stream geometry and moving substantial loads of nutrients and sediment. Likewise, sustained periods of low precipitation reduce baseflow as the groundwater table recedes, which can subsequently reduce the physical extent of aquatic habitat (Bond and others, 2008; Rolls and others, 2012), concentrate nutrient and pollutant concentrations (Menció and Mas-Pla, 2010), reduce hydrologic connectivity between stream segments (Boulton, 2003), increase

WT (Dahm and others, 2003), and reduce DO—all of which can degrade aquatic community health (Sabater and Barceló, 2010).

Streamflow

Annual streamflow yield—the volume of streamflow generated per unit area—was calculated for each of the five intensive monitoring stations to inform hydrologic comparisons between watersheds of varying size (fig. 5A). Median annual streamflow yields were highest at FLAT and DIFF, 49.81 and 48.09 million cubic feet per square mile (ft^3/mi^2), respectively. DEAD, LONG, and SFLIL had considerably lower median annual streamflow yields of 34.10, 32.95, and 31.87 ft^3/mi^2, respectively.

Streamflow yields increased with annual precipitation at all stations, but the amount of precipitation exported as stormflow varied between stations as indicated by runoff ratio (fig. 5B). The proportion of annual streamflow exported as stormflow exceeded the proportion exported as baseflow, as indicated by SFI values greater than 0.5, during most years at most stations, apart from SFLIL (fig. 5C). Stormflow indices and runoff ratios were positively related to annual precipitation at all stations except LONG; however, at this station the validity of the runoff ratio and SFI may be compromised by backwater produced at the confluence of LONG and ACC. The 10-year mean runoff ratios were noticeably higher at DIFF (0.25) and FLAT (0.23) than the other three stations, which contributes to the higher annual streamflow yields observed in these watersheds. The elevated runoff ratio and streamflow yield at FLAT may be partly attributable to the relatively low groundwater storage capacity of soils in the Triassic Lowlands (Froelich and Zenone, 1985a). At DIFF, a relatively

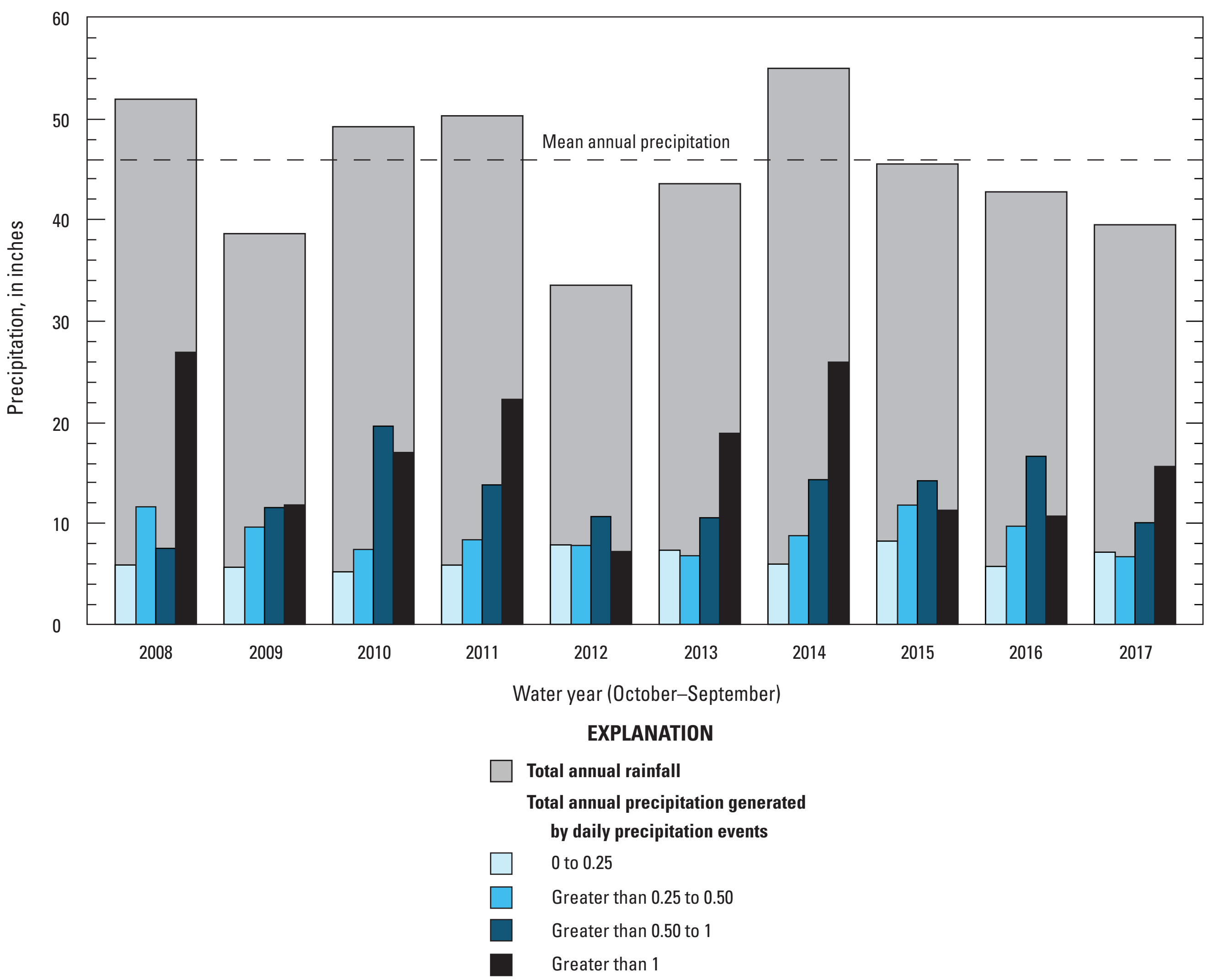

Figure 4. Annual precipitation data (gray bars) from Parameter-elevation Regressions on Independent Slopes Model (PRISM) for water years 2008 through 2017. A water year begins October 1 and ends September 30.

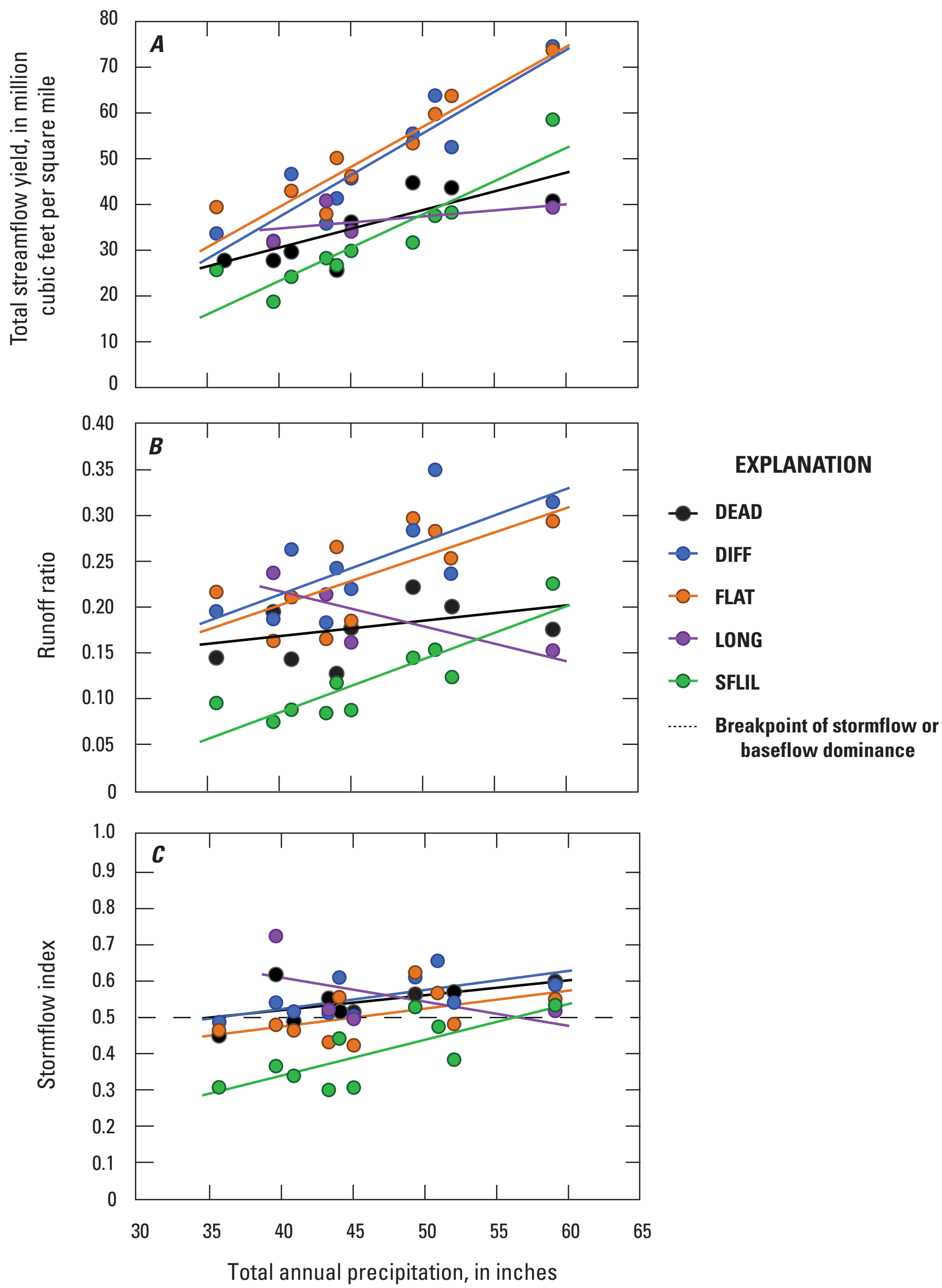

Figure 5. Annual water year (WY) streamflow yields (*A*), runoff ratio (*B*), and stormflow index (*C*) at each of the five intensive monitoring stations compared to total annual (WY) precipitation with fit lines. Annual metrics are presented as points with line of best fit. The dashed line in *C* indicates the breakpoint of stormflow or baseflow dominance. A water year begins October 1 and ends September 30. Station names are defined in table 1.

thin clay-rich saprolite that slows infiltration and generates more runoff than more permeable soils (Froelich and Zenone, 1985a) may contribute to similar conditions. Although total watershed impervious coverage was similar in DIFF and DEAD (31 and 35 percent, respectively) and both watersheds are in the Piedmont, streamflow yields and runoff ratios were lower at DEAD (fig. 5). This difference may be attributed to the geology underlying DEAD, which has a thicker, well-drained saprolite that sits atop well-drained schists (Obermeier and Langer, 1986) compared to clay-rich saprolite in DIFF. The SFLIL watershed, which has similar soil characteristics to DIFF, typically has the lowest streamflow yield and SFI because it contains the least amount of impervious land cover of the intensive sites (16 percent).

Monthly streamflow yields were compared to monthly precipitation totals to evaluate watershed responses to precipitation and explore changes in these relations in two sequential 5-year periods (fig. 6). Overall, the five intensively monitored watersheds generated similar streamflow yields in months receiving 2 in. of precipitation or less. Regardless of the period (WYs 2008–12 and 2013–17), FLAT and DIFF yielded more streamflow than the other three watersheds when monthly rainfall totals exceeded 2 in. Further, ANCOVA revealed that the slope of the relation between streamflow and precipitation decreased significantly at FLAT and DIFF between the periods WY 2008–12 and WY 2013–17; no significant change was observed for SFLIL or DEAD between these time periods (appendix 1; table 1.1, 1.2). Monthly precipitation totals were similar between 2008–12 and 2013–17 based on a monthly comparison of all pairs using a Steele-Dwass test, so these results indicate that DIFF and FLAT exported less streamflow during wet months in the second 5-year period than the first. Evidence of this pattern is also present in the lower streamflow yields and runoff ratios observed in the most recent 3 years at DIFF and FLAT. The decreases in these metrics may be related to BMP implementations or other changes in land use; however, the relation between these metrics and landscape change and BMP implementation were beyond the scope of this report.

Streamflow yields have been shown to increase with increasing impervious land cover (Beighley and Moglen, 2002; Pappas and others, 2008; Rasmussen and Gatotho, 2013; Aulenbach and others, 2017). Impervious surfaces cover about 30 percent of DIFF, DEAD, LONG, and FLAT and about 15 percent of SFLIL. These differences likely explain why SFLIL had a lower SFI and runoff ratio compared to the other stations. Streamflow yields at these urban stations were five times higher than South Fork Quantico Creek (SFQ, 7.62 mi^2 USGS station identifier 01658500), a primarily undeveloped watershed in neighboring Prince William County. Runoff ratios observed at DEAD, FLAT, DIFF, and LONG were comparable to those in a similar study of urban watersheds in the Baltimore, Maryland metropolitan area, which ranged from 0.17 to 0.34 (Brun and Band, 2000; Groffman and others, 2004). Meanwhile, the mean runoff ratio at SFLIL (0.11) was more comparable to the SFQ watershed (0.13).

Stream Flashiness and Stormflow Event Duration

A visual examination of storm hydrographs between monitoring stations can provide useful insights into the variability of watershed-specific hydrologic response to precipitation-runoff events. These comparisons can elucidate differences in peak streamflow, flashiness, and event duration; factors that play important roles in overall stream health. A hydrographic comparison at the five intensive monitoring stations and the SFQ reference station during a storm event that delivered approximately 1 in. of precipitation across Fairfax County and Prince William County on January 10, 2016, is shown in figure 7. During this event, DEAD had the highest peak but one of the shortest event durations. FLAT and DIFF had lower peaks than DEAD and LONG, even though the watersheds have similar levels of impervious cover. The storm response curves for these urban watersheds in Fairfax County fit the classic example of the hydrologic regime in a highly urbanized watershed where impervious land cover produces rapid runoff and limits groundwater infiltration. The hydrologic response at SFQ provides a contrast to DEAD. The rising and falling limb in SFQ were more gradual and the peak was substantially lower, reflective of greater infiltration owing to limited land development.

Duration curves of streamflow yield were used to provide a quantitative summary of streamflow characteristics in each of the intensively monitored watersheds (fig. 8) and expand upon the qualitative assessments in figure 7. Peak streamflow yields (0–0.01 nonexceedance) as well as the highest 25 percent of streamflow yields (0–0.25 nonexceedance), which represent stormflow conditions, were highest at FLAT and DIFF. Further, FLAT, DIFF, and SFLIL had higher baseflows, 0.25–0.75 nonexceedance, than DEAD and LONG. Additionally, the lowest streamflows, 0.75–0.999 nonexceedance, which typically occur during periods of extended drought, were much lower at LONG than the other stations. These patterns demonstrate variability in high, moderate, and low streamflow characteristics across the monitored watersheds, as well as metrics that measure response to precipitation such as runoff ratio and flashiness. For example, elevated stormflow yields at DIFF and FLAT are likely related to geologic factors that reduce infiltration (clay-rich saprolite and shallow soils, respectively). Elevated baseflows in these two watersheds may be the result of watershed area, which allows for greater storages and longer residence times of groundwater, as well as geologic factors that promote connectivity to the stream network. Likewise, the longer recession curves pictured in figure 7 are likely attributable to greater time of transit owing to the larger area of those two watersheds. Meanwhile elevated baseflows in SFLIL may also be attributable to geologic factors; however, the relatively low impervious land cover in this watershed may also be a key driver. Lower baseflows at DEAD and LONG are likely related to greater rates of storm runoff (flashiness) and poor connectivity to shallow groundwater storages.

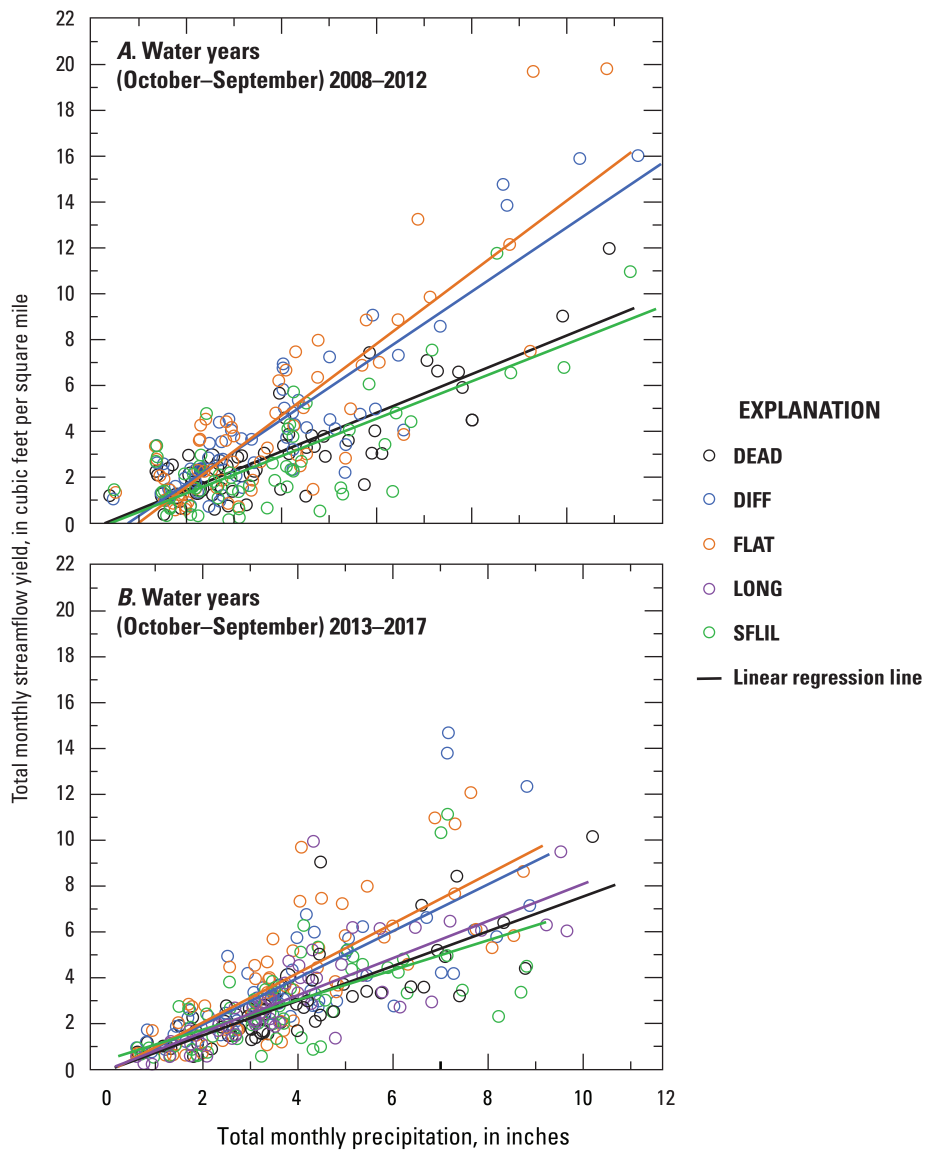

Figure 6. Monthly streamflow yield compared to monthly precipitation at each of the five intensively monitored watersheds between water years (WYs) 2008 through 2012 (*A*) and WYs 2013 through 2017 (*B*). A water year begins October 1 and ends September 30. Station names are defined in table 1.

The RBI was computed using all streamflow timeseries data from each intensive monitoring station collected during the period of study. DEAD was the flashiest watershed, indicated by the highest RBI score (0.417) and SFLIL the lowest within the network (0.169), and the reference station SFQ was the lowest overall (0.107). For the 20 trend stations, stage-based PERIOD5 ranged from 0.10 percent of the time at CASTLE to 0.66 percent of the time at DEAD and was positively correlated with impervious land cover (Pearson's r = 0.72, p=0.0003; fig. 9). On average, a 10-percent increase in watershed imperviousness resulted in a 20-percent (0.1 percentage points) increase in stage-based PERIOD5. Stage-based PERIOD5 at DEAD was greater than would be expected based only on impervious coverage and highlights that other watershed properties such as depth to bedrock, soil porosity, and effective impervious cover (areas directly connected to urban drainage systems) may contribute to these storm responses. Both RBI scores and stage-based PERIOD5 indices were stable in most watersheds throughout the study period. DEAD had the greatest reduction in stage-based PERIOD5; however, RBI scores indicate that stream flashiness was unchanged at this station. The number of times water-level rises by 0.5 ft (PERIOD5) is affected by changes in stream geometry, which is constantly evolving at all stations as a

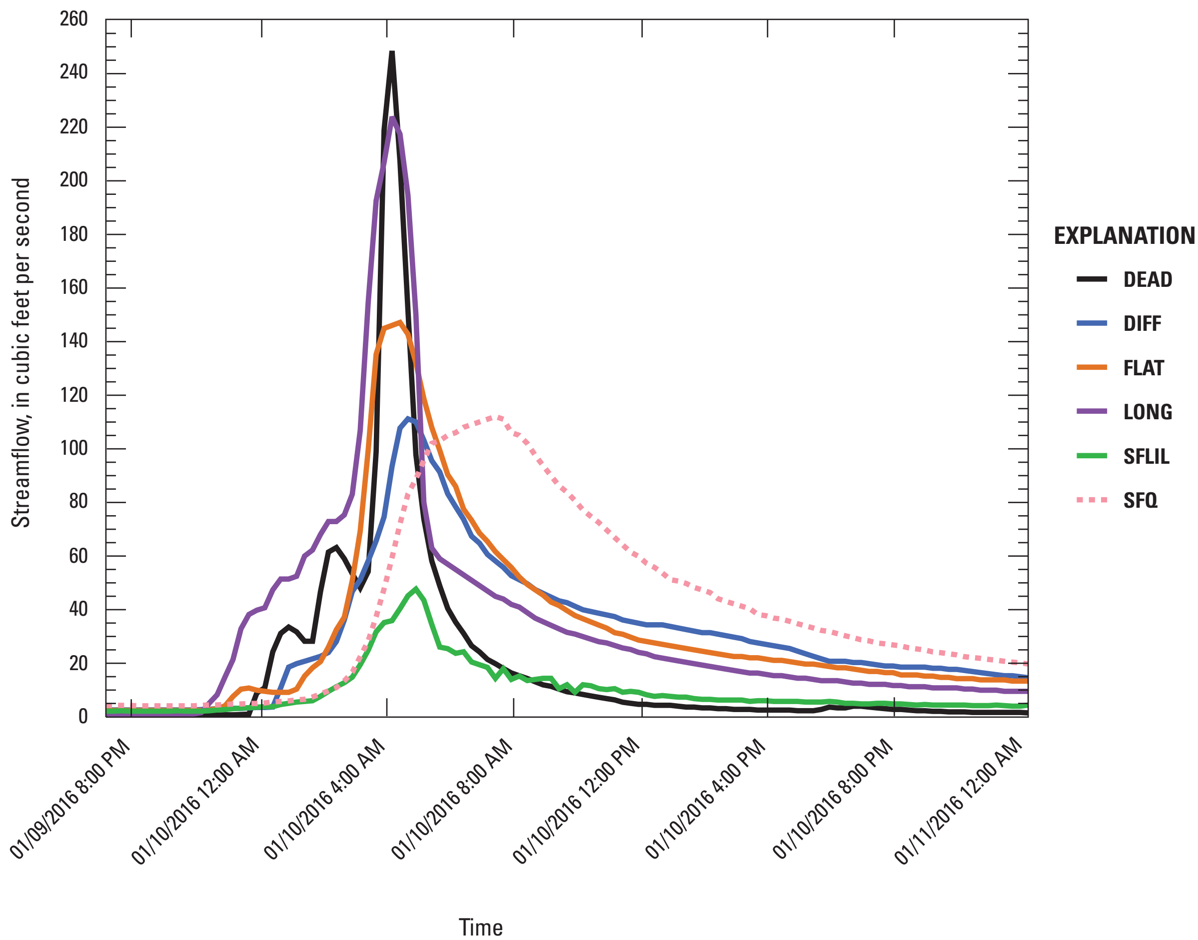

Figure 7. Hydrographs from the five intensively monitored watersheds and reference station (SFQ) during a 1-inch precipitation event that occurred on January 10, 2016. Station names are defined in table 1.

result of bank erosion, channel scour, or channel aggradation. The reductions in PERIOD5 at DEAD may therefore be affected by a widening and deepening of the channel.

Trends and Temporal Patterns in Streamflow

Multidecadal trends in baseflow indices and runoff ratios were evaluated at two stations where sufficiently long records were available, DRGF and ACC (fig. 10A, B). Increasing runoff ratios are most likely the product of increased impervious land cover and stormwater infrastructure, landscape changes that both reduce groundwater recharge and increase surface runoff (Klein, 1979; Rose and Peters, 2001; Hardison and others, 2009). These patterns are reflective of long-term shifts in the water budgets of these watersheds—much of the water that prior to development would have been intercepted by riparian buffers, lost to evapotranspiration, or stored in the soil column or aquifers, is now channeled directly to the stream. Notably, during the 10 years of the study period, a slower rate of change in these metrics was evident, and in some instances, the direction of these patterns reversed—increasing baseflows and decreasing runoff.

Statistically significant increases of about 1 percent per year were observed in the top 10-percent of mean daily flows at DRGF and ACC between 1946 and 2017 and 1948 and 2017, respectively (fig. 11A; red points on upper righthand side). Decreases occurred in the lower half of mean daily flows at both stations, but with greater significance and magnitude at ACC (fig. 11A; bottom left). Total impervious land cover in the ACC watershed increased from 3 percent in 1949 to 33 percent in 1994 and coincident to this period streamflow increased by 48 percent for periods with moderate rain and by 75 percent during periods of extreme rain (Jennings and Taylor Jarnagin, 2002), consistent with previously described relations between urbanization and hydrology. Mean daily streamflow trends between 2008 and 2018 at these stations were almost entirely nonsignificant but generally decreased by around 5 percent above the 10th percentile of mean daily flows. Below these values, conditions were relatively unchanged at DRGF and increased by as much as 5 percent at ACC (fig. 11B).

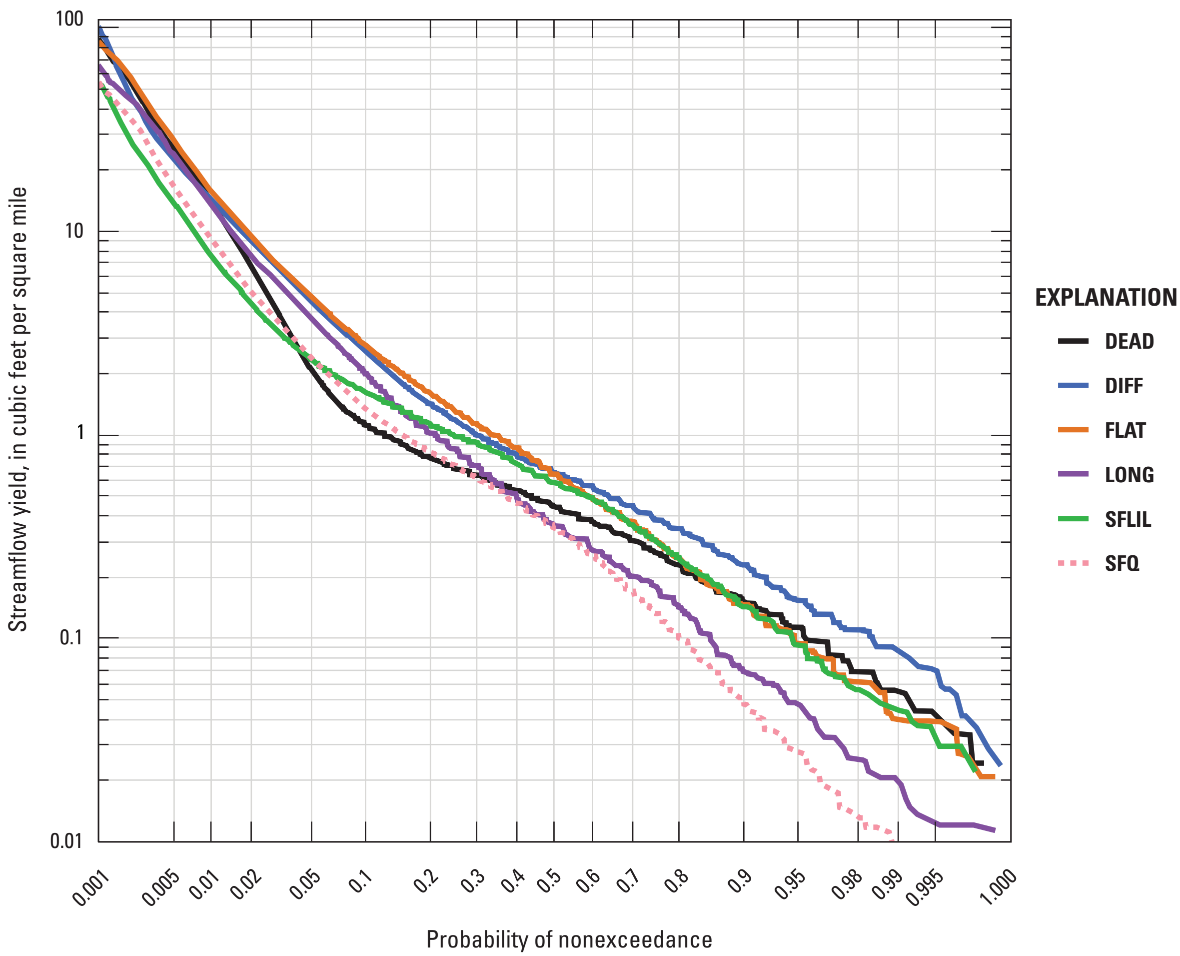

Figure 8. Flow-duration curve of instantaneous streamflow yield for 2008–17 water years at DIFF, FLAT, DEAD, and SFLIL, and for 2013–17 water years at LONG. A water year begins October 1 and ends September 30. Station names are defined in table 1.

There were few significant trends in mean daily streamflow between 2008 and 2018 at DEAD, FLAT, and DIFF, and no significant trends at SFLIL; however, the general patterns were similar to those observed over the same period at DRGF and ACC (fig. 12). No trends were observed for most quantiles at most stations; however, the typical pattern among stations indicated a decline in mean daily streamflow values between the 10th and 90th percentiles by as much as 10 percent. The top 10 percentiles of mean daily streamflow also declined at all stations except DEAD. The bottom 10 percentiles of mean daily streamflow were relatively unchanged at SFLIL and DIFF but increased at DEAD and FLAT. Patterns of decreasing high flows and increasing low flows may result from stormwater management practices designed to intercept direct runoff and promote groundwater infiltration, climate and precipitation patterns, or a combination of these and other factors (Hopkins and others, 2020).

Streamflow Annual Exceedance Probability

At all four monitoring stations the peak of record had an AEP of 0.09, or an 11-year storm (fig. 13; table 1.3). At DEAD, the peak occurred in August 2010 resulting from a localized high-intensity convective system, at FLAT and SFLIL the peak occurred in October 2011 during Tropical Storm Lee, and at DIFF in 2008 during Tropical Storm Hanna. At DRGF and ACC, the largest storm observed during the 10-year period occurred during Tropical Storm Lee in 2011. When multidecadal data were used to compute the recurrence intervals for these events at DRGF and ACC, the storms represented 42- and 72-year recurrences, respectively. When this analysis was conducted for DRGF and ACC using data only from the concomitant 10-year study period, both WY 2011 AEPs were 0.09 (11-year storm reoccurrence). The differences in computed AEPs highlights the skew and uncertainty in estimations at the four intensive monitoring stations as a result of record length and indicates that return intervals for these storms may be higher than the values reported above.

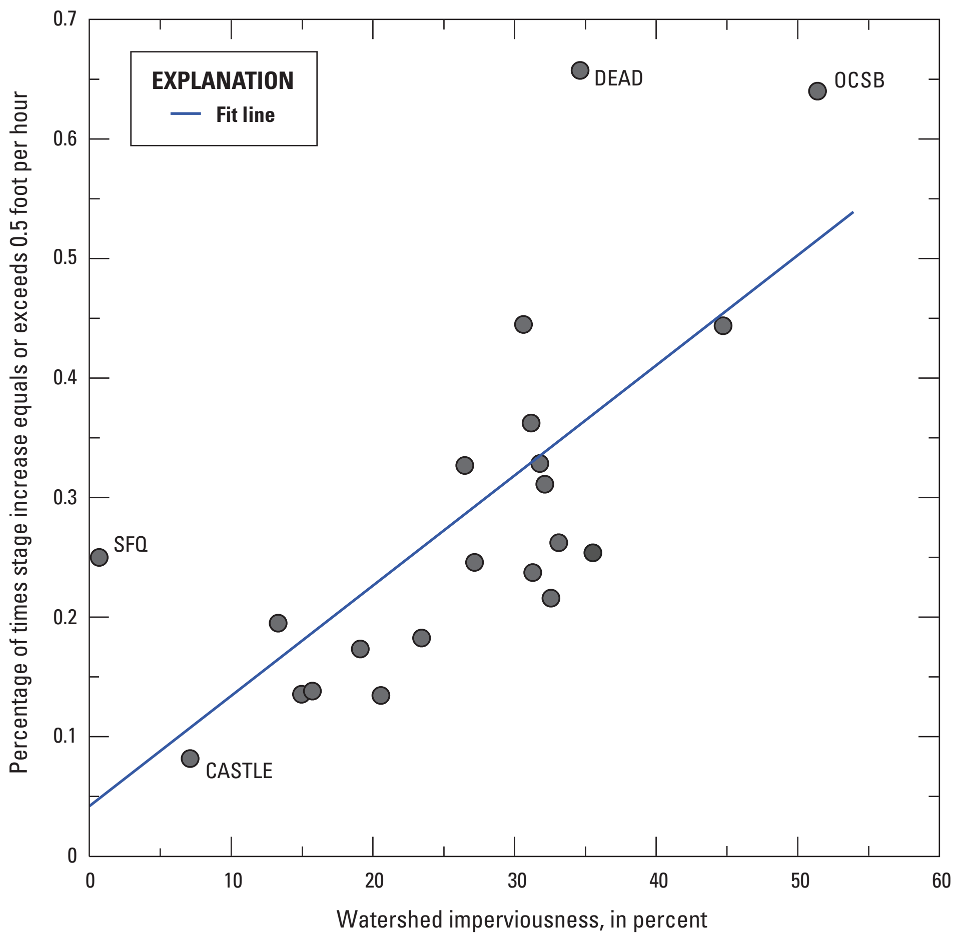

Figure 9. Flashiness, computed as the percentage of times stage increases by 0.5 feet per hour or greater, of 20 monitored streams in Fairfax County compared to the percentage of watershed area covered by impervious surfaces. Station names are defined in table 1.

Water-Chemistry Conditions

Spatial differences in a suite of water-chemistry constituents were explored to assess the aquatic condition of Fairfax County streams and to identify how water-chemistry differences may be related to land use, geology, and other watershed properties. Relations between water-chemistry, streamflow, and time of year are analyzed to develop an understanding of the primary delivery pathways and the environmental fate of various constituents. These analyses will support future work aimed at developing an understanding between watershed management and water-chemistry responses. This report includes the analysis of all data collected through March 2018. The collection of monthly samples began in April 2008 at the initial 14 monitoring stations (a total of 120 samples), and October 2013 at 6 add-on stations (a total of 66 samples) (table 1). A total of 1,882 storm samples were collected at the 5 intensive monitoring stations.

Constituent loads were computed for eight constituents at each of the five intensively monitored watersheds to provide a holistic evaluation of the complex and often integrated watershed processes that affect both water quantity and quality (Barber and others, 2006). For DIFF, FLAT, and SFLIL, loads and yields were computed for WYs 2008 through 2017; for DEAD, loads and yields were computed for WYs 2009 through 2017; and for LONG, loads and yields were computed for WYs 2014 through 2017 (Porter and others, 2020).

Water-chemistry trends were assessed at 14 stations with 10 years of monitoring data to describe how conditions have changed over time (Porter and others, 2020). Monotonic trends were analyzed between April 2008 and March 2018 in WT, DO, pH, SC, turbidity, nitrogen, phosphorous, and SS, and for certain constituents, FN trends were computed to document water-quality trends more closely associated with watershed changes than interannual hydrologic variability.

Water Temperature and Dissolved Oxygen

Water temperature is a fundamental water-quality parameter given its role in regulating chemical and biological reactions and governing the structure of aquatic communities (Mulholland and others, 2001; Hillebrand and others, 2010;

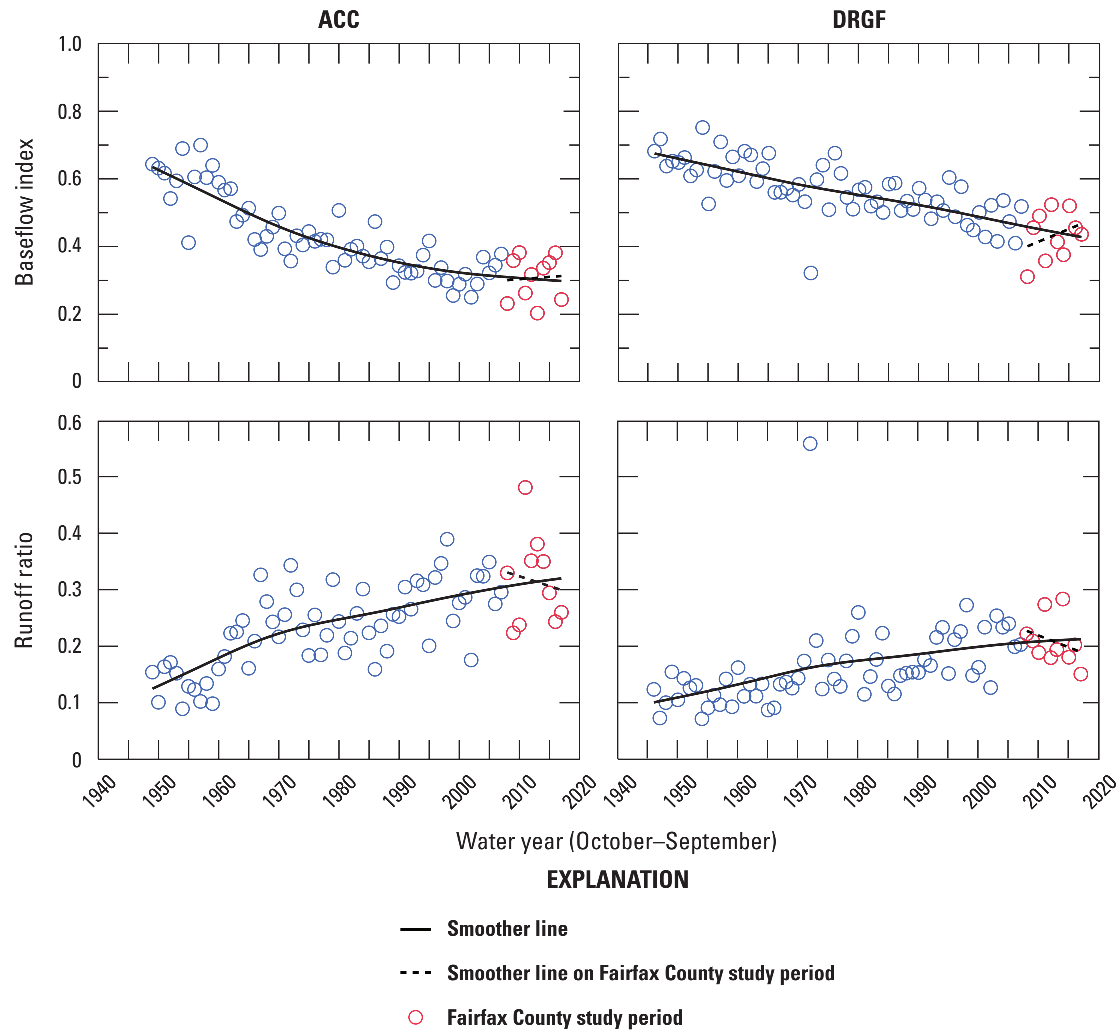

Figure 10. Annual baseflow index (*A*) and annual runoff ratio (*B*) at Accotink Creek near Annandale, Virginia (ACC) and Difficult Run near Great Falls, Virginia (DRGF), between water years 1949–2017 and 1946–2017, respectively, with a line of best fit. Water years 2007–17 (red dots) represent the period of study in Fairfax County. A water year begins October 1 and ends September 30.

Demars and others, 2011). A positive correlation between watershed imperviousness and stream temperature is commonly observed (Galli, 1991; O'Driscoll and others, 2010) as a result of reduced baseflows, increased runoff, and as a result of the low albedo of roads, sidewalks, and buildings, which gain and hold more heat, and consequently increase the temperature of overland runoff. Additionally, increased runoff has been shown to result in short-term temperature oscillations and spikes (Nelson and Palmer, 2007). Collectively, these effects can stress temperature-sensitive aquatic species.

Although DO varies by watershed owing to chemical and biological oxygen demands and processes such as photosynthesis and aeration that add oxygen, the solubility of oxygen is inversely related to WT, and as a result stream DO concentrations have both daily and seasonal cycles. The concentration of DO in streams is an indicator of the balance between processes that produce and consume oxygen (Hem, 1985), and the resultant net concentration is critical to the survival of aquatic organisms that require oxygen for respiration; therefore, DO is widely used as an indicator of stream health and in Virginia the minimum criterion for healthy streams is 4.0 milligrams per liter (mg/L; Commonwealth of Virginia, 1997a).

Hydrologic, Seasonal, and Spatial Patterns

Water temperatures in the monthly samples were between 0 and 28.1 degrees Celsius (°C) and from 0 to 29.0 °C in the continuously collected data, and never exceeded the Virginia maximum temperature criterion of 32.0 °C (appendix 2; fig. 2.1; Commonwealth of Virginia, 1997a) at any of the 20 stations over the 10 years of monitoring. Water temperatures were seasonally variable with a median cool season temperature of 6.5 °C and median warm season temperature of 19.0 °C networkwide. The greatest range in daily mean

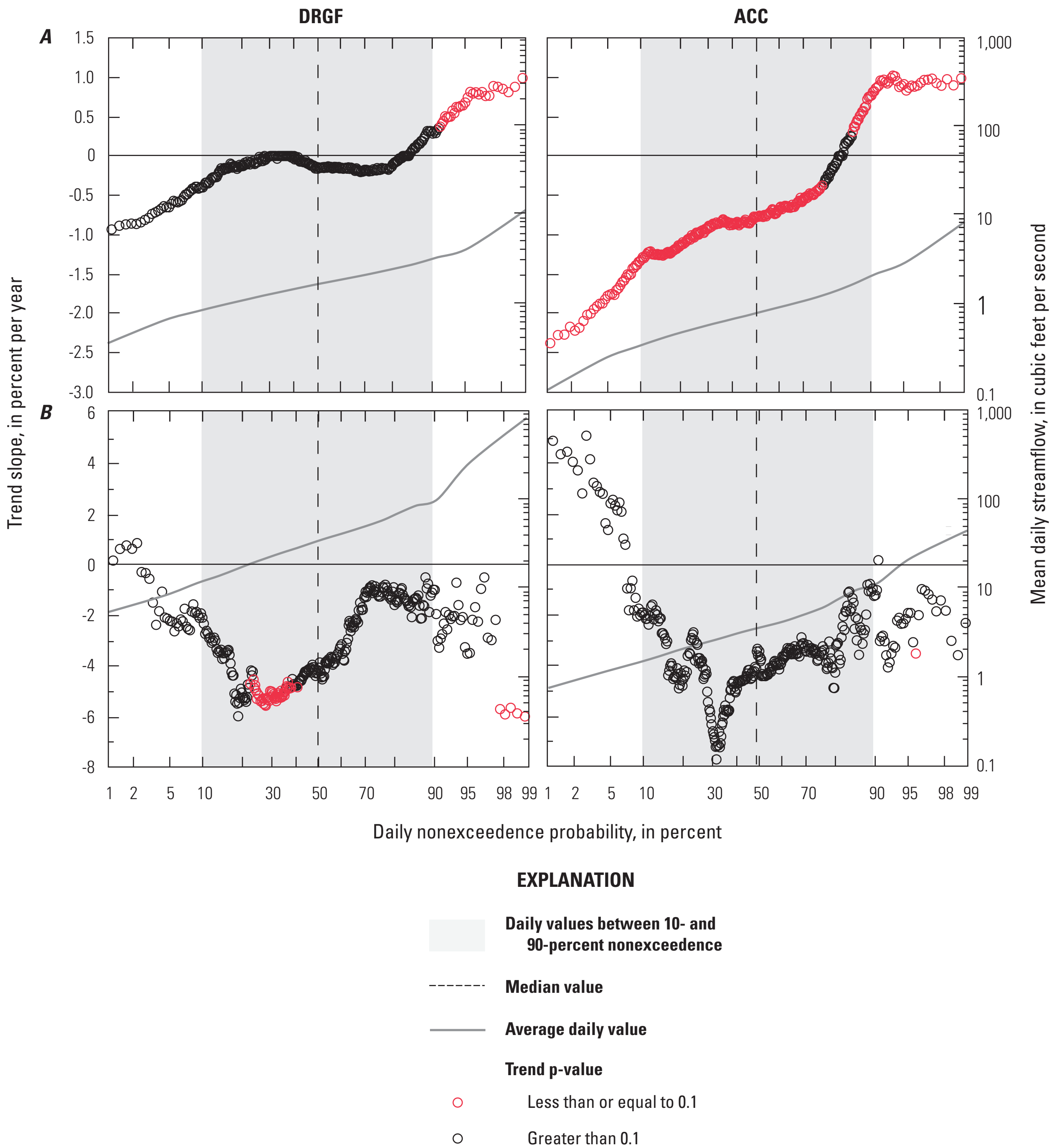

Figure 11. Trends in mean daily streamflow at Difficult Run near Great Falls, Virginia (DRGF) and Accotink Creek near Annandale, Virginia (ACC) *A*, between 1946–2017 and 1948–2017, respectively, and *B*, 2008–18 in years beginning April 1 and ending March 31 with nonexceedance probabilities of mean daily streamflow.

values from the continuous data at the five intensive monitoring stations were observed during spring months (fig. 14A). This pattern is attributed to daily fluctuations in WT caused by similar fluctuations in air temperature and from heating by solar radiation owing to a lack of lack of leaf cover in the tree canopy (fig. 14A; Johnson, 2004). Water temperature violated the 2-degree per hour change standard (Commonwealth of Virginia, 1997b) approximately 0.01 percent of the time across the five intensive monitoring stations. Violations were observed at all five intensive monitoring stations, but most commonly at DEAD (51 percent of all occurrences) and is likely related to stream flashiness. These occurrences were primarily during extreme storm events in warm months and

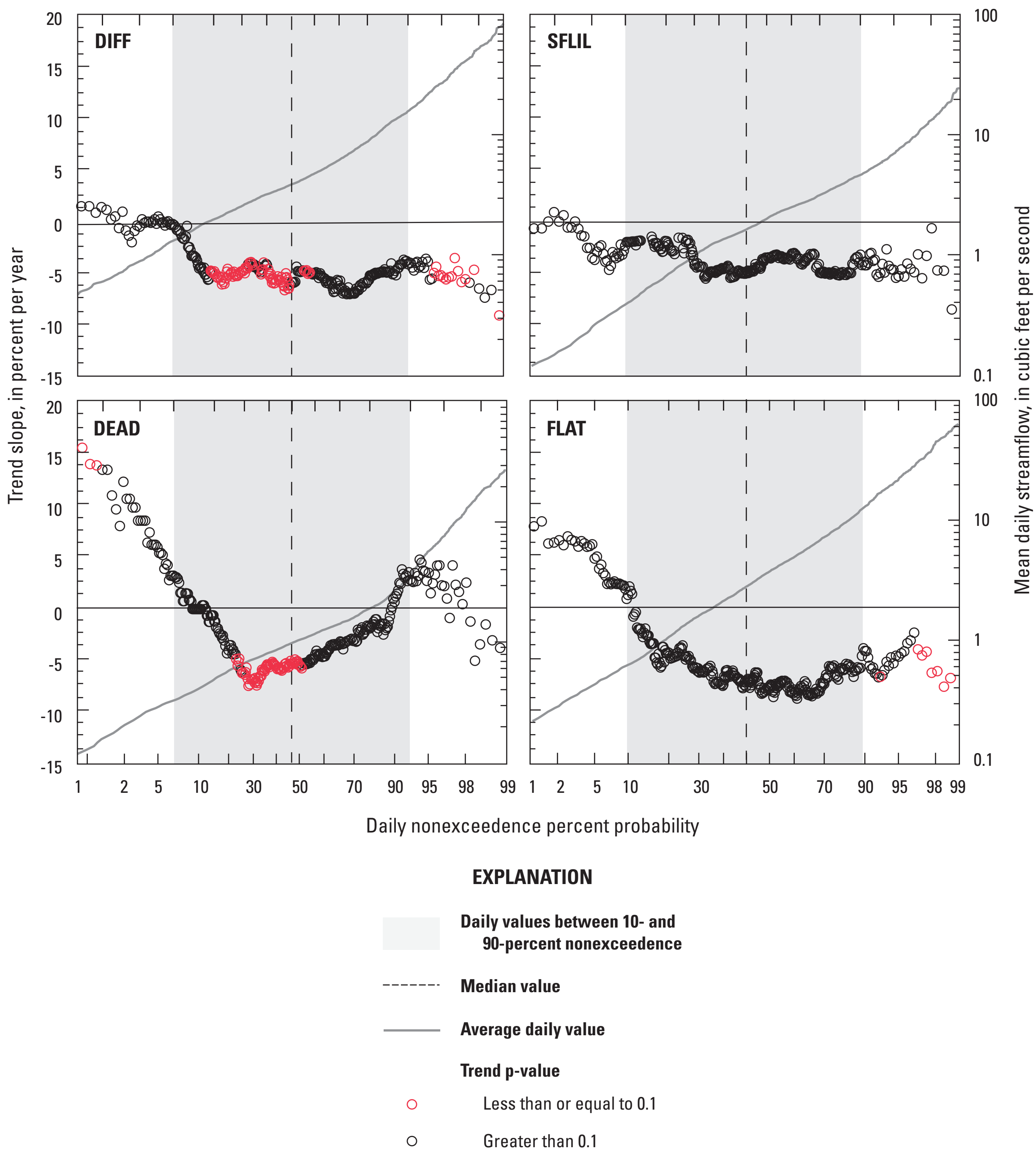

Figure 12. Trends in mean daily streamflow at the four intensive monitoring stations between April 2008 and March 2018, with nonexceedance probabilities of mean daily streamflow.

likely the result of rapid runoff from solar-heated impervious surfaces. Station-specific mean WT ranged from 12.2 to 14.8 °C and was typically lowest in the least developed watersheds.

Dissolved oxygen varied seasonally across monitored streams with median concentrations typically 4.0 mg/L higher in the cool season than the warm season. Median concentrations measured in the monthly samples varied across stations, with the highest concentrations generally observed at CASTLE and INDIAN (10.3 mg/L) and the lowest at PSB (8.3 mg/L; fig. 15). Median DO was typically lowest at PSB in the Coastal Plain and across all Triassic Lowlands streams, and highest in the Piedmont. Low median DO at PSB may have been the result of increased biological oxygen demand associated with storage of organic matter (Munn and others, 2018) and low topographic relief, which reduces the turbulence-induced dissolution of oxygen into stream water.

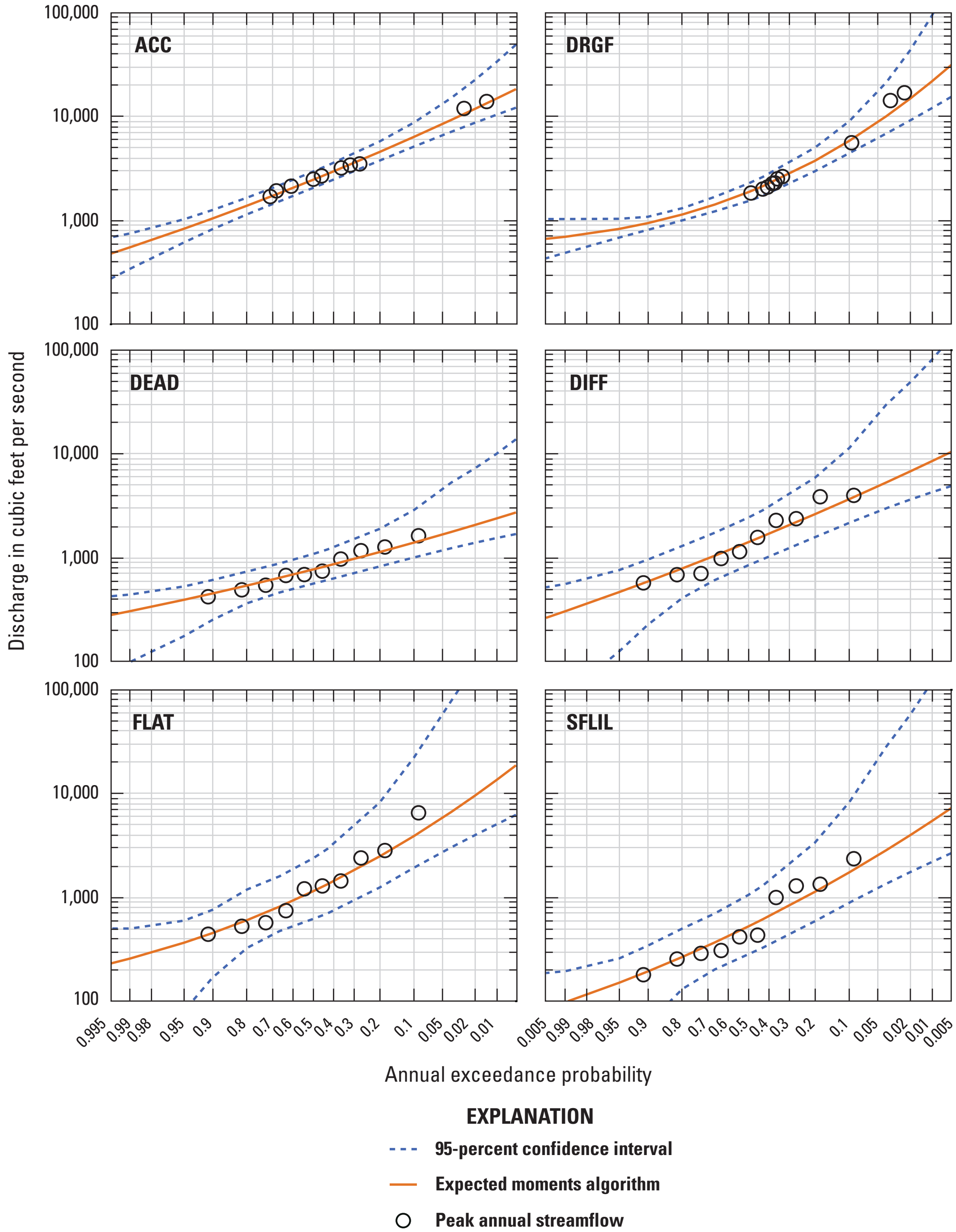

Figure 13. Annual exceedance probability plot and fitted distributions of peak annual streamflow for Accotink Creek near Annandale, Virginia (ACC), Difficult Run near Great Falls, Virginia (DRGF), and at four intensive monitoring stations in Fairfax County. Station names are defined in table 1.

More than 99 percent of the DO measurements from monthly samples were above the minimum criterion of 4.0 mg/L, with only 13 violations, all of which occurred during the warm season. Nine of these occurrences were observed at PSB, located within the Coastal Plain, from WYs 2008–2015 and may be attributed to the factors already discussed. Violations did not occur in DOGUE, and this may provide some insight into the geologic differences in these two Coastal Plain watersheds. DOGUE is underlain by coarse sediments that promote oxic conditions, whereas sediments underlying PSB have a greater clay and organic matter content that creates anoxic conditions. These differences are supported by lower soil permeability in PSB (3.37 inches/hour [in/hr]) than in other watersheds that drain the Coastal Plain

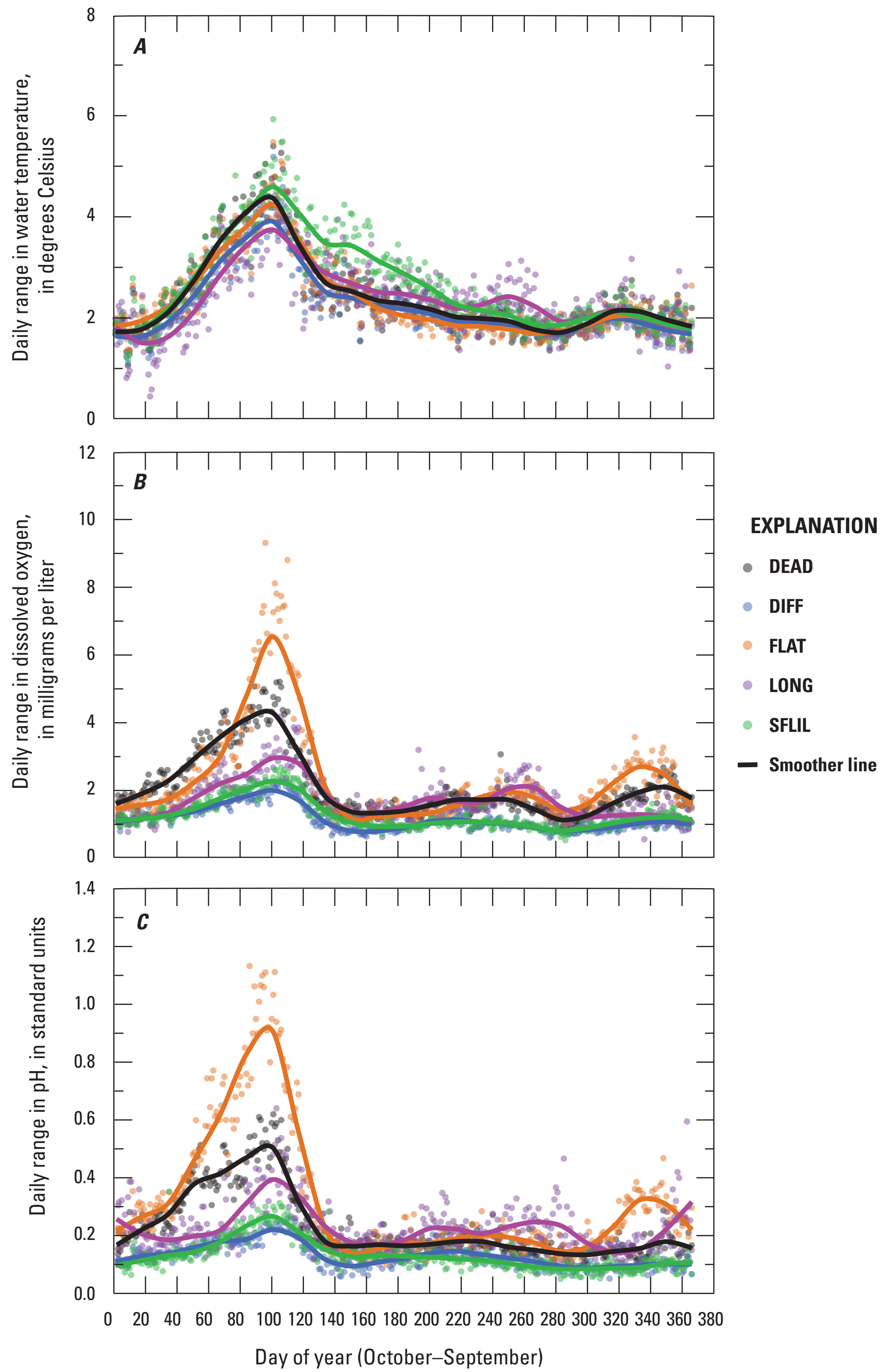

Figure 14. Daily ranges of water temperature (*A*), dissolved oxygen (*B*), and pH *(C*) summarized from continuous measurements recorded at the intensive monitoring stations and plotted against day of the year, where 1 = October 1 and 365 = September 30 in a nonleap year.

(4.26–5.19 in/hr; U.S. Geological Survey, 2016) and may explain differences in nutrient concentrations between these stations (discussed later). Violations also were recorded on single occasions at TRKYCK and FROG, and in two instances at HPEN, all of which are low-gradient systems outside of the Piedmont.

Pronounced diel cycling was apparent in continuous data during the spring at all five intensive monitoring stations; however, the greatest fluctuations were observed at FLAT, where DO varied by as much as 10 mg/L per day (fig. 14B). Fluctuations at FLAT and relatively low DO concentrations at all Triassic Lowlands stations were most likely related to

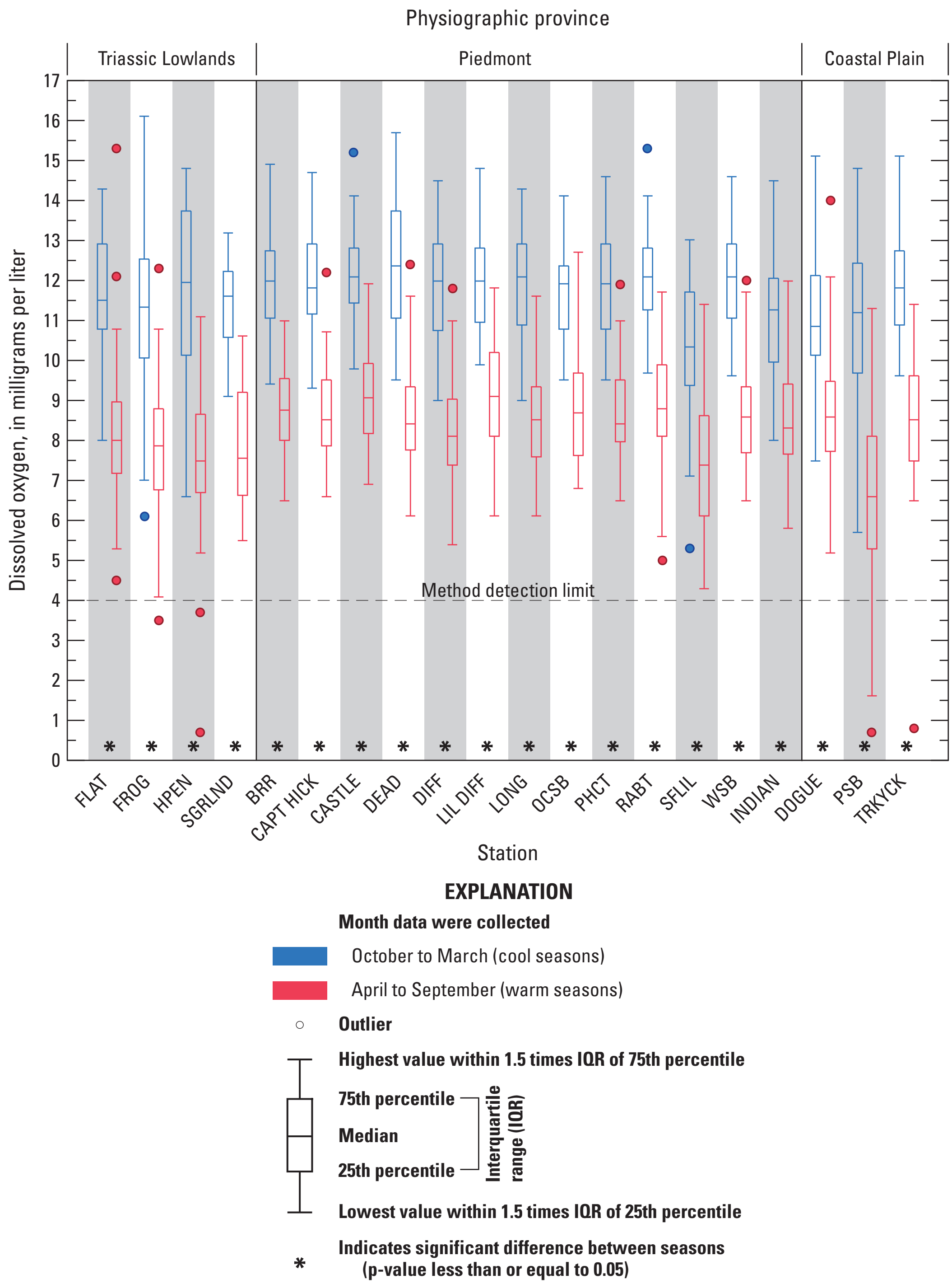

Figure 15. Dissolved oxygen results from the monthly sampling at 20 monitoring stations in Fairfax County comparing data collected during the cool (October-March) and warm (April-September) seasons. Station names are defined in table 1.

the combined effect of (1) readily available pools of soluble reactive phosphorus that promote photosynthesis that were previously deposited in ancient lakebed sediments, and (2) increased solar radiation in the early spring prior to leaf out (McCormick and Laing, 2003; Frost and others, 2006).

Trends

No trend in WT (in monthly samples) occurred at most stations and the combined trend result from all stations was nonsignificant (table 4, fig. 16A; Porter and others, 2020). A mean annual WT change of +0.03 °C, or about 0.2 percent, was observed from the network. Although WT changes were nonsignificant at most stations, their comparison to long-term and regional patterns provides useful insights. Mean annual changes in the 2008–2018 study period are similar to the long-term (1985–2016) significant trends observed at DRGF and ACC of +0.04 °C per year and to the regional trend of +0.028 °C per year between 1960 and 2010 documented in Chesapeake Bay streams (Rice and Jastram, 2015). There was almost no change in median to maximum mean daily WTs at four of the intensive monitoring stations (fig. 17A).

At most stations, no trend in DO was observed over the 10-year study period, but the combined trend result from all monitoring stations revealed a significant decrease of about 0.33 percent per year, or about 0.03 mg/L per year (table 4, fig. 16B; Porter and others, 2020). The largest change occurred at FROG, where a statistically significant decrease of approximately 2 percent per year was observed. The median decrease from all stations of –0.04 mg/L is nearly identical to the average annual decline observed at ACC between 1985 and 2016.

pH

pH is a measure of the relative concentration of free hydrogen and hydroxyl ions in water, which dictates the acidity or basicity of a substance. pH also affects the solubility of nutrients, which governs speciation and concentration, and

Table 4. Results from Regional Seasonal Kendall trend tests.

[Significance based on $p \leq 0.1$. Green text indicates a significant increasing trend and orange text indicates a significant decreasing trend. mg/L, milligrams per liter; FNU, Formazin nephelometric units]

Response, units	Abbreviation	Number of stations	Flow normalized			Nonflow normalized		
			p-value	Median annual change	Median annual percent change	p-value	Median annual change	Median annual percent change
Water temperature, degrees Celsius	WT	14	0.2825	0.04	0.03	0.5669	0.20	0.16
Dissolved oxygen, mg/L	DO	14	0.1016	–0.02	–0.03	0.0457	–0.31	–0.33
pH, standard units	pH	14	0.0025	–0.013	–0.02	0.0015	–0.06	–0.09
Specific conductance, uS/cm	SC	14	<0.0001	58.29	2.32	<0.0001	66.43	2.64
Total nitrogen, mg/L	TN	14	0.1648	–0.12	–0.59	0.1599	–0.10	–0.55
Total Kjeldahl nitrogen, mg/L	TKN	13	0.9134	0.02	0.67	0.6270	0.00	0.00
Total dissolved nitrogen, mg/L	TDN	14	0.7145	0.05	0.35	0.7927	0.00	0.00
Nitrate + nitrite, mg/L as nitrogen	NO_3^-	14	0.0994	–0.13	–1.33	0.0761	–0.16	–1.81
Dissolved total Kjeldhal nitrogen, mg/L	DTKN	13	<0.0001	0.12	4.73	0.0007	0.10	3.57
Total phosphorus, mg/L	TP	14	0.0041	0.01	3.90	0.0069	0.01	2.73
Total dissolved phosphorus, mg/L	TDP	14	<0.0001	0.01	8.13	<0.0001	0.01	10.56
Orthophosphate, mg/L	OP	10	0.0474	0.00	3.61	0.0069	0.01	6.98
Total particulate phosphorus, mg/L	TPP	12	0.0308	0.00	4.39	0.0454	0.00	0.00
Suspended sediment concentration, mg/L	SS	14	0.2396	0.56	1.78	0.6220	0.00	0.00
Turbidity, FNU	Turbidity	14	0.3186	–0.12	–0.79	0.2088	–0.43	–3.03

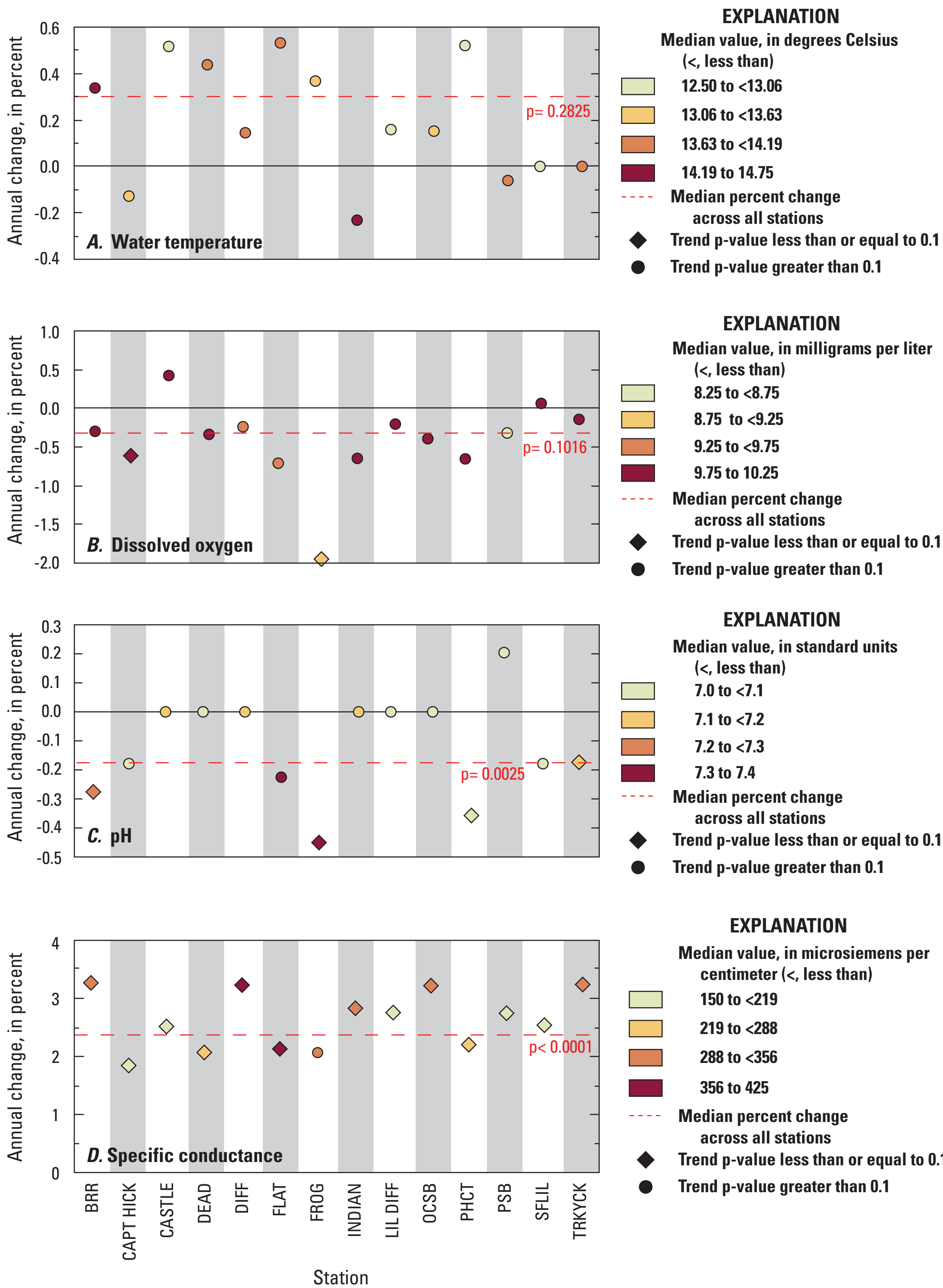

Figure 16. Water temperature (*A*), dissolved oxygen (*B*), pH (*C*), and specific conductance (*D*) trend results expressed as a percent change per year at 14 monitoring locations between March 2008 and April 2018. The p-value refers to the Regional Seasonal Kendall trend test. Station names are defined in table 1.

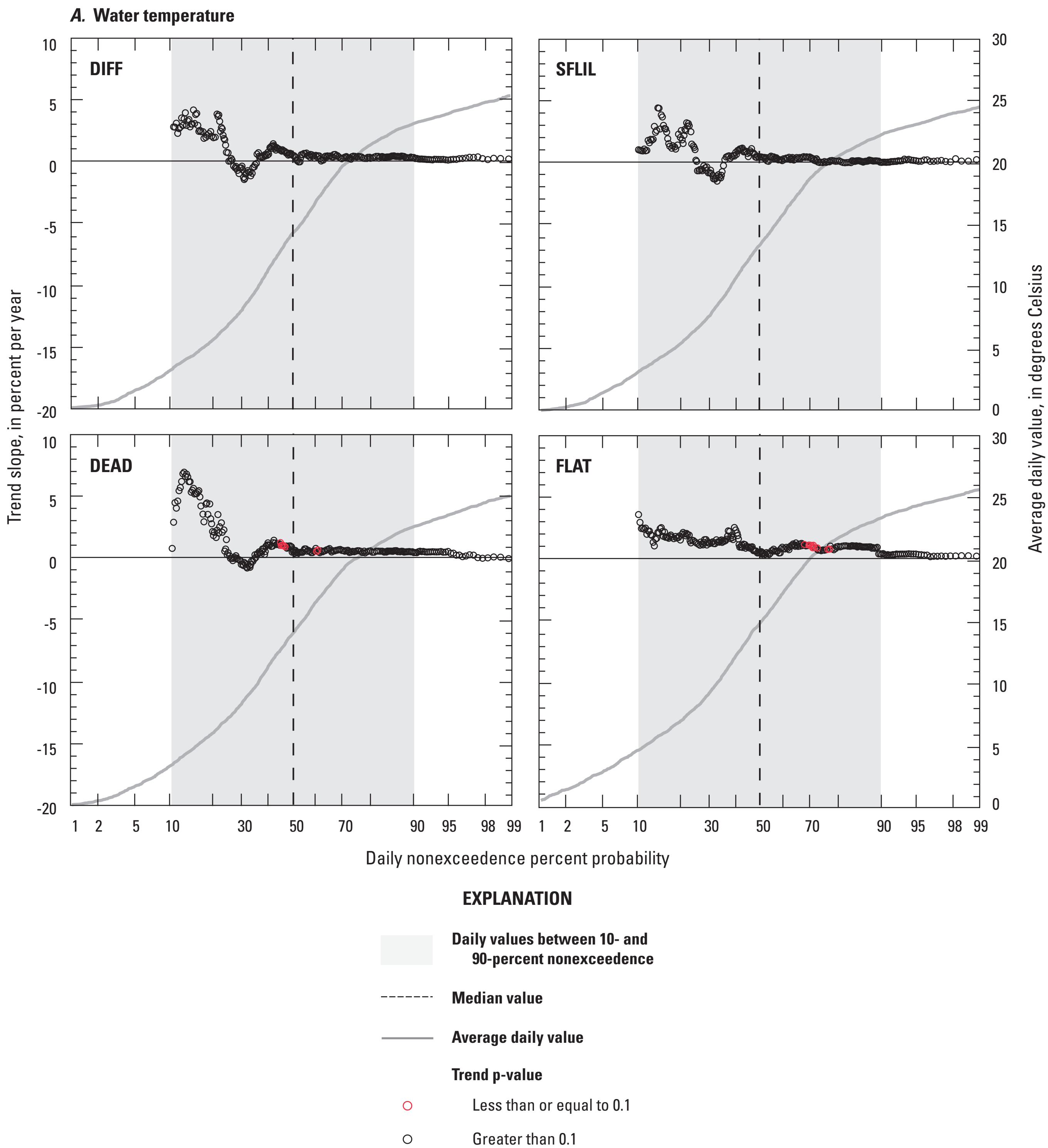

Figure 17. Trends in mean daily water temperature (*A*), pH (*B*), specific conductance (*C*), and turbidity (*D*) at four intensive monitoring stations between April 2008 and March 2018 with nonexceedance probabilities of mean daily values. Station names are defined in table 1.

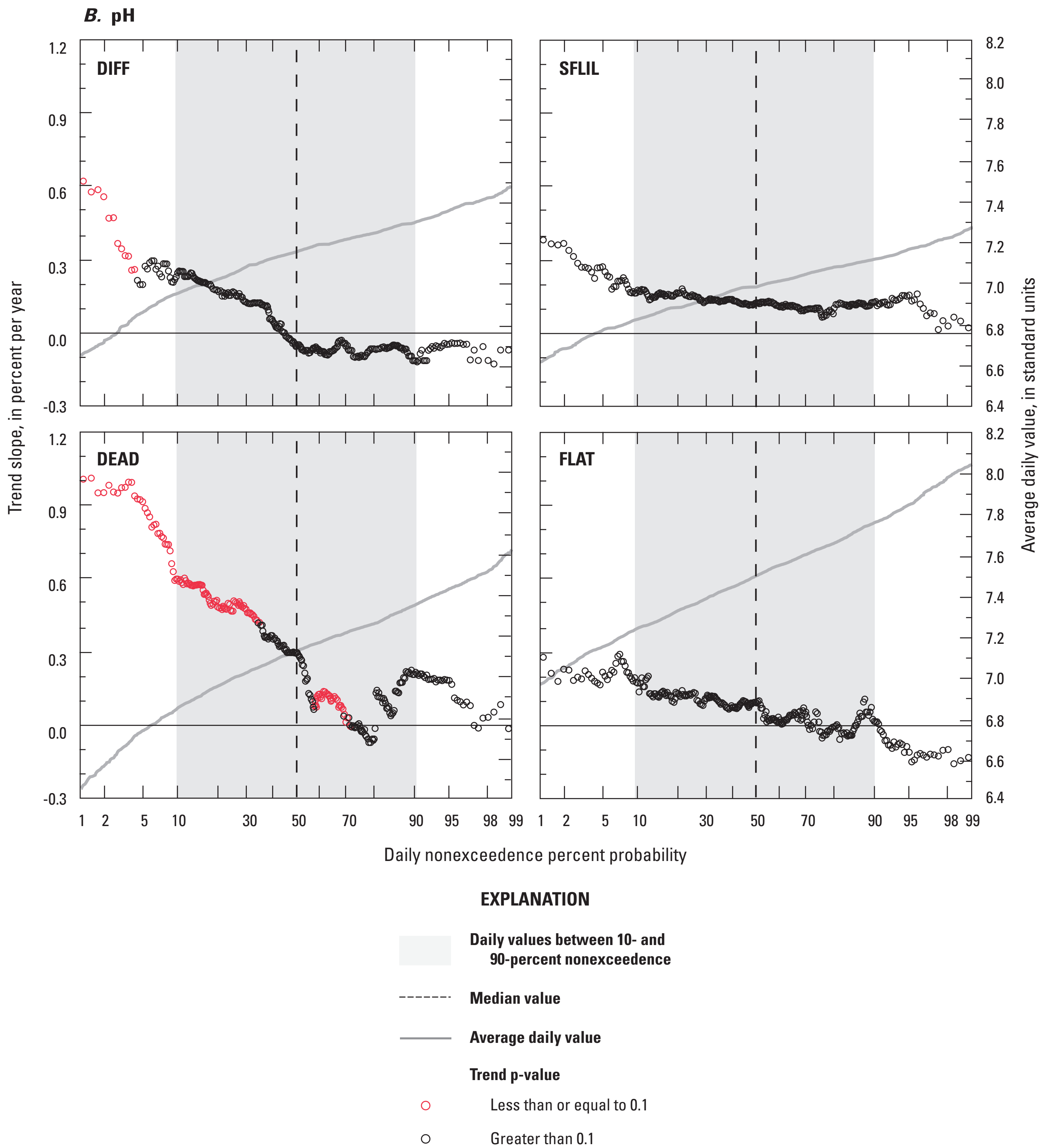

Figure 17. —Continued

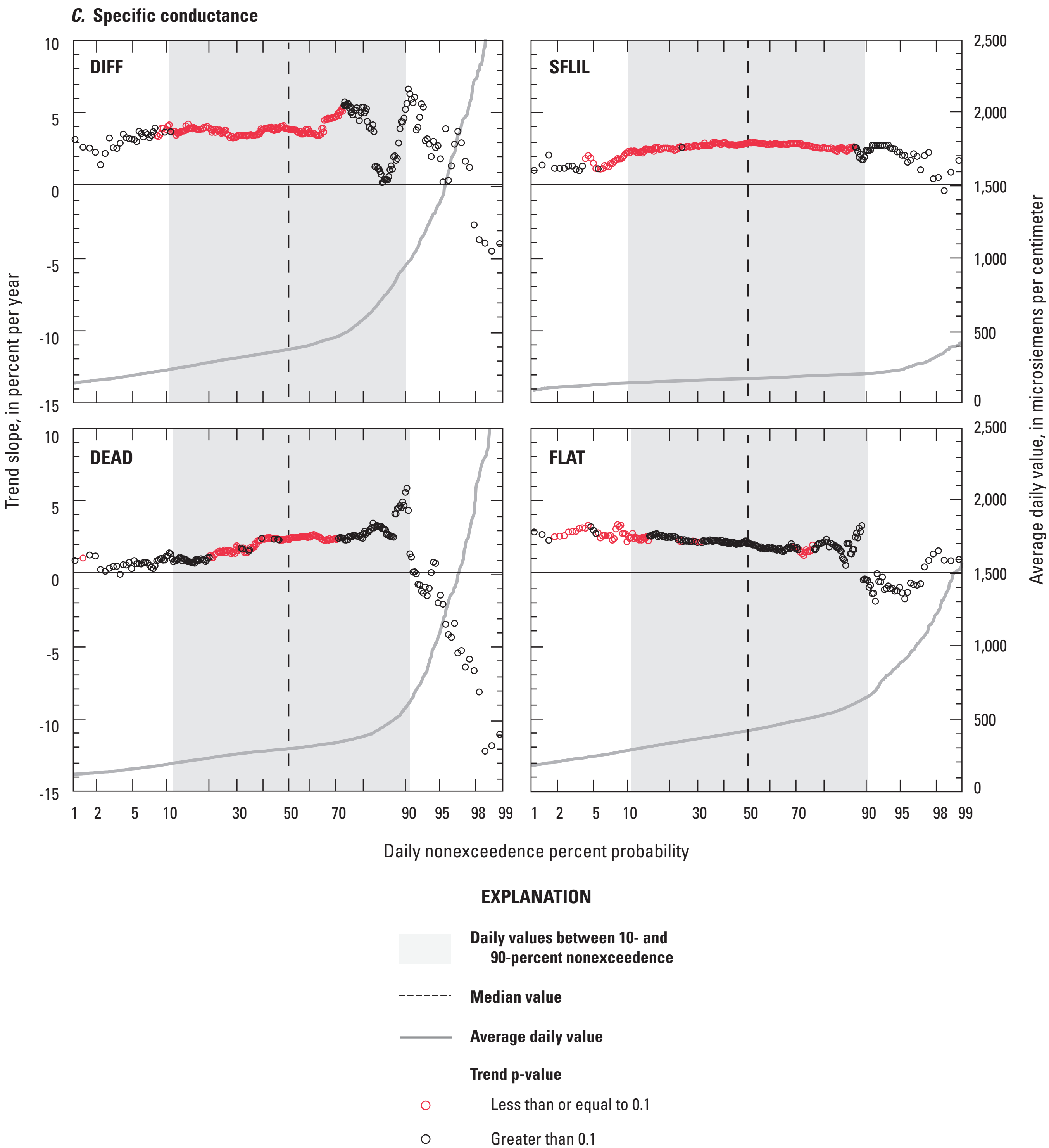

Figure 17. —Continued

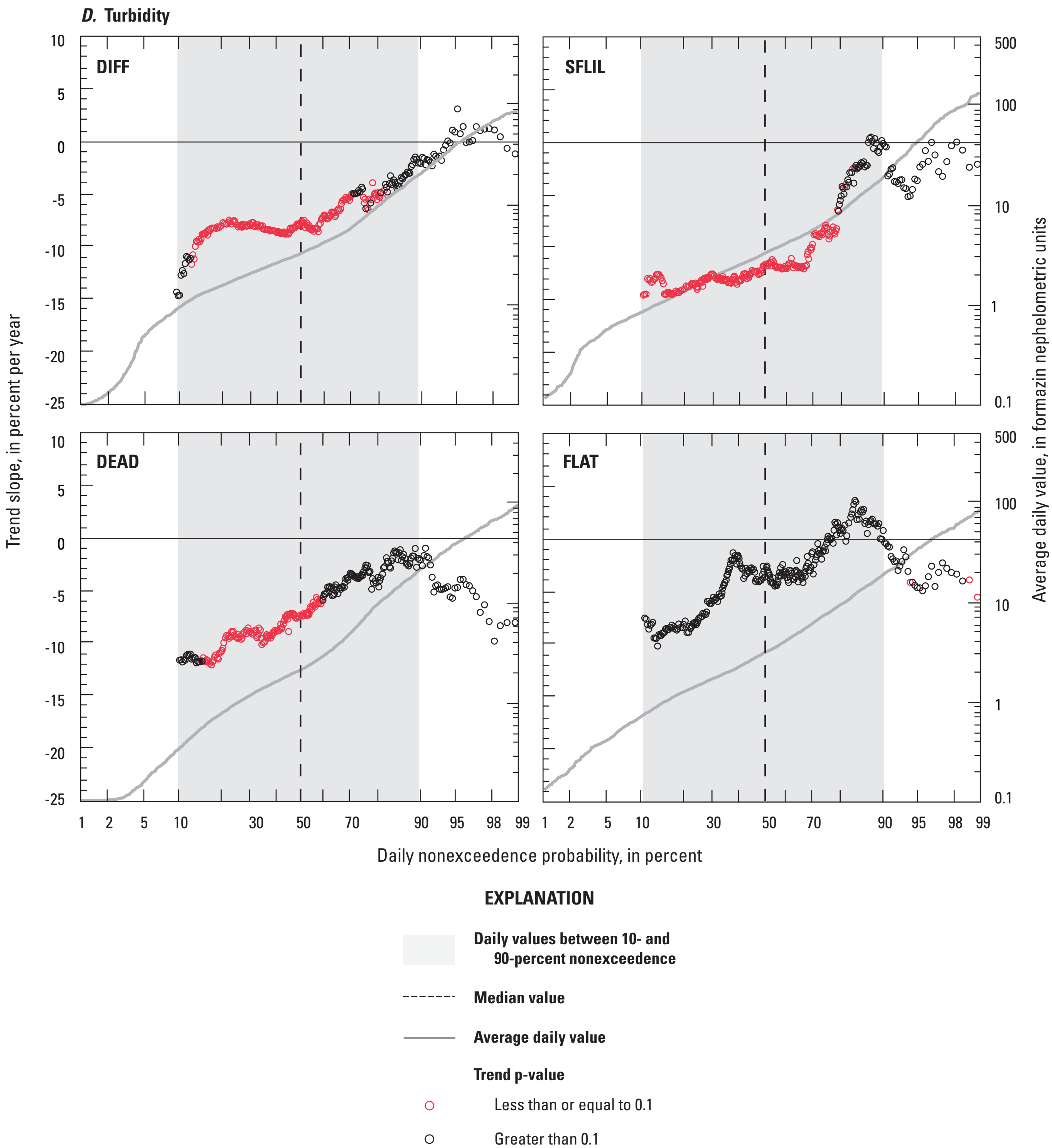

Figure 17. —Continued

consequently the biological availability of those constituents (Strauss and others, 2002; Li and others, 2013; Cerozi and Fitzsimmons, 2016). Stream pH has been shown to decrease with watershed imperviousness owing to increased runoff of rain, which is typically more acidic than that of fluvial waters (Deletic and Maksimovic, 1998; Barałkiewicz and others, 2014); however, increases in pH also have been cited (Conway, 2007; Nagy and others, 2012; Moore and others, 2017) from additions of calcium (Ca) and bicarbonate from concrete and asphalt weathering as well as lawn maintenance and road salts found in urban storm runoff (King and others, 2005; Li and others, 2013; Kaushal and others, 2017).

Hydrologic, Seasonal, and Spatial Patterns

pH was typically inversely related to streamflow owing to inputs of precipitation runoff during high flows (fig. 18). The median pH of rainwater in Virginia during the study period was 5.1 (National Atmospheric Deposition Program, 2016), whereas typical stream pH was approximately neutral (7.0±0.5 units). Within-station seasonal variability was minimal; however, median annual pH, which ranged from 6.7 to 7.5 units, indicated spatial variability across the 20 stations (fig. 19). Monthly pH measurements were within the range of natural waters (6.5–8.5, Hem, 1985) 95.9 percent of the time networkwide. The four stations with the highest median monthly pH all drain portions of the Triassic Lowlands; whereas the lowest monthly pH was observed at DOGUE, located in the Coastal Plain. The causes of elevated pH in the Triassic Lowlands streams are likely twofold: (1) increased photosynthesis that results from the dissolution of phosphorous-bearing geology removes hydrogen (H^+) ions from solution, and (2) calcium carbonate-rich groundwater discharging to streams (Froelich and Zenone, 1985b). Low pH observed at DOGUE and PSB may be related to the chemistry of the groundwater discharging to those streams. Ultisols, intensely weathered reddish clay soils that compose much of the Coastal Plain sediments, have a consistently low pH, low concentrations of calcium and magnesium (Mg), and high concentrations of iron (Fe) and aluminum (Al) (Virginia Department of Conservation and Recreation, Division of Natural Heritage, 2016). The chemistry of these soils affects groundwater pH by controlling the rate of carbonate-equilibrium reactions, which involves the hydrolysis of carbon dioxide (CO_2) to form carbonic acid, and ultimately disassociation to form H^+, carbonate, and bicarbonate ions (Focazio and others, 1992). Additionally, surface waters in the Coastal Plain are characteristically rich in organic, humic, and fluvic acids owing to the accumulation of organic matter and these acids naturally lower stream pH (Beck and others, 1974). Median pH was also low at RABT, located in the Piedmont region, which may have also resulted from organic matter accumulation. Organic matter was not measured directly; however, median TKN and DTKN concentrations, which contain dissolved organic nitrogen and form a subset of the dissolved organic matter pool (Hood and Christian, 2008; Sipler and Bronk, 2015), were higher at RABT than any other Piedmont station.

Seasonal variability in mean daily pH values was not observed in the continuous data at the five intensive stations; however, the range in daily values were typically greater from late February to mid-April, as well as in August to late September at FLAT (fig. 14C). The fine resolution of the continuous data revealed a daily pattern when streamflow was stable, in which pH values typically peaked during the warmest time of day and were at their lowest in the early morning hours. This pattern is controlled by a series of chemical reactions in which CO_2 reacts with water (H_2O) to form carbonic acid (H_2CO_3) and ultimately releases a H^+ ion into water. During the daytime, photosynthesizing organisms utilize CO_2 and H_2O and the consequent removal of H^+ ions causes water to become more basic; however, in the evening and early morning hours when photosynthesis is suspended, the concentration of H^+ ions increases, lowering pH. Respiration and decomposition processes also cause variability in pH owing to

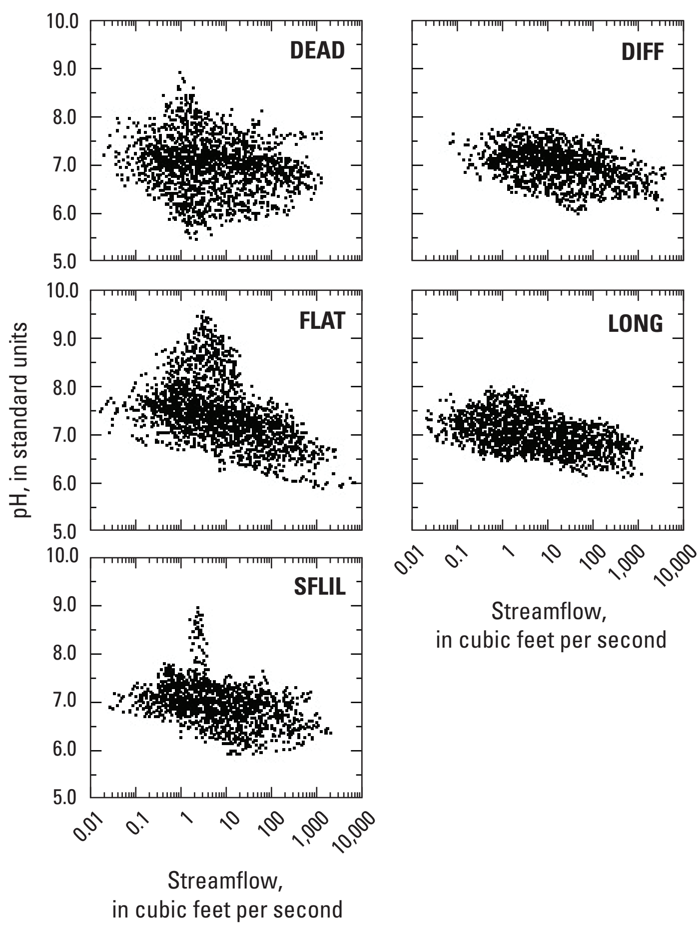

Figure 18. Continuous pH and streamflow data collected the five intensive monitoring stations. Station names are defined in table 1.

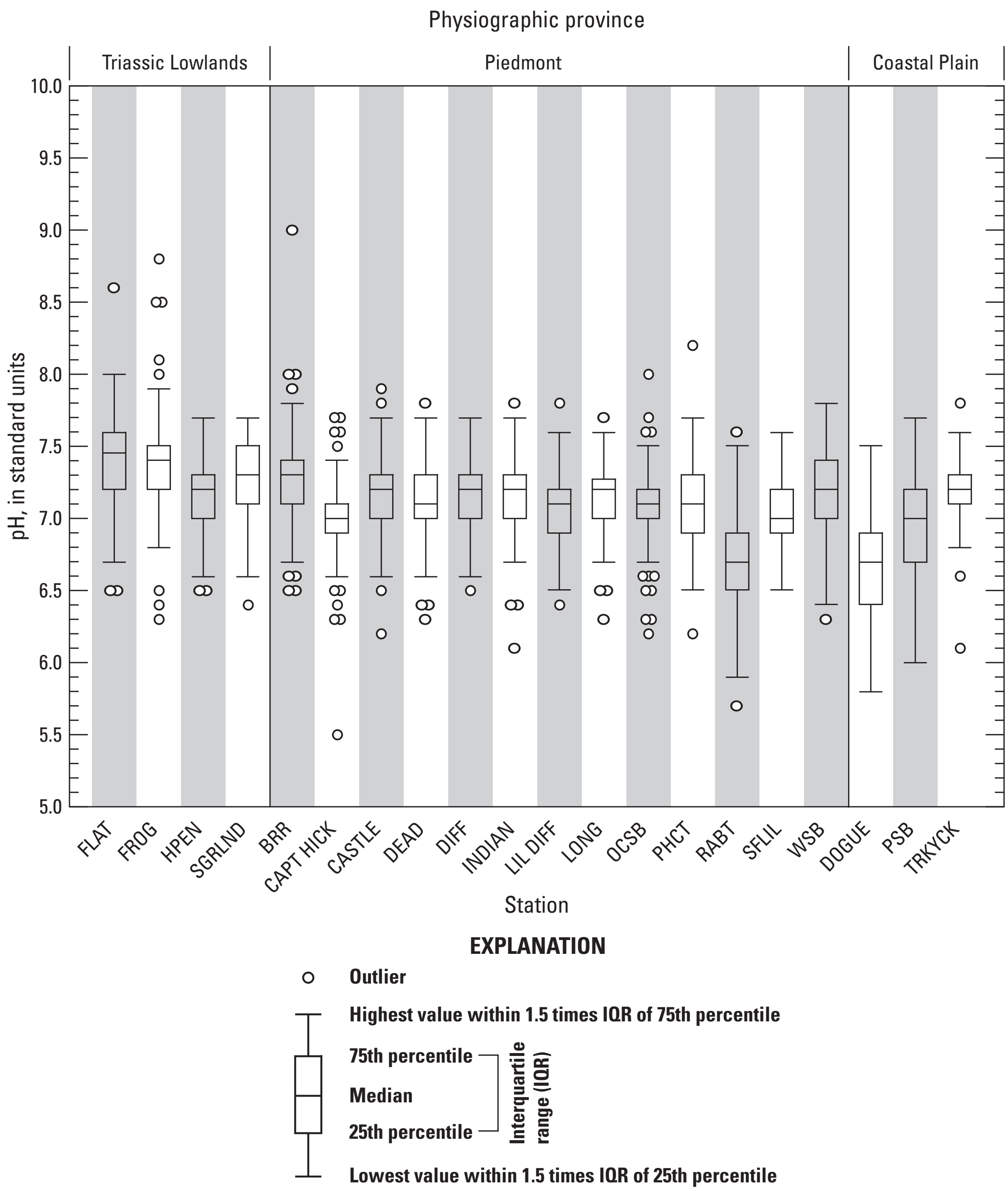

Figure 19. pH results from the monthly sampling at 20 monitoring stations in Fairfax County. Station names are defined in table 1.

the production of CO_2, which dissolves in water as carbonic acid. Diurnal swings were most pronounced prior to leaf-out in late winter and early spring when daytime solar heating caused the greatest fluctuation in daily WT, and consequently, biological activity. Diurnal pH fluctuations were greatest at FLAT and could be related to elevated phosphorous concentrations that increased photosynthetic rates.

Trends

The combined trend results from all monitoring stations (in the monthly data) revealed a significant decrease in pH over the 10-year study period; however, the network median change between 2008 and 2018 was less than 1 percent. Significant decreases occurred at four stations, where median changes ranged from about –0.2 to –0.5 percent. (table 4, fig. 16C; Porter and others, 2020). These changes are similar to the significant decrease in pH of 0.01 unit per year observed in ACC and DIFF between 1985 and 2016 (fig. 17B). Changes of as much as +1 percent per year were present in the lower 30th percentile of mean daily values, calculated from 15-min measurements at four of the intensive stations; a range of pH values between 6.5 and 7.0. Except for trends at DEAD, these changes mostly were not significant. Increasing pH values observed at DEAD may be attributed to increases in the delivery of base cations to streams, possibly as a result of increased road salt applications or from the dissolution of carbonate-bearing building materials (Kaushal and others, 2017). Lower pH values typically were observed during periods of elevated streamflow and values above this range, observed during baseflow, experienced smaller, nonsignificant changes. As discrete samples typically are collected during nonstormflow events, differences in the monthly trend results and mean daily value trend results reflect that temporal patterns in pH vary with hydrology.

Specific Conductance

Specific conductance is the ability of water to conduct electric current, corrected for temperature (typically 25 °C), and provides an indication of ion concentration in water (Hem, 1985). Factors that affect SC include temperature and geologic weathering (Hem, 1985), as well as anthropogenic sources such road deicing salts (Novotny and others, 2008; Daley and others, 2009), wastewater (Paul and Meyer, 2001; Potter and others, 2014), and weathering of concrete materials (Wright and others, 2011; Kaushal and others, 2017). Deicer applications have been linked with elevated ion concentrations, such as sodium and chloride, in streams. These applications are considered a major contributor to freshwater salinization in the urban environment and have been documented in Fairfax County streams (Sanford and others, 2012; Jastram, 2014; Hyer and others, 2016); similar relations have been observed throughout the northeastern and southeastern United States (Kaushal and others, 2005; Moore and others, 2020).

Freshwater salinization is a growing concern in urban watersheds where runoff is not typically mitigated by traditional stormwater management practices such as detention ponds (Snodgrass and others, 2017). Salinization can degrade stream and drinking water quality through the mobilization of nitrogen and phosphorous from soils (Steele and Aitkenhead-Peterson, 2013; Haq and others, 2018), the leaching of metals in water infrastructure (Kaushal, 2016; St. Clair and others, 2016), and has numerous negative impacts on aquatic life (Corsi and others, 2010). Annual stream-quality assessments based on macroinvertebrate sampling, physical habitat, and water chemistry consistently identify that 75 percent of Fairfax County streams are in fair to very poor condition (Fairfax County, 2017b). Chloride and sediment were identified as the most probable pollutant stressors causing the benthic impairments in ACC (Interstate Commission on the Potomac River Basin, 2017), and are likely contributors to poor benthic conditions in similar settings across Fairfax County (Fairfax County, 2017a). These concerns led to the development of a chloride surface-water standard in Virginia (Virginia Department of Environmental Quality, 2011) and the implementation of a chloride total maximum daily load (TMDL) in 2017 in ACC, the first such TMDL in the State in an urban setting.

Hydrologic, Seasonal, and Spatial Patterns

Median SC values ranged from 165 microsiemens per centimeter (µS/cm) at SFLIL to 418 µS/cm at FLAT (fig. 20) and typically were related inversely to streamflow networkwide, except during periods of ion enrichment following road deicing salt applications (fig. 21). This hydrologic dependence indicates that high-conductance groundwater dominates baseflows and low-conductance storm runoff dominates higher flows. Variability across stations is a function of geology and land cover. Although SC values are elevated by the delivery of salts applied to impervious surfaces, geologic effects also were evident in Fairfax County streams; the 10-year median values for Triassic Lowlands streams were significantly higher (376 µS/cm) than those in the Coastal Plain (243 µS/cm) or the Piedmont (226 µS/cm), all of which were higher than the EPA reference conditions for streams in most eastern ecoregions (<200 µS/cm; Griffith, 2014).

In the absence of anthropogenic disturbance, SC is controlled by three general processes: (1) the ionic composition of precipitation; (2) the ratio of evaporation to crystallization processes, which can concentrate or dilute the ionic composition of precipitation; and (3) the composition of the underlying rock (Gibbs, 1970; Griffith, 2014). Although these processes are not independent, given the relative proximity of monitored streams, it is reasonable to assume similar rates of evapocrystallization and precipitation chemistry; therefore, variability across physiographic provinces was most likely driven by the mineral composition of the underlying rock strata (Froelich and Zenone, 1985b). Ion concentration, and therefore SC, typically increases in groundwater with time of contact with the geologic materials (Gibbs, 1970; Matsubayashi and others, 1993), particularly when flowing through geology that lacks resistance to chemical weathering (Griffith, 2014). Therefore, groundwater SC likely was elevated in Triassic Lowlands streams owing to high concentrations of calcium and magnesium leached from highly weathered calcareous shale (Froelich and Zenone, 1985a).

Specific conductance increases with impervious land cover (Hem, 1985; Gregory and Calhoun, 2007; Peters, 2009), and is therefore a useful indicator of the effects of urbanization on stream quality. A positive relation (R^2=0.51, p=0.0004) between impervious land cover and mean SC was observed in Fairfax County streams (fig. 22) where SC increased nearly 100 µS/cm for every 10-percent increase in watershed imperviousness. Significant seasonal variability also was apparent networkwide with median SC ranging from 239 µS/cm in the warm season to 313 µS/cm in the cool season. Spikes in SC between 1,000 µS/cm and 5,000 µS/cm were observed in winter months (January, February, March) and were most pronounced at stations that drain watersheds with higher impervious land cover such, as OSCB, BRR, DEAD, and

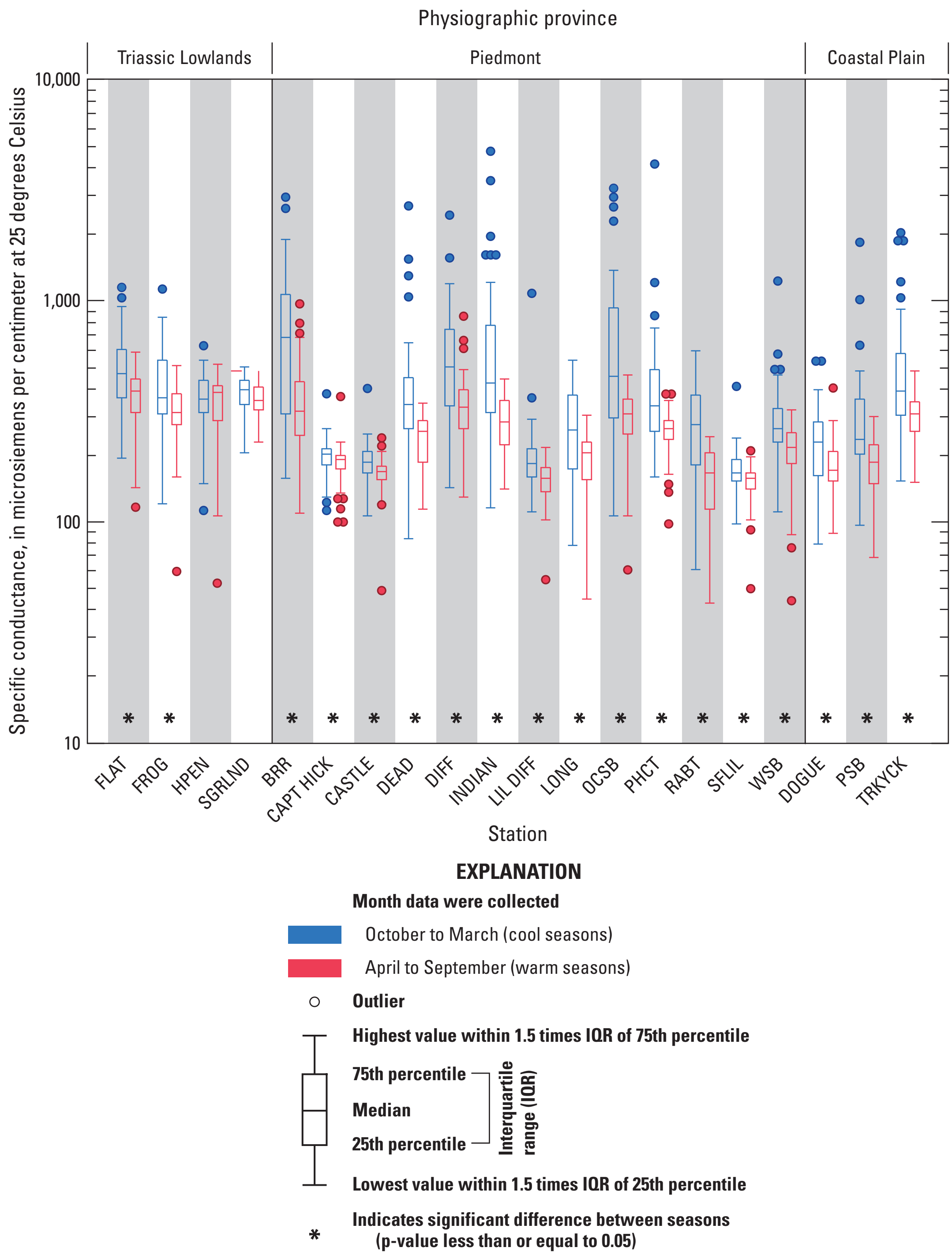

Figure 20. Specific conductance results from the monthly sampling at 20 monitoring stations in Fairfax County, with comparison of data collected during the cool (October–March) and warm (April–September) seasons. Station names are defined in table 1.

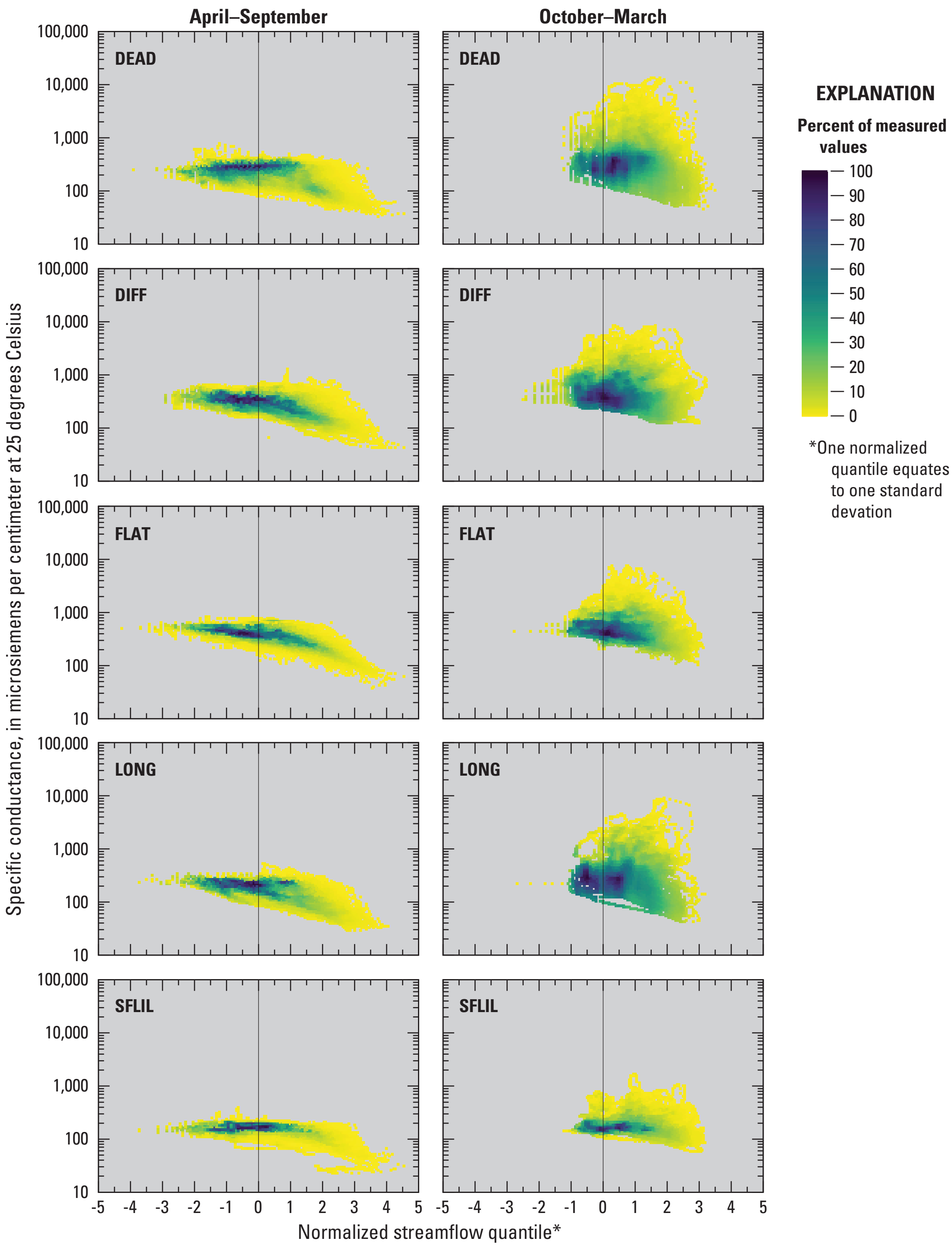

Figure 21. Continuous specific conductance data compared to normalized streamflow quantiles (one normalized quantile equals one standard deviation) measured at the five intensive monitoring stations in Fairfax County.

DIFF, than those that drain less intensively developed watersheds, such as CAPT HICK, SGRLND, CASTLE, and SFLIL. This pronounced difference was likely a function of the total area of roadways, sidewalks, and parking lots treated with deicing salts as well as greater connectivity of these surfaces to stormwater conveyances, and ultimately to stream channels. Impervious conveyance systems accelerate the transport of deicing salts, ions dissolved from weathered infrastructure, and other urban contaminants from land to stream (Hatt and others, 2004; Novotny and others, 2008). Although the application of deicing salts in winter months led to enrichment rather than dilution during runoff events at all five intensive stations, the effect was less pronounced at SFLIL, where the percentage of impervious land cover was lowest.

Trends

Significant increasing trends and (or) FN trends (in monthly samples) were observed in all streams with a median change of about 2.5 percent per year, or about 7.5 µS/cm per year (table 4; fig. 16D; Porter and others, 2020). The combined trend result from all stations indicates that SC has increased throughout the monitoring network. The largest annual change of 3.3 percent (11.6 µS/cm) occurred at BRR and the smallest annual change of 1.8 percent occurred at CAPT HICK (3.6 µS/cm). The median SC of BRR (356 µS/cm) is greater than that of CAPT HICK (197 µS/cm), but there was not a strong relation between median values and percent changes present throughout the network. These changes are similar to the long-term trends observed in DRGF and ACC of +5.3 and +5.9 µS/cm per year, respectively, which corresponds to about +2.8 percent per year.

Mean daily specific conductance, calculated from 15-min measurements, increased by about 2–3 percent per year at four of the intensive monitoring stations. Using a Mann-Kendall method (see trend quantification method 3 in the Methods section), SC increases of as much as 5 percent per year were observed during the lower 90 percent of mean daily values (approximately 100–500 µS/cm; fig. 17C). Most changes that occurred in the 10th to 90th percentile of mean daily values at DIFF, SFLIL, and DEAD were significant (shaded area in fig. 17C). The changes that occurred in the top 10 percent of mean daily values were less consistent and mostly nonsignificant. Using a novel method based on a GAM framework (see trend quantification method 4 in the Methods section; Yang and Moyer, 2020), significant increases of 2–3 percent occurred at DEAD (85 µS/cm over 10 years; fig. 23, table 1.4), DIFF (138 µS/cm), and SFLIL (38 µS/cm). A nonsignificant increase of 1.3 percent per year was observed at FLAT (62 µS/cm). Notably, the GAM method identified nonlinear trends in the mean daily values at DEAD and SFLIL, and linear trends at FLAT and DIFF over the 10-year period. Nonlinear trends demonstrate that, although there was a 10-year increase in SC, there were increasing, decreasing, and stable periods. This approach provides a daily estimation of SC that incorporates the effects of seasonality and streamflow, increasing the ability to link water-quality processes with watershed management.

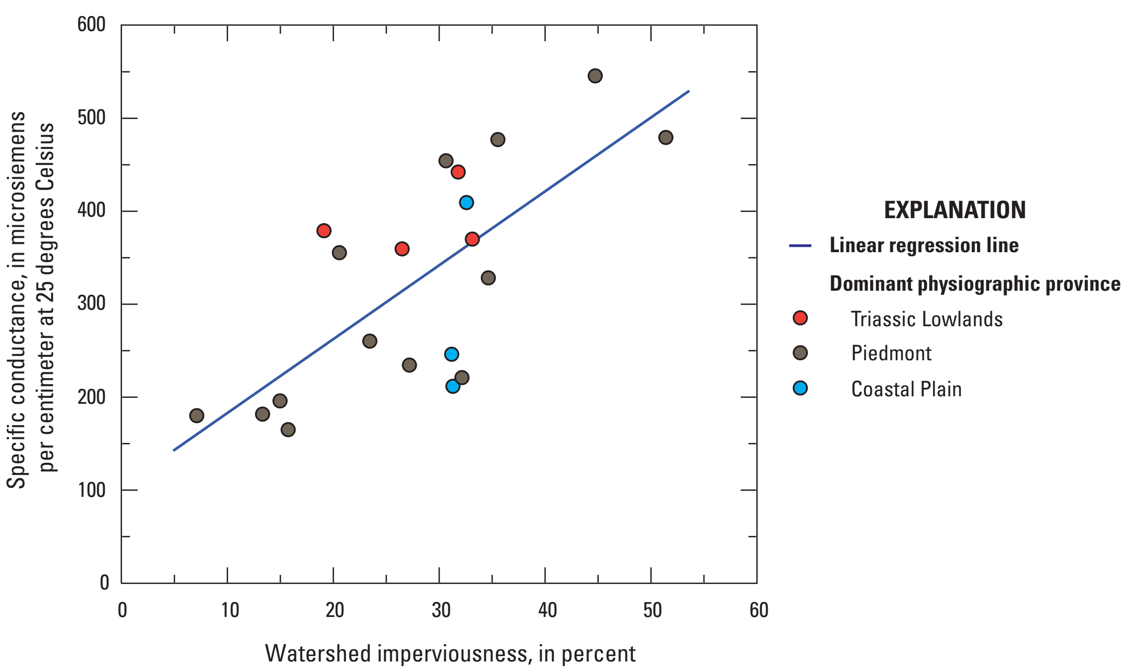

Figure 22. Mean specific conductance from the monthly sampling at the 20 monitoring stations in Fairfax County between water years 2008 and 2018 compared to the percentage of watershed covered by impervious area. A water year begins October 1 and ends September 30.

The magnitude of SC increases that occurred throughout the network varied by time of year. Significant increases at the 14 monitoring stations were most consistently observed in spring (March, April, and May) and fall (September, October, and November) months and occurred in about one-third of these station-month trend combinations (fig. 24). Increases in mean daily SC of as much as 5 percent per year were common at the four intensive monitoring locations during all seasons but were most often significant at all stations in the fall (fig. 25). Overall, the networkwide increases in SC during nonwinter months suggest that salts applied to deice roadways and other impervious surfaces are stored in the environment and released year-round. Other studies of urban watersheds have documented the transport of chloride to groundwater, which is slowly released to streams throughout the year (Perera and others, 2013; Corsi and others, 2015; Moore and others, 2020).

Turbidity and Suspended Sediment

Excess SS is a leading cause of water-quality and ecosystem impairment in urban streams. Although sediment transport occurs naturally and is controlled by fluctuations in streamflow, anthropogenic alterations to the landscape can

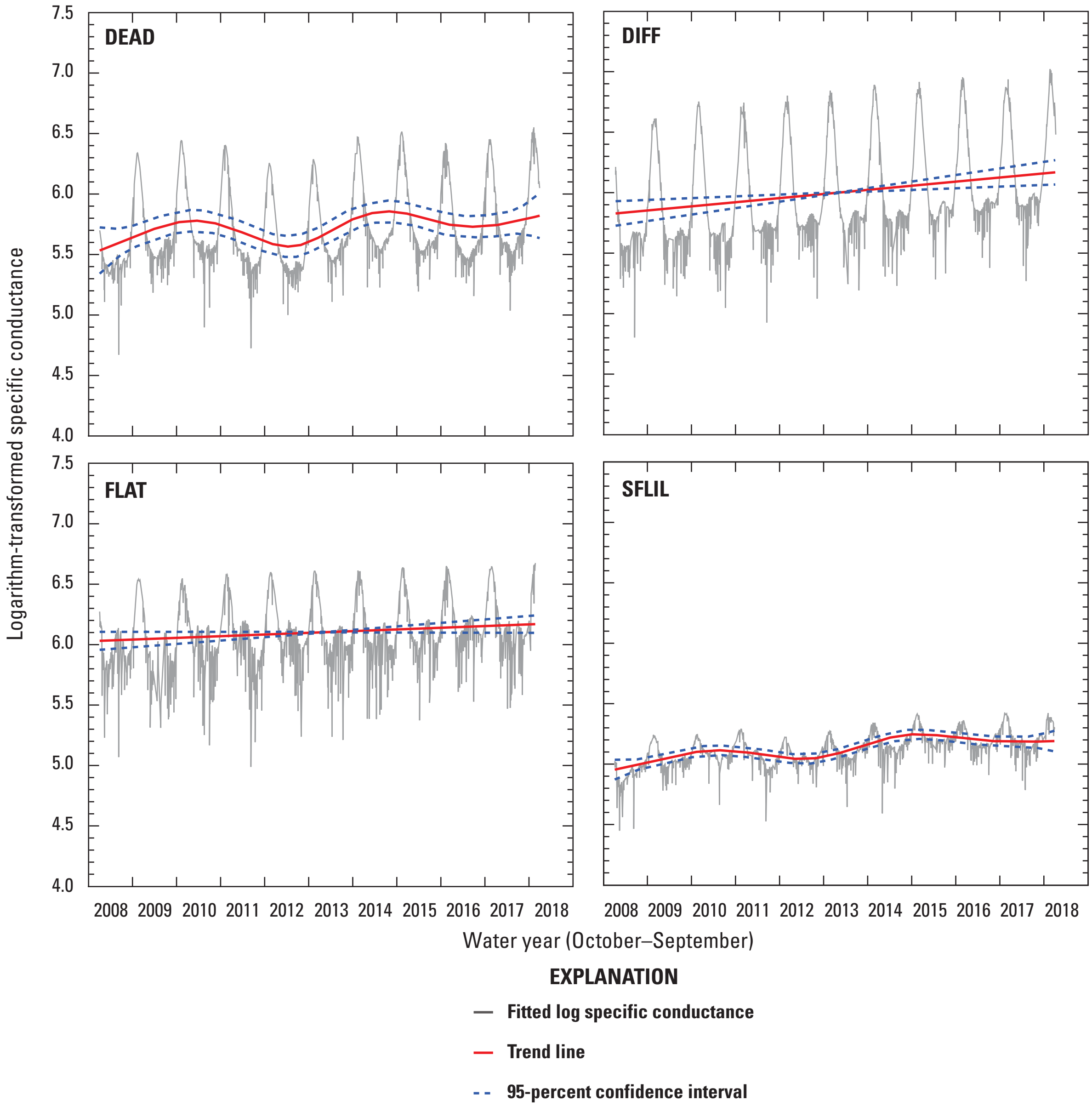

Figure 23. Trends in mean daily specific conductance at four intensive monitoring stations between April 2008 and March 2018 based on a generalized additive modeling approach, with 95-percent confidence intervals and fitted values. Station names are defined in table 1.

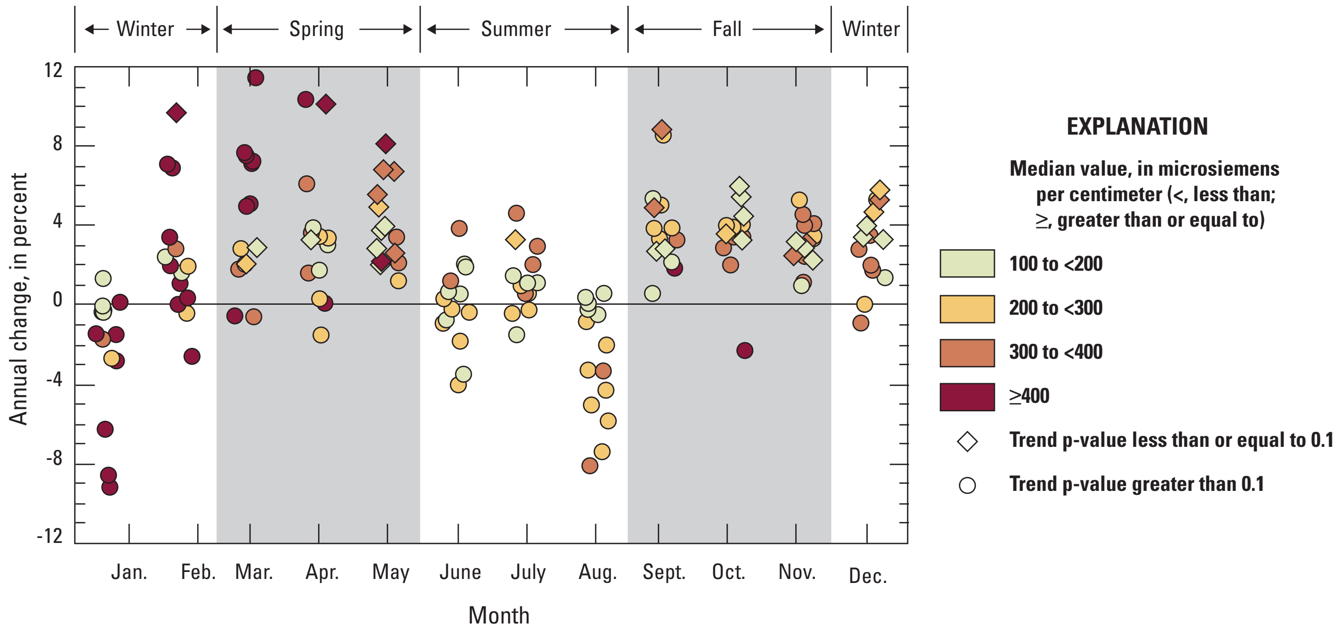

Figure 24. Monthly trends in specific conductance expressed as a percent change per year at 14 monitoring stations between April 2008 and March 2018.

increase erosional rates, decrease transport time to streams, and increase the magnitude and recurrence of peak flows that exacerbate stream-bed and -bank erosion (Paul and Meyer, 2001; Soulsby and others, 2006). Suspended fine sediments can (1) serve as vectors by which contaminants are transported downstream (U.S. Environmental Protection Agency, 2000b); (2) reduce light availability causing reduced photosynthesis and primary production (Wood, 1997); and (3) when deposited, can harm benthic macroinvertebrate communities, damage aquatic macrophyte beds, and alter the feeding, spawning, growth rate, and migration of fish (Luedtke and Brusven, 1976; Wood, 1997). Sediment transported to Chesapeake Bay carries 77 and 18 percent of annual TP and TN loads, respectively, and also conveys metals, pesticides, polychlorinated biphenyl, and organic contaminants (Zhang and others, 2015).

The highest yields of SS into Chesapeake Bay occur in the watersheds of the Piedmont physiographic province owing to soil availability and urban land development (Brakebill and others, 2010). Centuries of land-use change from forest to agriculture to urban have resulted in the accumulation of legacy sediments deposited in both uplands and stream channels (Gellis and others, 2009). Consequently, from 1952 to 2001, erosion rates in the Piedmont were nearly double the Valley and Ridge and 10 times higher than the Coastal Plain (Gellis and others, 2009). Other factors that influence streambank erosion are stream drainage area (Gellis and others, 2015, 2017; Hopkins and others, 2018), topography (Fenta and others, 2016), floods, freeze-thaw cycles (Wynn and others, 2008), increased WT and lower pH (Hoomehr and others, 2018), channel width (Schenk and others, 2013), soil density (Wynn and Mostaghimi, 2006), and vegetation type (Wynn and Mostaghimi, 2006).

Turbidity is a measure of the relative clarity of a volume of water and typically has a strong relation with SS concentration (Swenson and Baldwin, 1965). It is a particularly valuable water-quality parameter because it, unlike SS concentration, can be measured continuously and can often be used to estimate SS concentrations and loads more accurately than with models including only a streamflow term (Jastram and others, 2009; Rasmussen and others, 2009).

Hydrologic, Seasonal, and Spatial Patterns

Suspended-sediment concentrations in monthly samples, which typically represent baseflow conditions, were generally low (median = 3 mg/L) but were substantially higher in samples collected during stormflow conditions (median = 421 mg/L, maximum = 2,080 mg/L). Overall, a representative range of concentrations were sampled that allowed for accurate calculations of SS loads and transport dynamics. Suspended-sediment concentration increased with streamflow at all stations (fig. 26). Fine materials, such as silts and clays, typically were mobilized during low-flow conditions, but as streamflow increased, the associated increase in water velocity resulted in the entrainment of larger and heavier sand grains, particularly on the rising limb of storm hydrographs when shear stress was greatest (Kurashige, 1993). Although the largest storms typically transported the coarsest material, fine material still represented most of the SS concentration, which suggests that total SS loads at all stations were dominated by

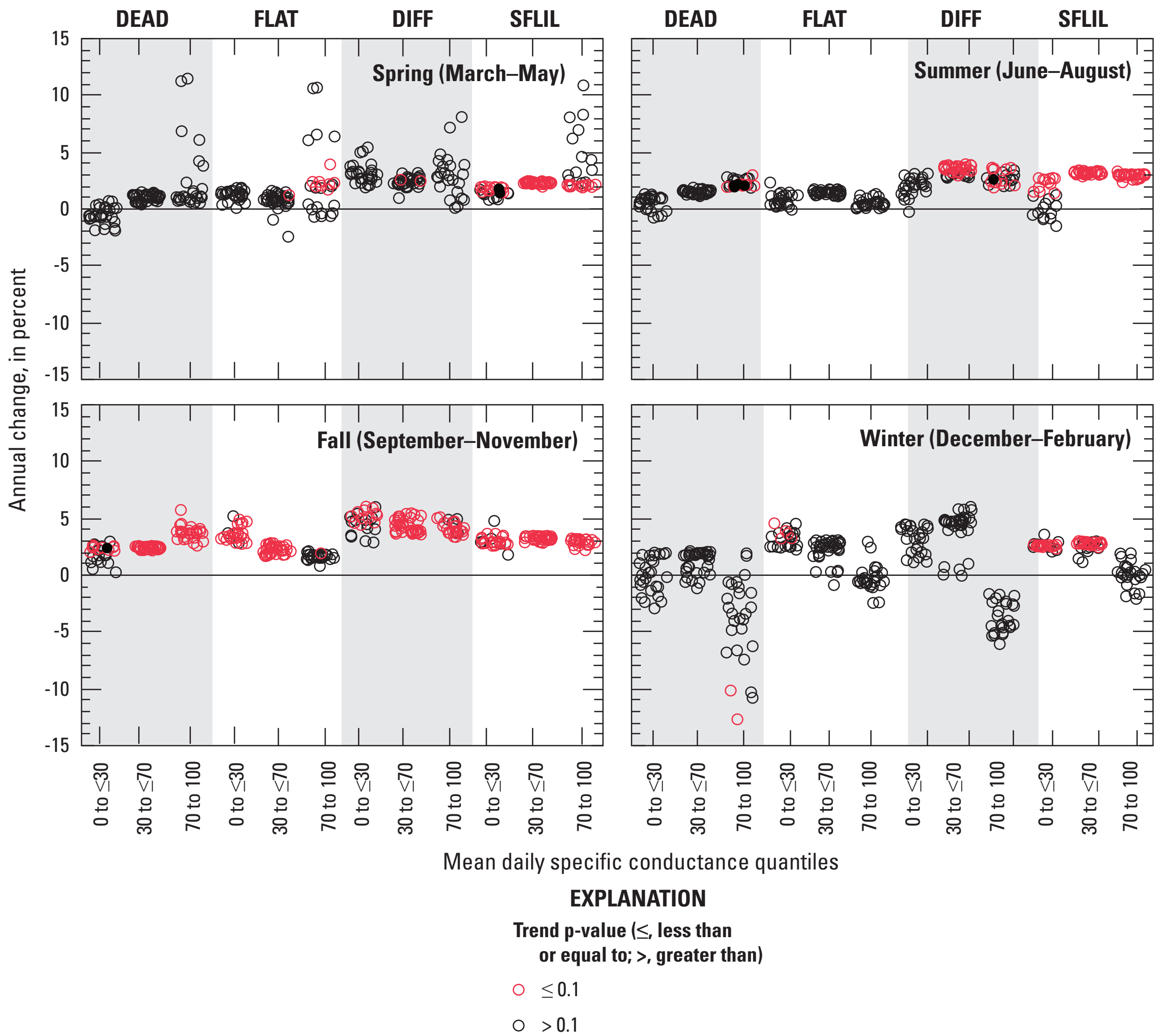

Figure 25. Seasonal trends in mean daily specific conductance at four intensive streamgages.

silts and clays (68–85 percent of the total sample). Fine sediments account for about 90 percent of the sediment inputs to the Chesapeake Bay (Zhang and Blomquist, 2018).

The timing of peak SS concentration on a hydrograph can provide useful insight into the source of SS and can be investigated by examining turbidity hysteresis patterns. Turbidity peaked within 1 hour of peak streamflow in 87 percent (222 out of 255 storms) of the storms examined across all stations (fig. 27), which suggests that sediment was quickly delivered to streams from storage within the stream channel network and from local streambank erosion (Landers and Sturm, 2013), but some between-station variability was present. In most storms, turbidity peaked less than 2 hours before streamflow at DIFF and FLAT (represented by positive LAG values on the x-axis of fig. 27). These storms would form a clockwise loop in a hysteresis plot (fig. 28A), indicating in-channel material and streambank erosion to be dominant sources of SS. This pattern was consistent with other studies in the Difficult Run watershed that reported suspended fine sediments were dominated by streambank material (91 percent of SS concentration; Cashman and others, 2018). The longer streamflow lags (>4 hours) observed at DIFF and FLAT are likely the result of an initial flush of instream material coupled with a longer transit time of runoff owing to watershed size. Turbidity peaks occurred less than 1 hour after streamflow (negative LAG values on the x-axis of fig. 27) during some storms at all stations but were the more common response at DEAD, LONG, and SFLIL. These storms would create a counterclockwise hysteresis loop and suggest that sediment sources such as upland material and erosion of upper streambank slopes are important components of the SS budget (fig. 28B). Although these analyses provide important insight, a complete understanding of the mechanisms that control event-based sediment transport has not been fully achieved owing to the myriad of processes affecting availability and mobilization such as seasonality,

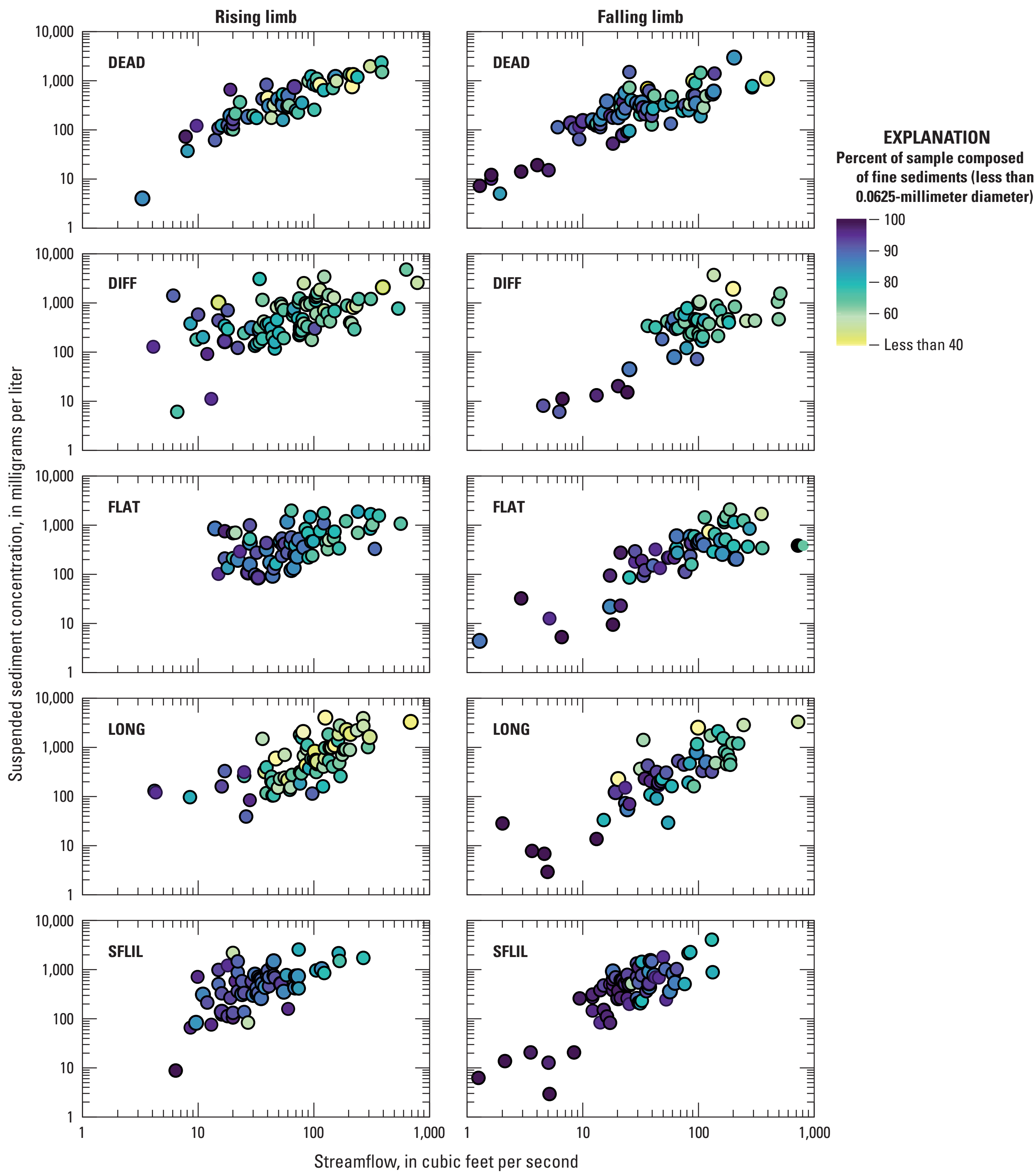

Figure 26. Suspended-sediment concentration compared to streamflow at the five intensive monitoring stations in Fairfax County, split by hydrologic condition (rising versus falling limb of the hydrograph). Color gradient reflects the percent of sample composed of fine sediments (less than 0.0625-millimeter diameter). Station names are defined in table 1.

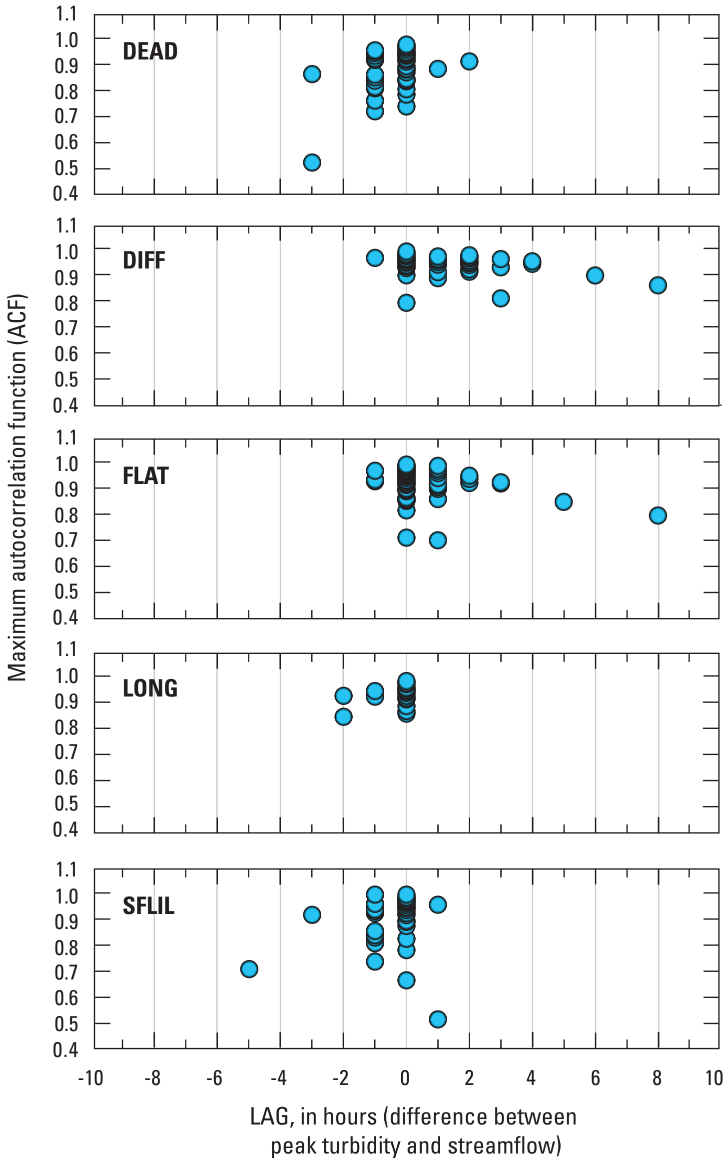

Figure 27. Cross-correlation analysis of turbidity and streamflow. Positive LAG values on the x-axis indicate that peak turbidity preceded peak streamflow, whereas negative values indicate that peak streamflow preceded peak turbidity. Each LAG unit represents a 1-hour difference between peak turbidity and streamflow. The strength of the relation between turbidity and streamflow is represented by the correlation function on the y-axis (1 = perfect correlation, 0 = no correlation). Red lines are presented for visual reference to aid interpretation of results. Station names are defined in table 1.

antecedent conditions, stormflow magnitude, and precipitation intensity (Lawler and others, 2006; McGuire and McDonnell, 2010; Lloyd and others, 2016).

Concentrations of SS measured at the five intensive monitoring stations were significantly higher in the warm season than the cool season at four out of five stations (fig. 29). In particular, concentrations were significantly lower in fall and winter months than spring months at DIFF, SFLIL, LONG, and DEAD. These patterns are consistent with two processes commonly associated with streambank erosion: hydrology and climate (Lawler and others, 1997). Streamflow yields in spring months (March-May) were nearly double those in fall months (September-November), which suggests that the hydrologic conditions required for sediment erosion and entrainment were more commonly met during the spring season. Additionally, climate-based factors such as increased bank erosion in late winter and spring has been attributed to soil weakening by freeze-thaw cycles (Lawler and others, 1997; Stott, 1997; Wynn and others, 2008) or by sudden increases in WT relative to soil temperature (Kelly and Gularte, 1981; Grabowski and others, 2011; Hoomehr and others, 2018; Akinola and others, 2019). The latter related to sudden WT increases is uniquely important in urban watersheds (Akinola and others, 2019) where warm weather thunderstorms can produce runoff from heated impervious surfaces that can substantially increase stream temperature (>7 °C; Nelson and Palmer, 2007; Hester and Bauman, 2013), but has a lesser effect on soil temperature. Cross-correlation analyses were used to evaluate seasonal patterns in the source of sediment (not presented), but a seasonal shift was not identified.

Median SS concentration ranged from 196 to 361 mg/L and did not vary significantly for most pairwise comparisons between the five intensive monitoring stations. The highest concentrations observed across the five intensive monitoring stations consistently occurred during stormflows at SFLIL (15 out of the highest 16). In urban streams, SS mobilization is often linked to changes to the hydrologic regime that result from urban development and transformation of uplands from pervious to impervious surfaces (Bledsoe and Watson, 2001; Paul and Meyer, 2001). Impervious land cover is lower at SFLIL than the other four intensively monitored watersheds and hydrologic metrics such as streamflow yield, flashiness, and runoff ratio, which are typically used to measure the effects of urbanization on streambank and -bed erosion, were low relative to other stations. Despite these properties, which are typically associated with limiting sediment transport, SS concentrations at SFLIL may be higher than the other watersheds during very large storms because there is more available sediment that has not been transported during smaller events as a result of in-channel and floodplain trapping (Skalak and Pizzuto, 2010; Hupp and others, 2013). Additionally, recent land development in this watershed converted a large portion of forest to residential lawn and impervious cover, potentially altering the hydrologic regime and promoting erosional processes.

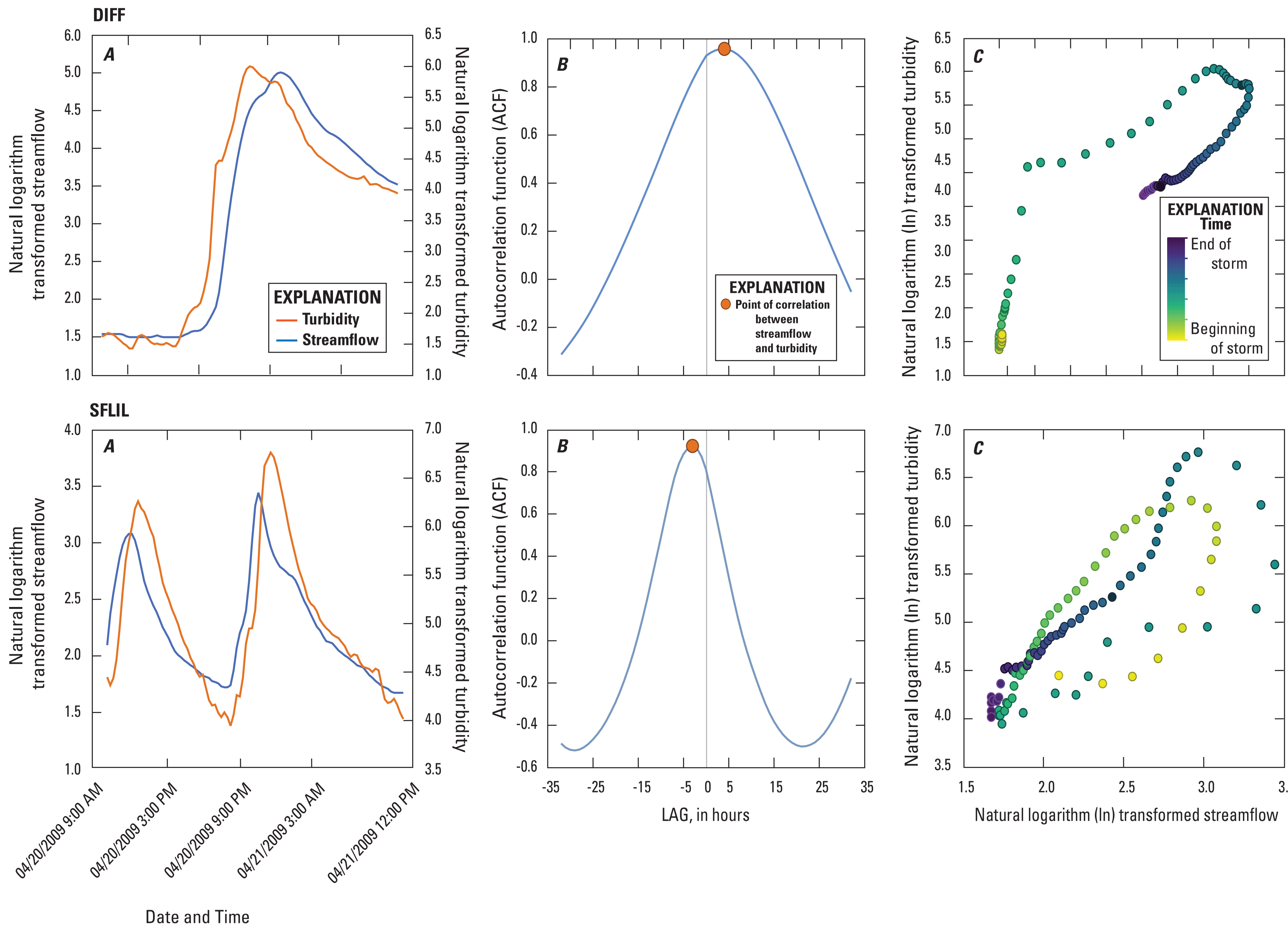

Figure 28. Natural logarithm transformed streamflow and turbidity timeseries (*A*), cross-correlation (*B*), and turbidity-streamflow hysteresis loops (*C*) from select storms at DIFF and SFLIL. Positive values on the cross-correlation x-axis indicate that peak turbidity preceded peak streamflow, whereas negative values indicate that peak streamflow preceded peak turbidity. The strength of the relation between turbidity and streamflow is represented by the correlation function on the y-axis (1 = perfect correlation, 0 = no correlation). The red circle indicates the maximum correlation between turbidity and streamflow. Station names are defined in table 1.

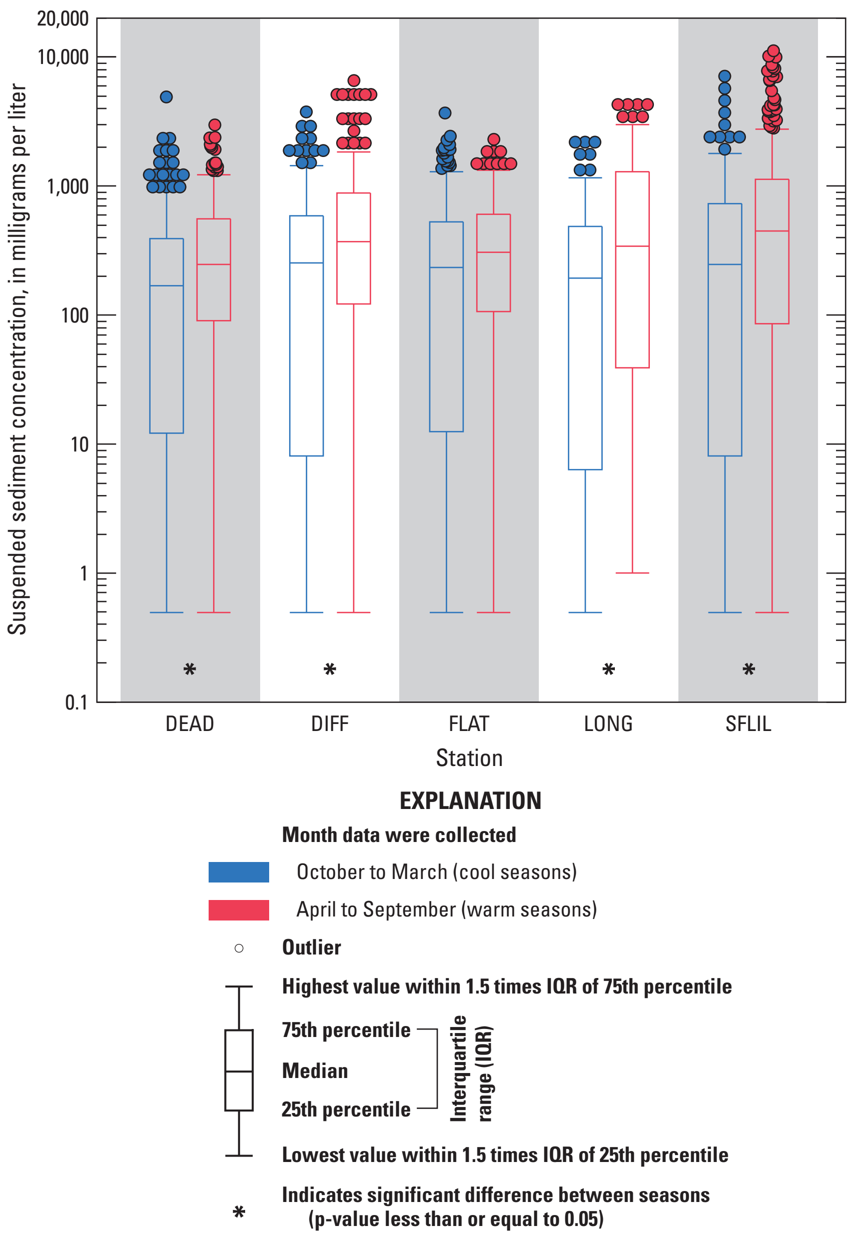

Figure 29. Suspended-sediment concentration results from the monthly sampling at 20 monitoring stations in Fairfax County, with comparison of data collected during the cool (October-March) and warm (April-September) seasons. Station names are defined in table 1.

Loads

At all five stations, turbidity and streamflow terms were strong predictors of SS concentration and explained more than 90 percent of variability (tables 1.5, 1.6). The wide range in measured and computed concentrations, and the strength of the sediment-turbidity relation highlights the importance of employing a continuous turbidity monitoring approach in studies of small, flashy urban streams. At SFLIL, seasonal terms also were included and may represent an increase in SS concentration in response to warmer temperatures or high-intensity thunderstorms in spring and summer months.

Substantial interannual variability was observed for SS loads at most stations and was strongly related to SFI (fig. 30; Porter and others, 2020). The highest yields at the five intensive monitoring stations occurred at SFLIL and DIFF during the wettest years (WYs 2008, 2011, and 2014). Notably, a large proportion of the total annual precipitation in these 3 years was generated during high-intensity events (daily precipitation equaled or exceeded 1 in.) and coincided with annual stormflow volumes that exceeded 10-year station-specific means. These two watersheds yielded considerably more SS than the other watersheds over the 10-year monitoring period, which was heavily influenced by these 3 wet years. The lack of annual variability in SS loads at DEAD during these years was likely related to a lack of variance in annual streamflow. At FLAT, lower SS yields in these years may be attributed to the wide channels, broad sloping topography, and shallow soils characteristic of the Triassic Lowlands, features that may limit streambank erosion and sediment availability. Cumulative loads were heavily weighted by isolated extreme events such as Tropical Storm Hanna in WY 2008, Tropical Storm Lee in WY 2011, and a series of record-setting daily rainfall totals in late April and early May of WY 2014 (fig. 31A). For example, these three events resulted in annual loads at DIFF that exceeded the 10-year mean by 139, 74, and 129 percent in WYs 2008, 2011, and 2014, respectively. Notably, precipitation totals were also above average in WY 2010 but did not coincide with high SS yields because there were few large, intense precipitation events during that year. Water year 2010 was the only year with annual precipitation greater than the 10-year mean that did not produce a storm with an AEP greater than 0.64 (approximately the 1.5-year recurrence interval), except at DEAD. Annual SS loads are typically better related to large precipitation events and peak streamflows than annual precipitation or streamflow volume (Jastram, 2014). The cumulative sediment yields are similar at DIFF and SFLIL during large stormflows but differ in other conditions; more sediment is transported in DIFF than SFLIL during small storms and baseflow. Watershed physiographic characteristics are similar between these adjacent watersheds; therefore, these differences were likely a result of greater impervious land cover at DIFF.

About 70 percent of the annual SS load in any given year was generated during weeks that received more than 2 in. of rainfall in DEAD, DIFF, FLAT, and SFLIL (fig. 32A). Less than half of the annual SS yields were delivered during these weeks at LONG. The timing of sediment yields at LONG may be affected by backwater conditions as a result of the sampling location and proximity to the Lake Accotink impoundment. Backwater conditions, which occur primarily during large storms, reduce water velocity and subsequently cause deposition of SS. This may explain the poor relation between SS yield and peak stage (not presented) at this station. The effects of backwater are evident around the monitoring station, as temporary sand bars and islands were commonly observed in the stream channel following large hydrologic events. Following storm events when backwater conditions did not occur, the remobilization of previously deposited sediments resulted in streambed scour and visually conspicuous changes to the channel structure. An alternative location for this streamgage has been identified upstream of the zone of backwater influence and relocation has been scheduled for WY 2020. Overall, relations between precipitation and SS yields highlight that the majority of sediment transport occurred during large storm events.

Comparison of SS yields from Fairfax County, Gwinnett County, Georgia, and the CB-NTN reflect three important factors that drive sediment loads in these watersheds: (1) the Piedmont region has more erosive soils and urbanized land than the adjacent physiographic provinces (Gellis and others, 2009), (2) headwater streams typically transport more sediment than higher order streams owing to a lack of opportunity for in-channel deposition and greater energy availability for entrainment (Smith and Wilcock, 2015), and (3) SS loads typically increase with urbanization (Paul and Meyer, 2001). Median SS yields in Fairfax County watersheds were comparable to those computed for the Gwinnett County watersheds (Aulenbach and others 2017); though Gwinnett County yields spanned a much greater range and contained a mix of high- and low-yielding watersheds (fig. 33A). Fairfax County streams typically yielded more SS than CB-NTN watersheds—likely because monitored Fairfax County watersheds are much smaller and contain more urban land use than CB-NTN watersheds (Donovan and others, 2015, 2016; Smith and Wilcock, 2015). Additionally, Fairfax County watersheds have steeper topography than most CB-NTN watersheds; previous studies have reported positive correlation between topographic relief and SS yield (Jansen and Painter, 1974; Syvitski and Morehead, 1999; Syvitski and others, 2000). Two stations within the CB-NTN, DRGF and ACC, are located within Fairfax County and, though considerably larger, had similar land use and land cover characteristics. These stations provided a more direct comparison to the watersheds in this study and had comparable yields to stations in the Fairfax

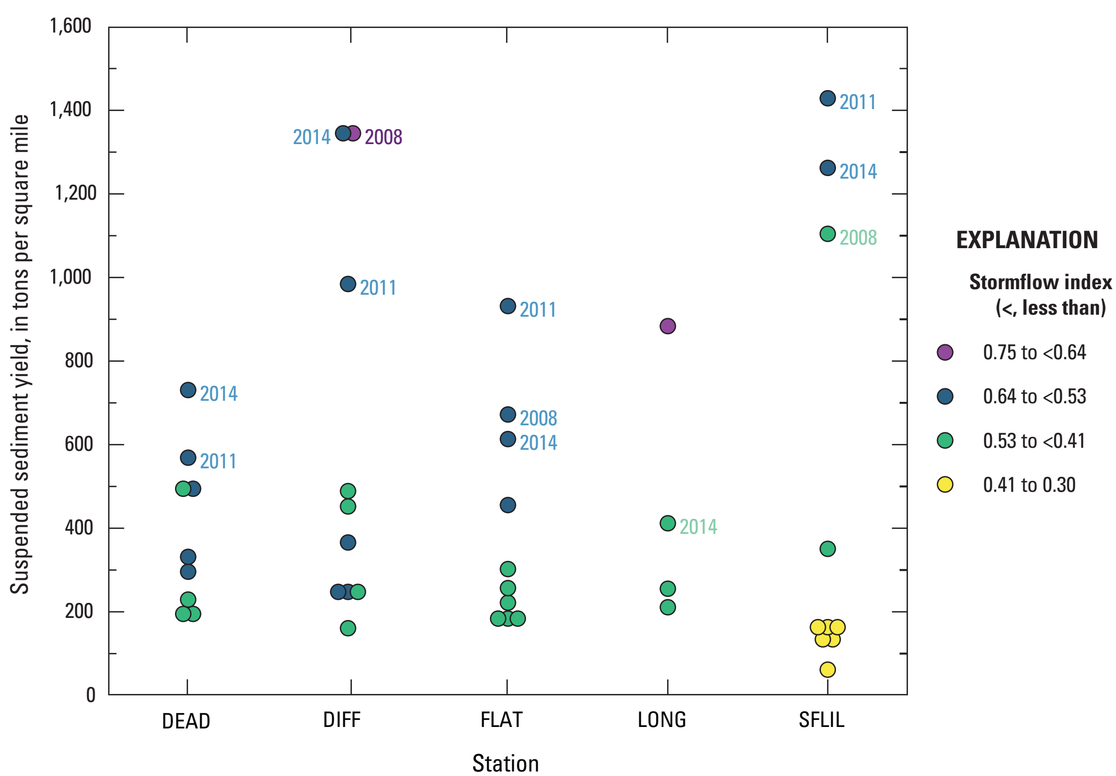

Figure 30. Annual suspended-sediment yields categorized by stormflow index for the five intensive monitoring stations in Fairfax County. Labeled years refer to water years (a period beginning October 1 and ending September 30). Station names are defined in table 1.

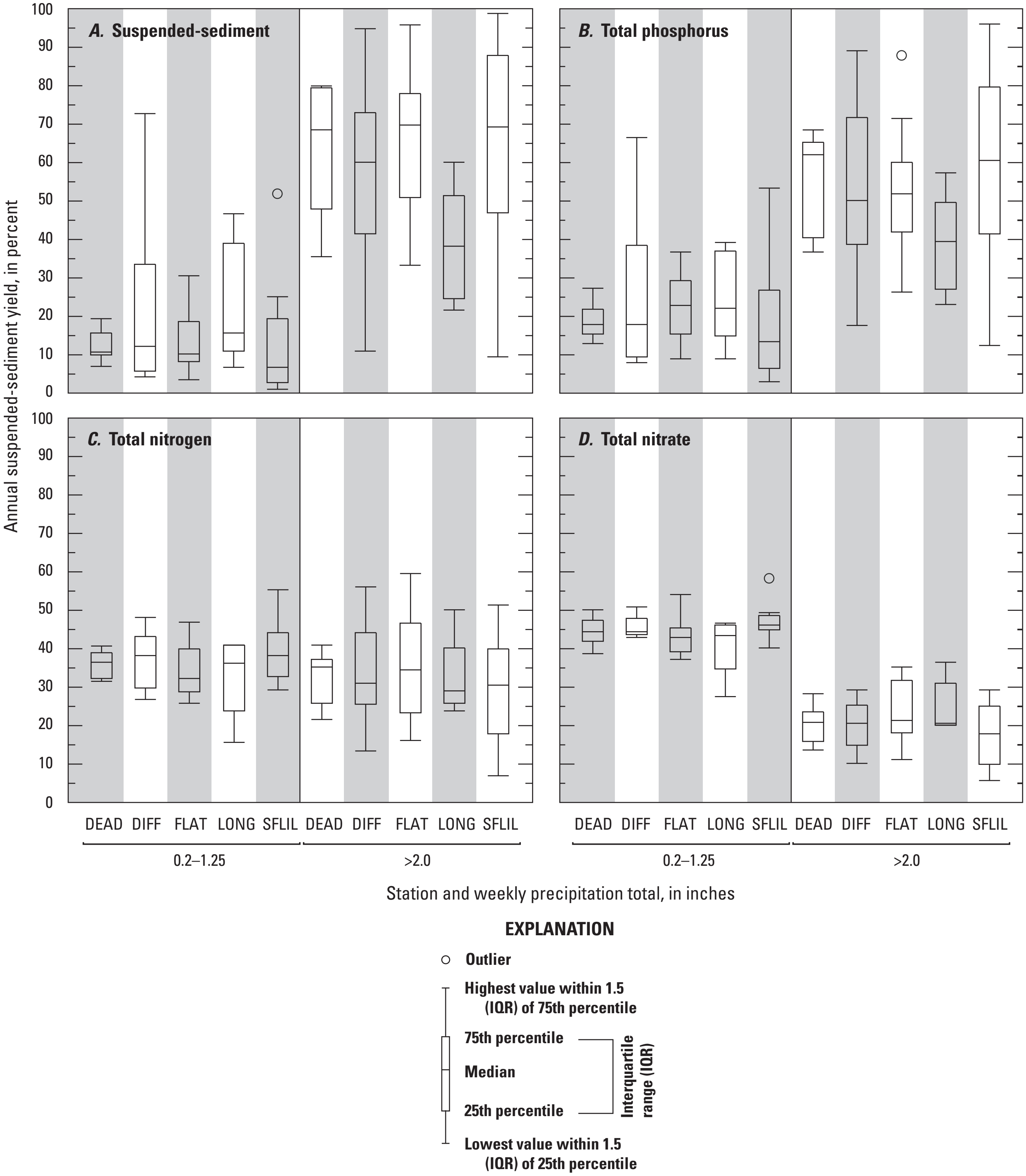

Figure 31. Percent of annual suspended-sediment (*A*), total phosphorus (*B*), total nitrogen (*C*), and nitrate (*D*) loads generated during weeks that received 0.2–1.25 inches of rain and more than 2 inches of rain for each of the five intensive monitoring locations. Station names are defined in table 1.

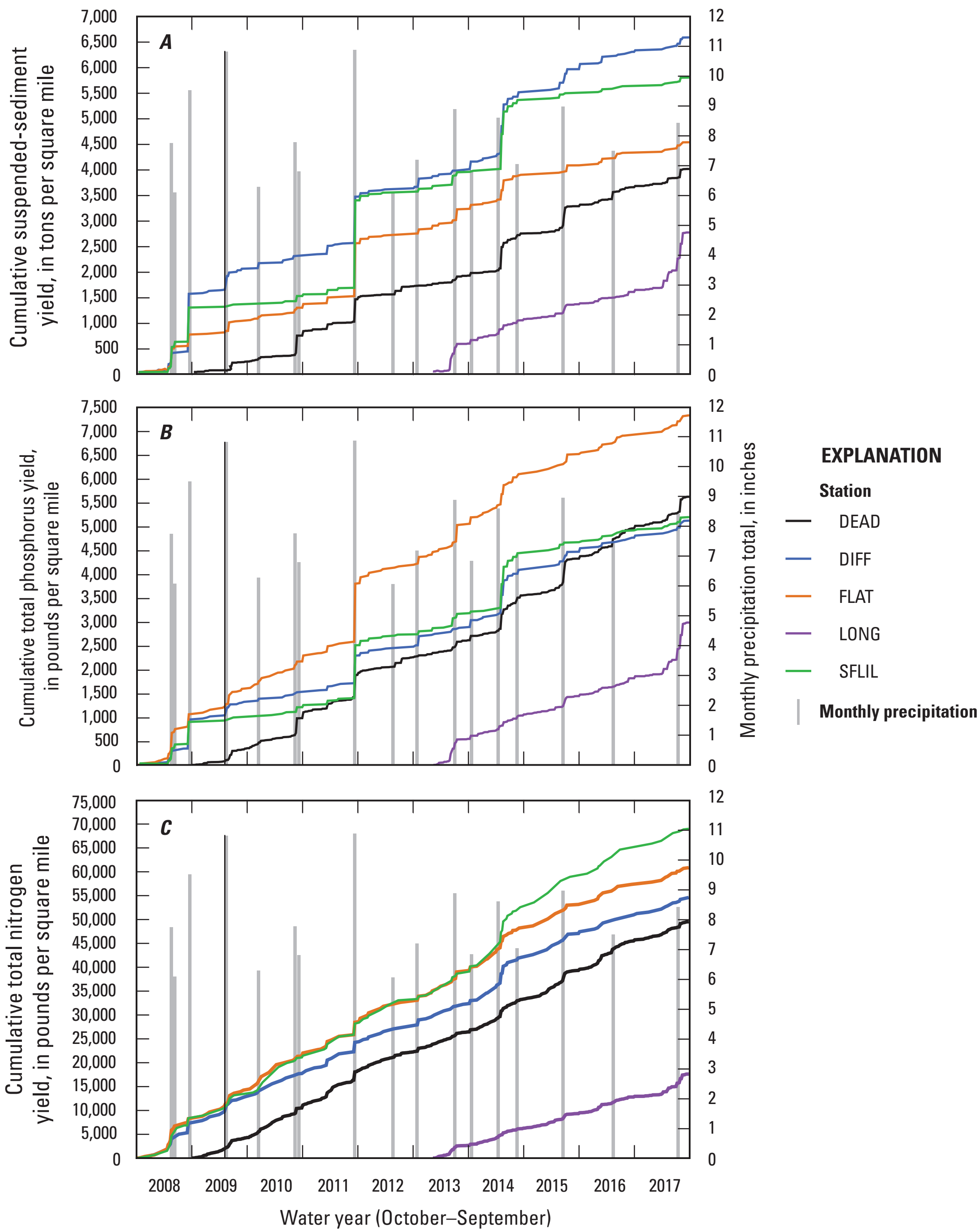

Figure 32. Cumulative estimated yield over the 10-year study period at the five intensive monitoring stations in Fairfax County for suspended sediment (*A*), total phosphorus (*B*), and total nitrogen (*C*). Monthly precipitation totals are presented for months when total rainfall was greater than or equal to 6 inches. Station names are defined in table 1.

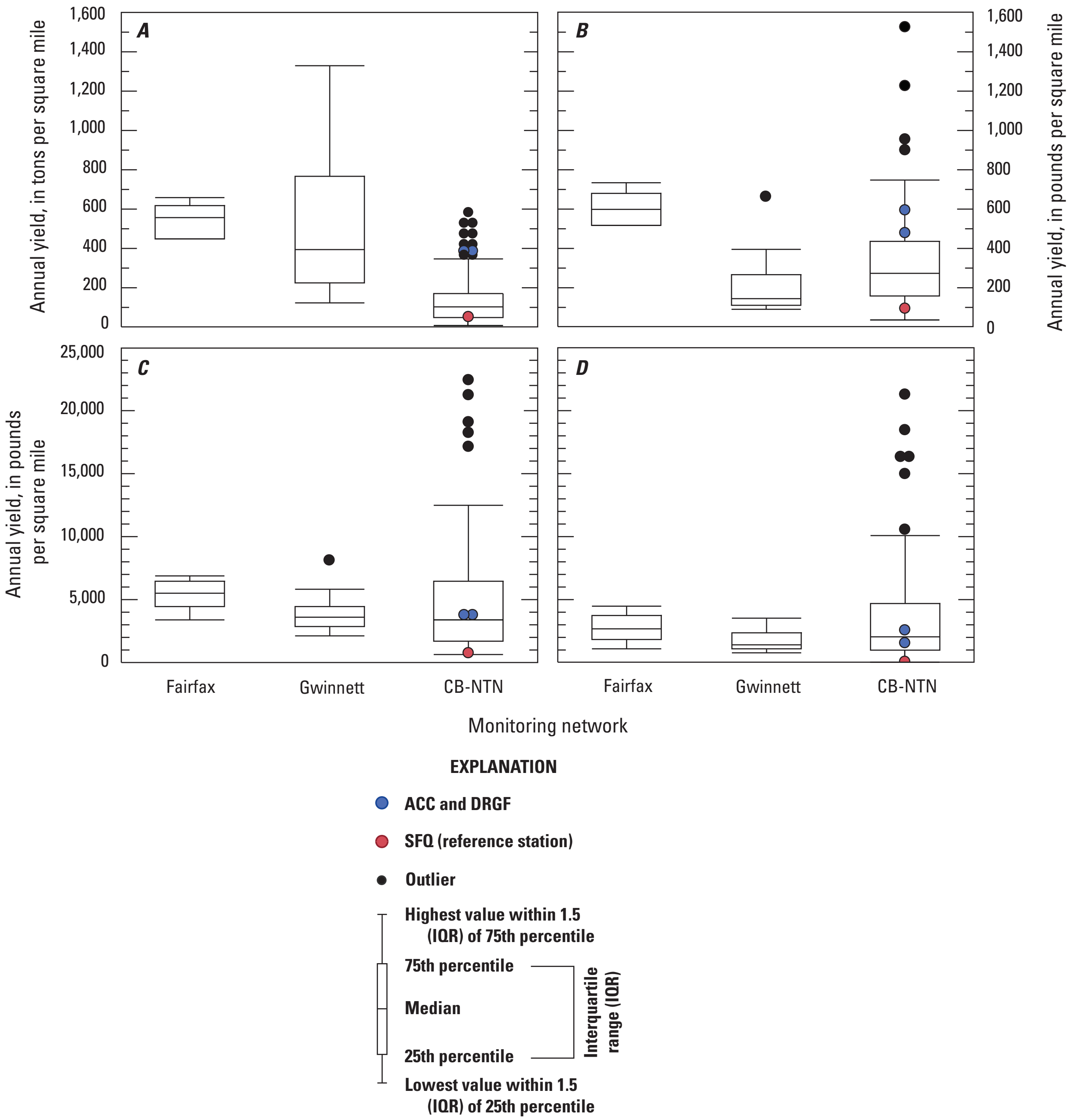

Figure 33. Suspended-sediment (*A*), total phosphorus (*B*), total nitrogen (*C*), and nitrate (*D*) yields from three monitoring networks—Fairfax County, Gwinnett County, Georgia, and the Chesapeake Bay Non-tidal Network. Blue points represent the mean yield at Accotink Creek near Annandale, Virginia (ACC) and Difficult Run near Great Falls, Virginia (DRGF), and red points represent the mean yield at the reference station, South Fork Quantico Creek near Independence Hill, Virginia (SFQ).

County monitoring network. Yields in the monitored Fairfax County watersheds were approximately seven times higher than at SFQ, the low-development reference watershed (Moyer and Blomquist, 2018), which highlights the effect of urbanization on SS mobilization.

Trends

At most stations, no trend was observed in turbidity or SS concentration in monthly samples over the 10-year study period and the combined trend result from all stations was nonsignificant for both constituents (table 4; fig. 34; Porter and others, 2020). The largest increases in SS concentration occurred in FLAT (11.5 percent, 0.34 milligram per liter per year [mg/L/yr]) and INDIAN (6.27 percent, 0.19 mg/L/yr), where turbidity increases of about 12 percent (0.24 Formazin nephelometric unit [FNU] per year) also occurred. The largest reductions in both SS concentration (–5.72 percent, –0.23 mg/L/yr) and turbidity (–9.81 percent, –0.31 FNU/yr) occurred at BRR. Changes in turbidity and SS concentration occurred relatively consistently over time in BRR and INDIAN but appear to have increased relatively quickly at FLAT between 2017 and 2018, a period when a stream restoration activity was occurring in proximity to the monitoring station. A Mann-Kendall method (see trend quantification method 3 in the Methods section) was used to investigate trends in mean daily turbidity calculated from 15-minute measurements at the intensive monitoring stations. Decreases in turbidity between 5 and 15 percent per year were observed in the lower 90 percent of mean daily values (approximately 1–10 FNU; fig. 17D) at all stations. Many of the changes that occurred in the 10th to 90th percentile of mean daily values at DEAD, DIFF, and SFLIL were significant (shaded area in fig. 17D). The changes that occurred in the top 10 percent of mean daily values were not typically significant at any station.

Trends in FN suspended-sediment concentration and load were estimated by WRTDS using a dataset of monthly and storm-targeted samples available from four intensive

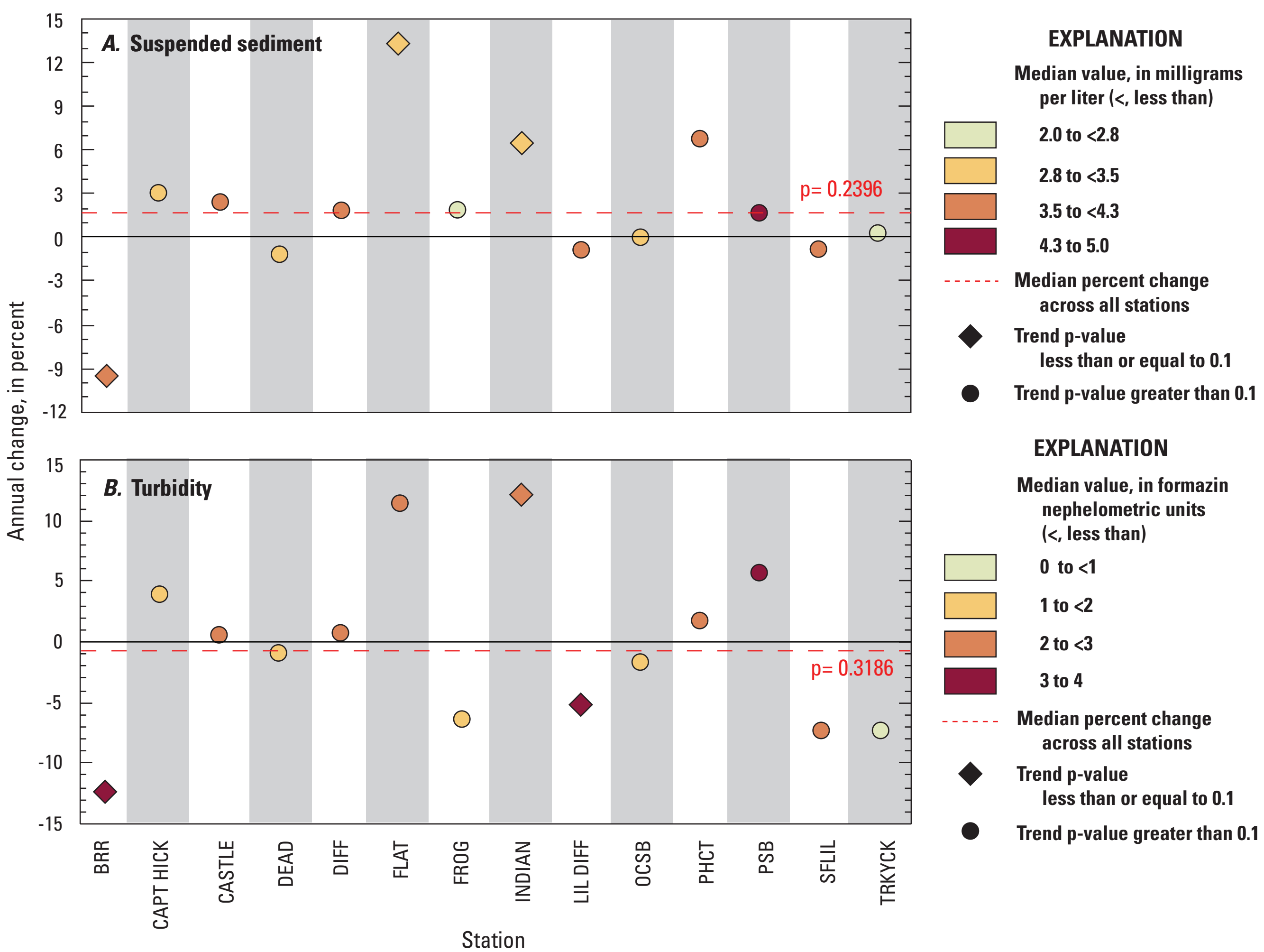

Figure 34. Suspended sediment (*A*) and turbidity (*B*) flow-normalized trend results expressed as a percent change per year at 14 monitoring locations between April 2008 and March 2018. P-value refers to the Regional Seasonal Kendall trend test. Station names are defined in table 1.

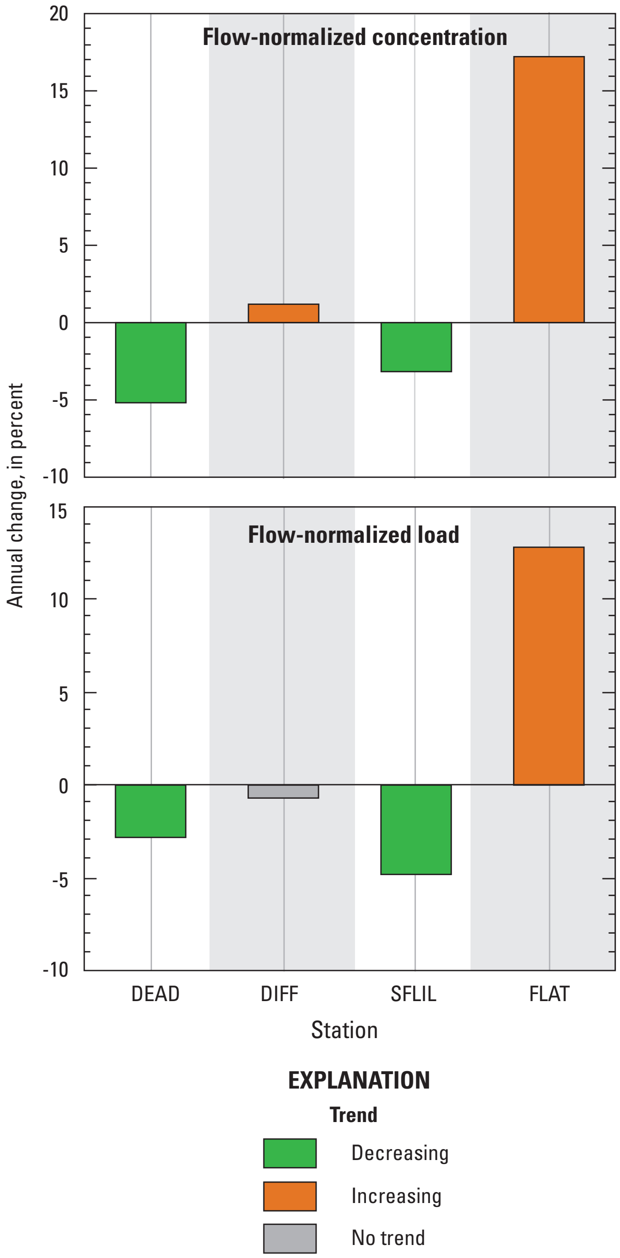

Figure 35. Trend in flow-normalized concentration and load of suspended sediment expressed as a percent change per year at four intensive monitoring locations between April 2008 and March 2018. Station names are defined in table 1.

monitoring stations (fig. 35). Both concentration and load declined at DEAD and SFLIL by as much as 5 percent per year and increased at FLAT by more than 10 percent per year. Changes in load at DIFF were nonsignificant, but concentrations had a significant increase of about 1 percent per year. Differences in FN concentration and load trends occur whenever the changes in water chemistry vary with flow; in this case, concentration increases may have been greater during low-flow conditions than high flows.

Phosphorus

Phosphorus is an essential nutrient required for the growth of plants and animals alike, but excess phosphorous in aquatic ecosystems can lead to eutrophication and, in turn, to ecosystem degradation. Phosphorus readily binds to soils and fluvial sediment, yet these matrices have a finite capacity to sorb phosphorous (Richardson and Craft, 1993). When available phosphorous sorption capacity is met, referred to as phosphorous saturation, through excess application of fertilizer or wastewater discharge, the unsorbed phosphorous fractions are exported to streams as dissolved phosphorous, and can result in degraded aquatic ecosystems (Conley and others, 2009). Transport and sources of phosphorous are higher in urban watersheds than undeveloped watersheds (Meybeck, 1998; Alvarez-Cobelas and others, 2009) and in some cases can equal the contribution from agricultural watersheds (Omernik, 1976; Paul and Meyer, 2001; Ator and others, 2011). Sources of phosphorous present in urban watersheds commonly include nonpoint sources (NPS) such as animal or pet waste, fertilizer, geologically derived phosphorous, and decomposition of plant and animal matter, as well as point-source discharges from municipal and industrial wastewater treatment facilities (La Valle, 1975; Paul and Meyer, 2001). There are no permitted point-source discharges of wastewater into the monitored Fairfax streams, highlighting the importance of understanding NPS inputs. Phosphorus inputs from these urban sources typically bind to sediments and are ultimately transported downstream by the erosion of streambeds, streambanks, floodplains, and upland areas by overland runoff and periods of elevated streamflow (Cowen and Lee, 1976; Yang and Toor, 2018).

Phosphorus can be temporarily immobilized in streambed or streambank sediments or deposited behind impoundments, which, in the short term, can reduce annual loads (Denver and others, 2010; Ator and others, 2011). Unfortunately, this temporarily stored phosphorous may be remobilized by erosion, impoundment overflow, maintenance dredging, or microbially mediated processes (Correll, 1998; Paul and Meyer, 2001; Ator and others, 2005). Even in watersheds where phosphorous inputs have been reduced, concentrations and loads may remain high owing to the ongoing desorption of phosphorous from sediments to the water column, and continued erosion of phosphorous-containing particulates (Denver and others, 2010; Wang and Liang, 2015). For example, phosphorous removal practices were implemented at the Norman M. Cole Pollution Control Plant in Fairfax County in the 1970s; however, a lag period of 10–15 years occurred between implementation of these practices and quantifiable reductions in phosphorous and an associated decline in phytoplankton as a result of continued sediment loading to the water column (Jones and others, 2017).

Increases in dissolved phosphorous can result from warming temperatures that affect both biotic and abiotic processes (Duan and others, 2012), the prevalence of anoxic conditions (House and Denison, 2002; Lehtoranta and Pitkänen, 2003), increased nutrient applications causing phosphorous-saturated soils (Sharpley, 1995), increased soil pH (James and Barko, 2004), or changing salinity levels (Haq and others, 2018). For example, in oxic environments phosphorous forms strong bonds to clays, iron and aluminum oxides, and organic matter, and may remain stored in streambank and streambed sediments (Manning and Wang, 1994; Lehtoranta and Pitkänen, 2003). Alternatively, in eutrophic environments, excessive primary production can cause anoxic conditions that can weaken these bonds and result in diffusion of dissolved phosphorous to the water column (Correll, 1998). Clay soils have a greater phosphorous sorption capacity than sandy soils due to grain size and their net negative charge, which affects surface area availability, increases aluminum and iron activity, and forms bonds with positively charged nutrients (Olsen and Watanabe, 1957; Ballard and Fiskell, 1974; Xu and others, 2006). Because of this affinity to bind to sediment, phosphorous generally enters surface waters through surficial flows, rather than groundwater, and is commonly associated with erosional processes and transported downstream by way of SS (Correll, 1998; Denver and others, 2010). A phosphorous criterion specific to Virginia streams currently does not exist; however, the EPA reference condition for streams in the ecoregions in Fairfax County (45, 64, and 65) are 0.03, 0.04, and 0.03 mg/L, respectively (U.S. Environmental Protection Agency, 2000a).

Hydrologic, Seasonal, and Spatial Patterns

Median TP concentrations ranged from 0.016 to 0.077 mg/L as phosphorous, with a networkwide median of 0.022 mg/L as phosphorous, and were composed primarily of dissolved phosphorous, which had a networkwide median concentration of 0.013 mg/L as phosphorous, most of which was orthophosphate (OP; networkwide median concentration of 0.012 mg/L as phosphorous; fig. 36). A strong positive relation between TP concentration and streamflow was apparent, and as streamflow increased the phosphorous composition became particulate dominant (fig. 37). Although phosphorous generally was present at low levels in Fairfax streams, concentrations and yields generally were higher than those measured in less developed watersheds throughout the Chesapeake Bay watershed (Moyer and others, 2017) Even small quantities of OP, the most biologically available form of phosphorous, can cause eutrophication in freshwaters (Correll, 1998) and has been associated with harmful algal blooms (Davis and others, 2010).

In 60 percent of stations, TP concentrations were significantly higher in the warm season than in the cool season (fig. 36). This pattern is consistent with temperature-dependent releases of OP from sediments (Duan and others, 2012) in which increased WT facilitates increased microbial metabolism that augments phosphorous mineralization and dissociation to surrounding waters (Duan and Kaushal, 2013; Sugiyama and Hama, 2013; Wilhelm and others, 2014). Additionally, increased decomposition and subsequent depletion of DO produces anoxic conditions in warmer months that then triggers the disassociation of phosphorous from iron, aluminum, and manganese in sediments and organic matter into the overlying water column (Duan and Kaushal, 2013). This seasonal effect also was related to SS concentration, which as previously discussed, was elevated in warm months and is strongly related to TP concentration. Of the stations with the overall highest TDP concentrations, the seasonal signal was weaker at DOGUE and RABT. This may indicate greater year-round phosphorous availability from a consistent input of nonpoint sources and, in the case of DOGUE, the low sorptive capacity of sandy soils.

Median TP concentrations in both monthly and storm samples were highest at stations located in the Triassic Lowlands (FROG, FLAT, and HPEN), two of the stations in the Coastal Plain (DOGUE and PSB), and two stations within the Piedmont (DEAD and RABT). Elevated TP at FROG, FLAT, and HPEN likely was a result of dissociation of phosphorous from the underlying geology—shale and limestone produced from particulate matter of plants and animals and consequently rich in phosphorous (Froelich and Zenone, 1985b). Additionally, poor drainage in these soils results in anoxic conditions that can lead to iron reduction and the subsequent release of iron-bound phosphorous to the water column (Lehtoranta and Pitkänen, 2003). Elevated TP in Coastal Plain stations may be a result of the low sorptive capacity of quartz sand-rich unconsolidated soils, which limits storage and promotes mobilization to streams (Nair and others, 2004; Chakraborty and others, 2012). Additionally, phosphorous may be elevated because of contributions from NPS such as septic system effluent or leaking sanitary sewer lines. At SFLIL, the highest TP concentrations were associated with the highest SS concentrations that typically occurred during the largest storm events. Spatial and seasonal results for TDP, OP, and total particulate phosphorus (TPP), similar to figure 36, are provided in appendix 2 in figures 2.2, 2.3, and 2.4, respectively.

Loads

Total phosphorous and TPP concentrations generally were well predicted by models that contained turbidity and streamflow terms, which reflects the strong relation between sediment and phosphorous transport (appendix 2, figs. 2.5, 2.6). The significance of either a seasonal or WT term in most models was indicative of seasonal fluctuations in phosphorous concentrations. A positive time term was included in several models, which was consistent with trends in phosphorous concentrations documented throughout the county and discussed in more detail below.p

Median annual TP yields were highest at FLAT and DEAD and ranged from 247 to 642 pounds per square mile (lbs/mi^2) networkwide (Porter and others, 2020). The 10-year cumulative TP yield was highest at FLAT because of relatively high phosphorous concentrations and streamflow yield (fig. 31B). The highest TP loads occurred in years with high

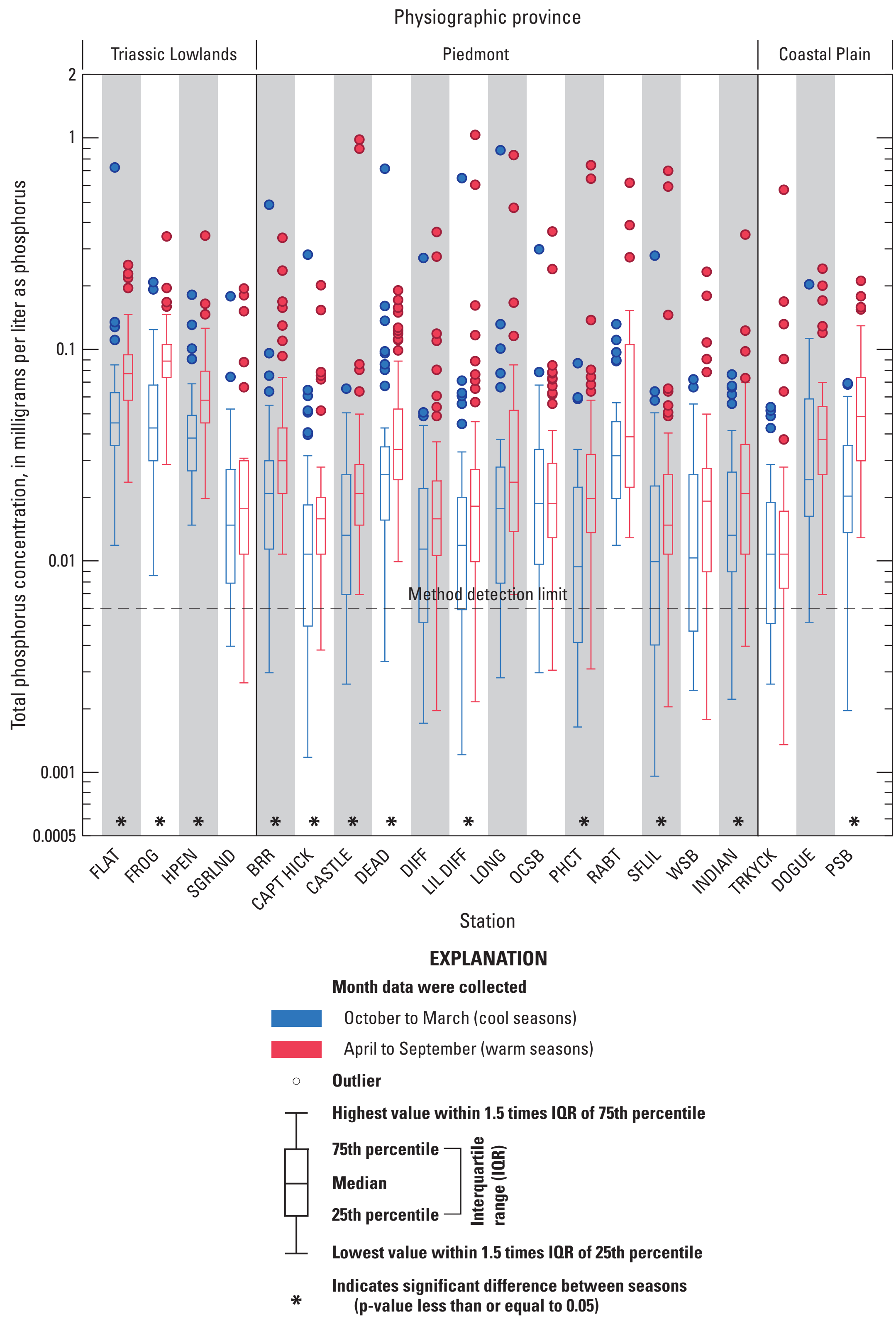

Figure 36. Total phosphorus results from monthly samples with comparison of data collected during the cool (October–March) and warm (April–September) seasons for the 20 monitoring stations in Fairfax County. Significant differences between warm and cool season sample concentration distributions were determined from a nonparametric Wilcoxon test with a p-value of ≤0.05. Stations are arranged by physiographic province and station names are defined in table 1.

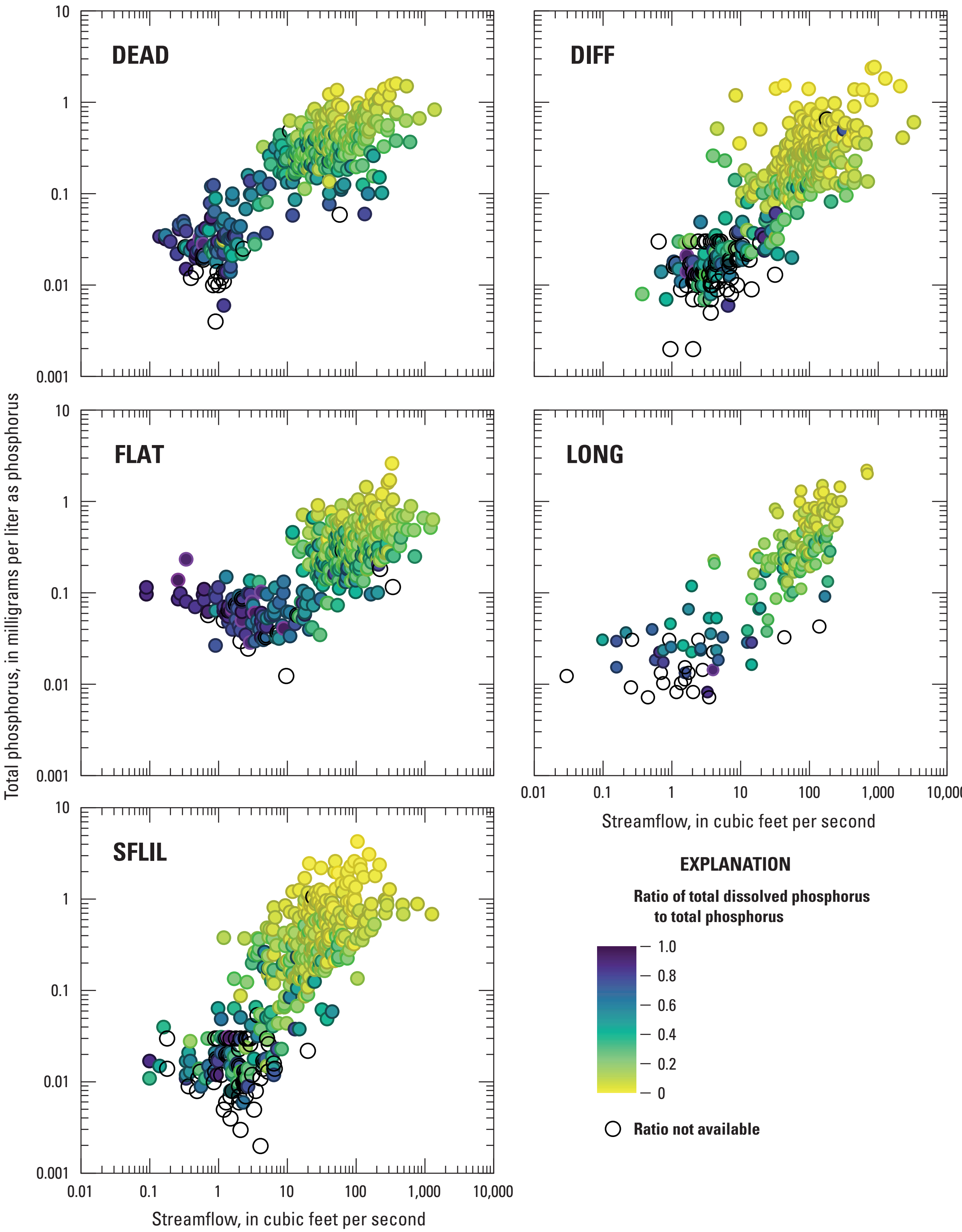

Figure 37. Total phosphorus concentrations compared to streamflow in the monthly and storm samples collected at the five intensive monitoring stations in Fairfax County. Station names are defined in table 1.

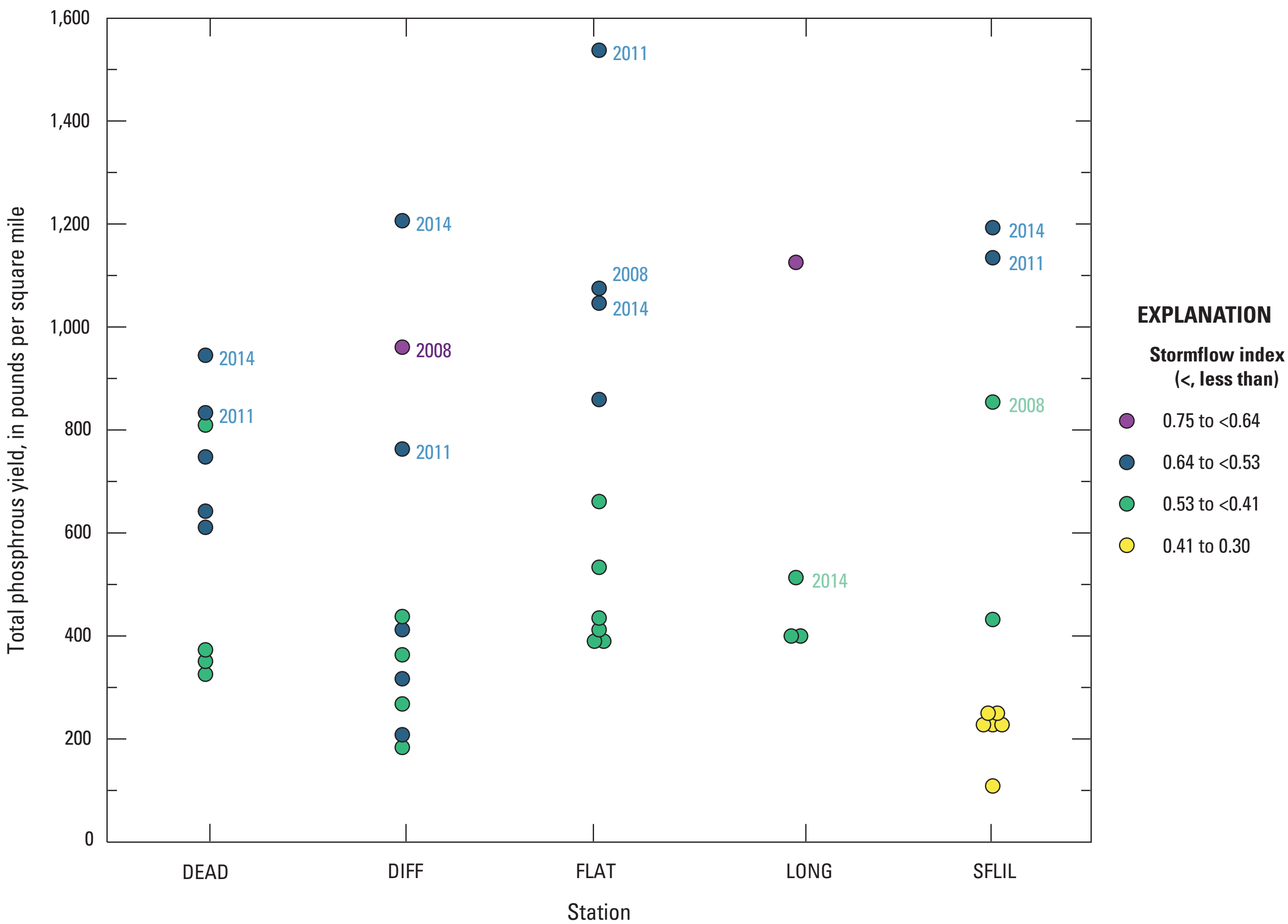

Figure 38. Annual total phosphorus yields for the five intensive monitoring stations in Fairfax County. Labeled years refer to water years (a period beginning October 1 and ending September 30). Station names are defined in table 1.

precipitation totals, which exported most streamflow as stormflow (fig. 38). Weeks in which more than 2 in. of rain fell generated about 50 percent of the annual TP loads (fig. 32B), highlighting the relation between streamflow and TP export. Interannual variability in phosphorous yields was most apparent at DIFF, FLAT, and SFLIL, where the highest loading years also were the wettest years during the study period and had the highest peak annual flows. For example, TP yields at SFLIL ranged from as high as 1,275 lbs/mi^2 in WY 2014 to as low as 103 lbs/mi^2 in WY 2009. The range in annual loads was much lower at DEAD and LONG because of low interannual variability in streamflow yield at those stations.

Phosphorus loads primarily were composed of TPP at all stations (fig. 39), but the composition varied both spatially and annually. The TPP portion of the TP load was greatest at all stations in the wettest years. The TPP:TP ratio was lowest at FLAT because of a greater composition of dissolved phosphorous, likely contributed by geologic materials. TDP loads at DEAD are typically higher than those at DIFF, LONG, or SFLIL and may result from physical or chemical processes that promote the desorption of phosphorus from stream sediments or from NPS contributions of phosphorous. Overall, the high proportion of particulate phosphorous at all watersheds suggests that management of phosphorous loads is strongly dependent on management of SS.

Total phosphorous yields from Fairfax County were higher than most yields reported in comparison studies—at or above the 75th percentile of yields from Gwinnett County, Georgia (Aulenbach and others 2017), and ranged between the 75th and 90th percentile of CB-NTN watersheds (fig. 33B). Yields from this study were comparable to those from the two predominantly urban CB-NTN watersheds in Fairfax County (ACC and DRGF), but five times higher than at SFQ. Elevated phosphorous yields in Fairfax County likely are related to the similarly high SS yields in these watersheds, given the strong relation of TP to sediment, and may be intrinsically higher than CB-NTN stations owing to factors related to stream order and watershed size. Larger watersheds and higher order streams typically have smaller yields than small headwater streams as a result of fluvial trapping of sediments (Smith and Wilcock, 2015). Total phosphorous yields were lower in Gwinnett County than Fairfax County, despite similar SS

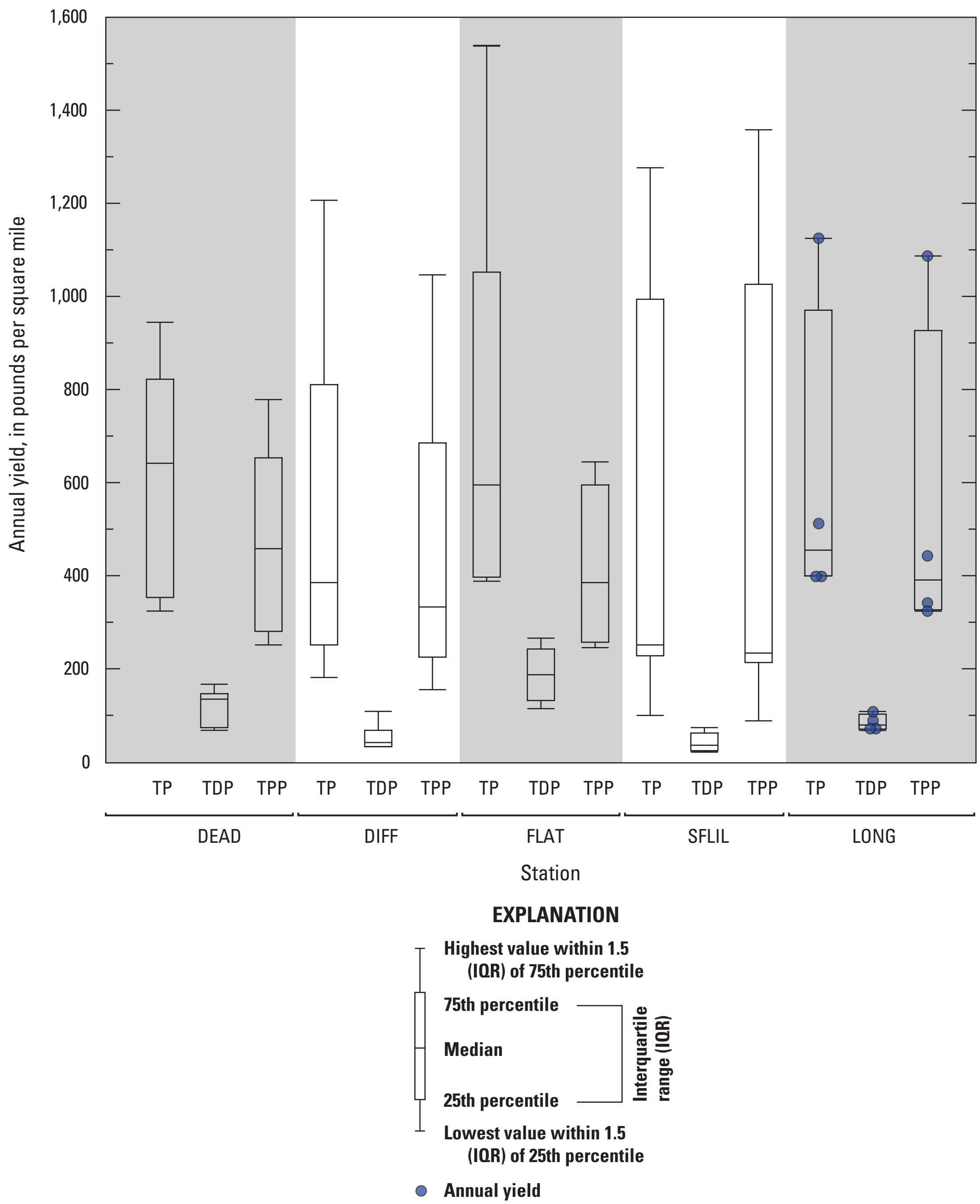

Figure 39. Boxplot of annual total phosphorus (TP), total dissolved phosphorus (TDP), and total particulate phosphorus (TPP) yields for the five intensive monitoring stations in Fairfax County. Points included for LONG owing to sample size (n=5). Note that it is possible for dissolved or particulate fractions to exceed the total due to model uncertainty. Station names are defined in table 1.

yields and nearly identical mean TDP:TP ratios (18.2 and 18.9 percent, respectively) (Aulenbach and others, 2017). This comparison suggests that TDP concentrations and (or) the phosphorous concentration of sediments are higher in Fairfax County streams than Gwinnett County streams, a condition that may result from differences in NPS phosphorous inputs or biogeochemical processes that affect the release of TDP from sediments.

Trends

The combined TP trend result (in monthly samples) from all stations revealed significant concentration and FN concentration increases of about 4 percent per year (table 4; fig. 40A; Porter and others, 2020). Samples in this trend analysis typically were collected during baseflow conditions when TP concentrations are relatively low. Therefore, these percent changes equate to small changes in concentration; the largest significant TP increase between 2008 and 2018 was 0.02 mg/L at PSB. FLAT and FROG have the highest median TP concentrations of all network stations; a significant TP decrease of about 4 percent per year (0.003 mg/L/yr) occurred at FROG.

Increases in TP observed throughout the network are consistent with increases observed in OP, TDP, and TPP (figs. 40B, 41; Porter and others, 2020). The combined trend result from all stations revealed significant concentration and FN concentration increases in each of these parameters. Dissolved phosphorous increases occurred in all streams except FLAT and FROG and most of these increases were significant. Median TDP increases were about 9 percent per year, but as with TP, TDP concentrations are very low in the samples used for this analysis (0.01 mg/L on average), so care should be applied when interpreting percent changes. A significant TDP decrease of about 5 percent per year occurred at FROG (–0.003 mg/L/yr), whereas no trend was observed at FLAT. Dissolved phosphorous and OP trends are similar in most streams—concentrations have increased at all stations but FLAT and FROG—because dissolved phosphorous is dominantly OP. The similarity of TP and TDP trends in most stations indicate that changes in particulate phosphorous were relatively small and that TP trends mostly resulted from dissolved phosphorous changes.

Trends in flow-normalized phosphorous concentration (in monthly samples) and load estimates by WRTDS (monthly and storm-targeted samples) indicate significant increases in TP concentrations and load at DIFF and FLAT by about 5 percent per year; whereas, concentration increased and load declined at DEAD and no trends occurred at SFLIL (fig. 42). The seemingly contradictory trends at DEAD result from decreasing TP concentrations during baseflows and increasing TP concentrations during stormflows, the latter of which

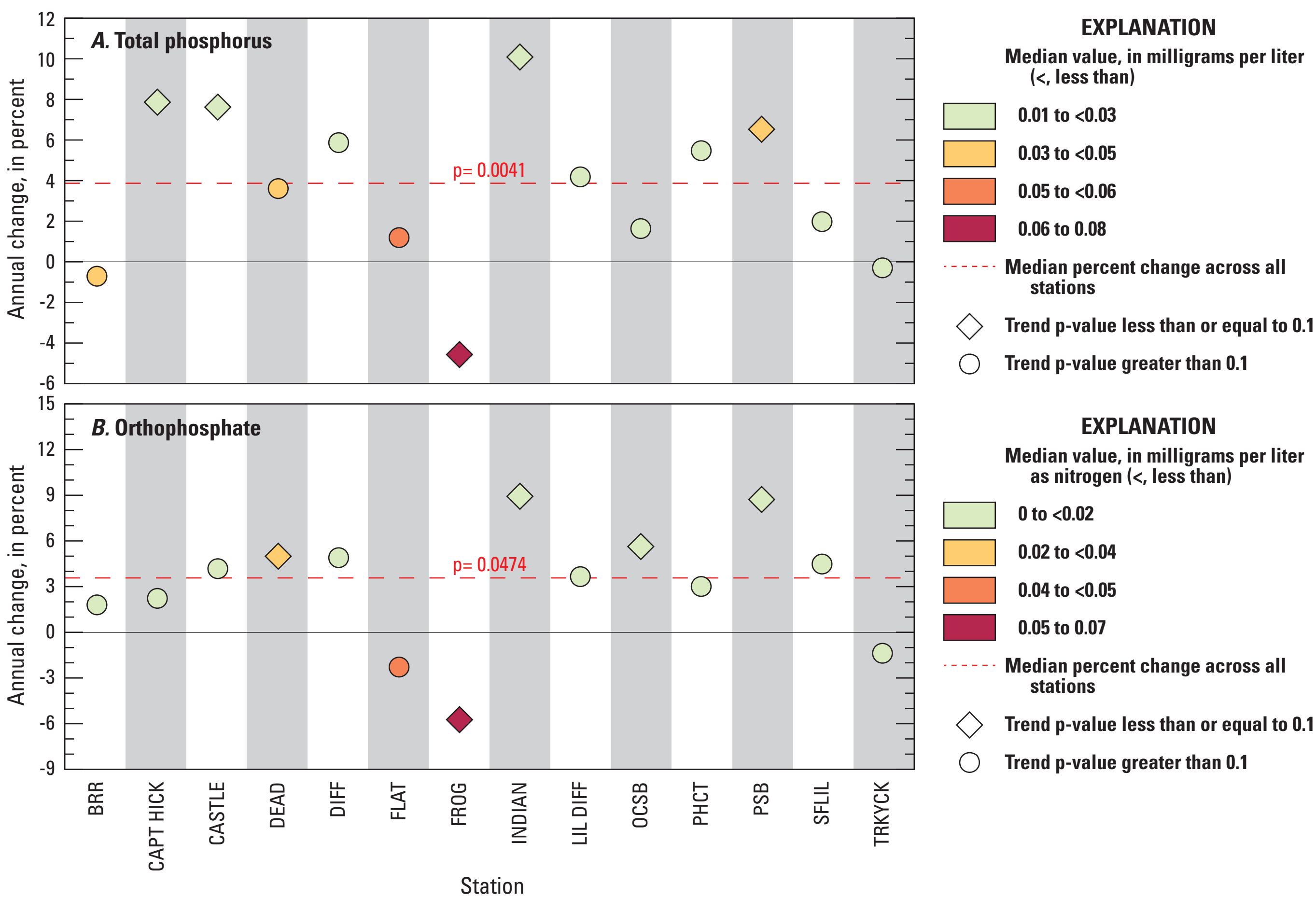

Figure 40. Total phosphorus (*A*) and orthophosphate (*B*) flow-normalized trend results expressed as a percent change per year at 14 monitoring locations between April 2008 and March 2018. The p-value refers to the Regional Seasonal Kendall trend test. Station names are defined in table 1.

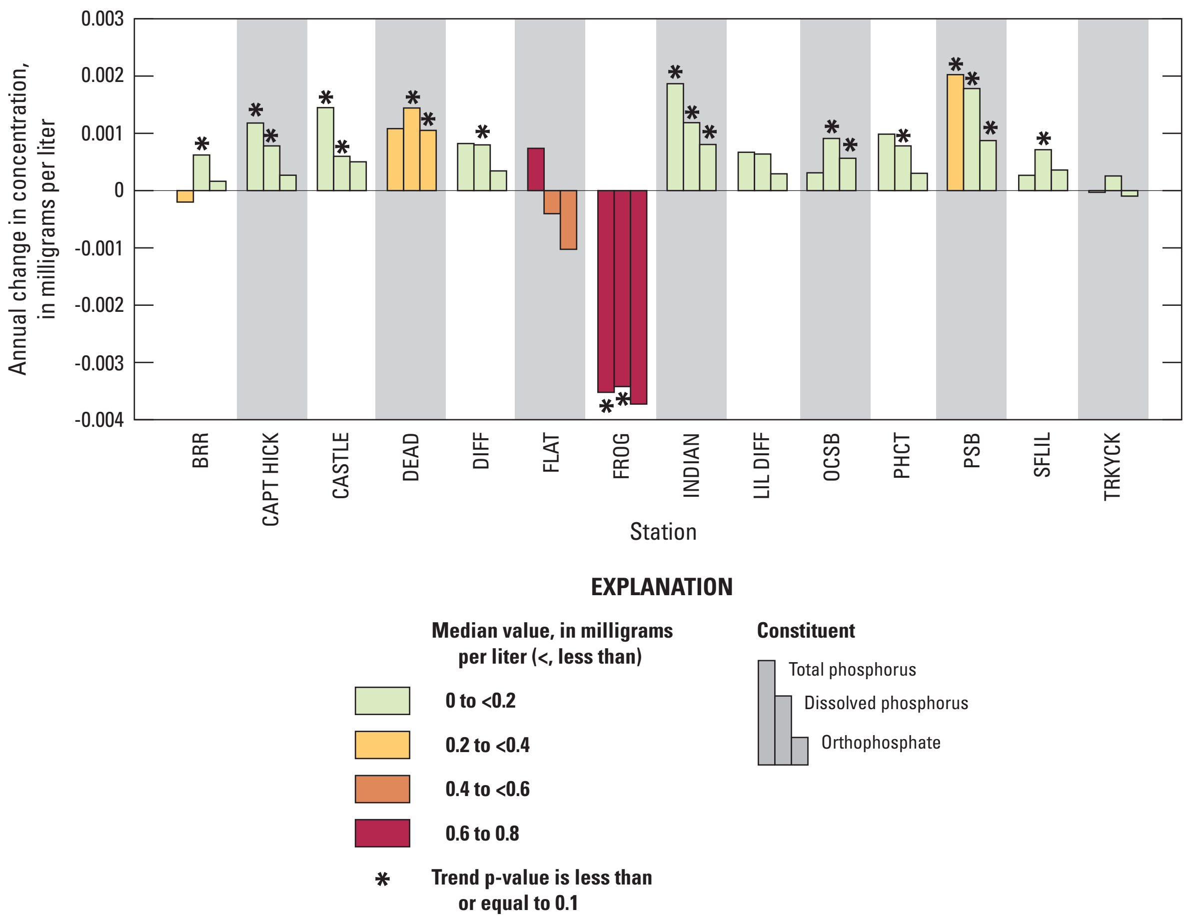

Figure 41. Annual change in flow-normalized concentrations of total phosphorus, dissolved phosphorus, and orthophosphate at 14 monitoring locations between April 2008 and March 2018. The p-value refers to the Regional Seasonal Kendall trend test. Station names are defined in table 1.

has a large influence on trends in load. Similar to the monthly concentration results previously discussed, increases in TDP also occurred in most stations. Unlike the monthly sample dataset, where trends in TPP were unavailable because most results were censored, the inclusion of storm samples allowed for computation of TPP trends in concentration and load. Increases in TPP concentration and load occurred at DIFF and FLAT, and decreases occurred at DEAD and SFLIL.

Nitrogen

Although nitrogen is naturally occurring and essential to the growth of plants and animals, inputs that exceed ecosystem processing and storage capacities may be exported to down-gradient waterbodies (Hem, 1985; Paul and Meyer, 2001). Nitrate, the biologically available dissolved form of nitrogen, is the primary delivery pathway of nitrogen to streams. This is a result of its high solubility, which enables it to move readily through land surfaces to groundwater, where it can persist for decades (Hem, 1985; Keeney and Follett, 1991). The average residence time of groundwater discharged to Fairfax County streams varies from about 4 to 14 years, with longer residence times associated with streams that drain Coastal Plain geology (Sanford and others, 2015); thus, some of the NO_3^- in Fairfax County streams likely entered these watersheds many years ago. Ultimately, excessive nitrogen promotes eutrophication and hypoxia and consequently degrades aquatic ecosystem health (Hem, 1985). Common urban nonpoint nitrogen inputs include anthropogenic sources such as atmospheric deposition, fertilizer application, leaking wastewater infrastructure, septic systems, and pet waste (Paul and Meyer, 2001; Bettez and Groffman, 2013; Hyer and others, 2016), as well as natural sources such as plant humic substances and biological fixation (Wanielista and others, 1977; Carpenter and others, 1998). The export of nitrogen associated with these inputs is positively correlated with urban development (Shields and others, 2008; Tasdighi and others, 2017), though nitrogen retention varies with watershed size (Groffman and others, 2004; Kaushal and others, 2008). A nitrogen criterion specific to Virginia streams does not currently exist; however, the EPA reference condition for streams in the ecoregions in Fairfax County (45, 64, and 65) are 0.61, 2.23, and 0.62 mg/L, respectively (U.S. Environmental Protection Agency, 2000a).

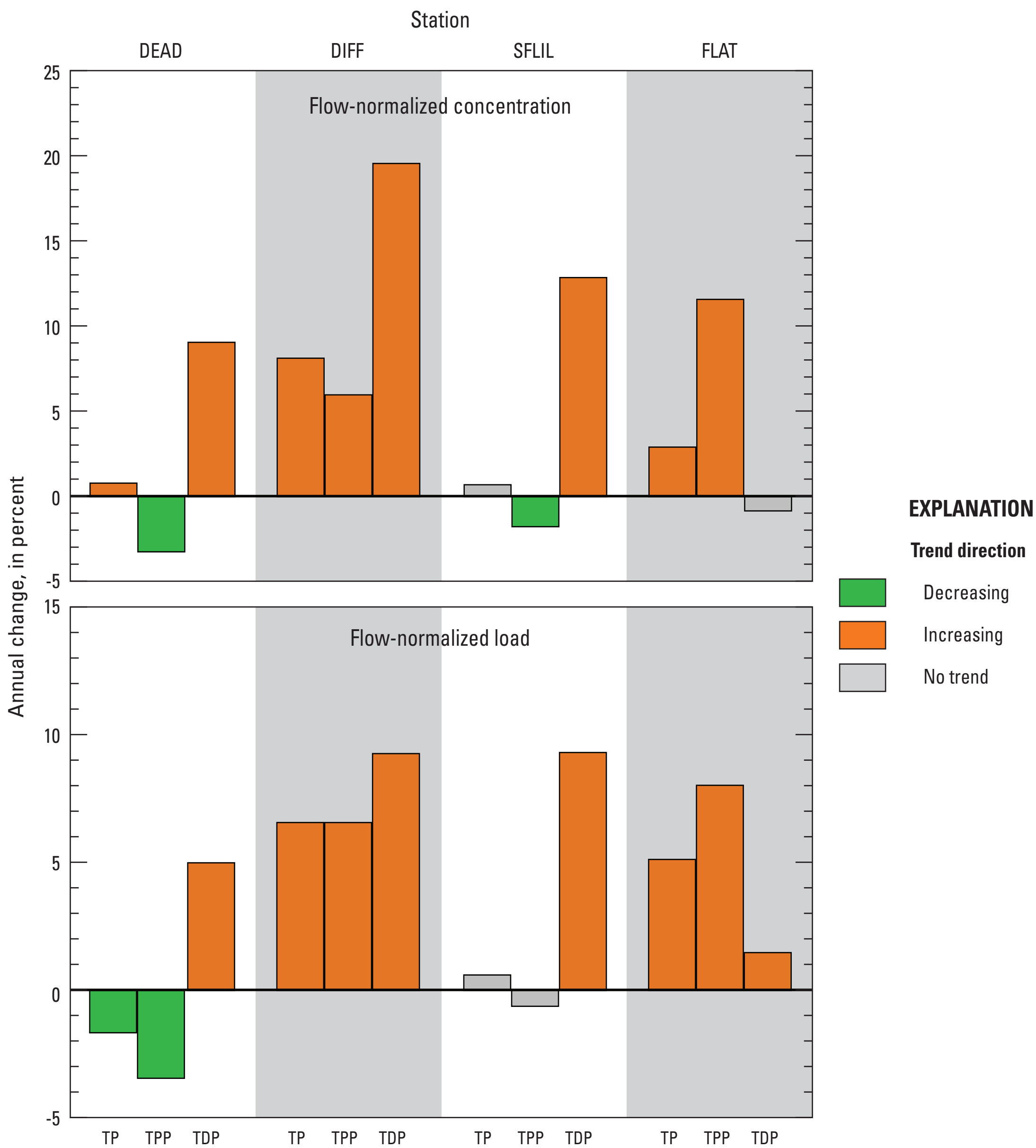

Figure 42. Trend in flow-normalized concentration and load of total phosphorous (TP), total particulate phosphorous (TPP), and total dissolved phosphorus (TDP), expressed as a percent change per year at four intensive monitoring locations between April 2008 and March 2018. Station names are defined in table 1.

Hydrologic, Seasonal, and Spatial Patterns

Total nitrogen, measured from monthly samples that commonly represented nonstormflow conditions, was primarily dissolved nitrogen (mean TDN:TN ratio of 94 percent), mostly delivered to streams as NO_3^- (mean NO_3^-:TDN ratio of 82 percent). Other forms of TDN included organic nitrogen, ammonia, and nitrite. Nitrate and nitrite were analyzed as a combined fraction for this study and will be referred to as nitrate or NO_3^- hereafter, as nitrite is quickly oxidized to NO_3^- in most stream conditions. Ammonia also was typically low because aerobic conditions transform ammonia to nitrite and nitrate through nitrification.

Nitrate concentrations were typically highest during low to intermediate streamflows and diluted during large flow events. These patterns are evident in monthly and storm samples collected from the five intensive monitoring stations and in the continuous NO_3^- data collected at SFLIL (fig. 43). Total nitrogen concentrations typically increased with streamflow, despite NO_3^- dilution, which indicates the importance of particulate nitrogen transport during storm flows (fig. 44). Dissolved nitrogen represented about 50–60 percent of TN in samples collected during stormflows, but the highest TN concentrations, greater than 10 mg/L at some stations, observed during the highest streamflow samples were almost entirely composed of particulate nitrogen. Coarse organic matter

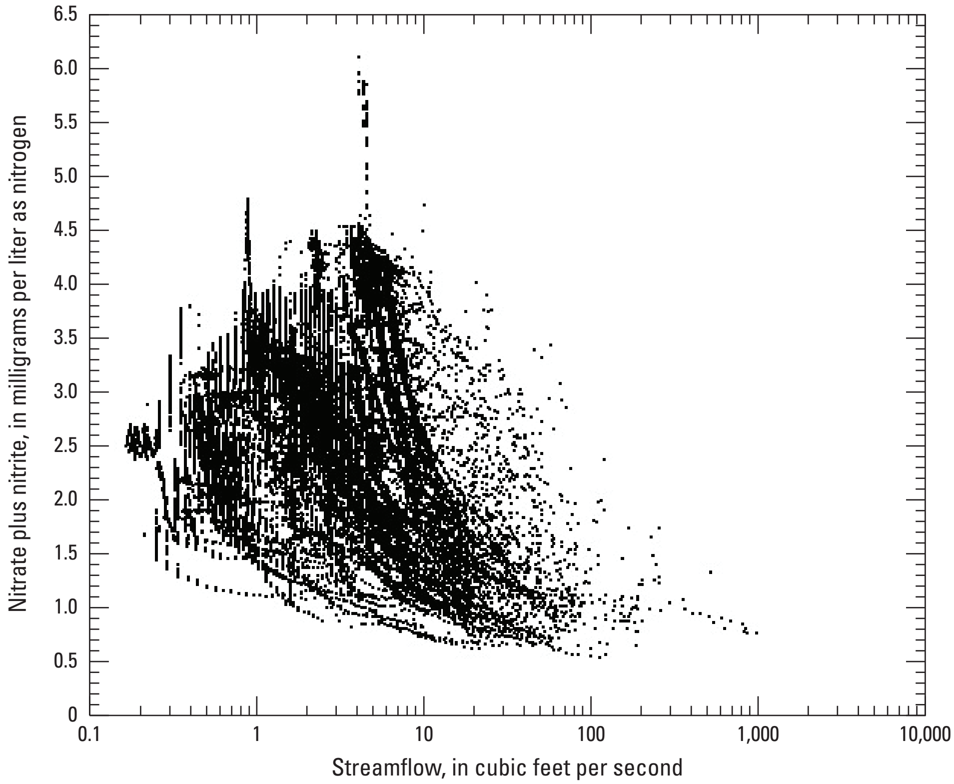

Figure 43. Continuous nitrate data compared to streamflow measured at the South Fork Little Difficult Run (SFLIL) streamgage in water year 2017. A water year begins October 1 and ends September 30.

dominates the particulate nitrogen budget during these large storm events and results from the transport of leaves, grass clippings, woody debris, and other allochthonous material carried in runoff to streams.

Total nitrogen concentrations varied by season at approximately half of the stations and were typically lowest in warm months when denitrification rates are greatest, though a few streams deviate from this pattern (fig. 45). The only station with significantly higher warm season concentrations was PHCT, where uncharacteristically high TN and dissolved nitrogen concentrations were observed in August and September in several years. These observations were coincident with the lowest annual streamflows and signal elevated dissolved nitrogen in deeper groundwater discharges. Terrestrial denitrification (reduction of NO_3^- to atmospheric N2) is often the dominant nitrogen loss term in nitrogen budgets of mid-Atlantic watersheds (Van Breemen and others, 2002) and similar seasonal nitrogen patterns (elevated cool season concentrations) have been documented in other urban watersheds (Tufford and others, 1998; Deek and others, 2010; Meng and others, 2018).

Denitrification rates vary in the Coastal Plain as a result of heterogenous lithology but are low in watersheds with predominantly sandy sediments that contain little organic material and where water remains oxic (Ator and others, 2005; Ator and Denver, 2015). Nitrate concentrations remain relatively stable throughout the year at DOGUE, a watershed in the Coastal Plain; whereas, a seasonal signal associated with denitrification was apparent at PSB, a neighboring Coastal Plain watershed. The sandy soils characteristic of DOGUE promote oxic conditions, which limit denitrification; whereas, PSB is underlain by clays and silts that produce greater rates of anoxic conditions that favor denitrification.

Nitrate also exhibited low seasonal variability at CAPT HICK (fig. 2.5), which is likely caused by year-round contributions of septic system effluent, a dominant nitrogen source in the watershed that is responsible for the elevated NO_3^- concentrations (Hyer and others, 2016). Streamflows are lowest during summer months and are primarily supported by groundwater discharges, which contain high NO_3^- concentrations at CAPT HICK. Although denitrification rates can be high in summer months, the concentrated groundwater contribution during this period may have offset expected reductions. The effect of concentrated low flows was most prevalent at PHCT, which also has a high density of septic system infrastructure. PHCT was the only station where the median TN concentration was significantly higher in the warm season, which was a result of anomalously high NO_3^- concentrations collected in some summer low-flow samples.

A network-wide median TN concentration of 1.6 mg/L occurred in the monthly discrete samples collected across all 20 watersheds during the study period, but concentrations

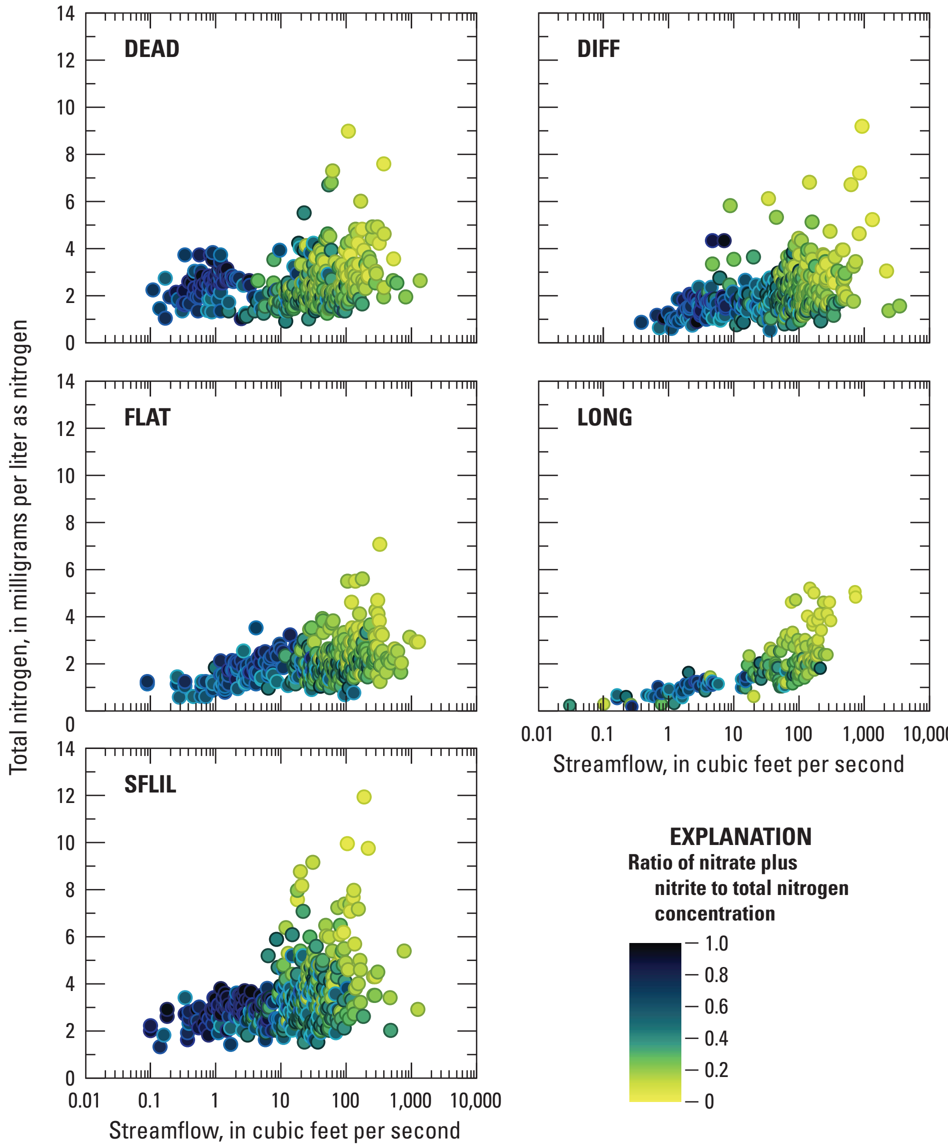

Figure 44. Total nitrogen concentrations compared to streamflow in the monthly and storm samples collected at the five intensive monitoring stations in Fairfax County. Station names are defined in table 1.

varied between stations. The highest NO_3^- concentrations were consistently observed at CAPT HICK and SFLIL, where previous research identified septic system effluent as the dominant source of nitrogen in these streams as a result of the high density of septic systems within the watersheds (Hyer and others, 2016). There is no indication of septic system failures in these watersheds, but conventional septic systems do not include NO_3^- removal capabilities and can impact surface-water quality when high NO_3^- groundwater is discharged to streams (Aravena and others, 1993; Lindsey and others, 2003). There is a positive relation (R^2=0.52, p=0.0003) between median NO_3^- concentrations and septic system densities throughout the monitoring network, which suggests the importance of septic effluent as a nitrogen source in Fairfax County streams not served by sanitary sewers (fig. 46). However, CAPT HICK, DOGUE, and DEAD all had median NO_3^- concentrations that were notably higher than would be expected based solely on this relation. This pattern may result from variability in (1) nitrogen sources and applications, with contemporary and legacy inputs other than septic effluent contributing to elevated concentrations; (2) denitrification rates; or (3) groundwater flow paths and septic system locations that affect how efficiently septic effluent is transported to streams. In CAPT HICK, areas immediately outside of the watershed also are served by septic systems and may contribute NO_3^- to the stream where groundwater flow paths cross watershed boundaries. In DOGUE, high NO_3^- concentrations may result from low denitrification rates associated with aerobic sandy

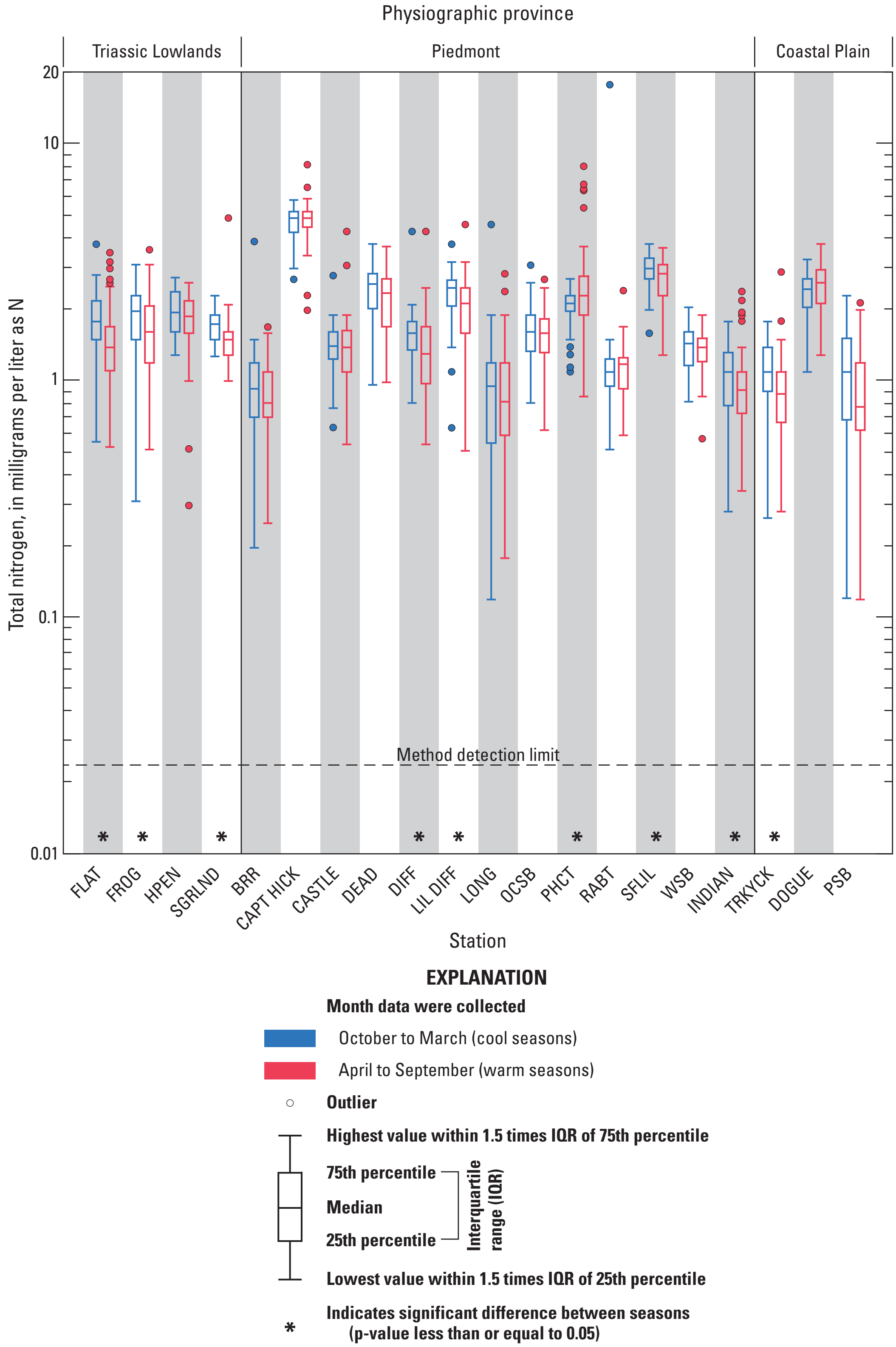

Figure 45. Total nitrogen results from the monthly sampling at 20 monitoring stations in Fairfax County with comparison of data collected during the cool (October–March) and warm (April–September) seasons. A significant difference between warm- and cool-season sample concentration distributions was determined from a nonparametric Wilcoxon test with a p-value of ≤0.05. Stations are arranged by physiographic province and station names are defined in table 1.

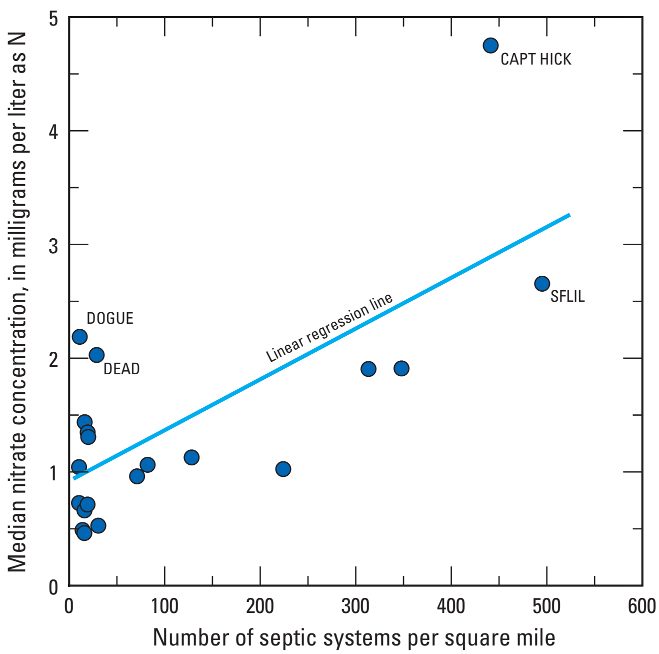

Figure 46. The relation of median nitrate concentrations collected between 2008 and 2018 at 20 monitoring locations and the number of septic systems per square mile within each location's drainage area. The blue line is a linear regression line. Station names are defined in table 1.

soils in some Coastal Plain watersheds. In DEAD, high NO_3^- concentrations may result from nonpoint nitrogen sources other than septic effluent, such as leaking sanitary sewer lines or fertilizer applications; however, the exact cause is not yet well understood. Spatial and seasonal boxplots of TDN and total particulate nitrogen (TPN), similar to figure 45, are provided in appendix 2 in figures 2.6 and 2.7, respectively.

Loads

The predictive power of TN, TDN, and NO_3^- concentration models varied across stations but were generally lower than for particulate constituents (tables 1.5, 1.6). Model predictions of TN were weakest, with the exception at LONG where particulate nitrogen dominated. Conversely, the use of turbidity as an explanatory variable resulted in strong predictions of TPN at all stations. Most TN, TDN, and NO_3^- models contained a seasonal term, which represents seasonal availability of NO_3^- due to denitrification. Most TN, TDN, and NO_3^- models also contained a positive SC term, which was reflective of higher NO_3^- concentrations during baseflow conditions when discharging groundwater dominated streamflow. Continuous NO_3^- data from the Satlantic SUNA in situ nitrate sensor was available for recalibration of TN and TDN models at SFLIL and subsequent recalculation of WY 2017 loads; the WY 2017 NO_3^- load was computed directly. The TDN model that included continuous NO_3^- as an explanatory variable explained approximately 20 percent more variability and reduced model bias as compared to the model that did not utilize continuous NO_3^-. The TN model that included continuous NO_3^- data showed minor improvements over the previous model but continued to underpredict the highest observed TN concentrations—periods when NO_3^- represents a minor fraction and coarse organic material represents a major fraction of the TN budget.

Median TN yields were similar across stations and ranged from about 3,600 to 6,300 lbs/mi² (Porter and others, 2020). Annual variability in the composition of TN yields were primarily driven by streamflow, with higher yields generated in wetter years (for example, 2014; fig. 47). These patterns are consistent with other studies of urban streams in which substantial decreases in nitrogen retention were observed between dry and wet years (O'Driscoll and others, 2010; Duncan and others, 2017). On average, TDN accounted for 70 percent of TN yields (fig. 48) and, although the overall TDN load increased in wet years, the ratio of TDN:TN decreased by approximately 15 percent as the composition shifted towards particulate nitrogen. In most years, NO_3^- represented about 50 percent of the TN yield at DEAD, DIFF, and FLAT. Nitrate yields were higher at SFLIL than the other monitoring stations and typically accounted for over two-thirds of the TN yield. Elevated NO_3^- yields in this watershed likely result from contributions of septic system effluent, as previously discussed. At LONG, NO_3^- yields accounted for only one-third of the TN yield and were lower than the other monitoring stations. The composition of these annual TN yields resulted from NO_3^- concentrations that consistently were lower than the other monitoring stations; NO_3^- rarely exceeded 1 mg/L as nitrogen at LONG. A combination of physical watershed properties that promote denitrification rates and (or) limited nonpoint nitrogen sources are likely responsible for these conditions.

The cumulative aggregation of TN yields occurs largely as a steady accumulation over time with small-magnitude step increases during major precipitation events (fig. 31*C*). These patterns highlight the importance of groundwater NO_3^- contributions to annual nitrogen loads. The year-round transport of NO_3^- to streams also is revealed in analyses of annual precipitation; weeks that received less than 1.25 in. of rain contributed a greater proportion of the annual NO_3^- load than weeks that received more than 2.0 in. of rain (fig. 30D). Because of particulate nitrogen contributions, both rainfall classifications contribute about 30–40 percent of the annual TN load at all stations (fig. 29C).

Total nitrogen and NO_3^- yields were higher in Fairfax County than for the Gwinnett County, Georgia, watersheds (fig. 33C, D) and ranged between the 40th and 75th quantiles of CB-NTN watersheds; however, CB-NTN yields spanned a greater range because of some low-yielding forested watersheds and high-yielding agricultural watersheds. Both TN and NO_3^- yields from ACC and DRGF were comparable to those in this study. Total nitrogen yields may be higher in monitored Fairfax County streams than in Gwinnett County streams because of greater nonpoint nitrogen source inputs or lower

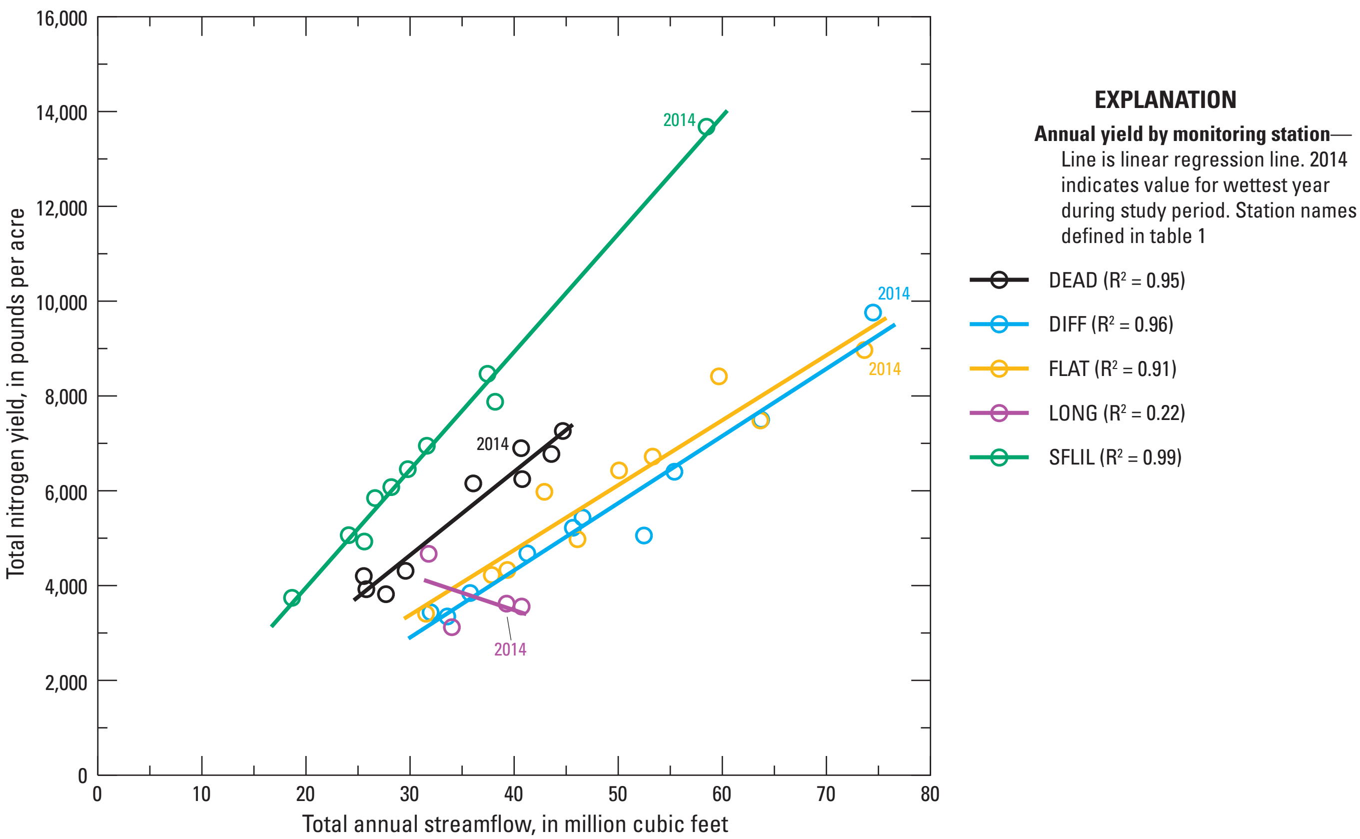

Figure 47. Annual total nitrogen yield compared to streamflow volume for the five intensive monitoring stations in Fairfax County. Data that correspond to the wettest year during the study period (2014), based on total annual precipitation, are labeled. Station names are defined in table 1.

rates of denitrification. Along with nitrogen availability and soil moisture, soil temperature is a major control on rates of terrestrial denitrification, with warmer conditions promoting greater rates of nitrogen loss (Pilegaard, 2013). Over a similar time period, median TN and NO_3^- yields were 6 and 29 times higher in the monitored Fairfax County watersheds than at SFQ, respectively (Moyer and Blomquist, 2018).

Trends

In the monthly samples, a significant decrease in TN concentrations and (or) FN concentrations occurred at five monitoring stations, but the combined trend result from all stations revealed no significant changes (table 4; figs. 49A, 50). Of the stations where TN declined, changes ranged from about –2 to –4 percent per year, or about –0.01 to –0.07 mg/L per year. A significant TN increase was only observed at SFLIL, a change of about 0.5 mg/L over the 10-year study period (about 2 percent per year). Though nonsignificant, concentrations and FN concentrations also increased at CAPT HICK, at rates of about 1 percent per year (0.05 mg/L/yr) and 0.66 percent per year (0.03 mg/L/yr), respectively. The 10-year TN increases of 1–2 percent per year at CAPT HICK and SFLIL are notable because the highest median TN concentrations in the monitoring network, 3–5 mg/L, are commonly observed at these stations.

Trends in NO_3^- and DTKN, the components of TDN, are useful in understanding TN changes. The combined trend results of NO_3^- concentration and FN concentration from all stations revealed a significant decrease, with a median reduction of about 0.15 mg/L over the 10-year monitoring period (fig. 49B). Conversely, the same measure of trend in DTKN revealed a significant 10-year increase of about 0.11 mg/L. The combined trend result for TDN from all stations was not significant, reflecting the offsetting patterns of these two dissolved components. For NO_3^-, trends and (or) FN trends decreased significantly at five stations (figs. 49B, 50B; Porter and others, 2020). Significant increases were observed at SFLIL and CAPT HICK, a notable result since these watersheds have the highest median NO_3^- concentrations in the network. For DTKN, increases occurred in concentration and (or) FN concentration in half of the monitoring stations. Dissolved TKN is composed of dissolved organic nitrogen and ammonia and is quickly converted to NO_3^- in most surface waters.

Trends in FN nitrogen concentration and load were estimated by WRTDS using a dataset of monthly and storm-targeted samples available from four of the intensive

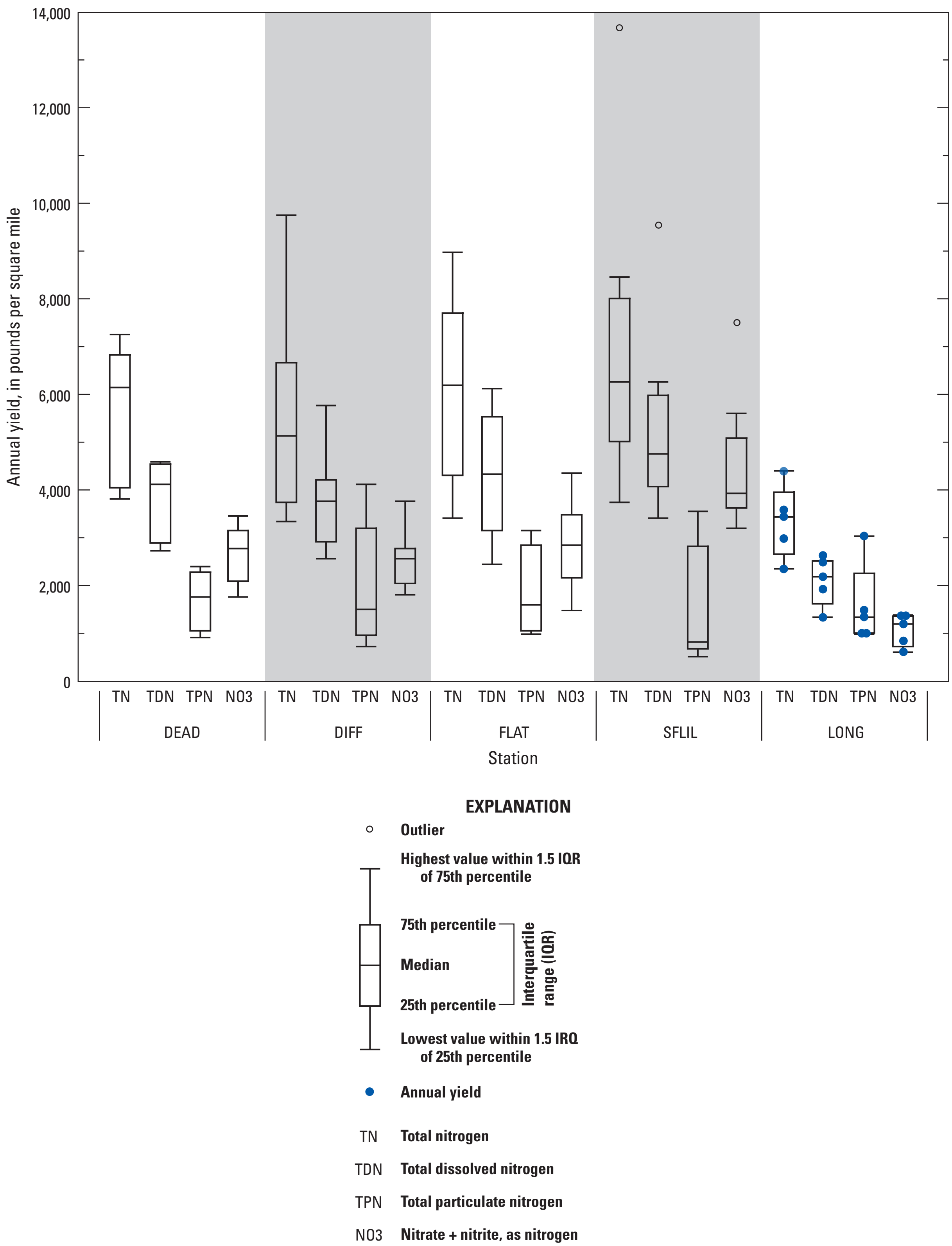

Figure 48. Boxplot of annual total nitrogen (TN), total dissolved nitrogen (TDN), total particulate nitrogen (TPN), and nitrate (NO3) yields for the five intensive monitoring stations in Fairfax County. Points included for LONG owing to sample size (n = 5). Station names are defined in table 1.

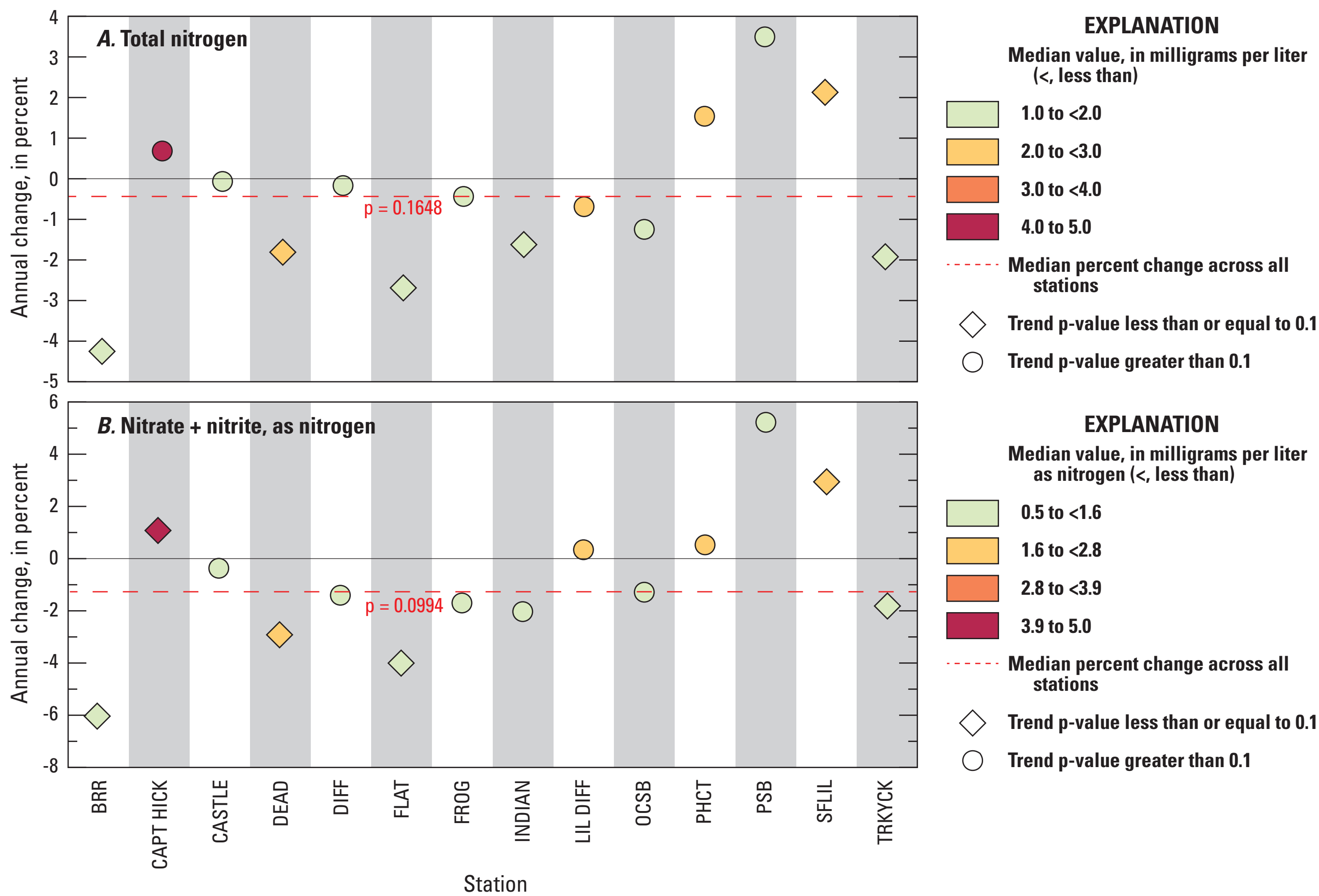

Figure 49. Total nitrogen (*A*) and nitrate + nitrite (*B*) flow-normalized concentration trend results expressed as a percent change per year at 14 monitoring locations between April 2008 and March 2018. The p-value refers to the Regional Seasonal Kendall trend test. Station names are defined in table 1.

monitoring stations (fig. 51). TN concentration and load declined at DEAD and FLAT by about 1–2 percent per year. No trend in concentration and an increase in load of about 1 percent per year was observed at DIFF. Differences in FN concentration and load trends occur whenever the changes in water chemistry vary with flow. TN concentration and load increased at SFLIL by about 1.35 percent per year, about 2,500 pounds over the study period.

Benthic Macroinvertebrates

Lotic water quality is typically evaluated by physical (for example, streamflow, turbidity) and chemical (for example, pH, DO, SC) metrics. Physicochemical metrics provide relevant snapshots of water quality, but unlike biological metrics, do not provide an integrated, comprehensive assessment of the health of a waterbody over time (Karr, 1999). Because benthic macroinvertebrates live in the aquatic environment and have varying degrees of tolerance to water-quality impairment, patterns in community structure and function can be used to indicate both positive and negative changes in their surroundings. Based on this premise, biomonitoring can be used to integrate the impact of physical and chemical urban stressors, such as altered streamflow and NPS pollution on aquatic ecosystems (Barbour and others, 1999; Poff and others, 2006). Urban stressors commonly are associated with reductions in community richness and composition and a shift from sensitive to tolerant species (Roy and others, 2003; Patrick and others, 2015). The presence and abundance of a species indicates if, and to what extent, its needs are being met by the surrounding ecosystem (Johnson, 2004). The absence of a species does not always indicate poor water quality but instead may be due to physical habitat suitability, which may be a function of physiography or anthropogenic disturbance. Although the relation between urbanization and decreased species abundance and diversity has been well established (Lenat and Crawford, 1994; Roy and others, 2003), the response to individual stressors such as increased stormflows, pollutant concentration, and sediment transport/deposition vary by species (O’Driscoll and others, 2010).

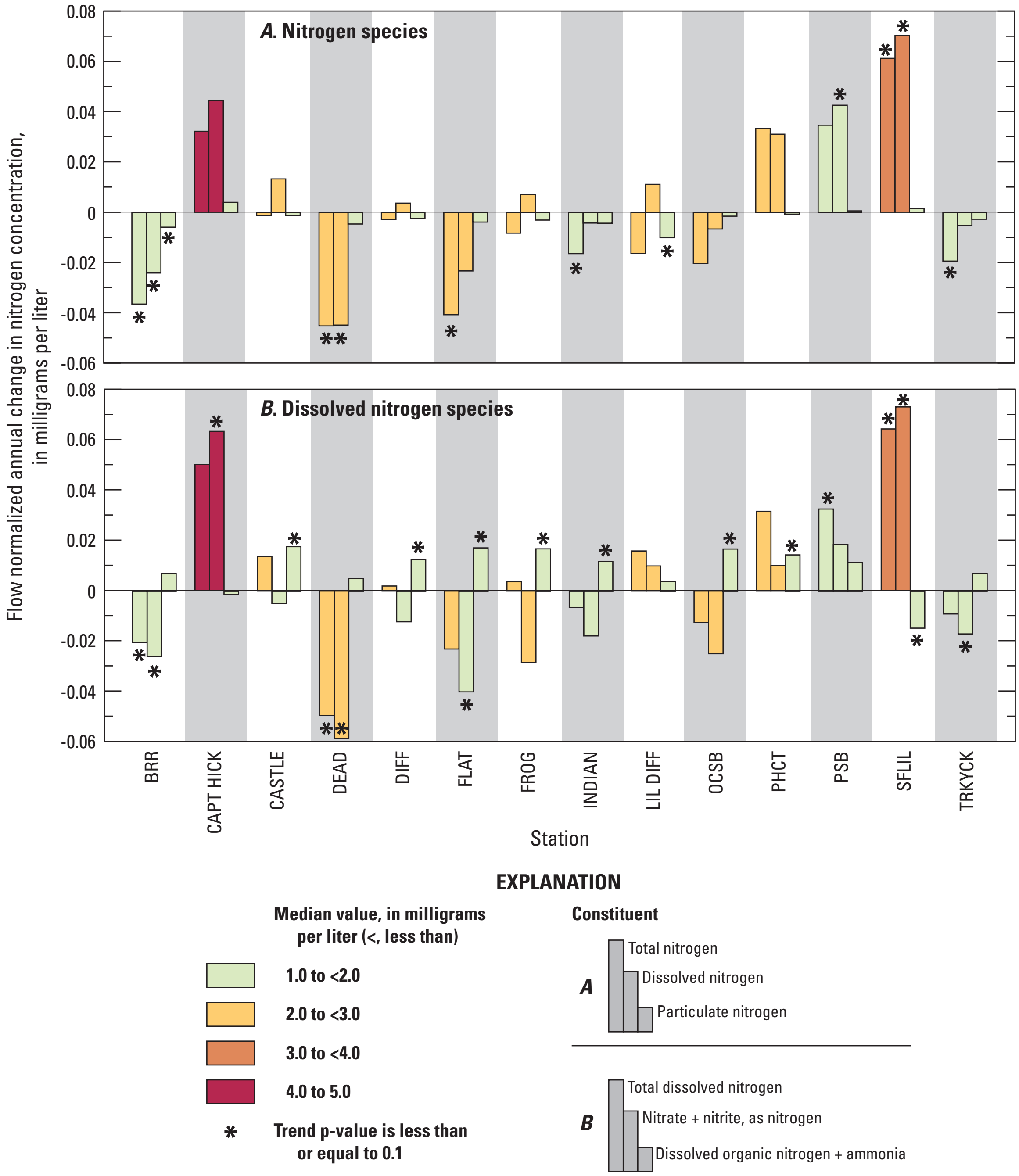

Figure 50. Annual change in flow-normalized concentrations of total, dissolved, and particulate nitrogen (*A*) and dissolved nitrogen, nitrate, and dissolved organic nitrogen (*B*) at 14 monitoring locations between April 2008 and March 2018. The p-value refers to the Regional Seasonal Kendall trend test. Note that it is possible for components of either dissolved or particulate fractions to be slightly higher than the total as a result of model uncertainty. Station names are defined in table 1.

A total of 139 macroinvertebrate samples were collected at the 14 monitoring stations for which trends in water quality were assessed. Samples were collected annually at each station, except for INDIAN in 2014 owing to construction activities. Seven additional samples were excluded as a result of inconsistencies in the sample sorting process; therefore, the total number of samples used in the analysis of trends was 132. These data were used to examine temporal trends in 20 benthic metrics at both the networkwide and station scale. Trends were computed on 10 years of data at most stations (2008–17), 9 years at three stations that were established in 2009 (OCSB, FLAT, and FROG), and 6 years at INDIAN.

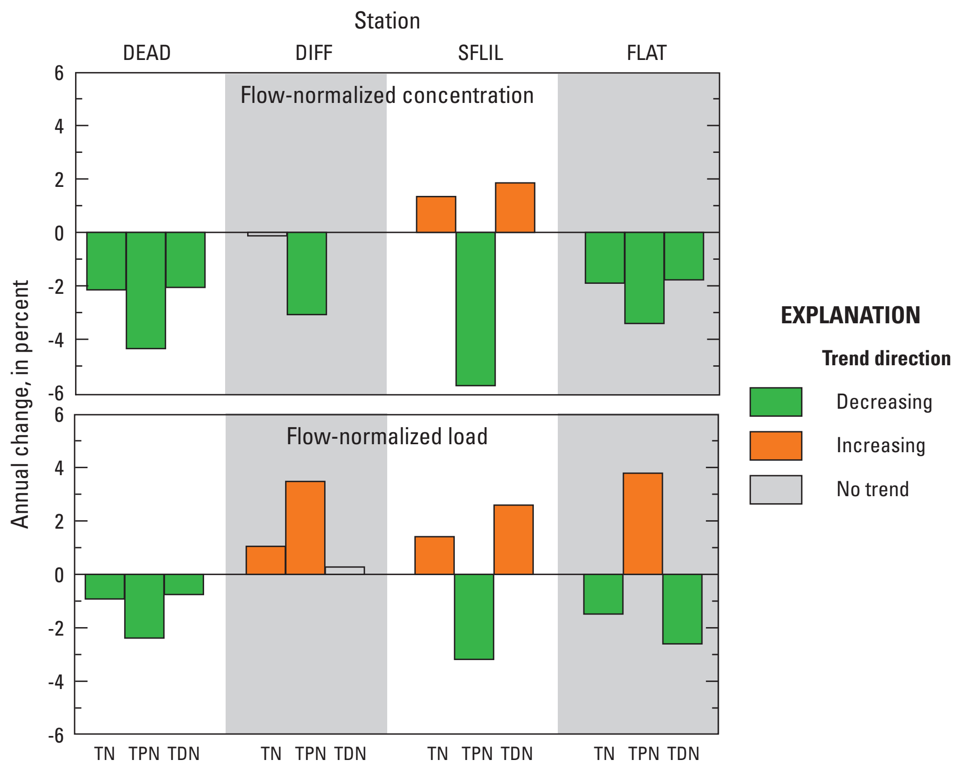

Figure 51. Trend in flow-normalized concentration and load of total nitrogen (TN), total particulate nitrogen (TPN), and total dissolved nitrogen (TDN) expressed as a percent change per year at four of the intensive monitoring locations between April 2008 and March 2018. Station names are defined in table 1.

Mixed-effect models were more sensitive to detecting change in analyses of networkwide trends than those at individual stations because the full dataset of 132 samples is leveraged, whereas the individual station regressions had a maximum of 10 samples. Percent composition metrics also tended to be more sensitive than the richness metrics at individual stations, likely owing to the limited species pool within the county and the degree of urbanization at each station.

Improvements in broad biodiversity metrics were observed across the network and at many individual stations between 2008 and 2017 (tables 5, 6; fig. 52A, B). The Fairfax IBI score increased significantly at the network scale, from a predicted score of 34.19 to 50.46 out of 100 (fig. 52A), an improvement that reflects nearly a full rating category (from poor to fair); significant increases also were observed at four individual stations. At 11 stations the IBI scores in 2017 were at least 1 qualitative group higher (for example, fair to good) than those in 2009 (the first year all 14 stations were sampled). Total taxa richness, as well as percent composition and the richness of both Ephemeroptera, Plecoptera, and Trichoptera (EPT) and Coleoptera, Odonata, Tricoptera, and Ephemeroptera (COTE) metrics also increased at the network scale. Although significant increases in composition metrics were observed at most individual stations, significant increases in richness metrics were rare at the station scale. Conversely, dominance (the relative abundance of the most common taxa in the sample) decreased significantly across the network and at most individual stations; this decline in homogeneity may be attributed to decreases in the percentage of Chironomidae (nonbiting midges) and Oligochaeta (worms), which include highly tolerant species.

A shift in functional composition was indicated by significant trends in functional feeding group (FFG) metrics. The structure and composition of trophic groups reflects resource availability (Barbour and others, 1999). Changes in FFGs can affect ecosystem processes such as nutrient mineralization, primary production, and organic matter decomposition (Wallace and others, 1982; Wallace and Webster, 1996; Diaz Villanueva and others, 2012; Ramírez and Gutiérrez-Fonseca, 2014). Composition and richness of filter feeders, predators, and scrapers increased across the 10-year period at the network scale. The proportion of filter feeders, predators, and scrapers increased significantly at most stations; conversely, no significant change was noted in the richness of filter feeders or predators at any station and scrapers taxa increased significantly at only two stations. Increases in tolerant filter-feeding caddisflies in the genera *Chimarra* spp., *Cheumatopsyche* spp., and *Hydropsyche* spp. (CCHs), and representatives of the order Odonata (damselflies and dragonflies), which contains many tolerant predators, may partly explain changes in EPT, COTE, filterer, and predator metrics. Notably, the pattern of increasing composition of filterer and predator FFGs

Table 5. The change in benthic macroinvertebrate composition metrics (number of target taxa in a standardized sample with 100 total individuals) between 2008 and 2018 at each monitoring station.

[The Index of Biological Integrity (IBI) represents the change in metric score, which also ranges from 0 to 100. Station names are defined in table 1. Orange text indicates a statistically significant increasing trend and green text a statistically significant decreasing trend ($p \leq 0.05$). EPT, Ephemeroptera, Plecoptera, and Trichoptera; COTE, Coleoptera, Odonata, Tricoptera, and Ephemeroptera; CCH, *Chimarra, Cheumatopsyche,* and *Hydropsyche*]

Station	IBI	EPT	COTE	Filterer	CCH	Predator	Odonata	Scraper	Gastropoda	Dominance	ChiroOligo
All stations	16.3	7.3	11.8	9.0	6.7	2.2	1.5	1.7	1.5	–15.3	–17.3
BRR	42.3	10.4	13.2	7.9	6.8	5.3	4.9	0.8	3.0	–10.4	–19.1
CAPT HICK	–4.5	3.9	4.9	10.2	9.8	0.9	1.2	–5.7	1.2	3.2	–0.6
CASTLE	–11.3	–13.4	11.8	12.0	12.5	1.7	1.3	2.0	1.7	0.6	10.7
DEAD	7.0	10.6	13.1	11.0	10.7	1.3	1.4	–0.2	–0.1	–24.4	–12.9
DIFF	28.2	1.1	15.5	3.6	1.1	3.1	2.3	14.7	0.9	–18.4	–21.1
FLAT	48.6	3.5	25.3	6.8	2.5	10.7	9.5	18.0	12.2	–34.6	–42.8
FROG	32.5	27.5	31.5	31.2	27.5	9.5	1.6	1.2	–0.3	–28.3	–35.3
INDIAN	36.6	27.6	31.9	31.3	27.6	9.9	1.9	1.3	–0.3	–32.6	–40.9
LIL DIFF	11.7	19.0	19.2	19.9	16.3	1.3	1.4	1.6	3.4	–27.2	–25.2
OCSB	–5.9	–2.2	–5.0	–3.0	–2.2	–3.1	–2.5	–0.9	0.7	0.8	0.2
PHCT	–1.8	1.9	2.1	2.5	1.7	0.5	0.6	–0.2	0.6	14.8	–1.1
PSB	11.9	1.1	2.1	2.0	1.1	1.0	0.7	1.2	0.9	–8.9	–5.4
SFLIL	29.0	20.0	22.3	19.4	19.7	3.1	0.2	3.2	2.2	–50.5	–45.3
TRKYCK	18.4	19.7	21.4	19.3	19.4	0.5	0.5	2.2	1.4	–13.7	–22.9
MEADOWS	3.0	13.3	29.5	–21.7	4.3	4.6	0.2	9.0	0.0	0.2	6.6

Table 6. The change in benthic macroinvertebrate richness metrics (number of unique taxa) between 2008 and 2018 at each monitoring station.

[Station names are defined in table 1. Orange text indicates a statistically significant increasing trend ($p \leq 0.05$).EPT, Ephemeroptera, Plecoptera, and Trichoptera; COTE, Coleoptera, Odonata, Tricoptera, and Ephemeroptera; CCH, *Chimarra, Cheumatopsyche,* and *Hydropsyche*]

Station	Total	EPT	COTE	Filterer	CCH	Predator	Odonata	Scraper	Gastropoda
All stations	5.1	1.1	3.1	1.1	0.6	1.7	1.5	1.4	1.3
BRR	15.0	3.2	8.4	2.0	1.2	5.2	4.7	2.6	2.3
CAPT HICK	1.3	–2.6	1.1	1.8	1.0	0.7	2.0	–0.4	2.0
CASTLE	3.6	–0.3	1.3	–1.1	–0.5	2.5	2.3	1.0	1.6
DEAD	–0.1	–0.5	0.8	0.1	–0.5	0.8	1.2	–0.3	–0.3
DIFF	7.3	0.1	1.9	2.0	0.0	1.8	0.7	2.1	1.0
FLAT	17.1	3.0	8.8	3.8	1.8	5.3	3.3	5.9	3.7
FROG	3.7	0.7	2.7	–1.2	0.1	1.2	0.8	3.4	2.4
INDIAN	2.2	1.9	3.2	2.4	1.9	0.4	0.9	0.5	–1.0
LIL DIFF	1.9	–0.5	3.5	–0.7	0.2	2.2	2.0	1.2	1.8
OCSB	–0.5	0.1	–0.5	–0.4	0.1	0.0	0.4	–1.8	–0.3
PHCT	2.4	1.0	1.7	1.1	0.2	1.0	1.2	1.0	0.7
PSB	5.8	1.2	2.3	2.0	1.2	0.8	0.3	1.5	0.8
SFLIL	3.2	1.1	0.9	–0.4	0.0	0.9	0.3	2.7	3.5
TRKYCK	3.7	0.6	1.9	0.0	0.1	0.6	0.5	1.3	1.2
MEADOWS	11.2	5.7	5.4	–0.3	0.1	5.2	0.5	2.8	0.0

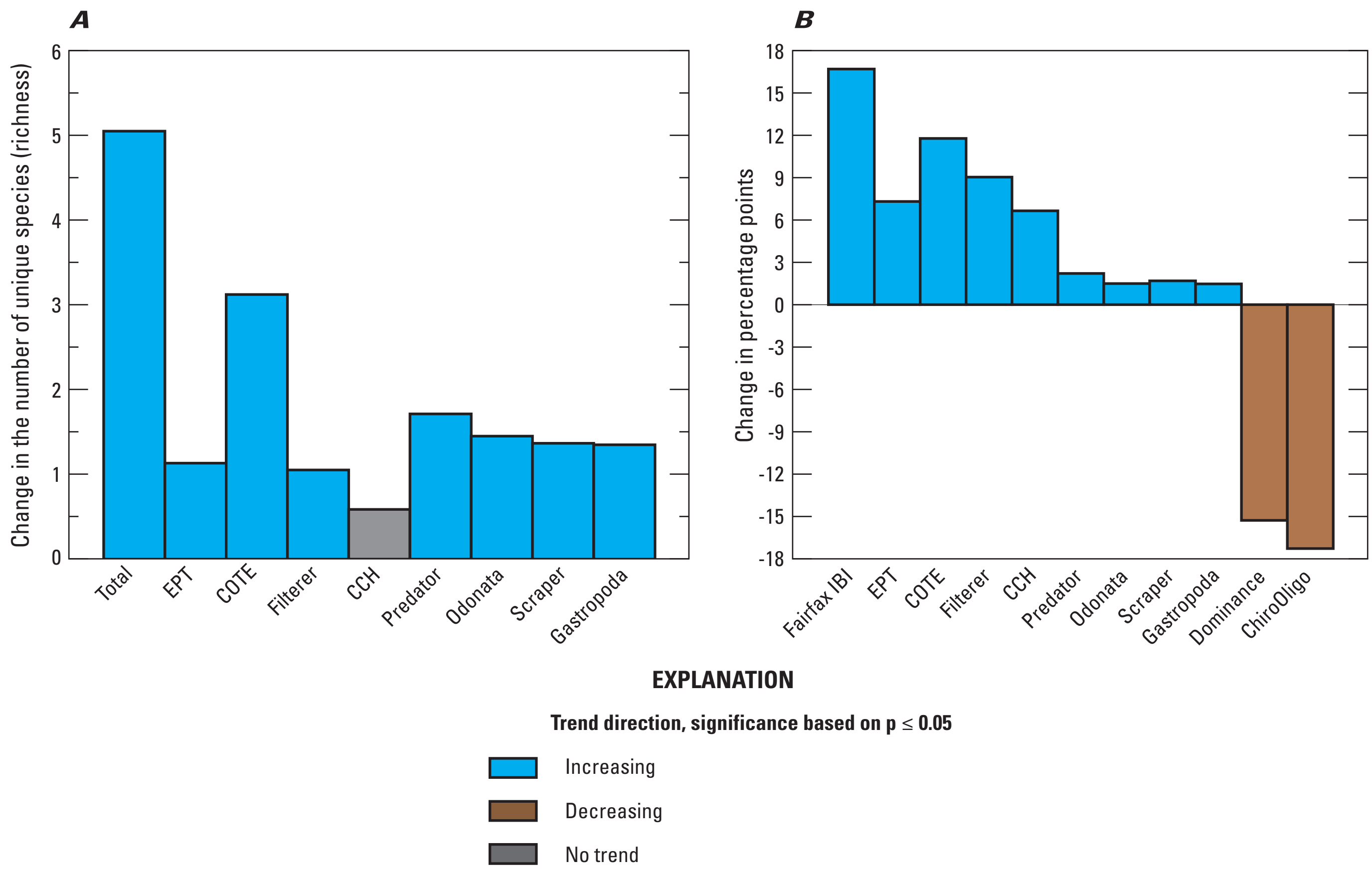

Figure 52. Predicted change at the network scale (data from all 14 stations) from April 2008 to March 2018 in richness metrics (number of unique taxa) (*A*), and composition metrics (number of target taxa in a standardized sample with 100 total individuals) (*B*). Fairfax IBI represents the change in metric score, which also ranges from 0 to 100. Metrics are defined in table 3.

and increases in EPT and COTE metrics was similar across several stations (BRR, INDIAN, LIL DIFF, DEAD, SFLIL, and TRKYCK), which suggests some similarities in the way conditions in these watersheds are changing despite exposure to different degrees of land-use change and best management practices (BMP) implementation.

Increases in the class Gastropoda, which contains many tolerant snails, were observed at most stations and likely explain increases in the composition and richness of the scraper FFG. The increase in scrapers may be related to decreased canopy cover resulting from increased urbanization and subsequent increase in photosynthetically active radiation (PAR). Additionally, increasing WT may be an important driving factor of increasing phosphorous concentrations, as was previously discussed. In freshwater ecosystems, increases in PAR and (or) phosphorous concentration can stimulate primary productivity (algal growth), a primary food source for scrapers. Collector and shredder FFGs (not presented) composed a small fraction of the total community; trends in composition and richness were nonsignificant at the network scale. Although the low proportion of shredders and collectors affects ecosystem processes such as organic matter decomposition, the increase in richness and composition of filterer, scraper, and especially predator FFGs is indicative of a more balanced community and altered ecosystem functioning.

To illustrate overall networkwide trends, and important deviations from it, consider SFLIL and CASTLE. The former was representative of most stations throughout the network in that conditions were initially poor based on the Fairfax IBI, and percent composition of EPT and COTE metrics but showed significant improvements over time. Improvements were coincident with the proliferation of more tolerant caddisflies (CCH), Gastropods, and Odonates, and a decrease in Chronomids and Oligochaetes. The improvements at SFLIL and many other stations has driven the overall positive networkwide trends in these metrics. Conversely, CASTLE was the least developed watershed over the study period and had the best mean annual Fairfax IBI score (85.13). This was the only station to initially be classified as excellent (based on the Fairfax IBI), which indicated high biodiversity and a balanced community structure. However, over the 10 years of monitoring, parts of this watershed were actively developed, and as a result the IBI score decreased from 95.73 in 2008 to 81.74 in 2018. Although declines in the IBI were statistically insignificant, it was accompanied by significant declines in overall EPT composition, and significant increases in Chironomids, Oligochaetes, and tolerant caddisflies (CCH), which indicates a shift from less tolerant to more tolerant taxa. Trends at CASTLE reveal a link between degrading benthic community health and recent land development, whereas SFLIL and many other stations previously characterized by poor biological conditions show signs of moderate recovery following decades of disturbance.

SFLIL and CASTLE can likewise be compared to a best-available, or reference, condition station, MEADOWS, located on a tributary downstream of SFQ in Prince William Forest National Park and sampled annually by Fairfax County Stormwater Planning Division (FCSWPD) between 2008 and 2017. MEADOWS had a mean annual Fairfax IBI score of 95.61 and showed significant increases in total taxa richness and the composition of EPTs and COTEs over the sampling period. Similar to SFLIL and CASTLE, a significant increase in the composition of tolerant caddisflies (CCHs) occurred at MEADOWS, but by a lesser magnitude than the composition of COTEs and EPTs, and it coincided with an increase in the composition of Coleoptera and Ephemeroptera (not presented). This pattern suggests that although tolerant caddisflies (CCHs) may have increased regionally across the urban gradient, the magnitude of change may depend on site condition (for example, physical habitat) or other factors unique to each station (for example, hydrology, water chemistry). Further, several similarities and differences of trends in FFGs between MEADOWS and Fairfax County stations were notable. Whereas the increase in CCHs at SFLIL and many other Fairfax County streams was attributed to an increase in filterers, a significant decrease in the composition of the filterers occurred at MEADOWS. This decrease coincided with a decrease in the composition of black flies (family Simuliidae, not presented). Similar to Fairfax County streams, an increase in the richness and composition of predator and scraper FFGs was observed at MEADOWS; however, unlike at SFLIL and many other stations, these changes did not coincide with an increase in Gastropods or Odonates. These results indicate that although there are some regional similarities in the direction of trends in FFGs, the taxonomic drivers of those changes may vary spatially as a result of station-specific factors.

Observed changes in the metrics considered here suggest that the biodiversity, function, and condition of streams in Fairfax County are improving, but many of these improvements are driven by increased diversity and percent composition of organisms that are tolerant of the urban environment. This is indicated by changes in taxa-specific metrics (for example, CCH and Odonata), which provide additional insight into the changes observed in broader biodiversity and FFG metrics. This appears to be particularly true for stations that were initially rated as poor based on the Fairfax IBI. For example, those stations that saw significant increases in richness and (or) composition of EPT, or decreased dominance had mean IBI scores between 20.5 and 22.9 in 2009. Regardless of the mechanism that underlies the increased heterogeneity and diversity of tolerant organisms, these improvements in condition provide valuable insight into understanding one potential trajectory that urban systems may take as conditions change and stabilize over time.

Summary

Fairfax County, Virginia, has experienced rapid urbanization since the mid-20th century and as a result, many streams are showing signs indicative of the so-called urban stream syndrome. The U.S. Geological Survey (USGS), in cooperation with Fairfax County Stormwater Planning Division, established a long-term water resources monitoring program in late 2007 to (1) assess water-quantity, -quality, and ecological conditions; (2) compute annual nutrient and sediment loads; and (3) evaluate trends in streamflow, water quality, and ecological condition. Results from the first 10 years of monitoring (water years [WY] 2008–17) indicate that Fairfax County streams show many of the classic symptoms of urbanization, such as increased storm runoff, localized hot spots of elevated nutrient concentrations, high rates of sediment transport, and low Index of Biological Integrity scores. Efforts to mitigate these detrimental effects are underway through the use of best management practices (BMPs) and stream restoration projects. An evaluation of watershed-scale response to these land and stream management implementations is ongoing.

Precipitation was highest in WYs 2008, 2011, and 2014 due in large part to short duration, high-intensity storm events. These precipitation periods had an outsized effect on hydrologic and water-quality conditions and contributed to substantial increases in annual nutrient and sediment loads at most stations. Streamflow yields varied by watershed, with FLAT and DIFF yielding more water than the other intensively monitored watersheds. Streamflow yield was positively correlated with annual rainfall at all stations; however, the amount of direct runoff, referred to as runoff ratio, also was higher at DIFF and FLAT (0.25 and 0.23, respectively). These differences likely can be attributed to watershed imperviousness and geologic and soil properties. The slope of the relation between precipitation and streamflow decreased at DIFF and FLAT between the first and second 5-year periods of monitoring, which indicated a reduction in the amount of streamflow produced by storm events; in the second 5- year period of monitoring the relation between monthly streamflow and precipitation yields were similar at all five stations. Stream flashiness, defined as the rate at which streamflow changes over time, was strongly correlated with watershed imperviousness (Pearson's r = 0.79), and every 10-percent increase in imperviousness increased flashiness by approximately 20 percent. The stage-based flashiness metric, which could be evaluated at all 20 stations, was lowest at CASTLE, the least impervious watershed, and highest at DEAD, the third most impervious watershed.

Decadal trends in mean daily streamflows were explored at four of the five intensive monitoring stations and revealed few significant trends but had a general pattern of increasing low and median mean daily flows and decreasing high-mean daily flows. Multidecadal trends in mean daily streamflow were investigated at two long-term CB-NTN stations (DRGF and ACC), with records dating back to the 1940s. At both stations, urbanization that occurred over the more than 70-year period resulted in statistically significant increases of approximately 1 percent per year in the top 10 percent of mean daily flows and decreases in low and median mean daily flows. Annual exceedance probabilities (AEPs), computed on peak annual streamflows at four of the intensive monitoring stations, indicated the occurrence of storms with an AEP of 0.09 (an approximately 11-year storm recurrence) at DEAD in 2010, FLAT and SFLIL in 2011, and DIFF in 2008. Conversely, these same events had AEPs between 0.02 and 0.01 (50- to 100-year storm recurrences) at ACC and DRGF when computed using multidecade records. Records of short length can skew AEP analyses and may have underestimated the AEP of storms at the four intensive monitoring stations.

Spatial and seasonal patterns in basic water-quality parameters (dissolved oxygen [DO], pH, specific conductance [SC], and water temperature [WT]) were assessed in the monthly data collected at all 20 stations and the continuous data collected at the 5 intensive monitoring stations. Patterns in all parameters reflect a mix of seasonal factors such as photosynthesis and denitrification, which are driven by monthly changes in air temperature, spatial patterns driven by differences in geologic and soil properties, and anthropogenic stressors such as deicing salt applications and septic infrastructure. Water temperature was seasonally dependent and never exceeded the Virginia maximum criterion. Nonsignificant trends in WT were observed at all stations, with a median change of +0.03 °C per year.

Dissolved oxygen varied both seasonally, owing to WT, and spatially owing to land use, physiographic province, and other factors. Dissolved oxygen was lowest in warm months and at stations located in the Triassic Lowlands, as well as PSB in the Coastal Plain. Stream DO was generally within range to support aquatic life (>4.0 milligrams per liter [mg/L]), though on occasion lower concentrations were measured in summer months (9 of 13 occurrences at PSB in the Coastal Plain). Dissolved oxygen decreased by less than 1 mg/L over the period of record at most stations, but most results were not statistically significant.

Stream pH was typically neutral (pH = 7±0.5) and decreased during periods of high streamflow as a result of inputs of acidic rainwater. The highest mean pH was observed in stations located in the Triassic Lowlands and was attributed to increased photosynthesis owing to elevated phosphorous and elevated calcium carbonate in groundwater resulting from the underlying geology. The lowest mean pH was observed in Coastal Plain stations and may be the result of carbonate-equilibrium reactions that increase groundwater acidity; additionally, Ultisol soils common in the Coastal Plain typically have low pH owing to their ionic composition. Continuous pH data revealed a diurnal pattern of daytime increases and nighttime decreases in pH as a result of photosynthetic processes. Trends in pH were generally nonsignificant (approximately 0.01 unit per year).

Spatial and seasonal patterns in SC were related strongly to physiographic province, impervious land cover and the application of deicing salts. Further, SC was inversely related to streamflow, which indicates groundwater-dominant baseflows and dilution by lower conductance storm runoff. Mean SC was significantly higher among stations in the Triassic Lowlands than the Piedmont or Coastal Plain as a result of natural geological processes that differ by region. Specific conductance was strongly correlated with increased impervious surface coverage. For each 10-percent increase in watershed imperviousness, there was an approximate 100-unit increase in SC. This relation was exacerbated in winter months when deicing salts were applied to roadways, parking lots, and sidewalks. Following salt applications, SC commonly increased by 1–2 orders of magnitude and did not typically return to baseline conditions until late spring or early summer. Spikes in SC represent wash-off of salts that can shock aquatic organisms and produce conditions that likely exceed impairment thresholds for freshwater species. Specific conductance increased at all stations by about 2.5 percent per year, or about 7.5 microsiemens per centimeter (µS/cm) per year. Specific conductance increases were most commonly observed in spring and fall months, which was likely a result of continued wash-off and resuspension of salts applied in the previous winter and from the transport of chloride stored in groundwater to streams.

Turbidity was a strong surrogate for suspended-sediment (SS) concentration and enabled strong predictions of SS loads (R^2>0.90 for all SS models). Suspended-sediment concentrations were highest in the spring and lowest in the fall. Seasonal variability in SS concentration likely reflects seasonal patterns in streamflow and sediment availability. Suspended-sediment loads, and yields were highly variable across WYs and strongly related to annual precipitation and peak streamflow. Although median annual yield did not vary significantly by station, annual yields at SFLIL and DIFF were more variable between wet and dry years. The three wettest WYs—2008, 2011, and 2014—produced substantially higher loads at SFLIL and DIFF than at the other stations; consequently, those stations yielded substantially more SS over the 10-year period. The range in annual yields at SFLIL and DIFF likely resulted from a greater range in streamflow and more erodible streambanks, particularly during extreme stormflows. Small decreases in turbidity of about 0.10 Formazin nephelometric unit (FNU) per year and no changes in SS concentration were observed at most stations, and most trend results were not statistically significant. The largest SS concentration increases occurred at FLAT, coincident with active construction of a stream restoration project in close proximity to the monitoring station.

Phosphorus concentration varied both spatially and seasonally, and typically increased with streamflow. The dominance of the particulate fraction in high-flow samples and in annual loads reflected the phosphorous sorption capacity of fine sediments in these watersheds. Concentrations were highest in watersheds that drain the Triassic Lowlands because of naturally occurring phosphorous concentrations contributed by geologic materials. Concentrations of phosphorous also were high at DOGUE, located in the Coastal Plain, which may reflect the low phosphorous sorptive capacity of sandy soils. Higher total phosphorous (TP) concentrations were observed throughout the network during warmer months as a result of temperature-dependent phosphorous desorption from streambed sediments and from increased sediment transport to streams during intense, frequent summer storms. The dominant species in monthly samples, which commonly were collected during baseflow conditions, was orthophosphate. Total phosphorous trends mostly were nonsignificant but increases of about 4 percent per year occurred at most stations; however, the station with the highest median TP concentrations (FROG) experienced a TP decrease of about 5 percent per year.

Nitrogen concentrations varied both spatially and seasonally. Nitrate (NO_3^-) concentrations were typically diluted by surface runoff during stormflow events; however, total nitrogen (TN) remained relatively constant owing to an increase of coarse organic material. Total nitrogen loads were primarily derived from NO_3^- in discharging groundwater and from the runoff or erosion of particulate-bound nitrogen; as a result, TN was mobilized to streams during both storm and nonstorm events. The highest median concentrations of NO_3^- during nonstormflow conditions were observed in watersheds with a high density of septic systems (CAPT HICK, SFLIL). Concentrations of nitrogen and subspecies were lowest in summer and highest in winter months at most stations owing to seasonal cycles of dentification. Total nitrogen yields were similar among stations (medians ranged from 3,600 to 6,300 pounds per square mile); variability in loads was primarily a function of annual streamflow volume. Total nitrogen and NO_3^- concentrations increased at the two stations with the highest median baseflow concentrations (CAPT HICK and SFLIL) but decreased by about 2 percent per year at most other stations.

The evaluation of the health of the aquatic communities in the streams monitored was assessed through annual benthic macroinvertebrate samples. Based on biological data collected at 40 randomly selected locations as part of the Fairfax County stream quality assessment program in 2017 it was reported that 75 percent of Fairfax County streams were generally of fair, poor, and very poor health; conditions that had been consistent dating back to 1999. However, many metrics assessed as part of this study showed an improving trend, especially at stations that were already in poor condition. Changes in all metrics suggest that the biodiversity, function, and condition of streams in Fairfax County is improving, but some of these improvements are driven by increased diversity and percent composition of organisms that are tolerant of the urban environment.

References Cited

Akinola, A.I., Wynn-Thompson, T., Olgun, C.G., Mostaghimi, S., and Eick, M.J., 2019, Fluvial erosion rate of cohesive streambanks is directly related to the difference in soil and water temperatures: Journal of Environmental Quality, v. 48, no. 6, p. 1741–1748, accessed August 2019 at https://doi.org/10.2134/jeq2018.10.0385.

Allen, D.M., 1974, The relationship between variable selection and data augmentation and a method for prediction: Technometrics, v. 16, no. 1, p. 125–127, accessed June 2019 at https://doi.org/10.1080/00401706.1974.10489157.

Alvarez-Cobelas, M., Sánchez-Carrillo, S., Angeler, D.G., and Sánchez-Andrés, R., 2009, Phosphorus export from catchments—A global view: Journal of the North American Benthological Society, v. 28, no. 4, p. 805–820, accessed May 2019 at https://doi.org/10.1899/09-073.1.

American Public Health Association, 1976, Standard methods for the examination of water and wastewater (14th ed.): Washington, D.C., American Public Health Association, 1,193 p.

American Society for Testing and Materials, 2007, Standard test methods for determining sediment concentration in water samples: West Conshohocken, Pa., American Society for Testing and Materials International, D3977–97, v. 11.02, p. 395–400.

Aravena, R., Evans, M.L., and Cherry, J.A., 1993, Stable isotopes of oxygen and nitrogen in source identification of nitrate from septic systems: Ground Water, v. 31, no. 2, p. 180–186, accessed July 2019 at https://doi.org/10.1111/j.1745-6584.1993.tb01809.x.

Ator, S.W., Brakebill, J.W., and Blomquist, J.D., 2011, Sources, fate, and transport of nitrogen and phosphorus in the Chesapeake Bay watershed—An empirical model: U.S. Geological Survey Scientific Investigations Report 2011–5167, 27 p., accessed April 2019 at https://doi.org/10.3133/sir20115167.

Ator, S.W., and Denver, J.M., 2015, Understanding nutrients in the Chesapeake Bay watershed and implications for management and restoration—the Eastern Shore—(ver. 1.2, June 2015): U.S. Geological Survey Circular 1406, 72 p., accessed May 2019 at https://doi.org/10.3133/cir1406.

Ator, S.W., Denver, J.M., Krantz, D.E., Newell, W.L., and Martucci, S.K., 2005, A surficial hydrogeologic framework for the mid-Atlantic Coastal Plain: U.S. Geological Survey Professional Paper 1680, 49 p.

Aulenbach, B.T., Joiner, J.K., and Painter, J.A., 2017, Hydrology and water quality in 13 watersheds in Gwinnett County, Georgia, 2001–15: U.S. Geological Survey Scientific Investigations Report 2017–5012, 82 p., accessed December 2018 at https://doi.org/10.3133/sir20175012.

Baker, D.B., Richards, R.P., Loftus, T.T., and Kramer, J.W., 2004, A new flashiness index—Characteristics and applications to midwestern rivers and streams: Journal of the American Water Resources Association, v. 40, no. 2, p. 503–522, accessed November 2018 at https://doi.org/10.1111/j.1752-1688.2004.tb01046.x.

Ballard, R., and Fiskell, J.G.A., 1974, Phosphorus retention in Coastal Plain forest soils—I. Relationship to soil properties: Soil Science Society of America Journal, v. 38, no. 2, p. 250–255, accessed May 2019 at https://doi.org/10.2136/sssaj1974.03615995003800020015x.

Barałkiewicz, D., Chudzińska, M., Szpakowska, B., Świerk, D., Gołdyn, R., and Dondajewska, R., 2014, Storm water contamination and its effect on the quality of urban surface waters: Environmental Monitoring and Assessment, v. 186, no. 10, p. 6789–6803, accessed May 2019 at https://doi.org/10.1007/s10661-014-3889-0.

Barber, L.B., Murphy, S.F., Verplanck, P.L., Sandstrom, M.W., Taylor, H.E., and Furlong, E.T., 2006, Chemical loading into surface water along a hydrological, biogeochemical, and land use gradient—A holistic watershed approach: Environmental Science & Technology, v. 40, no. 2, p. 475–486, accessed May 2019 at https://doi.org/10.1021/es051270q.

Barbour, M.T., Gerritsen, J., Snyder, B.D., and Stribling, J.B., 1999, Rapid bioassessment protocols for use in streams and wadeable rivers—Periphyton, benthic macroinvertebrates, and fish (2d ed.): U.S. Environmental Protection Agency, Office of Water, EPA 841-B-99-002, 337 p., accessed July 2019 at https://www3.epa.gov/region1/npdes/merrimackstation/pdfs/ar/AR-1164.pdf.

Barlow, P.M., Cunningham, W.L., Zhai, T., and Gray, M., 2017, U.S. Geological Survey Groundwater Toolbox version 1.3.1, a graphical and mapping interface for analysis of hydrologic data: U.S. Geological Survey software release, accessed February 2020 at https://doi.org/10.5066/F7R78C9G.

Bates, D., Mächler, M., Bolker, B., and Walker, S., 2015, Fitting linear mixed-effects models using lme4: Journal of Statistical Software, v. 67, no. 1, 48 p., accessed July 2019 at https://www.jstatsoft.org/article/view/v067i01.

Beck, K.C., Reuter, J.H., and Perdue, E.M., 1974, Organic and inorganic geochemistry of some coastal plain rivers of the southeastern United States: Geochimica et Cosmochimica Acta, v. 38, no. 3, p. 341–364, accessed February 2020 at https://doi.org/10.1016/0016-7037(74)90130-6.

Beighley, R.E., and Moglen, G.E., 2002, Trend assessment in rainfall-runoff behavior in urbanizing watersheds: Journal of Hydrologic Engineering, v. 7, no. 1, p. 27–34, accessed November 2018 at https://doi.org/10.1061/(ASCE)1084-0699(2002)7:1(27).

Bell, C.D., McMillan, S.K., Clinton, S.M., and Jefferson, A.J., 2016, Hydrologic response to stormwater control measures in urban watersheds: Journal of Hydrology (Amsterdam), v. 541, p. 1488–1500, accessed November 2018 at https://doi.org/10.1016/j.jhydrol.2016.08.049.

Bettez, N.D., and Groffman, P.M., 2013, Nitrogen deposition in and near an urban ecosystem: Environmental Science & Technology, v. 47, no. 11, p. 6047–6051, accessed November 2018 at https://doi.org/10.1021/es400664b.

Bhaskar, R., Porder, S., Balvanera, P., and Edwards, E.J., 2016, Ecological and evolutionary variation in community nitrogen use traits during tropical dry forest secondary succession: Ecology, v. 97, no. 5, p. 1194–1206, accessed December 2018 at https://doi.org/10.1890/15-1162.1.

Bledsoe, B.P., and Watson, C.C., 2001, Effects of urbanization on channel instability: Journal of the American Water Resources Association, v. 37, no. 2, p. 255–270, accessed May 2019 at https://doi.org/10.1111/j.1752-1688.2001.tb00966.x.

Blume, T., Zehe, E., and Bronstert, A., 2007, Rainfall—Runoff response, event-based runoff coefficients and hydrograph separation: Hydrological Sciences Journal, v. 52, no. 5, p. 843–862, accessed November 2019 at https://doi.org/10.1623/hysj.52.5.843.

Bond, N.R., Lake, P.S., and Arthington, A.H., 2008, The impacts of drought on freshwater ecosystems—An Australian perspective: Hydrobiologia, v. 600, no. 1, p. 3–16, accessed July 2019 at https://doi.org/10.1007/s10750-008-9326-z.

Bonneau, J., Fletcher, T.D., Costelloe, J.F., and Burns, M.J., 2017, Stormwater infiltration and the ‘urban karst’—A review: Journal of Hydrology (Amsterdam), v. 552, p. 141–150, accessed November 2018 at https://doi.org/10.1016/j.jhydrol.2017.06.043.

Boulton, A.J., 2003, Parallels and contrasts in the effects of drought on stream macroinvertebrate assemblages: Freshwater Biology, v. 48, no. 7, p. 1173–1185, accessed July 2019 at https://doi.org/10.1046/j.1365-2427.2003.01084.x.

Brakebill, J.W., Ator, S.W., and Schwarz, G.E., 2010, Sources of suspended-sediment flux in streams of the Chesapeake Bay Watershed—A regional application of the SPARROW model: Journal of the American Water Resources Association, v. 46, no. 4, p. 757–776, accessed June 2019 at https://doi.org/10.1111/j.1752-1688.2010.00450.x.

Brown, V.A., McDonnell, J.J., Burns, D.A., and Kendall, C., 1999, The role of event water, a rapid shallow flow component, and catchment size in summer stormflow: Journal of Hydrology (Amsterdam), v. 217, no. 3–4, p. 171–190, accessed December 2018 at https://doi.org/10.1016/S0022-1694(98)00247-9.

Brun, S.E., and Band, L.E., 2000, Simulating runoff behavior in an urbanizing watershed: Computers, Environment and Urban Systems, v. 24, no. 1, p. 5–22, accessed November 2018 at https://doi.org/10.1016/S0198-9715(99)00040-X.

Bussi, G., Dadson, S.J., Bowes, M.J., and Whitehead, P.G., 2017, Seasonal and interannual changes in sediment transport identified through sediment rating curves: Journal of Hydrologic Engineering, v. 22, no. 2, 8 p., accessed March 2019 at https://doi.org/10.1061/(ASCE)HE.1943-5584.0001466.

Carey, R.O., Hochmuth, G.J., Martinez, C.J., Boyer, T.H., Dukes, M.D., Toor, G.S., and Cisar, J.L., 2013, Evaluating nutrient impacts in urban watersheds—Challenges and research opportunities: Environmental Pollution, v. 173, p. 138–149. [Also available at https://doi.org/10.1016/j.envpol.2012.10.004.]

Carpenter, S.R., Caraco, N.F., Correll, D.L., Howarth, R.W., Sharpley, A.N., and Smith, V.H., 1998, Nonpoint Pollution of Surface Waters with Phosphorus and Nitrogen: Ecological Applications, v. 8, no. 3, p. 559–568, accessed February 2019 at https://doi.org/10.1890/1051-0761(1998)008[0559:NPOSWW]2.0.CO;2.

Cashman, M.J., Gellis, A., Sanisaca, L.G., Noe, G.B., Cogliandro, V., and Baker, A., 2018, Bank-derived material dominates fluvial sediment in a suburban Chesapeake Bay watershed: River Research and Applications, v. 34, no. 8, p. 1032–1044, accessed November 2018 at https://doi.org/10.1002/rra.3325.

Cerozi, B., and Fitzsimmons, K., 2016, The effect of pH on phosphorus availability and speciation in an aquaponics nutrient solution: Bioresource Technology, v. 219, p. 778–781, accessed May 2019 at https://doi.org/10.1016/j.biortech.2016.08.079.

Chakraborty, D., Nair, V.D., Harris, W.G., and Rhue, R.D., 2012, Environmentally relevant phosphorus retention capacity of sandy Coastal Plain soils: Soil Science, v. 177, no. 12, p. 701–707.

Chesapeake Bay Program Office, 2018, High-resolution land cover data for Chesapeake Bay watershed counties: Chesapeake Conservancy web page, accessed June 2018 at https://chesapeakeconservancy.org/conservation-innovation-center-2/high-resolution-data/land-use-data-project/.

Chesapeake Bay Scientific and Technical Advisory Committee, 2005, Understanding “lag times” affecting the improvement of water quality in the Chesapeake Bay: Chesapeake Bay Program STAC Publication 05–001, 19 p., accessed October 19, 2009, at http://www.chesapeake.org/stac/Pubs/LagTimeReport.pdf.

Cohn, T.A., England, J.F., Berenbrock, C.E., Mason, R.R., Stedinger, J.R., and Lamontagne, J.R., 2013, A generalized Grubbs-Beck test statistic for detecting multiple potentially influential low outliers in flood series: Water Resources Research, v. 49, no. 8, p. 5047–5058, accessed December 2018 at https://doi.org/10.1002/wrcr.20392.

Cohn, T.A., Gilroy, E.J., and Baier, W.G., 1992, Estimating fluvial transport of trace constituents using a regression model with data subject to censoring: American Statistical Association Section on Statistics and the Environment, proceedings, 9 p., accessed December 2018 at https://www.timcohn.com/Publications/CohnGilroyBaier1992.pdf.

Cohn, T.A., Lane, W.L., and Baier, W.G., 1997, An algorithm for computing moments-based flood quantile estimates when historical flood information is available: Water Resources Research, v. 33, no. 9, p. 2089–2096, accessed November 2018 at https://doi.org/10.1029/97WR01640.

Commonwealth of Virginia, 1997a, Numerical criteria for dissolved oxygen, pH, and maximum temperature, sec. 50 of State Water Control Board, chap. 260 of Environment: Virginia Administrative Code title 9, accessed April 2018 at https://law.lis.virginia.gov/admincode/title9/agency25/chapter260/section50/.

Commonwealth of Virginia, 1997b, Maximum hourly temperature change, sec. 70 of State Water Control Board, chap. 260 of Environment: Virginia Administrative Code title 9, accessed April 2018 at https://law.lis.virginia.gov/admincode/title9/agency25/chapter260/section70/.

Conley, D.J., Paerl, H.W., Howarth, R.W., Boesch, D.F., Seitzinger, S.P., Havens, K.E., Lancelot, C., and Likens, G.E., 2009, Controlling eutrophication—Nitrogen and phosphorus: Science, v. 323, no. 5917, p. 1014–1015.

Conway, T.M., 2007, Impervious surface as an indicator of pH and specific conductance in the urbanizing coastal zone of New Jersey, USA: Journal of Environmental Management, v. 85, no. 2, p. 308–316, accessed May 2019 at https://doi.org/10.1016/j.jenvman.2006.09.023.

Correll, D.L., 1998, The role of phosphorus in the eutrophication of receiving waters—A review: Journal of Environmental Quality, v. 27, no. 2, p. 261–266, accessed November 2018 at https://doi.org/10.2134/jeq1998.00472425002700020004x.

Corsi, S.R., De Ciccio, L.A., Lutz, M.A., and Hirsch, R.M., 2015, River chloride trends in snow-affected urban watersheds—Increasing concentrations outpace urban growth rate and are common among all seasons: The Science of the Total Environment, v. 508, p. 488–497, accessed April 2019 at https://doi.org/10.1016/j.scitotenv.2014.12.012.

Corsi, S.R., Graczyk, D.J., Geis, S.W., Booth, N.L., and Richards, K.D., 2010, A fresh look at road salt—Aquatic toxicity and water-quality impacts on local, regional, and national scales: Environmental Science & Technology, v. 44, no. 19, p. 7376–7382, accessed May 2019 at https://doi.org/10.1021/es101333u.

Cowen, W.F., and Lee, G.F., 1976, Phosphorus availability in particulate materials transported by urban runoff: Journal - Water Pollution Control Federation, v. 48, no. 3, p. 580–591.

Critchlow, D.E., and Flinger, M.A., 1991, On distribution-free multiple comparisons in the one-way analysis of variance: Communications in Statistics. Theory and Methods, v. 20, no. 1, p. 127–139, accessed February 2019 at https://doi.org/10.1080/03610929108830487.

Cuffney, T.F., Brightbill, R.A., May, J.T., and Waite, I.R., 2010, Responses of benthic macroinvertebrates to environmental changes associated with urbanization in nine metropolitan areas: Ecological Applications, v. 20, no. 5, p. 1384–1401, accessed December 2018 at https://doi.org/10.1890/08-1311.1.

Dahm, C.N., Baker, M.A., Moore, D.I., and Thibault, J.R., 2003, Coupled biogeochemical and hydrological responses of streams and rivers to drought: Freshwater Biology, v. 48, no. 7, p. 1219–1231, accessed July 2019 at https://doi.org/10.1046/j.1365-2427.2003.01082.x.

Daley, M.L., Potter, J.D., and McDowell, W.H., 2009, Salinization of urbanizing New Hampshire streams and groundwater—Effects of road salt and hydrologic variability: Journal of the North American Benthological Society, v. 28, no. 4, p. 929–940, accessed May 2019 at https://doi.org/10.1899/09-052.1.

Daly, C., Gibson, W., Taylor, G., Johnson, G., and Pasteris, P., 2002, A knowledge-based approach to the statistical mapping of climate: Climate Research, v. 22, p. 99–113, accessed November 2018 at https://doi.org/10.3354/cr022099.

Davis, T.W., Harke, M.J., Marcoval, M.A., Goleski, J., Orano-Dawson, C., Berry, D.L., and Gobler, C.J., 2010, Effects of nitrogenous compounds and phosphorus on the growth of toxic and non-toxic strains of Microcystis during cyanobacterial blooms: Aquatic Microbial Ecology, v. 61, no. 2, p. 149–162, accessed May 2019 at https://doi.org/10.3354/ame01445.

Deek, A., Emeis, K., and Struck, U., 2010, Seasonal variations in nitrate isotope composition of three rivers draining into the North Sea: Biogeosciences Discussions, v. 7, no. 4, p. 6051–6088, accessed February 2019 at https://doi.org/10.5194/bgd-7-6051-2010.

Deletic, A.B., and Maksimovic, C.T., 1998, Evaluation of water quality factors in storm runoff from paved areas: Journal of Environmental Engineering, v. 124, no. 9, p. 869–879, accessed May 2019 at https://doi.org/10.1061/(ASCE)0733-9372(1998)124:9(869).

Demars, B.O.L., Manson, J.R., Ólafsson, J.S., Gíslason, G.M., Gudmundsdóttir, R., Woodward, G., Reiss, J., Pichler, D.E., Rasmussen, J.J., and Friberg, N., 2011, Temperature and the metabolic balance of streams: Freshwater Biology, v. 56, no. 6, p. 1106–1121, accessed May 2019 at https://doi.org/10.1111/j.1365-2427.2010.02554.x.

Denver, J.M., Cravotta, C.A., III, Ator, S.W., and Lindsey, B.D., 2010, Contributions of phosphorus from groundwater to streams in the Piedmont, Blue Ridge, and Valley and Ridge Physiographic Provinces, Eastern United States: U.S. Geological Survey Scientific Investigations Report 2010–5176, 38 p., accessed May 2018 at https://doi.org/10.3133/sir20105176.

Diaz Villanueva, V., Albariño, R., and Canhoto, C., 2012, Positive effect of shredders on microbial biomass and decomposition in stream microcosms: Freshwater Biology, v. 57, no. 12, p. 2504–2513, accessed August 2019 at https://doi.org/10.1111/fwb.12023.

Dicken, C.L., Nicholson, S.W., Horton, J.D., Kinney, S.A., Gunter, G., Foose, M.P., and Mueller, J.A.L., 2005, Integrated geologic map databases for the United States—Delaware, Maryland, New York, Pennsylvania, and Virginia (ver. 1.0): U.S. Geological Survey Open-File Report 2005–1325, accessed June 2018 at https://doi.org/10.3133/ofr20051325.

Dingman, S.L., 2002, Physical hydrology: Upper Saddle River, New Jersey, Prentice Hall, 656 p.

Donovan, M., Miller, A., and Baker, M., 2016, Reassessing the role of milldams in Piedmont floodplain development and remobilization: Geomorphology, v. 268, p. 133–145, accessed March 2020 at https://doi.org/10.1016/j.geomorph.2016.06.007.

Donovan, M., Miller, A., Baker, M., and Gellis, A., 2015, Sediment contributions from floodplains and legacy sediments to Piedmont streams of Baltimore County, Maryland: Geomorphology, v. 235, p. 88–105, accessed March 2020 at https://doi.org/10.1016/j.geomorph.2015.01.025.

Duan, S., and Kaushal, S.S., 2013, Warming increases carbon and nutrient fluxes from sediments in streams across land use: Biogeosciences, v. 10, no. 2, p. 1193–1207, accessed February 2019 at https://doi.org/10.5194/bg-10-1193-2013.

Duan, S., Kaushal, S.S., Groffman, P.M., Band, L.E., and Belt, K.T., 2012, Phosphorus export across an urban to rural gradient in the Chesapeake Bay watershed: Journal of Geophysical Research. Biogeosciences, v. 117, no. G1, 12 p.

Duncan, J.M., Welty, C., Kemper, J.T., Groffman, P.M., and Band, L.E., 2017, Dynamics of nitrate concentration-discharge patterns in an urban watershed: Water Resources Research, v. 53, no. 8, p. 7349–7365, accessed February 2019 at https://doi.org/10.1002/2017WR020500.

England, J.F., Jr., Cohn, T.A., Faber, B.A., Stedinger, J.R., Thomas, W.O., Jr., Veilleux, A.G., Kiang, J.E., and Mason, R.R., Jr., 2018, Guidelines for determining flood flow frequency—Bulletin 17C: U.S. Geological Survey Techniques and Methods, book 4, chap. B5, 148 p., accessed December 2018 at https://doi.org/10.3133/tm4B5.

Fairfax County, 2017a, Stream quality assessment program: Fairfax County Public Works and Environmental Services web page, accessed May 20, 2019, at https://www.fairfaxcounty.gov/publicworks/stormwater/stream-quality-assessment-program.

Fairfax County, 2017b, Fairfax County stormwater status report: Fairfax County, Virginia, 59 p.

Fairfax County, 2018, Fairfax County geospatial data: Fairfax County Virginia Open Geospatial Data, accessed August 13, 2019, at https://www.fairfaxcounty.gov/maps/open-geospatial-data.

Fairfax County, 2019, Department of Public Works and Environmental Services policies and procedures—Stormwater Division Comprehensive Aquatic Monitoring Program standard operating procedures: Fairfax County Public Works and Environmental Services web page, accessed September 2019 at https://www.fairfaxcounty.gov/publicworks/sites/publicworks/files/assets/documents/pdf/publications/stream_assessment_sop.pdf.

Falcone, J.A., 2015, U.S. conterminous wall-to-wall anthropogenic land use trends (NWALT), 1974–2012: U.S. Geological Survey Data Series 948, 33 p. plus appendixes, accessed May 2019 at https://doi.org/10.3133/ds948.

Feminella, J.W., and Walsh, C.J., 2005, Urbanization and stream ecology—An introduction to the series: Journal of the North American Benthological Society, v. 24, no. 3, p. 585–587, accessed December 2018 at https://doi.org/10.1899/0887-3593(2005)024[0585:UASEAI]2.0.CO;2.

Fenneman, N.M., and Johnson, D.W., 1946, Physiographic divisions of the conterminous U.S.: U.S. Geological Survey NSDI Node database, accessed June 2018 at https://water.usgs.gov/lookup/getspatial?physio.

Fenta, A.A., Yasuda, H., Shimizu, K., Haregeweyn, N., and Negussie, A., 2016, Dynamics of soil erosion as influenced by watershed management practices—A case study of the Agula watershed in the semi-arid highlands of northern Ethiopia: Environmental Management, v. 58, no. 5, p. 889–905, accessed January 2019 at https://doi.org/10.1007/s00267-016-0757-4.

Flynn, K.M., Kirby, W.H., and Hummel, P.R., 2006, User's manual for program PeakFQ, annual flood-frequency analysis using bulletin 17B guidelines: U.S. Geological Survey Techniques and Methods, book 4, chap. B4, 42 p., accessed May 2018 at https://doi.org/10.3133/tm4B4.

Focazio, M.J., Speiran, G.K., and Rowan, M.E., 1992, Quality of ground water in the coastal plain physiographic province of Virginia: U.S Geological Survey Water-Resources Investigations Report 92-4175, 25 p.

Froelich, A.J., and Langer, W.H., 1983, Map showing geological provinces, landforms, drainage basin characteristics, and flooding in Fairfax County and vicinity, Virginia: U.S. Geological Survey Miscellaneous Investigations Series Map I-1421, scale 1:48,000.

Froelich, A.J., and Zenone, C., 1985a, Maps showing geologic terrane, drainage basins, overburden, and low flow of streams in Fairfax County, and vicinity, Virginia: U.S. Geological Survey Miscellaneous Investigations Series Map I-1534, scale 1:24,000.

Froelich, A.J., and Zenone, C., 1985b, The relation of water quality to geology and land use changes in Fairfax County and vicinity, Virginia: U.S. Geological Survey Miscellaneous Investigations Series Map I-1561, scale 1:48,000.

Frost, P.C., Larson, J.H., Johnston, C.A., Young, K.C., Maurice, P.A., Lamberti, G.A., and Bridgham, S.D., 2006, Landscape predictors of stream dissolved organic matter concentration and physicochemistry in a Lake Superior river watershed: Aquatic Sciences, v. 68, no. 1, p. 40–51, accessed April 2019 at https://doi.org/10.1007/s00027-005-0802-5.

Galli, J., 1991, Thermal impacts associated with urbanization and stormwater management best management practices. Metropolitan Washington Council of Governments, Maryland Department of Environment, 188 p.

Gellis, A.C., 2013, Factors influencing storm-generated suspended-sediment concentrations and loads in four basins of contrasting land use, humid-tropical Puerto Rico: Catena, v. 104, p. 39–57, accessed November 2018 at https://doi.org/10.1016/j.catena.2012.10.018.

Gellis, A.C., Hupp, C.R., Pavich, M.J., Landwehr, J.M., Banks, W.S.L., Hubbard, B.E., Langland, M.J., Ritchie, J.C., and Reuter, J.M., 2009, Sources, transport, and storage of sediment at selected sites in the Chesapeake Bay watershed: U.S. Geological Survey Scientific Investigations Report 2008–5186, 95 p.

Gellis, A.C., Myers, M.K., Noe, G.B., Hupp, C.R., Schenk, E.R., and Myers, L., 2017, Storms, channel changes, and a sediment budget for an urban-suburban stream, Difficult Run, Virginia, USA: Geomorphology, v. 278, p. 128–148, accessed May 2019 at https://doi.org/10.1016/j.geomorph.2016.10.031.

Gellis, A.C., Noe, G.B., Clune, J.W., Myers, M.K., Hupp, C.R., Schenck, E.R., and Schwarz, G.E., 2015, Sources of fine-grained sediment in the Linganore Creek watershed, Frederick and Carroll Counties, Maryland, 2008–10: U.S. Geological Survey Scientific Investigations Report 2014–5147, 56 p., accessed May 2019 at https://doi.org/10.3133/sir20145147.

Gibbs, R.J., 1970, Mechanisms controlling world water chemistry: Science, v. 170, no. 3962, p. 1088–1090, accessed May 2019 at https://doi.org/10.1126/science.170.3962.1088.

Grabowski, R.C., Droppo, I.G., and Wharton, G., 2011, Erodibility of cohesive sediment—The importance of sediment properties: Earth-Science Reviews, v. 105, no. 3–4, p. 101–120, accessed May 2019 at https://doi.org/10.1016/j.earscirev.2011.01.008.

Gregory, M.B., and Calhoun, D.L., 2007, Physical, chemical, and biological responses of streams to increasing watershed urbanization in the Piedmont ecoregion of Georgia and Alabama, 2003, chap. B *of* Effects of urbanization on stream ecosystems in six metropolitan areas of the United States: U.S. Geological Survey Scientific Investigations Report 2006–5101–B, 104 p., accessed December 2018 at https://doi.org/10.3133/sir20065101B.

Griffis, V.W., Stedinger, J.R., and Cohn, T.A., 2004, Log Pearson type 3 quantile estimators with regional skew information and low outlier adjustments: Water Resources Research, v. 40, no. 7, 17 p., accessed December 2018 at https://doi.org/10.1029/2003WR002697.

Griffith, M.B., 2014, Natural variation and current reference for specific conductivity and major ions in wadeable streams of the conterminous USA: Freshwater Science, v. 33, no. 1, p. 1–17, accessed May 2019 at https://doi.org/10.1086/674704.

Groffman, P.M., Law, N.L., Belt, K.T., Band, L.E., and Fisher, G.T., 2004, Nitrogen fluxes and retention in urban watershed ecosystems: Ecosystems (New York, N.Y.), v. 7, no. 4, p. 393–403, accessed November 2018 at https://doi.org/10.1007/s10021-003-0039-x.

Guy, H., 1969, Laboratory theory and methods for sediment analysis: U.S. Geological Survey Techniques of Water-Resources Investigations, book 5, chap. C1, 58 p.

Hall, F.R., 1968, Base-flow recessions—A review: Water Resources Research, v. 4, no. 5, p. 973–983, accessed July 2019 at https://doi.org/10.1029/WR004i005p00973.

Hall, M.J., 1977, The effect of urbanization on storm runoff from two catchment areas in North London: International Association of Hydrological Sciences, no. 123, p. 144–152, accessed February 2019 at http://hydrologie.org/redbooks/a123/iahs_123_0144.pdf.

Han, X., Hovland, E., and Khaja, F., 2018, Demographic reports 2018: County of Fairfax, Virginia, Economic, Demographic and Statistical Research, accessed May 2019 at https://www.fairfaxcounty.gov/demographics/sites/demographics/files/assets/demographicreports/fullrpt2018.pdf.

Haq, S., Kaushal, S.S., and Duan, S., 2018, Episodic salinization and freshwater salinization syndrome mobilize base cations, carbon, and nutrients to streams across urban regions: Biogeochemistry, v. 141, no. 3, p. 463–486, accessed May 2019 at https://doi.org/10.1007/s10533-018-0514-2.

Hardison, E.C., O'Driscoll, M.A., DeLoatch, J.P., Howard, R.J., and Brinson, M.M., 2009, Urban land use, channel incision, and water table decline along Coastal Plain streams, North Carolina: Journal of the American Water Resources Association, v. 45, no. 4, p. 1032–1046, accessed July 2019 at https://doi.org/10.1111/j.1752-1688.2009.00345.x.

Hatt, B.E., Fletcher, T.D., Walsh, C.J., and Taylor, S.L., 2004, The influence of urban density and drainage infrastructure on the concentrations and loads of pollutants in small streams: Environmental Management, v. 34, no. 1, p. 112–124, accessed November 2018 at https://doi.org/10.1007/s00267-004-0221-8.

Helsel, D.R., 2005, Insider censoring—Distortion of data with nondetects: Human and Ecological Risk Assessment, v. 11, no. 6, p. 1127–1137, accessed October 2018 at https://doi.org/10.1080/10807030500278586.

Helsel, D.R., and Frans, L.M., 2006, Regional Kendall test for trend: Environmental Science & Technology, v. 40, no. 13, p. 4066–4073, accessed March 2020 at https://doi.org/10.1021/es051650b.

Helsel, D.R., and Hirsch, R.M., 2002, Statistical methods in water resources: New York, Elsevier, 529 p.

Hem, J.D., 1985, Study and interpretation of the chemical characteristics of natural water (3d ed.): U.S. Geological Survey Water-Supply Paper 2254, 263 p.

Hester, E.T., and Bauman, K.S., 2013, Stream and retention pond thermal response to heated summer runoff from urban impervious surfaces: Journal of the American Water Resources Association, v. 49, no. 2, p. 328–342, accessed May 2019 at https://doi.org/10.1111/jawr.12019.

Hillebrand, H., Soininen, J., and Snoeijs, P., 2010, Warming leads to higher species turnover in a coastal ecosystem: Global Change Biology, v. 16, no. 4, p. 1181–1193, accessed May 2019 at https://doi.org/10.1111/j.1365-2486.2009.02045.x.

Hirsch, R.M., 2019, Daily streamflow trend analysis: U.S. Geological Survey Water Data for the Nation Blog web page, accessed January 5, 2018, at https://waterdata.usgs.gov/blog/quantile-kendall/.

Hirsch, R.M., Moyer, D.L., and Archfield, S.A., 2010, Weighted Regressions on Time, Discharge, and Season (WRTDS), with an application to Chesapeake Bay river inputs: Journal of the American Water Resources Association, v. 46, no. 5, p. 857–880, accessed March 2019 at https://doi.org/10.1111/j.1752-1688.2010.00482.x.

Hirsch, R.M., Slack, J.R., and Smith, R.A., 1982, Techniques of trend analysis for monthly water quality data: Water Resources Research, v. 18, no. 1, p. 107–121, accessed June 2019 at https://doi.org/10.1029/WR018i001p00107.

Hobbie, S.E., Finlay, J.C., Janke, B.D., Nidzgorski, D.A., Millet, D.B., and Baker, L.A., 2017, Contrasting nitrogen and phosphorus budgets in urban watersheds and implications for managing urban water pollution: Proceedings of the National Academy of Sciences of the United States of America, v. 114, no. 16, p. 4177–4182, accessed November 2018 at https://doi.org/10.1073/pnas.1618536114.

Hollis, G.E., 1975, The effect of urbanization on floods of different recurrence interval: Water Resources Research, v. 11, no. 3, p. 431–435, accessed November 2018 at https://doi.org/10.1029/WR011i003p00431.

Hood, R.R., and Christian, J.R., 2008, Ocean nitrogen cycle modeling, chap. 33 of Capone, D.G., Bronk, D.A., Mulholland, M.R., and Carpenter, E.J., eds., Nitrogen in the Marine Environment (2d ed.): San Diego, Academic Press, p. 1445–1495, accessed February 2020 at https://doi.org/10.1016/B978-0-12-372522-6.00033-5.

Hoomehr, S., Akinola, A.I., Wynn-Thompson, T., Garnand, W., and Eick, M.J., 2018, Water temperature, pH, and road salt impacts on the fluvial erosion of cohesive streambanks: Water (Basel), v. 10, no. 302, 16 p., accessed May 2019 at https://doi.org/10.3390/w10030302.

Hopkins, K.G., Bhaskar, A.S., Woznicki, S.A., and Fanelli, R.M., 2020, Changes in event-based streamflow magnitude and timing after suburban development with infiltration-based stormwater management: Hydrological Processes, v. 34, no. 2, p. 387–403, accessed February 2020 at https://doi.org/10.1002/hyp.13593.

Hopkins, K.G., Noe, G.B., Franco, F., Pindilli, E.J., Gordon, S., Metes, M.J., Claggett, P.R., Gellis, A.C., Hupp, C.R., and Hogan, D.M., 2018, A method to quantify and value floodplain sediment and nutrient retention ecosystem services: Journal of Environmental Management, v. 220, p. 65–76, accessed May 2019 at https://doi.org/10.1016/j.jenvman.2018.05.013.

House, W.A., and Denison, F.H., 2002, Total phosphorus content of river sediments in relationship to calcium, iron and organic matter concentrations: The Science of the Total Environment, v. 282–283, p. 341–351, accessed September 2019 at https://doi.org/10.1016/S0048-9697(01)00923-8.

Hupp, C.R., Noe, G.B., Schenk, E.R., and Benthem, A.J., 2013, Recent and historic sediment dynamics along Difficult Run, a suburban Virginia Piedmont stream: Geomorphology, v. 180–181, p. 156–169, accessed July 2019 at https://doi.org/10.1016/j.geomorph.2012.10.007.

Hyer, K.E., Denver, J.M., Langland, M.J., Webber, J.S., Bohlke, J.K., and Hively, W.D., 2016, Spatial and temporal variation of stream chemistry associated with contrasting geology and land-use patterns in the Chesapeake Bay watershed—Summary of results from Smith Creek, Virginia; Upper Chester River, Maryland; Conewago Creek, Pennsylvania; and Difficult Run, Virginia, 2010–2013: U.S. Geological Survey Scientific Investigations Report 2016–5093, 211 p., accessed December 2018 at https://doi.org/10.3133/sir20165093.

Interstate Commission on the Potomac River Basin, 2017, Volume III Chloride TMDLs for the Accotink Creek watershed, Fairfax County: Prepared for Virginia Department of Environmental Quality, 110 p., accessed May 2019 at https://www.deq.virginia.gov/portals/0/DEQ/Water/TMDL/apptmdls/potrvr/Vol_III_Final_CL_TMDL.pdf.

James, W.F., and Barko, J.W., 2004, Diffusive fluxes and equilibrium processes in relation to phosphorus dynamics in the upper Mississippi River: River Research and Applications, v. 20, no. 4, p. 473–484, accessed May 2019 at https://doi.org/10.1002/rra.761.

Jansen, I.M.L., and Painter, R.B., 1974, Predicting sediment yield from climate and topography: Journal of Hydrology (Amsterdam), v. 21, no. 4, p. 371–380, accessed March 2020 at https://doi.org/10.1016/S0022-1694(74)80006-5.

Jastram, J., 2014, Streamflow, water quality, and aquatic macroinvertebrates of selected streams in Fairfax County, Virginia, 2007–12: U.S. Geological Survey Scientific Investigations Report 2014–5073, 68 p., accessed January 2016 at https://doi.org/10.3133/sir20145073.

Jastram, J.D., Moyer, D.L., and Hyer, K.E., 2009, A comparison of turbidity-based and streamflow-based estimates of suspended-sediment concentrations in three Chesapeake Bay tributaries: U.S. Geological Survey Scientific Investigations Report 2009–5165, 37 p., accessed April 2015 at https://doi.org/10.3133/sir20095165.

Jennings, D.B., and Taylor Jarnagin, S., 2002, Changes in anthropogenic impervious surfaces, precipitation and daily streamflow discharge—A historical perspective in a mid-Atlantic subwatershed: Landscape Ecology, v. 17, no. 5, p. 471–489, accessed December 2018 at https://doi.org/10.1023/A:1021211114125.

Johnson, H.O., Gupta, S.C., Vecchia, A.V., and Zvomuya, F., 2009, Assessment of water quality trends in the Minnesota River using non-parametric and parametric methods: Journal of Environmental Quality, v. 38, no. 3, p. 1018–1030, accessed August 2019 at https://doi.org/10.2134/jeq2008.0250.

Johnson, S.L., 2004, Factors influencing stream temperatures in small streams—Substrate effects and a shading experiment: Canadian Journal of Fisheries and Aquatic Sciences, v. 61, no. 6, p. 913–923, accessed July 2019 at https://doi.org/10.1139/f04-040.

Jones, C.R., de Mutsert, K., and Fowler, A., 2017, An ecological study of Gunston Cove: Prepared for the Department of Public Works and Environmental Services, County of Fairfax, VA, 178 p., accessed March 3, 2020, at http://mars.gmu.edu/handle/1920/11346.

Karr, J.R., 1999, Defining and measuring river health: Freshwater Biology, v. 41, no. 2, p. 221–234, accessed August 2019 at https://doi.org/10.1046/j.1365-2427.1999.00427.x.

Kaushal, S.S., 2016, Increased salinization decreases safe drinking water: Environmental Science & Technology, v. 50, no. 6, p. 2765–2766, accessed May 2019 at https://doi.org/10.1021/acs.est.6b00679.

Kaushal, S.S., Duan, S., Doody, T.R., Haq, S., Smith, R.M., Newcomer Johnson, T.A., Newcomb, K.D., Gorman, J., Bowman, N., Mayer, P.M., Wood, K.L., Belt, K.T., and Stack, W.P., 2017, Human-accelerated weathering increases salinization, major ions, and alkalinization in fresh water across land use: Applied Geochemistry, v. 83, p. 121–135, accessed May 2019 at https://doi.org/10.1016/j.apgeochem.2017.02.006.

Kaushal, S.S., Groffman, P.M., Band, L.E., Shields, C.A., Morgan, R.P., Palmer, M.A., Belt, K.T., Swan, C.M., Findlay, S.J., and Fisher, G.T., 2008, Interaction between urbanization and climate variability amplifies watershed nitrate export in Maryland: Environmental Science & Technology, v. 42, no. 16, p. 5872–5878, accessed May 2019 at https://doi.org/10.1021/es800264f.

Kaushal, S.S., Groffman, P.M., Likens, G.E., Belt, K.T., Stack, W.P., Kelly, V.R., Band, L.E., and Fisher, G.T., 2005, Increased salinization of fresh water in the northeastern United States: Proceedings of the National Academy of Sciences of the United States of America, v. 102, no. 38, p. 13517–13520, accessed May 2019 at https://doi.org/10.1073/pnas.0506414102.

Keeney, D.R., and Follett, R.F., 1991, Managing nitrogen for groundwater quality and farm profitability—Overview and introduction 1, chap. 1 *of* Follet, R.F., Keeney, D.R., and Cruse, R.M. eds., Managing nitrogen and groundwater quality and farm profitability—Proceedings of a symposium: Madison, Soil Science Society of America, v. 1, p. 1–7, accessed March 2018 at https://doi.org/10.2136/1991.managingnitrogen.c1.

Kelly, W.E., and Gularte, R.C., 1981, Erosion resistance of cohesive soils: Journal of the Hydraulics Division, v. 107, no. 10, p. 1211–1224.

King, R.S., Baker, M.E., Whigham, D.F., Weller, D.E., Jordan, T.E., Kazyak, P.F., and Hurd, M.K., 2005, Spatial considerations for linking watershed land cover to ecological indicators in streams: Ecological Applications, v. 15, no. 1, p. 137–153, accessed December 2018 at https://doi.org/10.1890/04-0481.

Klein, R.D., 1979, Urbanization and stream quality impairment: Journal of the American Water Resources Association, v. 15, no. 4, p. 948–963, accessed November 2018 at https://doi.org/10.1111/j.1752-1688.1979.tb01074.x.

Kurashige, Y., 1993, Mechanism of suspended sediment supply to headwater rivers and its seasonal variation in west central Hokkaido, Japan: Japanese Journal of Limnology, v. 54, no. 4, p. 305–315. [Rikusuigaku Zasshi], accessed May 2019 at https://doi.org/10.3739/rikusui.54.305.

Kutznetsova, A., Brockhoff, P.B., and Christensen, R.H.B., 2017, lmerTest Package—Tests in linear mixed effects models: Journal of Statistical Software, v. 82, no. 13, 26 p., accessed July 2019 at https://doi.org/10.18637/jss.v082.i13.

Lammers, R.W., and Bledsoe, B.P., 2017, What role does stream restoration play in nutrient management?: Critical Reviews in Environmental Science and Technology, v. 47, no. 6, p. 335–371, accessed November 2018 at https://doi.org/10.1080/10643389.2017.1318618.

Landers, M.N., and Sturm, T.W., 2013, Hysteresis in suspended sediment to turbidity relations due to changing particle size distributions: Water Resources Research, v. 49, no. 9, p. 5487–5500, accessed May 2018 at https://doi.org/10.1002/wrcr.20394.

Langland, M.J., Blomquist, J.D., Sprague, L.A., and Edwards, R.E., 2000, Trends and status of flow, nutrients, and sediments for selected nontidal sites in the Chesapeake Bay watershed, 1985–98: U.S. Geological Survey Open-File Report 99-451, 46 p., accessed June 2019 at https://doi.org/10.3133/ofr99451.

La Valle, P.D., 1975, Domestic sources of stream phosphates in urban streams: Water Research, v. 9, no. 10, p. 913–915, accessed November 2018 at https://doi.org/10.1016/0043-1354(75)90041-X.

Lawler, D.M., Petts, G.E., Foster, I.D.L., and Harper, S., 2006, Turbidity dynamics during spring storm events in an urban headwater river system—The Upper Tame, West Midlands, UK: The Science of the Total Environment, v. 360, no. 1–3, p. 109–126, accessed May 2019 at https://doi.org/10.1016/j.scitotenv.2005.08.032.

Lawler, D.M., Thorne, C.R., and Hooke, J.M., 1997, Bank erosion and instability, *in* Thorne, C.R., and Hooke, J.M., eds., Applied Fluvial Geomorphology for River Engineering and Management: New York, John Wiley & Sons, p. 137–172.

Lehtoranta, J., and Pitkänen, H., 2003, Binding of phosphate in sediment accumulation areas of the eastern Gulf of Finland, Baltic Sea: Hydrobiologia, v. 492, no. 1–3, p. 55–67, accessed May 2019 at https://doi.org/10.1023/A:1024869929510.

Lenat, D.R., and Crawford, J.K., 1994, Effects of land use on water quality and aquatic biota of three North Carolina Piedmont streams: Hydrobiologia, v. 294, no. 3, p. 185–199, accessed August 2019 at https://doi.org/10.1007/BF00021291.

Leopold, L.B., 1968, Hydrology for urban land planning—A guidebook on the hydrologic effects of urban land use: U.S. Geological Survey Circular 554, 18 p., accessed November 2017 at https://doi.org/10.3133/cir554.

Leopold, L.B., and Dunne, T., 1978, Water in environmental planning: San Francisco, W.H. Freeman, 815 p.

Li, H., Liu, L., Li, M., and Zhang, X., 2013, Effects of pH, temperature, dissolved oxygen, and flow rate on phosphorus release processes at the sediment and water interface in storm sewer: Journal of Analytical Methods in Chemistry, 7 p., accessed May 1, 2019, at https://www.hindawi.com/journals/jamc/2013/104316/.

Lindsey, B.D., Phillips, S.W., Donnelly, C.A., Speiran, G.K., Plummer, L.N., Böhlke, J.-K., Focazio, M.J., Burton, W.C., and Busenberg, E., 2003, Residence times and nitrate transport in ground water discharging to streams in the Chesapeake Bay watershed: U.S. Geological Survey Water-Resources Investigations Report 2003–4035, 201 p., accessed December 2019 at https://doi.org/10.3133/wri034035.

Lloyd, C.E.M., Freer, J.E., Johnes, P.J., and Collins, A.L., 2016, Using hysteresis analysis of high-resolution water quality monitoring data, including uncertainty, to infer controls on nutrient and sediment transfer in catchments: The Science of the Total Environment, v. 543, p. 388–404, accessed July 2019 at https://doi.org/10.1016/j.scitotenv.2015.11.028.

Loader, C., 2013, locfit—Local regression, likelihood and density estimation (ver. 1.5-9.1): The Comprehensive R Archive Network web page, accessed May 2019 at https://CRAN.R-project.org/package=locfit.

Lorenz, D., 2017, restrend—ESTimate TRENDs (ver. 0.4.2): U.S. Geological Survey GitHub web page, accessed June 2018 at https://github.com/USGS-R/restrend.

Lorenz, D., Runkel, R., and De Cicco, L., 2015, rloadest—River load estimation (ver. 0.4.5): U.S. Geological Survey GitHub web page, accessed August 2018 at https://github.com/USGS-R/rloadest.

Luedtke, R.J., and Brusven, M.A., 1976, Effects of sand sedimentation on colonization of stream insects: Journal of the Fisheries Research Board of Canada, v. 33, no. 9, p. 1881–1886, accessed February 2019 at https://doi.org/10.1139/f76-240.

Maidment, D.R., 1993, Handbook of hydrology: New York, McGraw-Hill, 1,424 p.

Mallows, C.L., 1973, Some comments on Cp: Technometrics, v. 15, no. 4, p. 661–675.

Manning, P.G., and Wang, X., 1994, Ferric oxide and the binding of phosphorus, lead and carbon in river particulate matter: Canadian Mineralogist, v. 32, p. 211–221.

Matsubayashi, U., Velasquez, G.T., and Takagi, F., 1993, Hydrograph separation and flow analysis by specific electrical conductance of water: Journal of Hydrology (Amsterdam), v. 152, no. 1–4, p. 179–199, accessed November 2019 at https://doi.org/10.1016/0022-1694(93)90145-Y.

Maxted, J.R., Barbour, M.T., Gerritsen, J., Poretti, V., Primrose, N., Silvia, A., Penrose, D., and Renfrow, R., 2000, Assessment framework for mid-Atlantic coastal plain streams using benthic macroinvertebrates: Journal of the North American Benthological Society, v. 19, no. 1, p. 128–144, accessed July 2019 at https://doi.org/10.2307/1468286.

McCormick, P.V., and Laing, J.A., 2003, Effects of increased phosphorus loading on dissolved oxygen in a subtropical wetland, the Florida Everglades: Wetlands Ecology and Management, v. 11, no. 3, p. 199–216.

McGuire, K.J., and McDonnell, J.J., 2010, Hydrological connectivity of hillslopes and streams—Characteristic time scales and nonlinearities: Water Resources Research, v. 46, no. 10, 17 p., accessed May 2019 at https://doi.org/10.1029/2010WR009341.

McMahon, G., Bales, J.D., Coles, J.F., Giddings, E.M.P., and Zappia, H., 2003, Use of stage data to characterize hydrologic conditions in an urbanizing environment: Journal of the American Water Resources Association, v. 39, no. 6, p. 1529–1546, accessed October 2018 at https://doi.org/10.1111/j.1752-1688.2003.tb04437.x.

Meals, D.W., Dressing, S.A., and Davenport, T.E., 2010, Lag time in water quality response to best management practices—A review: Journal of Environmental Quality, v. 39, no. 1, p. 85–96, accessed March 2020 at https://doi.org/10.2134/jeq2009.0108.

Menció, A., and Mas-Pla, J., 2010, Influence of groundwater exploitation on the ecological status of streams in a Mediterranean system (Selva Basin, NE Spain): Ecological Indicators, v. 10, no. 5, p. 915–926, accessed July 2019 at https://doi.org/10.1016/j.ecolind.2010.02.001.

Meng, Z., Yang, Y., Qin, Z., and Huang, L., 2018, Evaluating temporal and spatial variation in nitrogen sources along the lower reach of Fenhe River (Shanxi Province, China) using stable isotope and hydrochemical tracers: Water, v. 10, no. 2, 16 p.

Meybeck, M., 1998, Man and river interface—Multiple impacts on water and particulates chemistry illustrated in the Seine river basin, *in* Amiard, J.-C., Le Rouzic, B., Berthet, B., and Bertru, G., eds., Oceans, Rivers and Lakes—Energy and Substance Transfers at Interfaces: Dordrecht, Springer Netherlands, p. 1–20, accessed March 2019 at https://doi.org/10.1007/978-94-011-5266-2_1.

Meyer, J.L., Paul, M.J., and Taulbee, W.K., 2005, Stream ecosystem function in urbanizing landscapes: Journal of the North American Benthological Society, v. 24, no. 3, p. 602–612, accessed December 2019 at https://doi.org/10.1899/04-021.1.

Miller, M.P., Susong, D.D., Shope, C.L., Heilweil, V.M., and Stolp, B.J., 2014, Continuous estimation of baseflow in snowmelt-dominated streams and rivers in the upper Colorado River basin—A chemical hydrograph separation approach: Water Resources Research, v. 50, no. 8, p. 6986–6999, accessed December 2018 at https://doi.org/10.1002/2013WR014939.

Moore, J., Bird, D.L., Dobbis, S.K., and Woodward, G., 2017, Nonpoint source contributions drive elevated major ion and dissolved inorganic carbon concentrations in urban watersheds: Environmental Science & Technology Letters, v. 4, no. 6, p. 198–204, accessed February 2020 at https://doi.org/10.1021/acs.estlett.7b00096.

Moore, J., Fanelli, R.M., and Sekellick, A.J., 2020, High-frequency data reveal deicing salts drive elevated specific conductance and chloride along with pervasive and frequent exceedances of the U.S. Environmental Protection Agency aquatic life criteria for chloride in urban streams: Environmental Science & Technology, v. 54, no. 2, p. 778–789, accessed February 2020 at https://doi.org/10.1021/acs.est.9b04316.

Moring, J.B., 2006, Effects of urbanization on the chemical, physical, and biological characteristics of small Blackland Prairie streams in and near the Dallas-Fort Worth metropolitan area, Texas, chap. C *of* Effects of urbanization on stream ecosystems in six metropolitan areas of the United States: U.S. Geological Survey Scientific Investigations Report 2006–5101–C, 31 p.

Moyer, D.L., and Blomquist, J.D., 2018, Nitrogen, phosphorus, and suspended-sediment loads and trends measured at the Chesapeake Bay river input monitoring stations—Water years 1985–2017: U.S. Geological Survey data release, accessed August 2019 at https://doi.org/10.5066/P96NUK3Q.

Moyer, D.L., Langland, M.J., Blomquist, J.D., and Yang, G., 2017, Nitrogen, phosphorus, and suspended-sediment loads and trends measured at the Chesapeake Bay Nontidal Network stations—Water years 1985–2016: U.S. Geological Survey data release, accessed June 2018 at https://doi.org/10.5066/F7RR1X68.

Mulholland, P.J., Fellows, C.S., Tank, J.L., Grimm, N.B., Webster, J.R., Hamilton, S.K., Martí, E., Ashkenas, L., Bowden, W.B., Dodds, W.K., Mcdowell, W.H., Paul, M.J., and Peterson, B.J., 2001, Inter-biome comparison of factors controlling stream metabolism: Freshwater Biology, v. 46, no. 11, p. 1503–1517, accessed May 2019 at https://doi.org/10.1046/j.1365-2427.2001.00773.x.

Munn, M.D., Frey, J.W., Tesoriero, A.J., Black, R.W., Duff, J.H., Lee, K.E., Maret, T.R., Mebane, C.A., Waite, I.A., and Zelt, R.B., 2018, Understanding the influence of nutrients on stream ecosystems in agricultural landscapes: U.S. Geological Survey Circular 1437, 80 p., accessed April 2019 at https://doi.org/10.3133/cir1437.

Muthukrishnan, S., Madge, B., Selvakumar, A., and Sullivan, D., 2004, The use of best management practices (BMPs) in urban watersheds: U.S. Environmental Protection Agency EPA/600/R-04/184, 271 p., accessed September 2018 at https://nepis.epa.gov/Exe/ZyPDF.cgi/P100O0RJ.PDF?Dockey=P100O0RJ.PDF.

Nagy, R.C., Lockaby, B.G., Kalin, L., and Anderson, C., 2012, Effects of urbanization on stream hydrology and water quality—The Florida Gulf Coast: Hydrological Processes, v. 26, no. 13, p. 2019–2030, accessed April 2019 at https://doi.org/10.1002/hyp.8336.

Nair, V.D., Portier, K.M., Graetz, D.A., and Walker, M.L., 2004, An environmental threshold for degree of phosphorus saturation in sandy soils: Journal of Environmental Quality, v. 33, no. 1, p. 107–113, accessed May 2019 at https://doi.org/10.2134/jeq2004.1070.

Nash, J.E., and Sutcliffe, J.V., 1970, River flow forecasting through conceptual models part I—A discussion of principles: Journal of Hydrology (Amsterdam), v. 10, no. 3, p. 282–290, accessed May 2019 at https://doi.org/10.1016/0022-1694(70)90255-6.

National Atmospheric Deposition Program, 2016, National Atmospheric Deposition Program 2015 annual summary: National Atmospheric Deposition Program Data Report 2016–02, 28 p., accessed April 30, 2019, at http://nadp.slh.wisc.edu/lib/data/2015as.pdf.

Nelson, K.C., and Palmer, M.A., 2007, Stream temperature surges under urbanization and climate change—Data, models, and responses: Journal of the American Water Resources Association, v. 43, no. 2, p. 440–452, accessed May 2019 at https://doi.org/10.1111/j.1752-1688.2007.00034.x.

Noe, G., Skalak, K., Cashman, M., Gellis, A., Hopkins, K., Hupp, C., Moyer, D., Brakebill, J., Langland, M., Sekellick, A., Benthem, A., Maloney, K., Zhang, Q., Hogan, D., and others, 2017, Chesapeake sediment synthesis—Reviewing sediment sources, transport, delivery, and impacts in the Chesapeake Bay watershed to guide management actions (ver. 3): Chesapeake Bay Scientific and Technical Advisory Committee, accessed November 2019 at http://www.chesapeake.org/stac/presentations/286_Sediment%20Synthesis_Noe.pdf.

Novotny, E.V., Murphy, D., and Stefan, H.G., 2008, Increase of urban lake salinity by road deicing salt: The Science of the Total Environment, v. 406, no. 1–2, p. 131–144.

Obermeier, S.F., and Langer, W.H., 1986, Relationships between geology and engineering characteristics of soils and weathered rocks of Fairfax County and vicinity, Virginia: U.S. Geological Survey Professional Paper 1344, 30 p., accessed June 2019 at https://doi.org/10.3133/pp1344.

O'Driscoll, M., Clinton, S., Jefferson, A., Manda, A., and McMillan, S., 2010, Urbanization effects on watershed hydrology and in-stream processes in the southern United States: Water (Basel), v. 2, no. 3, p. 605–648, accessed October 2018 at https://doi.org/10.3390/w2030605.

Olsen, S.R., and Watanabe, F.S., 1957, A method to determine a phosphorus adsorption maximum of soils as measured by the Langmuir Isotherm: Soil Science Society of America Journal, v. 21, no. 2, p. 144–149, accessed May 2019 at https://doi.org/10.2136/sssaj1957.03615995002100020004x.

Omernik, J.M., 1976, The influence of land use on stream nutrient levels: U.S. Environmental Protection Agency EPA–600/2–76–014, 106 p., accessed April 2018 at https://nepis.epa.gov/Exe/ZyPDF.cgi?Dockey=9100T18Y.PDF.

Omernik, J.M., 1987, Ecoregions of the conterminous United States: Annals of the Association of American Geographers, v. 77, no. 1, p. 118–125, accessed May 2019 at https://doi.org/10.1111/j.1467-8306.1987.tb00149.x.

Pappas, E.A., Smith, D.R., Huang, C., Shuster, W.D., and Bonta, J.V., 2008, Impervious surface impacts to runoff and sediment discharge under laboratory rainfall simulation: Catena, v. 72, no. 1, p. 146–152, accessed April 2018 at https://doi.org/10.1016/j.catena.2007.05.001.

Patrick, M.S., Jean-Marie, T.M., and Nadine, M.L., 2015, Benthic macroinvertebrates as indicators of water quality—A case-study of urban Funa Stream (in Kinshasa, Democratic Republic of Congo): Open Journal of Water Pollution and Treatment, v. 2, no. 1, p. 8–24, accessed June 2019 at https://doi.org/10.15764/WPT.2015.01002.

Paul, M.J., and Meyer, J.L., 2001, Streams in the urban landscape: Annual Review of Ecology and Systematics, v. 32, no. 1, p. 333–365, accessed July 2019 at https://doi.org/10.1146/annurev.ecolsys.32.081501.114040.

Perera, N., Gharabaghi, B., and Howard, K., 2013, Groundwater chloride response in the Highland Creek watershed due to road salt application—A re-assessment after 20 years: Journal of Hydrology (Amsterdam), v. 479, p. 159–168, accessed February 2018 at https://doi.org/10.1016/j.jhydrol.2012.11.057.

Peters, N.E., 2009, Effects of urbanization on stream water quality in the city of Atlanta, Georgia, USA: Hydrological Processes, v. 23, no. 20, p. 2860–2878, accessed June 2018 at https://doi.org/10.1002/hyp.7373.

Peters, E., and van Lanen, H.A.J., 2005, Separation of base flow from streamflow using groundwater levels—Illustrated for the Pang catchment (UK): Hydrological Processes, v. 19, no. 4, p. 921–936, accessed February 2018 at https://doi.org/10.1002/hyp.5548.

Pilegaard, K., 2013, Processes regulating nitric oxide emissions from soils: Philosophical Transactions of the Royal Society, v. 368, no. 1621, p. 20130126, accessed July 2019 at https://doi.org/10.1098/rstb.2013.0126.

Pinder, G.F., and Jones, J.F., 1969, Determination of the ground-water component of peak discharge from the chemistry of total runoff: Water Resources Research, v. 5, no. 2, p. 438–445, accessed February 2019 at https://doi.org/10.1029/WR005i002p00438.

Poff, N.L., Bledsoe, B.P., and Cuhaciyan, C.O., 2006, Hydrologic variation with land use across the contiguous United States—Geomorphic and ecological consequences for stream ecosystems: Geomorphology, v. 79, no. 3–4, p. 264–285, accessed August 2019 at https://doi.org/10.1016/j.geomorph.2006.06.032.

Porter, A.J., Webber, J.S., Jastram, J.D., and Witt, J.W., 2020, Inputs and selected outputs used to assess spatial and temporal patterns in streamflow, water-chemistry, and aquatic macroinvertebrates of selected streams in Fairfax County, Virginia, 2007–2018: U.S. Geological Survey data release, https://doi.org/10.5066/P95S9RFV.

Potter, J.D., McDowell, W.H., Helton, A.M., and Daley, M.L., 2014, Incorporating urban infrastructure into biogeochemical assessment of urban tropical streams in Puerto Rico: Biogeochemistry, v. 121, no. 1, p. 271–286, accessed May 2019 at https://doi.org/10.1007/s10533-013-9914-5.

R Core Team, 2018, R—A language and environment for statistical computing: R Foundation for Statistical Computing, Vienna, Austria, accessed June 2019 at https://www.R-project.org/.

Raffensperger, J.P., Baker, A.C., Blomquist, J.D., and Hopple, J.A., 2017, Optimal hydrograph separation using a recursive digital filter constrained by chemical mass balance, with application to selected Chesapeake Bay watersheds: U.S. Geological Survey Scientific Investigations Report 2017–5034, 51 p., accessed December 2018 at https://doi.org/10.3133/sir20175034.

Ramírez, A., and Gutiérrez-Fonseca, P.E., 2014, Functional feeding groups of aquatic insect families in Latin America—A critical analysis and review of existing literature: Revista de Biología Tropical, v. 62, no. 2, p. 155–167, accessed August 2019 at https://doi.org/10.15517/rbt.v62i0.15785.

Rantz, S.E., and others, 1982, Measurement and computation of streamflow—Volume 1. Measurement of stage and discharge: U.S. Geological Survey Water Supply Paper 2175, 299 p.

Rasmussen, T., and Gatotho, J., 2013, Water-quality variability and constituent transport in streams of Johnson County, Kansas, using continuous monitoring and regression models, 2003–11: U.S. Geological Survey Scientific Investigations Report 2013–5221, 53 p., accessed December 2018 at https://doi.org/10.3133/sir20135221.

Rasmussen, P.P., Gray, J.R., Glysson, G.D., and Ziegler, A.C., 2009, Guidelines and procedures for computing timeseries suspended-sediment concentrations and loads from in-stream turbidity-sensor and streamflow data: U.S. Geological Survey Techniques and Methods, book 3, chap. C4, 52 p.

Ratzlaff, J.R., 1994, Mean annual precipitation, runoff, and runoff ratio for Kansas, 1971–1990: Transactions of the Kansas Academy of Science, v. 97, no. 3–4, p. 94–101.

Resh, V.H., Myers, M.J., and Hannaford, M.J., 1996, Macroinvertebrates as biotic indicators of environmental quality, *in* Hauer, F.R., and Lamberti, G.A., eds., Methods in stream ecology: New York, Academic Press, p. 674.

Rice, K.C., and Jastram, J.D., 2015, Rising air and stream-water temperatures in Chesapeake Bay region, USA: Climatic Change, v. 128, no. 1–2, p. 127–138, accessed August 2017 at https://doi.org/10.1007/s10584-014-1295-9.

Richards, K.D., Scudder, B.C., Fitzapatrick, F.A., Steuer, J.J., Bell, A.H., Peppler, M.C., Stewart, J.S., and Harris, M.A., 2006, Effects of urbanization on stream ecosystems along an agriculture-to-urban land-use gradient, Milwaukee to Green Bay, Wisconsin, 2003–2004, chap. E *of* Effects of urbanization on stream ecosystems in six metropolitan areas of the United States: U.S. Geological Survey Scientific Investigations Report 2006–5101–E, 210 p.

Richardson, C.J., and Craft, C.B., 1993, Effective phosphorus retention in wetlands—Fact or fiction? *in* Moshiri, G.A., ed., Constructed Wetlands for Water Quality Improvement: Boca Raton, Fla., Lewis Publishers, p. 271–282.

Robertson, D.M., Hubbard, L.E., Lorenz, D.L., and Sullivan, D.J., 2018, A surrogate regression approach for computing continuous loads for the tributary nutrient and sediment monitoring program on the Great Lakes: Journal of Great Lakes Research, v. 44, no. 1, p. 26–42, accessed September 2018 at https://doi.org/10.1016/j.jglr.2017.10.003.

Rolls, R.J., Leigh, C., and Sheldon, F., 2012, Mechanistic effects of low-flow hydrology on riverine ecosystems—Ecological principles and consequences of alteration: Freshwater Science, v. 31, no. 4, p. 1163–1186, accessed July 2019 at https://doi.org/10.1899/12-002.1.

Rose, S., and Peters, N.E., 2001, Effects of urbanization on streamflow in the Atlanta area (Georgia, USA)—A comparative hydrological approach: Hydrological Processes, v. 15, no. 8, p. 1441–1457, accessed July 2019 at https://doi.org/10.1002/hyp.218.

Rosenberg, D.M., and Resh, V.H., 1993, Freshwater biomonitoring and benthic macroinvertebrates: London, Chapman and Hall, 461 p.

Roy, A.H., Rosemond, A.D., Paul, M.J., Leigh, D.S., and Wallace, J.B., 2003, Stream macroinvertebrate response to catchment urbanisation (Georgia, U.S.A.): Freshwater Biology, v. 48, no. 2, p. 329–346, accessed August 2019 at https://doi.org/10.1046/j.1365-2427.2003.00979.x.

Runkel, R.L., Crawford, C.G., and Cohn, T.A., 2004, Load Estimator (LOADEST)—A FORTRAN program for estimating constituent loads in streams and rivers: U.S. Geological Survey Techniques and Methods, book 4, chap. A5, 75 p.

Sabater, S., and Barceló, D., eds., 2010, Water scarcity in the Mediterranean—Perspectives under global change: Heidelberg, Springer-Verlag, 234 p., accessed July 2019 at https://doi.org/10.1007/978-3-642-03971-3.

Sanford, W.E., Casile, G., and Haase, K.B., 2015, Dating base flow in streams using dissolved gases and diurnal temperature changes: Water Resources Research, v. 51, no. 12, p. 9790–9803, accessed May 2019 at https://doi.org/10.1002/2014WR016796.

Sanford, W., Nelms, D.L., Pope, J.P., and Selnick, D.L., 2012, Quantifying components of the hydrologic cycle in Virginia using chemical hydrograph separation and multiple regression analysis: U.S. Geological Survey Scientific Investigations Report 2011–5198, 152 p. [Also available at https://doi.org/10.3133/sir20115198.]

Sauer, V.B., 2002, Standards for the analysis and processing of surface-water data and information using electronic methods: U.S. Geological Survey Water-Resources Investigations Report 01–4044, 91 p.

Schenk, E.R., Hupp, C.R., Gellis, A., and Noe, G., 2013, Developing a new stream metric for comparing stream function using a bank-floodplain sediment budget—A case study of three Piedmont streams: Earth Surface Processes and Landforms, v. 38, no. 8, p. 771–784, accessed May 2019 at https://doi.org/10.1002/esp.3314.

Schilling, K.E., Sea-Won, K., and Jones, C.S., 2017, Use of water quality surrogates to estimate total phosphorus concentrations in Iowa rivers—Journal of Hydrology, v: Regional Studies, v. 12, p. 111–121.

Schwientek, M., Osenbrück, K., and Fleischer, M., 2013, Investigating hydrological drivers of nitrate export dynamics in two agricultural catchments in Germany using high-frequency data series: Environmental Earth Sciences, v. 69, no. 2, p. 381–393, accessed November 2019 at https://doi.org/10.1007/s12665-013-2322-2.

Searcy, J.K., 1959, Flow-duration curves; Manual of Hydrology—Part 2. Low-flow techniques: U.S. Geological Survey Water-Supply Paper 1542-A, 33 p.

Sharpley, A.N., 1995, Soil phosphorus dynamics—Agronomic and environmental impacts: Ecological Engineering, v. 5, no. 2–3, p. 261–279, accessed May 2019 at https://doi.org/10.1016/0925-8574(95)00027-5.

Shields, C.A., Band, L.E., Law, N., Groffman, P.M., Kaushal, S.S., Savvas, K., Fisher, G.T., and Belt, K.T., 2008, Streamflow distribution of non–point source nitrogen export from urban-rural catchments in the Chesapeake Bay watershed: Water Resources Research, v. 44, no. 9, 13 p., accessed June 2019 at https://doi.org/10.1029/2007WR006360.

Shreve, E.A., and Downs, A.C., 2005, Quality-assurance plan for the analysis of fluvial sediment by the U.S. Geological Survey Kentucky Water Science Center Sediment Laboratory: U.S. Geological Survey Open-File Report 2005–1230, 28 p.

Sipler, R.E., and Bronk, D.A., 2015, Dynamics of dissolved organic nitrogen, chap. 4 *of* Hansell, D.A., and Carlson, C.A., eds., Biogeochemistry of marine dissolved organic matter (2d ed.): Boston, Academic Press, p. 127–232.

Skalak, K., and Pizzuto, J., 2010, The distribution and residence time of suspended sediment stored within the channel margins of a gravel-bed bedrock river: Earth Surface Processes and Landforms, v. 35, no. 4, p. 435–446, accessed July 2019 at https://doi.org/10.1002/esp.1926.

Sloto, R.A., and Crouse, M.Y., 1996, HYSEP—A computer program for streamflow hydrograph separation and analysis: U.S. Geological Survey Water-Resources Investigations Report 96–4040, 46 p.

Smith, Z., Buchanan, C., and Nagel, A., 2017, Refinement of the basin-wide index of biotic integrity for non-tidal streams and wadeable rivers in the Chesapeake Bay watershed: Interstate Commission on the Potomac River Basin Report 17–2, 79 p.

Smith, S.M.C., and Wilcock, P.R., 2015, Upland sediment supply and its relation to watershed sediment delivery in the contemporary mid-Atlantic Piedmont (U.S.A.): Geomorphology, v. 232, p. 33–46, accessed May 2019 at https://doi.org/10.1016/j.geomorph.2014.12.036.

Snodgrass, J.W., Moore, J., Lev, S.M., Casey, D.R., Ownby, D.R., Flora, R.F., and Grant, I., 2017, Influence of modern stormwater management practices on transport of road salt to surface waters: Environmental Science & Technology, v. 51, no. 8, p. 4165–4172, accessed May 2019 at https://doi.org/10.1021/acs.est.6b03107.

Soulsby, C., Tetzlaff, D., Rodgers, P., Dunn, S., and Waldron, S., 2006, Runoff processes, stream water residence times and controlling landscape characteristics in a mesoscale catchment—An initial evaluation: Journal of Hydrology (Amsterdam), v. 325, no. 1–4, p. 197–221, accessed November 2018 at https://doi.org/10.1016/j.jhydrol.2005.10.024.

Sprague, L.A., Zeullig, R.E., and Dupree, J.A., 2006, Effects of urbanization on stream ecosystems in the South Platte River Basin, Colorado and Wyoming, chap. A *of* Effects of urbanization on stream ecosystems in six metropolitan areas of the United States: U.S. Geological Survey Scientific Investigations Report 2006–5101–A, 139 p.

St. Clair, J., Cartier, C., Triantafyllidou, S., Clark, B., and Edwards, M., 2016, Long-term behavior of simulated partial lead service line replacements: Environmental Engineering Science, v. 33, no. 1, p. 53–64, accessed May 2019 at https://doi.org/10.1089/ees.2015.0337.

Steele, M.K., and Aitkenhead-Peterson, J.A., 2013, Salt impacts on organic carbon and nitrogen leaching from senesced vegetation: Biogeochemistry, v. 112, no. 1–3, p. 245–259, accessed May 2019 at https://doi.org/10.1007/s10533-012-9722-3.

Steele, T.D., 1969, Digital-computer applications in chemical-quality studies of surface water in a small watershed, in The use of analog and digital computers in hydrology: Gentbrugge, Belgium, International Association of Scientific Hydrology, Proceedings of the Tucson Symposium, v. 1, p. 203–214.

Stenback, G.A., Crumpton, W.G., Schilling, K.E., and Helmers, M.J., 2011, Rating curve estimation of nutrient loads in Iowa rivers: Journal of Hydrology (Amsterdam), v. 396, no. 1–2, p. 158–169, accessed June 2019 at https://doi.org/10.1016/j.jhydrol.2010.11.006.

Stewart, M., Cimino, J., and Ross, M., 2007, Calibration of base flow separation methods with streamflow conductivity: Ground Water, v. 45, no. 1, p. 17–27, accessed December 2018 at https://doi.org/10.1111/j.1745-6584.2006.00263.x.

Stott, T., 1997, A comparison of stream bank erosion processes on forested and moorland streams in the Balquhidder Catchments, central Scotland: Earth Surface Processes and Landforms, v. 22, no. 4, p. 383–399, accessed May 2019 at https://doi.org/10.1002/(SICI)1096-9837(199704)22:4<383::AID-ESP695>3.0.CO;2-4.

Strauss, E.A., Mitchell, N.L., and Lamberti, G.A., 2002, Factors regulating nitrification in aquatic sediments—Effects of organic carbon, nitrogen availability, and pH: Canadian Journal of Fisheries and Aquatic Sciences, v. 59, no. 3, p. 554–563, accessed May 2019 at https://doi.org/10.1139/f02-032.

Sugiyama, S., and Hama, T., 2013, Effects of water temperature on phosphate adsorption onto sediments in an agricultural drainage canal in a paddy-field district: Ecological Engineering, v. 61, p. 94–99, accessed February 2019 at https://doi.org/10.1016/j.ecoleng.2013.09.053.

Sullivan, D.J., Vecchia, A.V., Lorenz, D.L., Gilliom, R.J., and Martin, J.D., 2009, Trends in pesticide concentrations in corn-belt streams, 1996–2006: U.S. Geological Survey Scientific Investigations Report 2009–5132, 75 p., accessed August 2019 at https://pubs.usgs.gov/sir/2009/5132/pdf/sir20095132.pdf.

Swenson, H.A., and Baldwin, H.L., 1965, A primer on water quality: U.S. Geological Survey General Information Product, 27 p., accessed February 2019 at https://doi.org/10.3133/7000057.

Syvitski, J.P., and Morehead, M.D., 1999, Estimating river-sediment discharge to the ocean—Application to the Eel margin, northern California: Marine Geology, v. 154, no. 1–4, p. 13–28, accessed March 2020 at https://doi.org/10.1016/S0025-3227(98)00100-5.

Syvitski, J.P., Morehead, M.D., Bahr, D.B., and Mulder, T., 2000, Estimating fluvial sediment transport—The rating parameters: Water Resources Research, v. 36, no. 9, p. 2747–2760, accessed March 2020 at https://doi.org/10.1029/2000WR900133.

Tasdighi, A., Arabi, M., and Osmond, D.L., 2017, The relationship between land use and vulnerability to nitrogen and phosphorus pollution in an urban watershed: Journal of Environmental Quality, v. 46, no. 1, p. 113–122, accessed May 2019 at https://doi.org/10.2134/jeq2016.06.0239.

Terando, A.J., Costanza, J., Belyea, C., Dunn, R.R., McKerrow, A., and Collazo, J.A., 2014, The southern megalopolis—Using the past to predict the future of urban sprawl in the southeast U.S.: PLoS One, v. 9, no. 7, 8 p., accessed February 2020 at https://doi.org/10.1371/journal.pone.0102261.

Tufford, D.L., McKellar, H.N., Jr., and Hussey, J.R., 1998, In-stream nonpoint source nutrient prediction with land-use proximity and seasonality: Journal of Environmental Quality, v. 27, no. 1, p. 100–111, accessed February 2019 at https://doi.org/10.2134/jeq1998.00472425002700010015x.

United Nations, 2018, World urbanization prospects—The 2018 revision: United Nations, Department of Economic and Social Affairs, Population Division, 103 p., accessed December 2018 at https://population.un.org/wup/Publications/Files/WUP2018-KeyFacts.pdf.

U.S. Census Bureau, 2014, Cartographic boundary file, state-county for United States, 1:500,000: U.S. Census Bureau Data.gov web page, accessed July 2018 at https://catalog.data.gov/dataset/2014-cartographic-boundary-file-state-county-for-united-states-1-500000.

U.S. Census Bureau, 2012, 2010 Census of population and housing—Population and housing unit counts: Virginia, U.S, U.S. Census Bureau, 117 p.

U.S. Environmental Protection Agency, 2000a, Ambient water quality criteria recommendations—Information supporting the development of state and tribal nutrient criteria for rivers and streams in nutrient ecoregion IX: U.S. Environmental Protection Agency, EPA 822-B-00-019, 108 p., accessed May 2019 at https://nepis.epa.gov/Exe/ZyPDF.cgi/20003EHB.PDF?Dockey=20003EHB.PDF.

U.S. Environmental Protection Agency, 2000b, The quality of our nation's waters; A summary of the national water quality inventor—1998 report to congress: U.S. Environmental Protection Agency EPA841-S-00-001, 20 p., accessed August 2018 at https://www.epa.gov/sites/production/files/2015-09/documents/2000_07_07_305b_98report_98brochure.pdf.

U.S. Environmental Protection Agency, 2011, A national evaluation of the Clean Water Act section 319 program: U.S. Environmental Protection Agency, 197 p., accessed November 2011 at https://www.epa.gov/sites/production/files/2015-09/documents/319evaluation.pdf.

U.S. Environmental Protection Agency, 2018, Clean Water Act analytical methods: U.S. Environmental Protection Agency web page, accessed August 14, 2018, at https://water.epa.gov/scitech/methods/cwa/.

U.S. Geological Survey, 2016, The StreamStats program: U.S. Geological Survey StreamStats web page, accessed July 2018 at https://www.usgs.gov/mission-areas/water-resources/science/streamstats/.

U.S. Geological Survey, 2018, USGS water data for the Nation: U.S. Geological Survey National Water Information System database, accessed May 8, 2018, at https://doi.org/10.5066/F7P55KJN.

Van Breemen, N., Boyer, E.W., Goodale, C.L., Jaworski, N.A., Paustian, K., Seitzinger, S.P., Lajtha, K., Mayer, B., Van Dam, D., Howarth, R.W., Nadelhoffer, K.J., Eve, M., and Billen, G., 2002, Where did all the nitrogen go? Fate of nitrogen inputs to large watersheds in the northeastern U.S.A, *in* Boyer, E.W., and Howarth, R.W., eds., The nitrogen cycle at regional to global scales: Dordrecht, Netherlands, Springer, p. 267–293, accessed June 2019 at https://doi.org/10.1007/978-94-017-3405-9_8.

Van Metre, P.C., Waite, I.R., Qi, S., Mahler, B., Terando, A., Wieczorek, M., Meador, M., Bradley, P., Journey, C., Schmidt, T., and Carlisle, D., 2019, Projected urban growth in the southeastern USA puts small streams at risk: PLoS One, v. 14, no. 10, 17 p., accessed September 2019 at https://doi.org/10.1371/journal.pone.0222714.

Veilleux, A.G., Cohn, T.A., Flynn, K., Mason, R.R., Jr., and Hummel, P., 2013, Estimating magnitude and frequency of floods using the PeakFQ 7.0 program: U.S. Geological Survey Fact Sheet 2013–3108, 2 p.

Virginia Department of Conservation and Recreation, Division of Natural Heritage, 2016, Overview of the physiography and vegetation of Virginia: Virginia Department of Conservation and resources web page, accessed May 2019 at https://www.dcr.virginia.gov/natural-heritage/natural-communities/document/ncoverviewphys-veg.pdf.

Virginia Department of Environmental Quality, 2011, 9VAC25–260–140. Criteria for surface water, in 9VAC25–260 Virginia water quality standards: State Water Control Board, Statutory Authority—62.1-44.15 3a of the Code of Virginia, with amendments effective January 6, 2011, p. 14–34, accessed March 2019 at https://www.deq.virginia.gov/Portals/0/DEQ/Water/WaterQualityMonitoring/TOX/TR2017/Appendices/Appendix_A_DEQ_Water_Quality_Standards_Jan2011.pdf.

Wagner, R.J., Boulger, R.W., Jr., Oblinger, C.J., and Smith, B.A., 2006, Guidelines and standard procedures for continuous water-quality monitors—Station operation, record computation, and data reporting: U.S. Geological Survey Techniques and Methods, book 1, chap. D3, 51 p., 8 attachments, accessed April 10, 2006, at https://doi.org/10.3133/tm1D3.

Wallace, J.B., and Webster, J.R., 1996, The role of macroinvertebrates in stream ecosystem function: Annual Review of Ecology and Systematics, v. 41, p. 115–139.

Wallace, J.B., Webster, J.R., and Cuffney, T.F., 1982, Stream detritus dynamics—Regulation by invertebrate consumers: Oecologia, v. 53, no. 2, p. 197–200, accessed August 2019 at https://doi.org/10.1007/BF00545663.

Walsh, C.J., Roy, A.H., Feminella, J.W., Cottingham, P.D., Groffman, P.M., and Morgan, R.P., II, 2005, The urban stream syndrome—Current knowledge and the search for a cure: Journal of the North American Benthological Society, v. 24, no. 3, p. 706–723, accessed November 2018 at https://doi.org/10.1899/04-028.1.

Wang, L., and Liang, T., 2015, Distribution characteristics of phosphorus in the sediments and overlying water of Poyang Lake: PLoS One, v. 10, no. 5, 12 p., accessed May 2019 at https://doi.org/10.1371/journal.pone.0125859.

Wanielista, M.P., Yousef, Y.A., and McLellon, W.M., 1977, Nonpoint source effects on water quality: Journal - Water Pollution Control Federation, v. 49, no. 3, p. 441–451.

Weiss, L.A., 1990, Effects of urbanization on peak streamflows in four Connecticut communities, 1980–84: U.S. Geological Survey Water-Resources Investigation Report 89–4167, 40 p.

Wilhelm, S.W., LeCleir, G.R., Bullerjahn, G.S., McKay, R.M., Saxton, M.A., Twiss, M.R., and Bourbonniere, R.A., 2014, Seasonal changes in microbial community structure and activity imply winter production is linked to summer hypoxia in a large lake: FEMS Microbiology Ecology, v. 87, no. 2, p. 475–485, accessed February 2019 at https://doi.org/10.1111/1574-6941.12238.

Williams, G.P., 1989, Sediment concentration versus water discharge during single hydrologic events in rivers: Journal of Hydrology (Amsterdam), v. 111, no. 1–4, p. 89–106, accessed May 2019 at https://doi.org/10.1016/0022-1694(89)90254-0.

Wittenberg, H., 2003, Effects of season and man-made changes on baseflow and flow recession—Case studies: Hydrological Processes, v. 17, no. 11, p. 2113–2123, accessed December 2019 at https://doi.org/10.1002/hyp.1324.

Wood, P.J., 1997, Biological effects of fine sediment in the lotic environment: Environmental Management, v. 21, no. 2, p. 203–217, accessed February 2019 at https://doi.org/10.1007/s002679900019.

Wright, I.A., Davies, P.J., Findlay, S.J., and Jonasson, O.J., 2011, A new type of water pollution—Concrete drainage infrastructure and geochemical contamination of urban waters: Marine and Freshwater Research, v. 62, no. 12, p. 1355–1361, accessed April 2020 at https://doi.org/10.1071/MF10296.

Wynn, T.M., Henderson, M.B., and Vaughan, D.H., 2008, Changes in streambank erodibility and critical shear stress due to subaerial processes along a headwater stream, southwestern Virginia, USA: Geomorphology, v. 97, no. 3–4, p. 260–273, accessed May 2019 at https://doi.org/10.1016/j.geomorph.2007.08.010.

Wynn, T., and Mostaghimi, S., 2006, The effects of vegetation and soil type on streambank erosion, southwestern Virginia, USA: Journal of the American Water Resources Association, v. 42, no. 1, p. 69–82, accessed May 2019 at https://doi.org/10.1111/j.1752-1688.2006.tb03824.x.

Xu, D., Xu, J., Wu, J., and Muhammad, A., 2006, Studies on the phosphorus sorption capacity of substrates used in constructed wetland systems: Chemosphere, v. 63, no. 2, p. 344–352, accessed May 2019 at https://doi.org/10.1016/j.chemosphere.2005.08.036.

Yang, G., and Moyer, D.L., 2020, Estimation of nonlinear water-quality trends in high-frequency monitoring data: The Science of the Total Environment, v. 715, p. 136686, accessed February 2020 at https://doi.org/10.1016/j.scitotenv.2020.136686.

Yang, Y.-Y., and Toor, G.S., 2018, Stormwater runoff driven phosphorus transport in an urban residential catchment—Implications for protecting water quality in urban watersheds: Scientific Reports, v. 8, no. 1, 10 p., accessed November 2018 at https://doi.org/10.1038/s41598-018-29857-x.

Yu, Z., and Schwartz, F.W., 1999, Automated calibration applied to watershed-scale flow simulations: Hydrological Processes, v. 13, no. 2, p. 191–209, accessed December 2018 at https://doi.org/10.1002/(SICI)1099-1085(19990215)13:2<191::AID-HYP706>3.0.CO;2-N.

Zhang, Q., and Blomquist, J.D., 2018, Watershed export of fine sediment, organic carbon, and chlorophyll-a to Chesapeake Bay—Spatial and temporal patterns in 1984-2016: The Science of the Total Environment, v. 619–620, p. 1066–1078, accessed May 2019 at https://doi.org/10.1016/j.scitotenv.2017.10.279.

Zhang, Q., Brady, D.C., Boynton, W.R., and Ball, W.P., 2015, Long-term trends of nutrients and sediment from the nontidal Chesapeake watershed—An assessment of progress by river and season: Journal of the American Water Resources Association, v. 51, no. 6, p. 1534–1555, accessed June 2019 at https://doi.org/10.1111/1752-1688.12327.

Appendix 1 Results of Hypotheses Tests, Annual Exceedance Probabilities, General Additive Models, and Load and Concentration Models

Table 1.1. Difference in slope, with standard error and p-value for each pairwise comparison from an analysis of covariance testing for differences in the slopes of regression lines for monthly streamflow and monthly precipitation for all station by station combinations within each observation period (2008–12 and 2013–17).

[Significant differences are in red, based on p≤0.05. DEAD, Dead Run at Whann Avenue near Mclean, VA; DIFF, Difficult Run above Fox Lake near Fairfax, VA; FLAT, Flatlick Branch above Frog Branch at Chantilly, VA; LONG, Long Branch near Annandale, VA; SFLIL, South Fork Little Difficult Run above mouth near Vienna, VA]

Period	Station	Station	Difference	Standard error	p-value
2008–12	DIFF	DEAD	0.285	0.063	<0.001
2008–12	DIFF	SFLIL	0.293	0.068	<0.001
2008–12	FLAT	DIFF	0.077	0.085	0.365
2008–12	FLAT	SFLIL	0.371	0.082	<0.001
2008–12	FLAT	DEAD	0.366	0.078	<0.001
2008–12	DEAD	SFLIL	0.011	0.060	0.85
2013–17	DIFF	DEAD	0.130	0.070	0.064
2013–17	DIFF	SFLIL	0.185	0.079	0.021
2013–17	DIFF	LONG	0.106	0.073	0.149
2013–17	DIFF	FLAT	–0.029	0.082	0.725
2013–17	FLAT	DEAD	0.160	0.066	0.021
2013–17	FLAT	SFLIL	0.214	0.078	0.007
2013–17	FLAT	LONG	0.135	0.071	0.061
2013–17	SFLIL	LONG	–0.079	0.067	0.245
2013–17	DEAD	SFLIL	0.053	0.065	0.422
2013–17	DEAD	LONG	–0.026	0.057	0.654

Table 1.2. Differences in slope with standard error and p-value from an analysis of covariance testing for differences in the slopes of regression lines for monthly streamflow and monthly precipitation at each station across the two observation periods (2008–12 and 2013–17). Significant differences are in red, based on p≤0.05.

[[DEAD, Dead Run at Whann Avenue near Mclean, VA; DIFF, Difficult Run above Fox Lake near Fairfax, VA; FLAT, Flatlick Branch above Frog Branch at Chantilly, VA; LONG, Long Branch near Annandale, VA; SFLIL, South Fork Little Difficult Run above mouth near Vienna, VA; N/A, not available]

Station	Difference	Standard error	p-value
DEAD	–0.042	0.054	0.427
DIFF	–0.189	0.076	0.014
FLAT	–0.241	0.087	0.007
SFLIL	–0.082	0.070	0.244
LONG	N/A	N/A	N/A

Table 1.3. Annual exceedance probabilities for each of the four intensive monitoring stations with a minimum 10-year record.

[DEAD, Dead Run at Whann Avenue near Mclean, VA; DIFF, Difficult Run above Fox Lake near Fairfax, VA; FLAT, Flatlick Branch above Frog Branch at Chantilly, VA; LONG, Long Branch near Annandale, VA; SFLIL, South Fork Little Difficult Run above mouth near Vienna, VA]

Water year	Station			
	DEAD	DIFF	FLAT	SFLIL
2008	0.18	0.09	0.27	0.27
2009	0.82	0.36	0.64	0.73
2010	0.09	0.82	0.73	0.64
2011	0.27	0.18	0.09	0.09
2012	0.64	0.91	0.36	0.45
2013	0.91	0.45	0.18	0.55
2014	0.36	0.27	0.55	0.36
2015	0.55	0.64	0.45	0.18
2016	0.46	0.73	0.91	0.91
2017	0.73	0.55	0.82	0.82

Table 1.4. Model results from generalized additive model run on the continuously collected data at the four intensive stations.

[DEAD, Dead Run at Whann Avenue near Mclean, VA; DIFF, Difficult Run above Fox Lake near Fairfax, VA; FLAT, Flatlick Branch above Frog Branch at Chantilly, VA; LONG, Long Branch near Annandale, VA; SFLIL, South Fork Little Difficult Run above mouth near Vienna, VA; CI, confidence interval, µS/cm, microsiemens per centimeter]

Station	Adjusted R^2	Trend	95-percent CI	p-value	Geometric median (µS/cm)	Change (µS/cm)
DEAD	0.44	0.29	0.02–0.56	0.04	305.9	93.7
DIFF	0.57	0.34	0.14–0.54	<0.01	403.5	148.7
FLAT	0.54	0.14	–0.01–0.28	0.06	446.7	64.0
SFLIL	0.38	0.24	0.12–0.35	<0.01	168.8	38.6

Table 1.5. Number of observations, coefficients, R^2, Nash-Sutcliffe index, and bias percentage of suspended sediment, total phosphorus, total dissolved phosphorus, total particulate phosphorus, total nitrogen, total dissolved nitrogen, total particulate nitrogen, and nitrate plus nitrite load models at the five intensive monitoring stations.

[Dependent variable is the natural logarithm of the constituent. Ln, natural logarithm; Q, streamflow; TB, turbidity; SC, specific conductance; WT, water temperature; dTime, decimal time; BASE, indicator variable (0 or 1) for hydrologic condition of either baseflow or stormflow; NO_3^-, nitrate; R^2, coefficient of determination; n/a, not applicable; –, variable not included in selected model; Nash-Sutcliffe, Nash Sutcliffe efficiency index; DEAD, Dead Run at Whann Avenue near Mclean, VA; DIFF, Difficult Run above Fox Lake near Fairfax, VA; FLAT, Flatlick Branch above Frog Branch at Chantilly, VA; LONG, Long Branch near Annandale, VA; SFLIL, South Fork Little Difficult Run above mouth near Vienna, VA]

Station	Number of observations	Intercept	Ln Q	Ln Q^2	Ln TB	Ln SC	WT	pH	dTime	$dTime^2$	SIN (dTime2π)	COS (dTime2π)	BASE	Ln TB * BASE	Ln NO_3^-	Adjusted R^2	Nash-Sutcliffe	Bias percentage
Suspended sediment																		
DEAD	401	–5.0854	1.3458	n/a	0.3056	n/a	n/a	n/a	n/a	n/a	n/a	n/a	0.2198	0.3717	n/a	97.9	0.210	27.86
DIFF	387	–5.5976	1.2060	n/a	0.8266	n/a	n/a	n/a	n/a	n/a	n/a	n/a	0.7065	n/a	n/a	97.4	0.907	2.58
FLAT	398	–5.8721	1.2174	n/a	0.7678	n/a	n/a	n/a	n/a	n/a	n/a	n/a	0.9575	n/a	n/a	97.5	0.755	9.24
LONG	209	–5.1363	1.2063	n/a	0.8497	n/a	n/a	n/a	n/a	n/a	n/a	n/a	0.0011	n/a	n/a	95.8	0.941	4.02
SFLIL	367	–5.0534	1.3124	n/a	0.2981	n/a	n/a	n/a	n/a	n/a	0.0814	–0.1851	–0.2337	n/a	n/a	97.8	0.987	8.65
Total phosphorus																		
DEAD	378	–74.2039	1.1882	n/a	0.3418	n/a	n/a	n/a	0.0360	n/a	–0.1491	–0.2382	n/a	n/a	n/a	97.8	0.763	14.02
DIFF	384	–104.3999	1.0620	n/a	0.6031	–0.3175	n/a	n/a	0.0512	n/a	n/a	n/a	n/a	n/a	n/a	97.1	0.659	–3.59
FLAT	367	1.0886	0.9702	0.0360	0.4259	n/a	n/a	n/a	n/a	n/a	–0.1075	–0.1576	n/a	n/a	n/a	96.5	0.512	7.38
LONG	181	–2.7638	1.2399	n/a	0.3873	n/a	0.0248	n/a	n/a	n/a	n/a	n/a	n/a	n/a	n/a	97.3	0.842	–11.03
SFLIL	352	–107.5302	1.1609	n/a	0.5007	n/a	0.0337	n/a	0.0516	n/a	n/a	n/a	0.5402	n/a	n/a	96.5	0.277	18.59
Total dissolved phosphorus																		
DEAD	379	–118.6668	0.9838	n/a	0.2007	–0.2844	n/a	n/a	0.0587	n/a	–0.2235	–0.0664	n/a	n/a	n/a	97.8	0.708	14.56
DIFF	378	–0.3311	1.0541	n/a	0.0886	–0.4700	n/a	n/a	0.0517	–0.0105	n/a	n/a	n/a	n/a	n/a	93.4	0.298	–1.84
FLAT	368	2.1807	0.9361	0.0175	0.0972	–0.1736	n/a	n/a	n/a	n/a	–0.3192	–0.2455	n/a	n/a	n/a	96.9	0.912	4.54
LONG	182	–0.6805	1.0297	n/a	0.1278	–0.3238	n/a	n/a	n/a	n/a	n/a	n/a	n/a	n/a	n/a	96.8	0.868	6.29
SFLIL	349	1.8337	1.0184	–0.0315	0.1977	–0.5348	n/a	n/a	n/a	n/a	–0.3253	–0.1035	n/a	n/a	n/a	93.9	0.934	10.74
Total particulate phosphorus																		
DEAD	378	–2.7933	1.2450	n/a	0.4266	n/a	n/a	n/a	n/a	n/a	n/a	n/a	n/a	n/a	n/a	96.3	0.708	14.56
DIFF	373	98.5008	1.0381	n/a	0.6732	–0.2548	n/a	n/a	0.0479	n/a	n/a	n/a	n/a	n/a	n/a	96.2	0.650	–5.08
FLAT	366	–8.2868	1.1327	n/a	0.6138	n/a	0.0151	0.6412	n/a	n/a	n/a	n/a	n/a	n/a	n/a	95.9	0.572	4.20
LONG	181	–3.5143	1.2784	n/a	0.4496	n/a	0.0302	n/a	n/a	n/a	n/a	n/a	n/a	n/a	n/a	96.6	0.867	–9.00
SFLIL	343	–106.7709	1.2106	n/a	0.54933	n/a	0.0253	n/a	0.0511	n/a	n/a	n/a	0.4443	n/a	n/a	95.6	–0.206	28.60
Total nitrogen																		
DEAD	383	3.7037	1.0567	0.0143	n/a	0.1997	n/a	n/a	–0.0075	–0.0095	0.0458	–0.1222	n/a	n/a	n/a	98.1	0.776	0.88
DIFF	373	4.2135	0.9730	0.0172	0.1504	0.1134	n/a	n/a	n/a	n/a	0.1287	–0.0018	n/a	n/a	n/a	97.6	0.826	–2.91
FLAT	366	38.1489	1.0477	n/a	0.0535	n/a	n/a	n/a	–0.0180	n/a	0.1563	–0.0153	n/a	n/a	n/a	97.7	0.882	–2.98

Table 1.5. Number of observations, coefficients, R^2, Nash-Sutcliffe index, and bias percentage of suspended sediment, total phosphorus, total dissolved phosphorus, total particulate phosphorus, total nitrogen, total dissolved nitrogen, total particulate nitrogen, and nitrate plus nitrite load models at the five intensive monitoring stations.—Continued

[Dependent variable is the natural logarithm of the constituent. Ln, natural logarithm; Q, streamflow; TB, turbidity; SC, specific conductance; WT, water temperature; dTime, decimal time; BASE, indicator variable (0 or 1) for hydrologic condition of either baseflow or stormflow; NO_3^-, nitrate; R^2, coefficient of determination; n/a, not applicable; –, variable not included in selected model; Nash-Sutcliffe, Nash Sutcliffe efficiency index; DEAD, Dead Run at Whann Avenue near Mclean, VA; DIFF, Difficult Run above Fox Lake near Fairfax, VA; FLAT, Flatlick Branch above Frog Branch at Chantilly, VA; LONG, Long Branch near Annandale, VA; SFLIL, South Fork Little Difficult Run above mouth near Vienna, VA]

Station	Number of observations	Intercept	Ln Q	Ln Q^2	Ln TB	Ln SC	WT	pH	dTime	$dTime^2$	SIN ($dTime2\pi$)	COS ($dTime2\pi$)	BASE	Ln TB * BASE	Ln NO_3^-	Adjusted R^2	Nash-Sutcliffe	Bias percentage
LONG	181	1.2281	1.1308	n/a	0.1196	n/a	n/a	n/a	n/a	n/a	0.1888	–0.1208	n/a	n/a	n/a	98.7	0.959	–3.07
SFLIL	363	1.5498	1.0969	n/a	n/a	0.2179	n/a	n/a	n/a	n/a	0.0772	–0.1354	n/a	n/a	n/a	97.6	0.783	–3.48
Total dissolved nitrogen																		
DEAD	379	2.2879	0.9962	–0.0115	–0.0823	0.2604	n/a	n/a	n/a	n/a	–0.0265	–0.1586	n/a	n/a	n/a	98.0	0.948	–1.65
DIFF	373	4.5605	0.9455	–0.0144	n/a	0.0868	n/a	n/a	n/a	n/a	0.1772	0.0255	n/a	n/a	n/a	97.5	0.904	–1.03
FLAT	368	51.0989	1.0650	n/a	–0.0661	0.2359	n/a	n/a	n/a	n/a	0.0980	–0.0638	n/a	n/a	n/a	97.1	0.829	–0.36
LONG	192	4.0873	1.0787	–0.0379	n/a	n/a	n/a	n/a	n/a	n/a	0.1241	–0.1059	n/a	n/a	n/a	98.4	0.947	0.09
SFLIL	343	–26.0213	1.0144	–0.0161	–0.0693	0.2667	n/a	n/a	0.0147	n/a	0.0653	–0.0674	n/a	n/a	n/a	98.0	0.920	–0.70
Total particulate nitrogen																		
DEAD	378	–1.3595	1.2249	n/a	0.2700	0.1182	0.0127	n/a	n/a	n/a	n/a	n/a	n/a	n/a	n/a	96.0	0.303	14.17
DIFF	373	1.6246	0.9366	0.0366	0.6178	n/a	n/a	n/a	n/a	n/a	n/a	n/a	n/a	n/a	n/a	95.6	0.644	6.16
FLAT	366	–1.1170	1.1549	n/a	0.3742	n/a	n/a	n/a	n/a	n/a	–0.0044	–0.1242	n/a	n/a	n/a	94.5	0.637	10.15
LONG	180	–2.0169	1.2512	n/a	0.4388	n/a	0.0215	n/a	n/a	n/a	n/a	n/a	n/a	n/a	n/a	97.1	0.958	–0.86
SFLIL	343	–1.2560	1.1208	n/a	0.4773	n/a	n/a	n/a	n/a	n/a	0.0494	–0.2013	n/a	n/a	n/a	94.0	0.517	15.16
Nitrate plus nitrite																		
DEAD	378	60.1177	0.9740	n/a	–0.1489	0.3814	n/a	n/a	–0.0298	n/a	–0.0610	–0.1618	n/a	n/a	n/a	95.4	0.918	0.45
DIFF	383	3.4050	0.8349	–0.0280	n/a	0.2129	n/a	n/a	n/a	n/a	0.1823	0.0601	n/a	n/a	n/a	94.6	0.791	–0.07
FLAT	368	87.3961	1.0396	–0.0217	–0.1024	0.359	n/a	n/a	–0.0422	n/a	n/a	n/a	n/a	n/a	n/a	95.6	0.886	–0.23
LONG	189	2.9278	1.0477	–0.0509	n/a	0.1071	n/a	n/a	n/a	n/a	n/a	n/a	n/a	n/a	n/a	95.8	0.880	2.24
SFLIL	351	–3.8118	0.9990	–	–0.1019	0.4205	n/a	0.6215	n/a	n/a	0.1515	–0.0064	n/a	n/a	n/a	95.3	0.903	2.75
Total nitrogen with continuous nitrate monitor																		
SFLIL	363	2.3717	1.1065	–	0.0210	n/a	n/a	n/a	n/a	n/a	0.0455	–0.1319	n/a	n/a	0.3078	97.9	0.774	–3.92
Total dissolved nitrogen with continuous nitrate monitor																		
SFLIL	363	2.1965	1.0084	n/a	n/a	n/a	n/a	n/a	n/a	n/a	0.0187	–0.0367	n/a	n/a	0.5456	99.1	0.869	2.78

Table 1.6. Number of observations, regression coefficients, R^2, Nash-Sutcliffe index, and model bias in percent for suspended sediment, total phosphorus, total dissolved phosphorus, total particulate phosphorus, total nitrogen, total dissolved nitrogen, total particulate nitrogen, and nitrate plus nitrite concentration models at the five intensive monitoring stations.

[Dependent variable is the natural logarithm of the constituent. Ln, natural logarithm; Q, streamflow; TB, turbidity; SC, specific conductance; WT, water temperature; dTime, decimal time; BASE, indicator variable (0 or 1) for hydrologic condition of either baseflow or stormflow; NO_3^-, nitrate; R^2, coefficient of determination; n/a, not applicable; –, variable not included in selected model; Nash-Sutcliffe, Nash Sutcliffe efficiency index; DEAD, Dead Run at Whann Avenue near Mclean, VA; DIFF, Difficult Run above Fox Lake near Fairfax, VA; FLAT, Flatlick Branch above Frog Branch at Chantilly, VA; LONG, Long Branch near Annandale, VA; SFLIL, South Fork Little Difficult Run above mouth near Vienna, VA]

Station	Number of obser-vations	Intercept	Ln Q	Ln Q^2	Ln TB	Ln SC	WT	pH	dTime	$dTime^2$	SIN (dTime2π)	COS (dTime2π)	BASE	Ln TB * BASE	Ln NO_3^-	Ad-justed R^2	Nash-Sut-cliffe	Bias per-cent-age
Suspended sediment																		
DEAD	401	0.8303	0.3458	n/a	0.3056	n/a	n/a	n/a	n/a	n/a	n/a	n/a	0.2198	0.3717	n/a	93.2	0.623	6.25
DIFF	387	0.3181	0.2026	n/a	0.8266	n/a	n/a	n/a	n/a	n/a	n/a	n/a	0.7065	n/a	n/a	92.8	0.721	3.61
FLAT	398	0.0435	0.2174	n/a	0.7678	n/a	n/a	n/a	n/a	n/a	n/a	n/a	0.9575	n/a	n/a	92.4	0.769	2.34
LONG	209	0.7894	0.2064	n/a	0.8497	n/a	n/a	n/a	n/a	n/a	n/a	n/a	0.0011	n/a	n/a	91.3	0.735	4.78
SFLIL	367	0.8623	0.3124	n/a	0.2981	n/a	n/a	n/a	n/a	n/a	0.0814	–0.1851	–0.2337	n/a	n/a	94.3	0.806	10.13
Total phosphorus																		
DEAD	378	–75.8891	0.1882	n/a	0.3418	n/a	n/a	n/a	0.0360	n/a	–0.1491	–0.2382	n/a	n/a	n/a	85.9	0.641	2.88
DIFF	384	–106.0851	0.0620	n/a	0.6031	–0.3175	n/a	n/a	0.0512	n/a	n/a	n/a	n/a	n/a	n/a	87.7	0.567	–3.36
FLAT	367	–3.3945	–0.0298	0.0360	0.4259	n/a	n/a	n/a	n/a	n/a	–0.1075	–0.1576	n/a	n/a	n/a	74.1	0.527	–1.92
LONG	181	–4.4491	0.2399	n/a	0.3873	n/a	0.0248	n/a	n/a	n/a	n/a	n/a	n/a	n/a	n/a	85.8	0.729	–0.47
SFLIL	352	–109.2154	0.1609	n/a	0.5007	n/a	0.0337	n/a	0.0516	n/a	n/a	n/a	0.5402	n/a	n/a	88.4	0.644	0.46
Total dissolved phosphorus																		
DEAD	379	–120.3532	–0.0162	n/a	0.2007	–0.2844	n/a	n/a	0.0587	n/a	–0.2235	–0.0664	n/a	n/a	n/a	72.3	0.592	2.19
DIFF	378	–2.0164	0.0541	n/a	0.0886	–0.4700	n/a	n/a	0.0517	–0.0105	n/a	n/a	n/a	n/a	n/a	39.0	0.120	–6.55
FLAT	368	–2.3024	–0.0639	0.0175	0.0972	–0.1736	n/a	n/a	n/a	n/a	–0.3192	–0.2455	n/a	n/a	n/a	54.1	0.449	0.48
LONG	182	–2.3658	0.0297	n/a	0.1278	–0.3238	n/a	n/a	n/a	n/a	n/a	n/a	n/a	n/a	n/a	59.4	0.526	1.62
SFLIL	349	–1.9479	0.0184	–0.0315	0.1977	–0.5348	n/a	n/a	n/a	n/a	–0.3253	–0.1035	n/a	n/a	n/a	58.6	0.472	–0.47
Total particulate phosphorus																		
DEAD	378	–4.4786	0.2450	n/a	0.4266	n/a	n/a	n/a	n/a	n/a	n/a	n/a	n/a	n/a	n/a	82.2	0.579	3.89
DIFF	373	–100.1860	0.0381	n/a	0.6732	–0.2548	n/a	n/a	0.0479	n/a	n/a	n/a	n/a	n/a	n/a	85.2	0.557	–2.99
FLAT	366	–9.9720	0.1327	n/a	0.6138	n/a	0.0151	0.6412	n/a	n/a	n/a	n/a	n/a	n/a	n/a	81.7	0.602	–0.91
LONG	181	–5.1996	0.2784	n/a	0.4496	n/a	0.0302	n/a	n/a	n/a	n/a	n/a	n/a	n/a	n/a	85.2	0.725	–0.40
SFLIL	343	–108.4561	0.2106	n/a	0.54933	n/a	0.0253	n/a	0.0511	n/a	n/a	n/a	0.4443	n/a	n/a	86.0	0.622	2.11
Total nitrogen																		
DEAD	383	–0.2202	0.0566	0.0143	n/a	0.1997	n/a	n/a	–0.0075	–0.0095	0.0458	–0.1222	n/a	n/a	n/a	28.2	0.232	–0.32
DIFF	373	–0.6436	–0.0270	0.0172	0.1504	0.1134	n/a	n/a	n/a	n/a	0.1287	–0.0018	n/a	n/a	n/a	49.4	0.471	–0.41

Table 1.6. Number of observations, regression coefficients, R^2, Nash-Sutcliffe index, and model bias in percent for suspended sediment, total phosphorus, total dissolved phosphorus, total particulate phosphorus, total nitrogen, total dissolved nitrogen, total particulate nitrogen, and nitrate plus nitrite concentration models at the five intensive monitoring stations.—Continued

[Dependent variable is the natural logarithm of the constituent. Ln, natural logarithm; Q, streamflow; TB, turbidity; SC, specific conductance; WT, water temperature; dTime, decimal time; BASE, indicator variable (0 or 1) for hydrologic condition of either baseflow or stormflow; NO_3^-, nitrate; R^2, coefficient of determination; n/a, not applicable; –, variable not included in selected model; Nash-Sutcliffe, Nash Sutcliffe efficiency index; DEAD, Dead Run at Whann Avenue near Mclean, VA; DIFF, Difficult Run above Fox Lake near Fairfax, VA; FLAT, Flatlick Branch above Frog Branch at Chantilly, VA; LONG, Long Branch near Annandale, VA; SFLIL, South Fork Little Difficult Run above mouth near Vienna, VA]

Station	Number of observations	Intercept	Ln Q	Ln Q^2	Ln TB	Ln SC	WT	pH	dTime	$dTime^2$	SIN (dTime2π)	COS (dTime2π)	BASE	Ln TB * BASE	Ln NO_3^-	Adjusted R^2	Nash-Sutcliffe	Bias percentage
FLAT	366	36.4637	0.0477	n/a	0.0535	n/a	n/a	n/a	–0.0180	n/a	0.1563	–0.0153	n/a	n/a	n/a	35.6	0.291	–0.13
LONG	181	–0.4872	0.1085	n/a	0.1196	n/a	n/a	n/a	n/a	n/a	0.1888	–0.1208	n/a	n/a	n/a	79.2	0.671	0.71
SFLIL	363	–0.1354	0.0969	n/a	n/a	0.2179	n/a	n/a	n/a	n/a	0.0772	–0.1354	n/a	n/a	n/a	27.6	0.265	–0.42
Total dissolved nitrogen																		
DEAD	379	–0.6360	–0.0038	–0.0115	–0.0823	0.2604	n/a	n/a	n/a	n/a	–0.0265	–0.1586	n/a	n/a	n/a	62.8	0.588	–0.10
DIFF	373	–0.2966	–0.0545	–0.0144	n/a	0.0868	n/a	n/a	n/a	n/a	0.1772	0.0255	n/a	n/a	n/a	34.5	0.301	–0.13
FLAT	368	49.4136	0.0650	n/a	–0.0661	0.2359	n/a	n/a	n/a	n/a	0.0980	–0.0638	n/a	n/a	n/a	28.3	0.248	0.12
LONG	192	0.0023	0.0787	–0.0379	n/a	n/a	n/a	n/a	n/a	n/a	0.1241	–0.1059	n/a	n/a	n/a	50.4	0.330	1.02
SFLIL	343	–29.8029	0.0144	–0.0161	–0.0693	0.2667	n/a	n/a	0.0147	n/a	0.0653	–0.0674	n/a	n/a	n/a	52.6	0.524	0.19
Total particulate nitrogen																		
DEAD	378	–3.0448	0.2249	n/a	0.2700	0.1182	0.0127	n/a	n/a	n/a	n/a	n/a	n/a	n/a	n/a	75.1	0.528	–0.54
DIFF	373	–3.2324	–0.0635	0.0366	0.6178	n/a	n/a	n/a	n/a	n/a	n/a	n/a	n/a	n/a	n/a	79.5	0.693	1.14
FLAT	366	–2.8022	0.1549	n/a	0.3742	n/a	n/a	n/a	n/a	n/a	–0.0044	–0.1242	n/a	n/a	n/a	69.6	0.563	1.69
LONG	180	–3.7021	0.2512	n/a	0.4388	n/a	0.0215	n/a	n/a	n/a	n/a	n/a	n/a	n/a	n/a	85.0	0.768	–1.24
SFLIL	343	–2.9412	0.1208	n/a	0.4773	n/a	n/a	n/a	n/a	n/a	0.0494	–0.2013	n/a	n/a	n/a	77.0	0.626	1.20
Nitrate plus nitrite																		
DEAD	378	58.4325	–0.0260	n/a	–0.1489	0.3814	n/a	n/a	–0.0298	n/a	–0.0610	–0.1618	n/a	n/a	n/a	73.7	0.651	0.02
DIFF	383	–1.4521	–0.1651	–0.0280	n/a	0.2129	n/a	n/a	n/a	n/a	0.1823	0.0601	n/a	n/a	n/a	56.1	0.461	–0.47
FLAT	368	82.9130	0.0396	–0.0217	–0.1024	0.359	n/a	n/a	–0.0422	n/a	n/a	n/a	n/a	n/a	n/a	50.9	0.473	–0.52
LONG	189	–0.1633	0.0476	–0.0509	n/a	0.1071	n/a	n/a	n/a	n/a	n/a	n/a	n/a	n/a	n/a	27.3	0.168	2.52
SFLIL	351	–12.1487	–0.0013	–	–0.1019	0.4205	n/a	0.6215	n/a	n/a	0.1515	–0.0064	n/a	n/a	n/a	68.1	0.689	0.58
Total nitrogen with continuous nitrate monitor																		
SFLIL	363	0.6864	0.1065	–	0.0210	n/a	n/a	n/a	n/a	n/a	0.0455	–0.1319	n/a	n/a	0.3078	35.5	0.292	–0.42
Total dissolved nitrogen with continuous nitrate monitor																		
SFLIL	363	0.5113	0.0084	n/a	n/a	n/a	n/a	n/a	n/a	n/a	0.0187	–0.0367	n/a	n/a	0.5456	78.09	0.816	0.09

Appendix 2 Water Temperature, Orthophosphate, Nitrate Plus Nitrite, and Dissolved and Particulate Components of Phosphorus and Nitrogen at Each Monitoring Station by Season

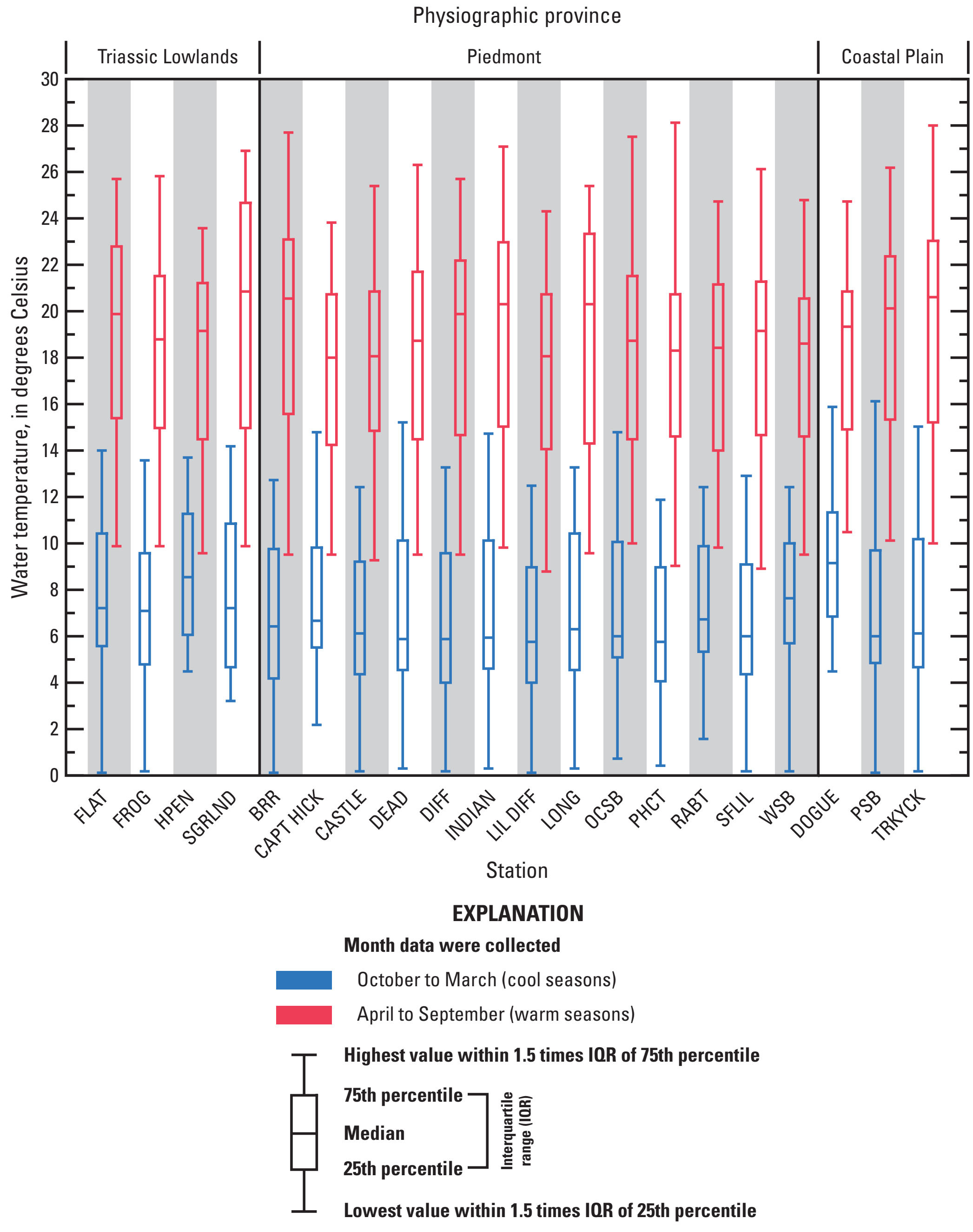

Figure 2.1. Water temperature results from the monthly sampling at 20 monitoring stations in Fairfax County, with comparison of data collected during the cool (October-March) and warm (April-September) seasons. The effect of season is statistically significant at all stations, based on $p \leq 0.05$. Stations are arranged by physiographic province. Station names are defined as DEAD, Dead Run at Whann Avenue near Mclean, VA; DIFF, Difficult Run above Fox Lake near Fairfax, VA; FLAT, Flatlick Branch above Frog Branch at Chantilly, VA; LONG, Long Branch near Annandale, VA; SFLIL, South Fork Little Difficult Run above mouth near Vienna, VA; BRR, Big Rocky Run at Stringfellow Rd near Chantilly, VA; CAPT HICK, Captain Hickory Run at Route 681 near Great Falls, VA; CASTLE, Castle Creek at Newman Road at Clifton, VA; DOGUE, Douge Creek Tributary at Woodley Drive at Mount Vernon, VA; FROG, Frog Branch above Flatlick Branch at Chantilly, VA; HPEN, Horsepen Rn above Horsepen Run Tributary near Herndon, VA; INDIAN, Indian Run at Bren Mar Drive at Alexandria, VA; LIL DIFF, Little Difficult Run near Vienna, VA; OCSB, Old Courthouse Spring Branch near Vienna, VA; PHCT, Popes Head Creek tributary near Fairfax Station, VA; PSB, Paul Spring Br above North Branch near Gum Springs, VA; RABT, Rabbit Branch Tributary above Lake Royal near Burke, VA; SGRLND, Sugarland Run Tributary below Crayton Road near Herndon, VA; TRKYCK, Turkeycock Run at Edsall Road at Alexandria, VA; WSB, Willow Springs Branch at Highway 29 near Centreville, VA.

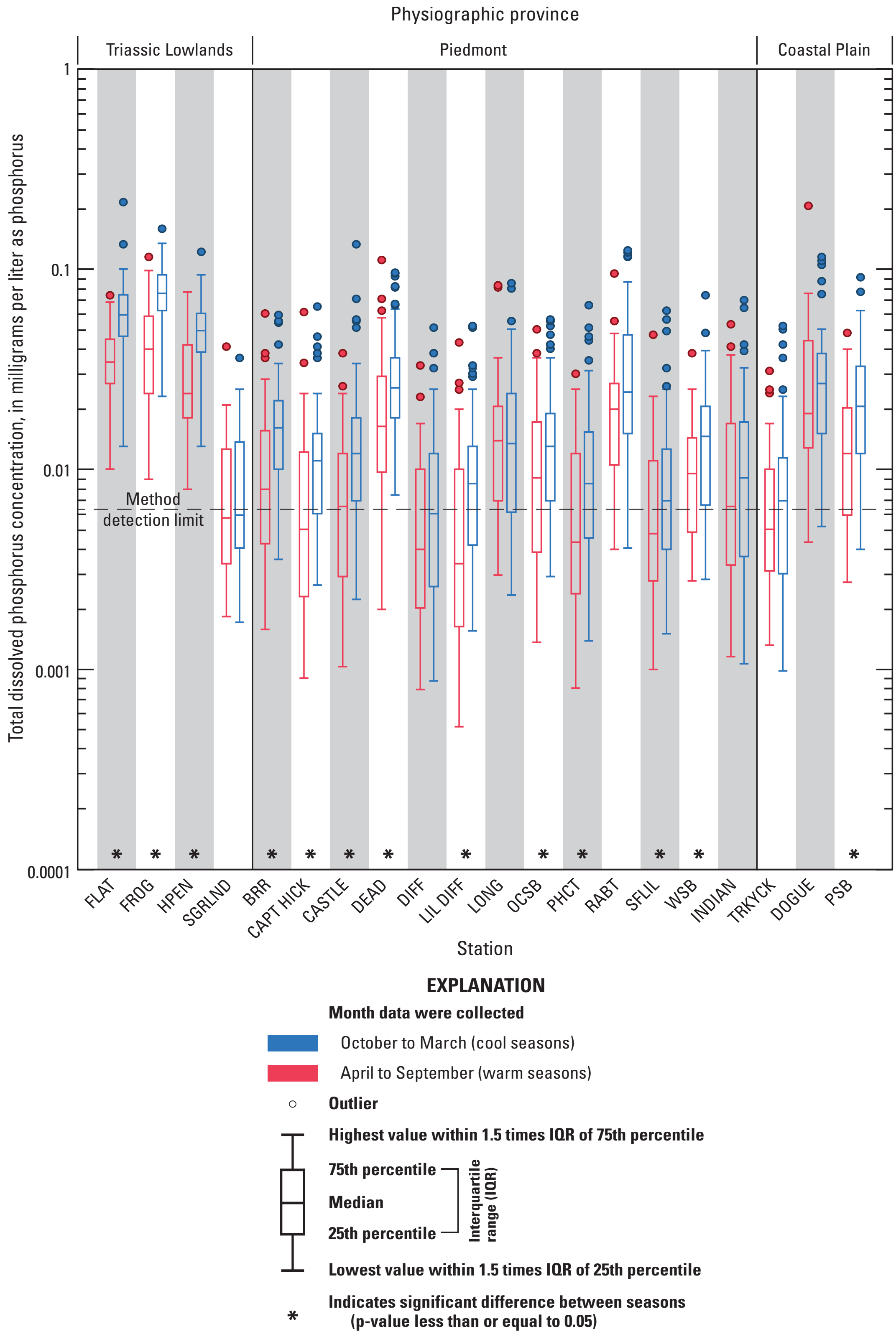

Figure 2.2. Total dissolved phosphorus results from the monthly sampling at 20 monitoring stations in Fairfax County, with comparison of data collected during the cool (October-March) and warm (April-September) seasons. A significant difference between warm and cool season sample concentration distributions was determined from a nonparametric Wilcoxon test with a p-value of ≤0.05. Stations are arranged by physiographic province. Station names are defined in figure 2.1.

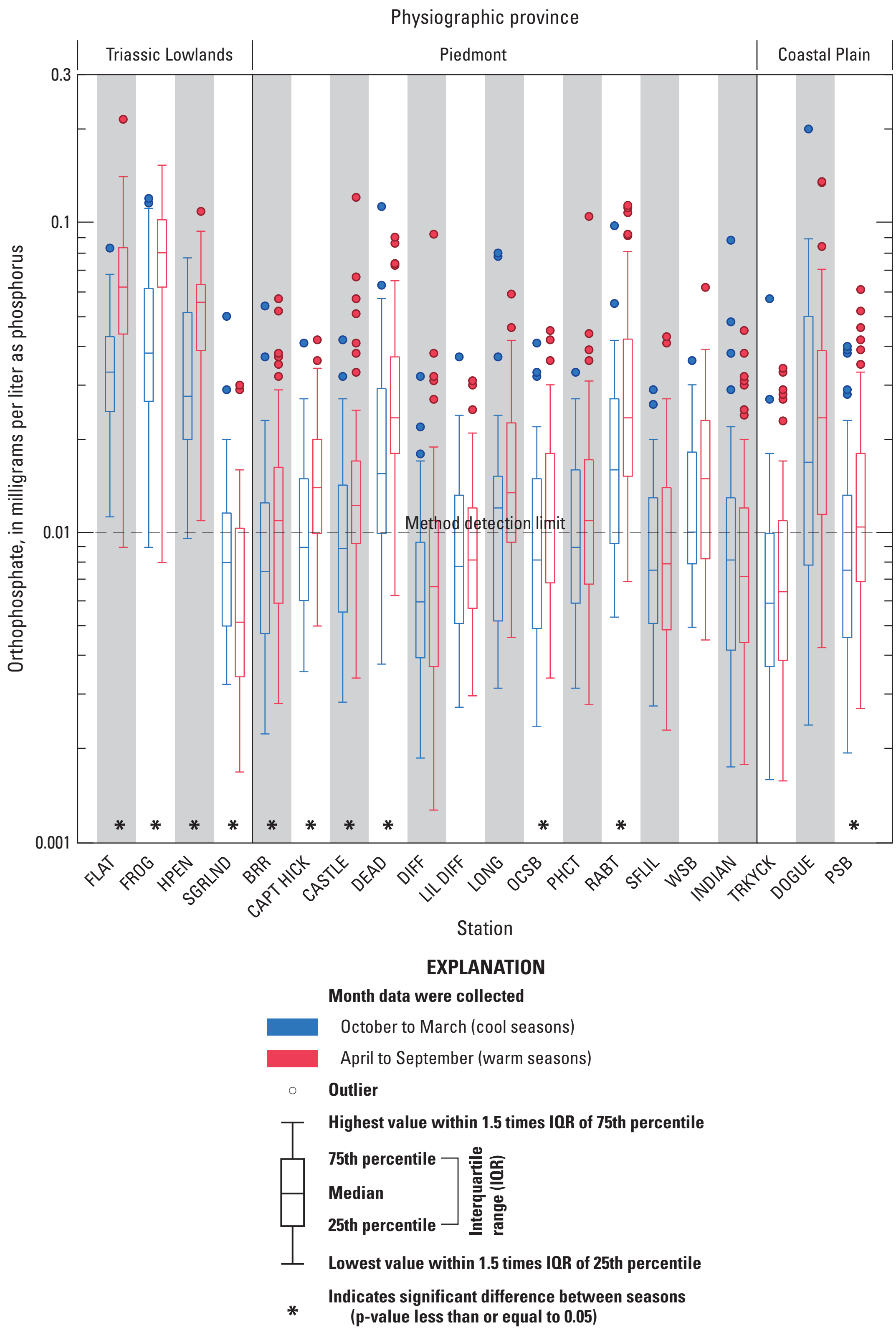

Figure 2.3. Orthophosphate results from the monthly sampling at 20 monitoring stations in Fairfax County, with comparison of data collected during the cool (October-March) and warm (April-September) seasons. A significant difference between warm and cool season sample concentration distributions was determined from a nonparametric Wilcoxon test with a p-value of ≤0.05. Stations are arranged by physiographic province. Station names are defined in figure 2.1.

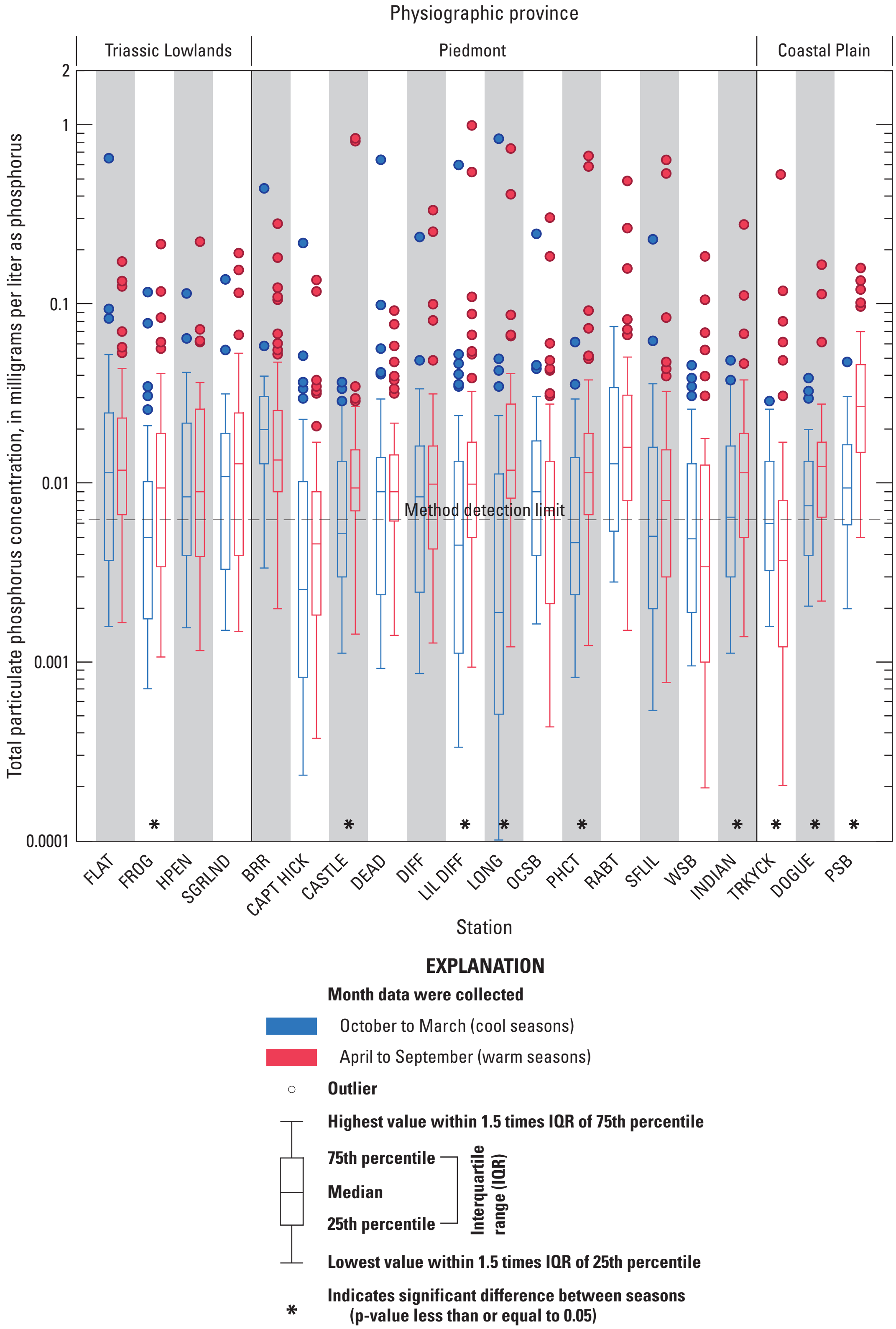

Figure 2.4. Total particulate phosphorus results from the monthly sampling at 20 monitoring stations in Fairfax County, with comparison of data collected during the cool (October-March) and warm (April-September) seasons. A significant difference between warm and cool season sample concentration distributions was determined from a nonparametric Wilcoxon test with a p-value of ≤0.05. Stations are arranged by physiographic province. Station names are defined in figure 2.1.

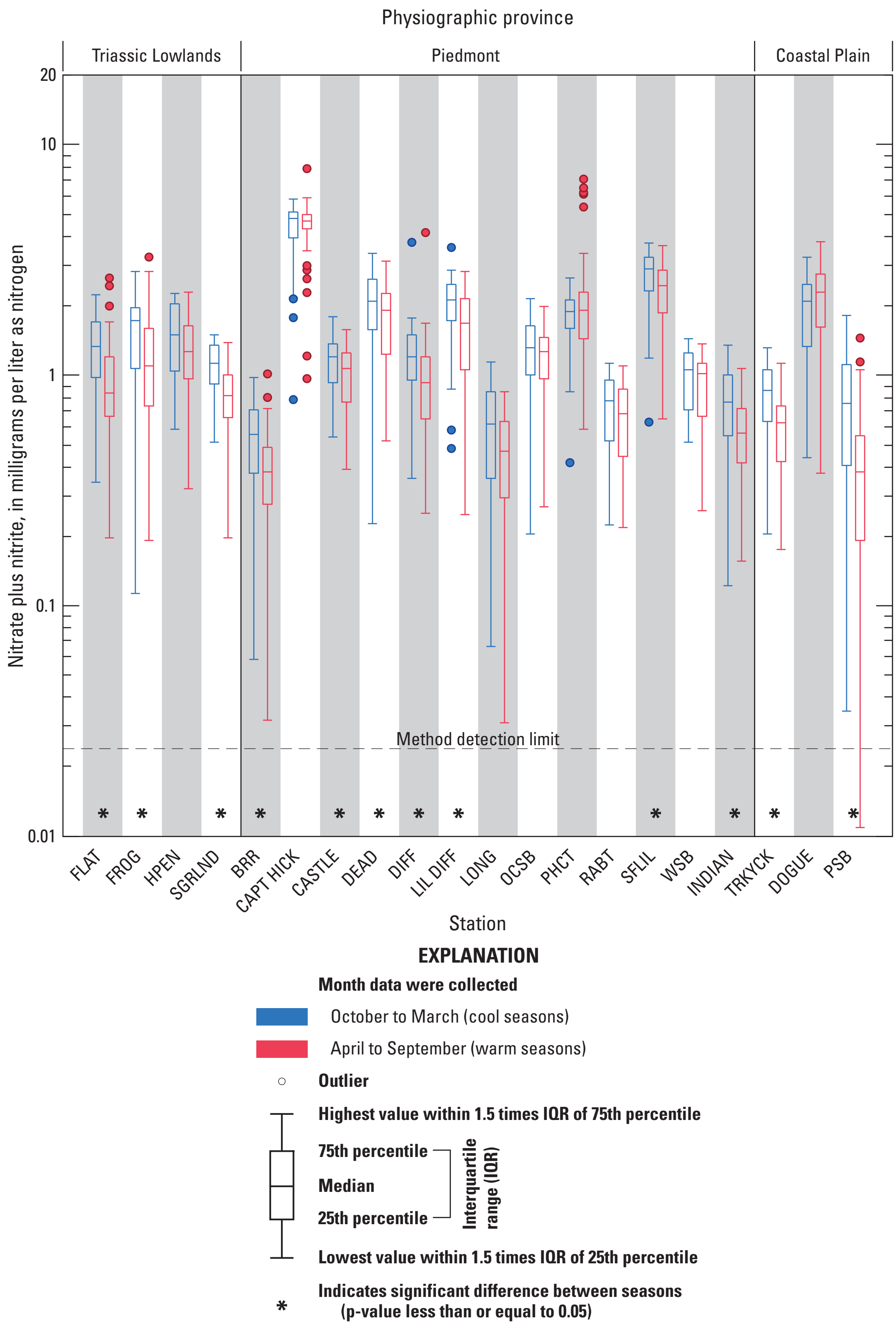

Figure 2.5. Nitrate plus nitrite results from the monthly sampling at 20 monitoring stations in Fairfax County, with comparison of data collected during the cool (October-March) and warm (April-September) seasons. A significant difference between warm and cool season sample concentration distributions was determined from a nonparametric Wilcoxon test with a p-value of ≤0.05. Stations are arranged by physiographic province. Station names are defined in figure 2.1.

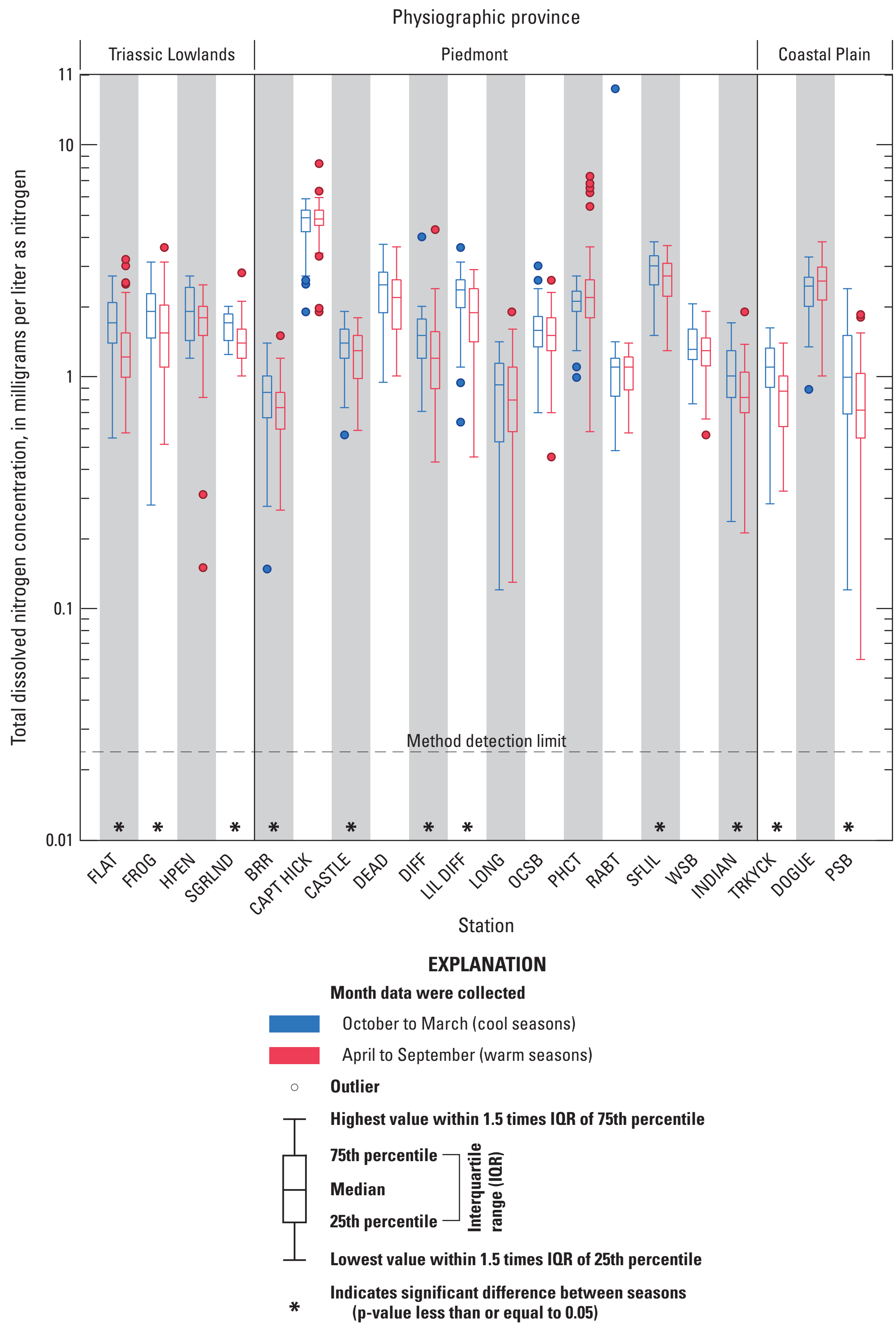

Figure 2.6. Total dissolved nitrogen results from the monthly sampling at 20 monitoring stations in Fairfax County, with comparison of data collected during the cool (October-March) and warm (April-September) seasons. A significant difference between warm and cool season sample concentration distributions was determined from a nonparametric Wilcoxon test with a p-value of ≤0.05. Stations are arranged by physiographic province. Station names are defined in figure 2.1.

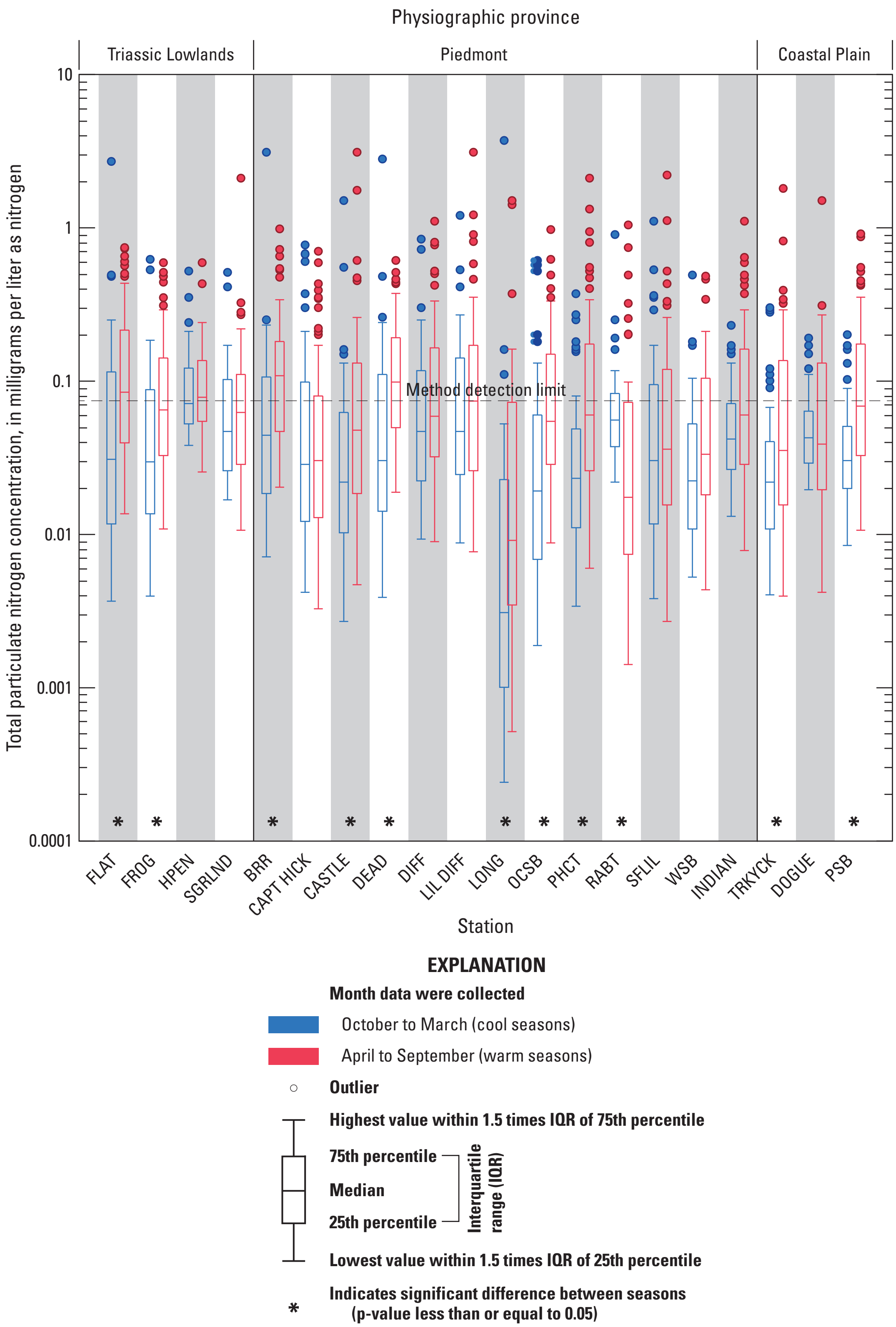

Figure 2.7. Total particulate nitrogen results from the monthly sampling at 20 monitoring stations in Fairfax County, with comparison of data collected during the cool (October-March) and warm (April-September) seasons. A significant difference between warm and cool season sample concentration distributions was determined from a nonparametric Wilcoxon test with a p-value of ≤0.05. Stations are arranged by physiographic province. Station names are defined in figure 2.1.

Director, Virginia and West Virginia Water Science Center,
U.S. Geological Survey
1730 E. Parham Road, Richmond, VA 23228
Publishing support provided by the West Trenton Publishing Service Center.

Porter and others—**Spatial and Temporal Patterns in Selected Streams in Fairfax County, Virginia, 2007–18**—SIR 2020–5061

ISBN 978-1-4113-4376-4

ISSN 2328-031X (print)
ISSN 2328-0328 (online)
https://doi.org/10.3133/sir20205061